TURKISH SOCIETY OF MEDICAL ONCOLOGY
In pursuit of science for life...

ISSN: 2651-4532 / E-ISSN: 2452-3364

Journal of ONCOLOGICAL SCIENCES

Official Journal of Turkish Society of Medical Oncology

Volume: 12 Issue: 1 April 2026

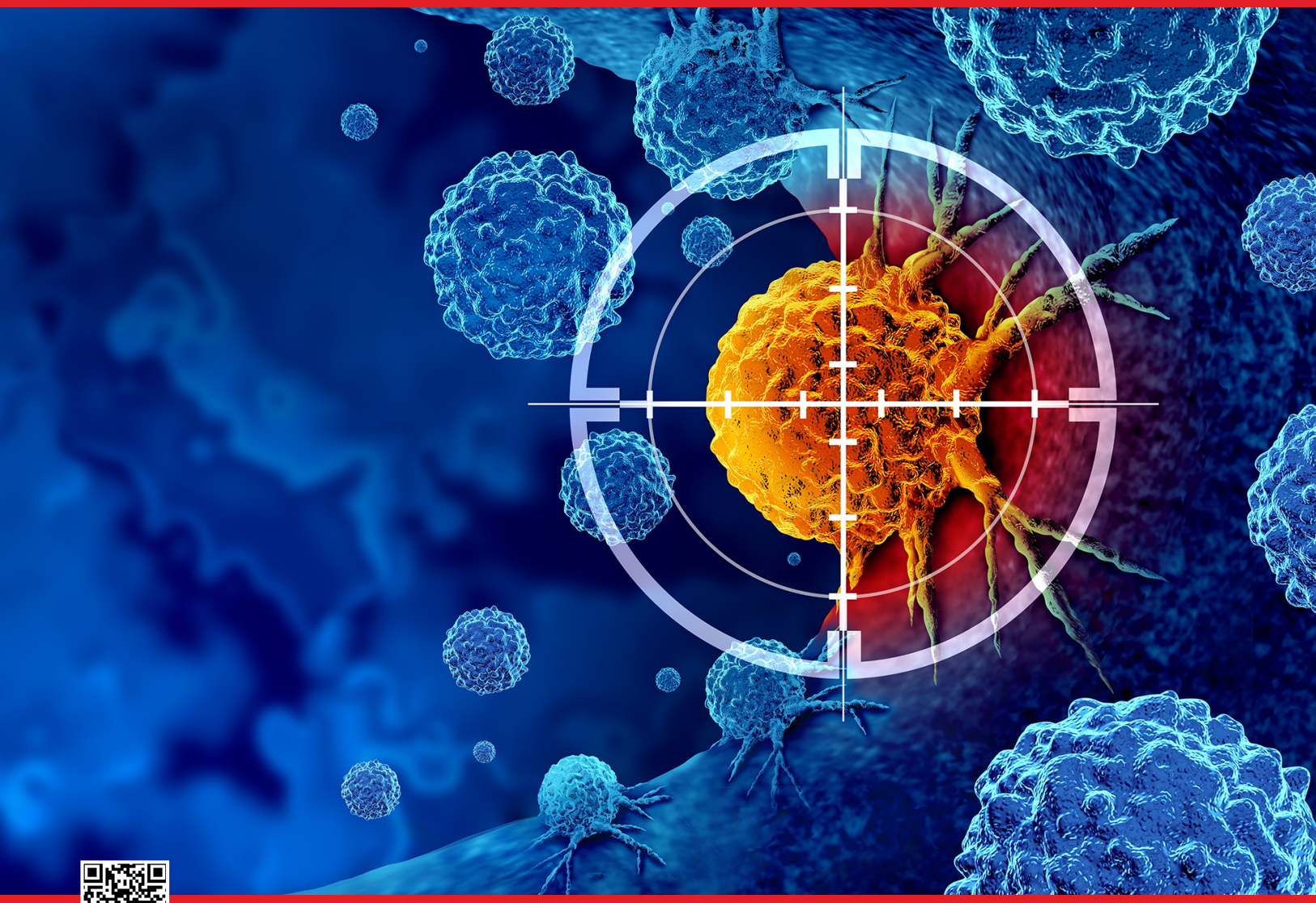

journalofoncology.org

galenos yayinevi

Journal of
ONCOLOGICAL
SCIENCES

VOLUME: 12 | ISSUE: 1 | APRIL 2026

EDITORIAL BOARD

Publisher Contact
Address: Molla Gürani Mah. Kaçamak Sk. No: 21/1 34093 İstanbul, Turkey
Phone: +90 (530) 177 30 97 / +90 (539) 307 32 03
E-mail: info@galenos.com.tr/yayin@galenos.com.tr
Web: www.galenos.com.tr
Publisher Certificate Number: 14521

Publication Date: March 2026

ISSN: 2651-4532 / **E-ISSN:** 2452-3364

International periodical journal published three times in a year.

Journal of
ONCOLOGICAL
SCIENCES

VOLUME: 12 | ISSUE: 1 | APRIL 2026

EDITORIAL BOARD

Section Editors and Scientific Editorial Board

Journal of
ONCOLOGICAL
SCIENCES

VOLUME: 12 | ISSUE: 1 | APRIL 2026

EDITORIAL BOARD

Editorial Board

Journal of
ONCOLOGICAL
SCIENCES

VOLUME: 12 | ISSUE: 1 | APRIL 2026

Please refer to the journal's webpage (**journalofoncology.org**) for "Policies" and "Instructions".
The editorial and publication processes of the journal are conducted in accordance with the guidelines of the ICMJE, COPE, WAME, CSE and EASE.
Journal of Oncological Sciences is indexed in **TUBITAK/ULAKBIM**, **Scopus**, **DOAJ**, and **Turkey Citation Index**.
The journal is published online.
Owner: Murat Dinçer, on behalf of Turkish Society of Medical Oncology
Responsible Manager: Sercan Aksoy

Journal of
ONCOLOGICAL
SCIENCES

VOLUME: 12 | ISSUE: 1 | APRIL 2026

CONTENTS

Journal of
ONCOLOGICAL
SCIENCES

VOLUME: 12 | ISSUE: 1 | APRIL 2026

ORIGINAL ARTICLE

DOI: 10.37047/jos.galenos.2025.2025-11-2

J Oncol Sci 2026;12(1):1-8

Serum Vitamin D Levels as a Prognostic Biomarker in Patients Receiving Immune Checkpoint Inhibitors

Taha Koray ŞAHİN[1], Onur BAŞ[1], Gözde KAVGACI[1], Naciye GÜDÜK[2], Fırat ŞİRVAN[2], Serkan AKIN[1], Zafer ARIK[1], Neyran KERTMEN[1], Ömer DİZDAR[1], Mustafa ERMAN[1], Şuayib YALÇIN[1], Sercan AKSOY[1], Burak Yasin AKTAŞ[1], Deniz Can GÜVEN[1]

[1]Hacettepe University Cancer Institute, Department of Medical Oncology, Ankara, Türkiye
[2]Hacettepe University Faculty of Medicine, Department of Internal Medicine, Ankara, Türkiye

ABSTRACT

Objective: Vitamin D exerts pleiotropic effects on tumor biology and immune regulation, including modulation of T-cell function and antigen presentation. Preclinical evidence suggests that optimal vitamin D status may enhance immune checkpoint inhibitor (ICI) efficacy; however, data are limited among ICI-treated patients. We aimed to evaluate the prognostic significance of baseline serum 25(OH)D levels in patients receiving ICIs.

Material and Methods: A retrospective cohort of 244 patients with advanced solid tumors treated with ICI. Baseline serum 25(OH)D concentrations, obtained within 30 days prior to ICI initiation, were categorized as sufficient (>20 ng/mL), insufficient (12-20 ng/mL), or deficient (<12 ng/mL).

Results: The median age of the patients was 63 years; 65.2% were male. The most common tumor types were non-small cell lung cancer (32.8%), renal cell carcinoma (18.9%), and melanoma (14.3%). Vitamin D status was sufficient in 36.5%, insufficient in 34.8%, and deficient in 28.7% of patients. In multivariable analysis, vitamin D deficiency independently predicted shorter overall survival (OS) [hazard ratio (HR): 2.264, 95% confidence interval (CI): 1.553-3.300; p<0.001] compared with the vitamin D-sufficient group. Both vitamin D insufficiency (HR: 1.494; 95% CI: 1.067-2.092; p=0.019) and vitamin D deficiency (HR: 2.0; 95% CI: 1.411-2.833; p<0.001) were independently associated with inferior progression-free survival (PFS).

Conclusion: Baseline vitamin D deficiency is an independent adverse prognostic factor for OS and PFS in ICI-treated patients. Integrating vitamin D assessment into pretreatment evaluation may facilitate risk stratification and inform supportive care strategies, warranting prospective validation.

Keywords: Vitamin D; immune checkpoint inhibitors; prognostic biomarkers; survival

INTRODUCTION

Cancer cells create an immunosuppressive microenvironment in their vicinity, and its development is paramount to cancer progression.[1] Recently, it has been demonstrated that cell surface receptors called immune checkpoints, located on the surfaces of T-lymphocytes, play a crucial role in cancer progression and orchestrate immune evasion and exhaustion of anti-tumor T-cells.[2] Monoclonal antibodies targeting these checkpoints, known as immune checkpoint inhibitors (ICIs), have been developed and introduced into clinical practice over the last decade.[3] The ICIs became the foundation of modern immunotherapy and significantly changed the cancer treatment landscape.[4]

Although ICIs have improved outcomes in several tumor types, many patients still do not respond to ICIs.[5] In addition, toxicities, including class-specific adverse events, and the financial burden are concerning.[6] Biomarkers are urgently needed to identify patients who are most likely to benefit. There are several tumor- and microenvironment-based biomarkers. While microsatellite instability (MSI) status, tumor mutational burden, and tumor programmed death-ligand 1 (PD-L1) expression are well-established predictive biomarkers, they require invasive tissue sampling, are costly, and may not fully capture the dynamic interaction between host immunity and tumor biology.[7] These issues led to increased interest in peripheral blood-based biomarkers that evaluate various

Correspondence: Taha Koray ŞAHİN MD,
Hacettepe University Cancer Institute, Department of Medical Oncology, Ankara, Türkiye
E-mail: takorsah@gmail.com
ORCID ID: orcid.org/0000-0002-3590-0426

Received: 10.11.2025 **Accepted:** 23.12.2025 **Epub:** 22.01.2026 **Publication Date:** 18.03.2026

Cite this article as: Şahin TK, Baş O, Kavgacı G, et al. Serum vitamin D levels as a prognostic biomarker in patients receiving immune checkpoint inhibitors. J Oncol Sci. 2026;12(1):1-8

Available at journalofoncology.org

aspects of tumor-host interactions. From this perspective, simple biomarkers retrieved from the routine complete blood count and chemistry tests may be valuable and provide clues about the host's immune and nutritional status.

Vitamin D is an essential nutrient for bone health and also exerts antitumor effects, including the regulation of apoptosis, tumor-cell proliferation, invasion, angiogenesis, and metastasis.[8,9] vitamin D is a key immunomodulator, with its receptors prevalent on most immune cells.[10] Its active metabolite, 1,25-dihydroxyvitamin D [1,25-$(OH)_2$D], modulates immunity through effects on antigen-presenting cell differentiation, lymphocyte proliferation, and cytokine secretion.[11] Experimental studies indicate that Vitamin D may enhance tumor immunotherapy by activating natural killer (NK) cells and T-cells, mitigating immunosuppressive factors such as pro-inflammatory cytokines and PD-L1, and favorably altering the TME.[12,13] Preclinical models have shown improved immune-mediated tumor control and response to ICIs with higher vitamin D availability.[14] Despite these mechanistic rationales, clinical evidence remains limited and inconsistent, often stemming from small sample sizes and single-center studies.[15,16]

Based on the immunomodulatory role of vitamin D and emerging evidence suggesting its interaction with antitumor immune responses, we hypothesized that baseline serum vitamin D status may be associated with survival outcomes in patients treated with ICIs. Consequently, we aimed to evaluate the association between baseline vitamin D levels and survival outcomes among ICI-treated patients at our institution.

MATERIAL AND METHODS

Patients and Study Design

This retrospective cohort study included patients with metastatic or unresectable cancer who were treated with ICIs between September 2016 and August 2024. Exclusion criteria included participation in clinical trials or expanded access programs, absence of a baseline serum 25(OH)D measurement within 30 days prior to ICI initiation, incomplete clinical or survival data, and loss to follow-up within the first month after treatment initiation. Baseline serum 25(OH) D measurements were available for all patients and were obtained within 30 days prior to ICI initiation. Baseline patient demographics, Eastern Cooperative Oncology Group (ECOG) status, primary tumor type, metastasis sites, line of immunotherapy, type of ICI, survival outcomes, and baseline serum 25(OH)D levels were obtained from patient files and the electronic hospital registry. Serum 25(OH)D levels were obtained from blood samples drawn within 30 days prior to ICI initiation as part of routine clinical practice. Measurements were performed in the institutional biochemistry laboratory using a standardized chemiluminescent immunoassay. Vitamin D status was categorized into three groups according to baseline 25(OH)D concentration: deficiency (<12 ng/mL), insufficiency (12-20 ng/mL), and sufficiency (>20 ng/mL). These cut-offs were selected to ensure clinical relevance, biological interpretability, and comparability with prior literature.[17]

The authors state that they have obtained Hacettepe University Health Sciences Research Ethics Committee approval (date: 26.08.2025, approval number: SBA 25/743).

Statistical Analyses

We reported continuous data as medians with interquartile range (IQR), and categorical variables as frequencies with percentages. For categorical variables, comparisons between vitamin D categories were conducted using the chi-square test or Fisher's exact test; for continuous variables, the Kruskal-Wallis or Mann-Whitney U test was employed, as appropriate. The Kaplan-Meier approach was used to examine the influence of prognostic factors on survival. Univariable Cox proportional hazards models were used to estimate hazard ratios (HRs) with 95% confidence intervals (CIs) for potential prognostic factors. Variables yielding a p-value of less than 0.10 in the univariable analysis were subsequently included in a multivariable Cox regression to control for confounding effects. Statistical analyses were performed using SPSS version 24; p-values <0.05 were considered statistically significant.

RESULTS

A total of 798 patients with metastatic or unresectable solid tumors were treated with ICIs at our institution. Of these, 123 patients were excluded due to participation in clinical trials or expanded access programs. The remaining 675 patients were evaluated for eligibility. Among them, 349 patients did not have an available baseline serum 25-hydroxyvitamin D measurement obtained within 30 days of ICI initiation; 54 patients had incomplete clinical or survival data; and 28 patients were lost to follow-up within the first month after treatment initiation. After applying these exclusion criteria, 244 patients were included in the analyses (Figure 1).

The median age of patients was 63 years (IQR, 55-69); 65.2% of patients were male. The most common primary tumors were non-small cell lung cancer (NSCLC) (32.8%), renal cell carcinoma (18.9%), and melanoma (14.3%). Most patients (77.5%) had an ECOG performance status (PS) of 0-1, and 40.6% received ICIs in the second-line setting. Nivolumab was the most frequently administered agent (80.3%), followed by atezolizumab (8.6%) and pembrolizumab (7.4%).

Baseline vitamin D status was sufficient in 89 patients (36.5%), insufficient in 85 (34.8%), and deficient in 70 (28.7%). The baseline demographic and clinical characteristics are detailed in Table 1.

When patients were stratified by vitamin D status, no statistically significant differences were observed in age, sex, ECOG PS, primary tumor type, treatment line, or presence of liver or lung metastases (Table 2).

In univariable analysis of overall survival (OS), ECOG PS ≥2 (HR: 1.670, 95% CI: 1.178-2.369; p=0.004) and lower vitamin D levels were associated with worse outcomes. Compared with patients with sufficient vitamin D levels, those with insufficiency had an HR of 1.462 (95% CI: 1.012-2.113; p=0.043) and those with deficiency had an HR of 2.315 (95% CI: 1.606-3.337; p<0.001). In multivariable analysis, vitamin D deficiency remained an independent predictor of shorter OS (HR: 2.264, 95% CI: 1.553-3.300; p<0.001), whereas vitamin D insufficiency was not significantly associated with OS (HR: 1.380, 95% CI: 0.944-2.017; p=0.096) compared with the vitamin D-sufficient group (Table 3). Median OS was 19.1 months (95% CI: 11.0-27.1) in the sufficiency group, 12.0 months (95% CI: 8.8-15.1) in the insufficiency group, and 7.1 months (95% CI: 4.6-9.5) in the deficiency group (Figure 2). Additional sensitivity analyses stratified by tumor type

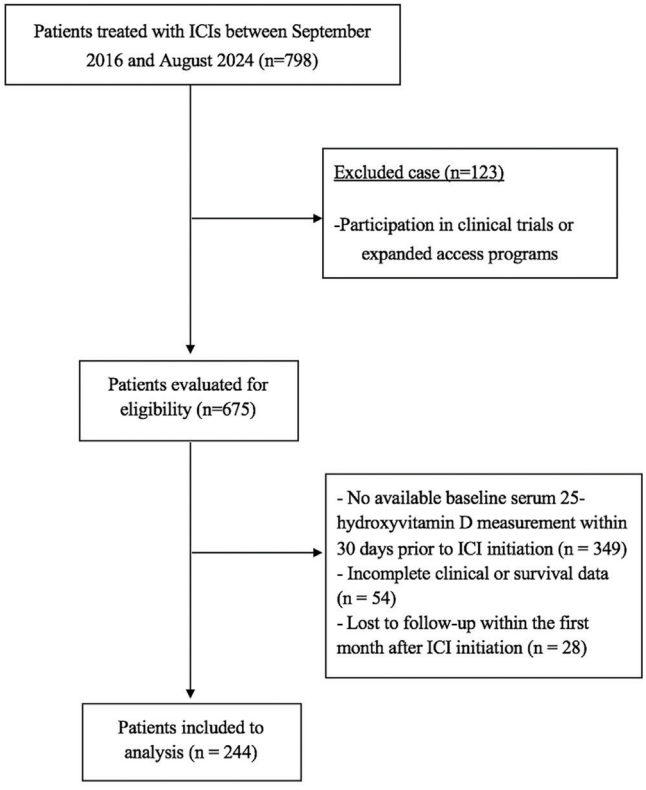

FIGURE 1: Flow diagram of patient selection process.
ICI: Immune checkpoint inhibitor

TABLE 1: Baseline patient characteristics of study cohort (n=244).

Clinical feature	n, (%)
Age at ICI treatment, median (IQR)	63 (55-69)
Sex	
Female	85 (34.8)
Male	159 (65.2)
ECOG PS	
0	109 (44.7)
1	80 (32.8)
2	39 (16.0)
3	16 (6.6)
Primary tumor	
NSCLC	80 (32.8)
RCC	46 (18.9)
Melanoma	35 (14.3)
HNC	22 (9)
SCLC	6 (2.5)
HCC	6 (2.5)
Urothelial cancer	6 (2.5)
Sarcoma	5 (2)
Others	38 (15.6)
Treatment line	
1	45 (18.4)
2	99 (40.6)
3	55 (22.5)
4 or later	45 (18.4)
Type of ICI	
Nivolumab	196 (80.3)
Nivolumab-Ipilimumab	8 (3.3)
Pembrolizumab	18 (7.4)
Atezolizumab	21 (8.6)
Avelumab	1 (0.4)
Liver metastases	
Absent	183 (75)
Present	61 (25)
Lung metastases	
Absent	105 (43)
Present	139 (57)
25-hydroxyvitamin D level	
Vitamin D sufficiency (>20 ng/mL)	89 (36.5)
Vitamin D insufficiency (12-20 ng/mL)	85 (34.8)
Vitamin D deficiency (<12 ng/mL)	70 (28.7)

ECOG PS: Eastern Cooperative Oncology Group performance status; HNC: Head and neck cancer; ICI: Immune checkpoint inhibitor; RCC: Renal cell carcinoma; NSCLC: Non-small cell lung cancer; SCLC: Small cell lung cancer; HCC: Hepatocellular carcinoma; IQR: Interquartile range.

TABLE 2: Comparison of baseline characteristics according to vitamin D status (n=244).

Characteristics	Vitamin D sufficiency (n=89)	Vitamin D insufficiency (n=85)	Vitamin D deficiency (n=70)	p-value
Age				0.687
<65 years	49 (55.1)	52 (61.2)	42 (60)	
≥65 years	40 (44.9)	33 (38.8)	28 (40)	
Sex, n (%)				0.776
Male	57 (64)	54 (63.5)	48 (68.6)	
Female	32 (36)	31 (36.5)	22 (31.4)	
ECOG PS, n (%)				0.115
0-1	68 (81.9)	62 (77.5)	46 (67.6)	
2-3	15 (18.1)	18 (22.5)	22 (32.4)	
Primary tumor, n (%)				0.759
NSCLC	26 (29.2)	29 (34.1)	25 (35.7)	
RCC	17 (19.1)	19 (22.4)	10 (14.3)	
Melanoma	12 (13.5)	12 (14.1)	11 (15.7)	
HNC	6 (6.7)	9 (10.6)	7 (10)	
SCLC	2 (2.2)	1 (1.2)	3 (4.3)	
HCC	4 (4.5)	0 (0)	2 (2.9)	
Urothelial cancer	3 (3.4)	1 (1.2)	2 (2.9)	
Sarcoma	1 (1.1)	2 (2.4)	2 (2.9)	
Others	18 (20.2)	12 (14.1)	8 (11.4)	
Treatment line, n (%)				0.779
1-2	50 (56.2)	51 (60)	43 (61.4)	
3 or later	39 (43.8)	34 (40)	27 (38.6)	
Liver metastases				0.520
Absent	65 (73)	62 (72.9)	56 (80)	
Present	24 (27)	23 (27.1)	14 (20)	
Lung metastases				0.761
Absent	39 (43.8)	34 (40)	32 (45.7)	
Present	50 (56.2)	51 (60)	38 (54.3)	

ECOG: Eastern Cooperative Oncology Group performance status; HNC: Head and neck cancer; RCC: Renal cell carcinoma; NSCLC: Non-small cell lung cancer; SCLC: Small cell lung cancer; HCC: Hepatocellular carcinoma.

demonstrated that vitamin D deficiency (HR: 2.23, 95% CI: 1.53-3.24) remained independently associated with shorter OS.

For progression-free survival (PFS), univariable analysis showed that ECOG PS ≥2 (HR: 1.504, 95% CI: 1.095-2.065, p=0.012) and lower vitamin D levels were associated with inferior outcomes. Compared with vitamin D sufficiency, insufficiency was associated with an HR of 1.610 (95% CI: 1.159-2.235; p=0.004), and deficiency was associated with an HR of 2.178 (95% CI: 1.549-3.064; p<0.001). In the multivariable analysis, both vitamin D insufficiency (HR: 1.494, 95% CI: 1.067-2.092; p=0.019) and vitamin D deficiency (HR: 2.0, 95% CI: 1.411-2.833; p<0.001) remained independent predictors of shorter PFS (Table 4). Median PFS was 10.4 months (95% CI: 7.0-13.7) for the vitamin D sufficiency group, 5.5 months (95% CI: 4.1-6.9) for the vitamin D insufficiency group, and 3.5 months (95% CI: 2.0-4.9) for the vitamin D deficiency group (Figure 3). Additional sensitivity analyses stratified by tumor type demonstrated that both vitamin D insufficiency (HR: 1.56, 95% CI: 1.11-2.19) and vitamin D deficiency (HR: 2.06, 95% CI: 1.45-2.92) remained independently associated with shorter PFS.

TABLE 3: Univariable and multivariable analyses for OS.						
	Univariable			Multivariable		
Variable	HR	95% CI	p	HR	95% CI	p
Age (≥65 vs. <65)	0.999	0.738-1.351	0.994			
Sex (male vs. female)	1.107	0.808-1.515	0.527			
ECOG status (≥2 vs. <2)	1.670	1.178-2.369	0.004	1.570	1.101-2.238	0.013
Liver metastases at baseline (yes vs. no)	1.231	0.885-1.714	0.217			
Lung metastases at baseline (yes vs. no)	1.319	0.975-1.785	0.072	1.292	0.944-1.770	0.110
ICI treatment line (1-2 vs. 3 or later)	1.010	0.750-1.360	0.948			
ICI agent (nivolumab vs. others)	1.297	0.914-1.841	0.146			
Tumor type	1.099	0.975-1.261	0.182			
Vitamin D status (vitamin D sufficiency)	Ref			Ref		
Vitamin D insufficiency	1.462	1.012-2.113	0.043	1.380	0.944-2.017	0.096
Vitamin D deficiency	2.315	1.606-3.337	<0.001	2.264	1.553-3.300	<0.001
ECOG: Eastern Cooperative Oncology Group; ICI: Immune checkpoint inhibitör; OS: Overall survival; HR: Hazard ratio; CI: Confidence interval.						

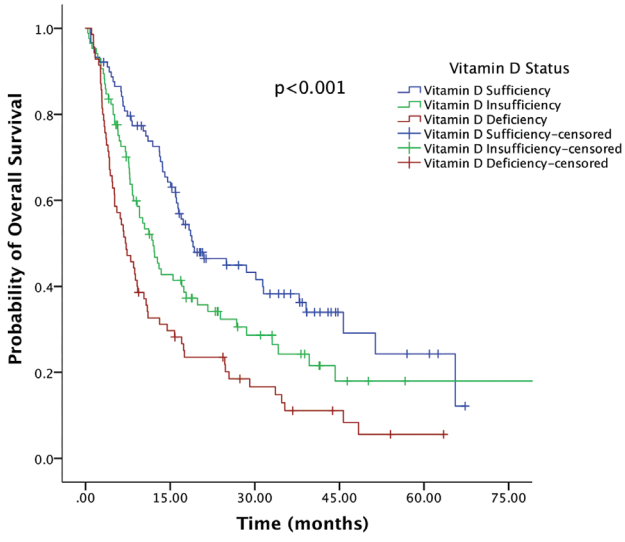

FIGURE 2: Overall survival of patients according to vitamin D status.

TABLE 4: Univariable and multivariable analyses for PFS.						
	Univariable			Multivariable		
Variable	HR	95% CI	p	HR	95% CI	p
Age (≥65 vs. <65)	0.984	0.748-1.293	0.906			
Sex (male vs. female)	0.979	0.739-1.296	0.880			
ECOG status (≥2 vs. <2)	1.504	1.095-2.065	0.012	1.432	1.042-1.968	0.027
Liver metastases at baseline (yes vs. no)	1.260	0.931-1.705	0.134			
Lung metastases at baseline (yes vs. no)	1.250	0.951-1.644	0.110			
ICI agent (nivolumab vs. others)	1.119	0.800-1.566	0.510			
Tumor type	1.060	0.934-1.202	0.368			
ICI treatment line (1-2 vs. 3 or later)	1.143	0.872-1.499	0.334			
Vitamin D status (vitamin D sufficiency)	Ref			Ref		
Vitamin D insufficiency	1.610	1.159-2.235	0.004	1.494	1.067-2.092	0.019
Vitamin D deficiency	2.178	1.549-3.064	<0.001	2.000	1.411-2.833	<0.001
ECOG PS: Eastern Cooperative Oncology Group; ICI: Immune checkpoint inhibitör; PFS: Progression-free survival; HR: Hazard ratio; CI: Confidence interval.						

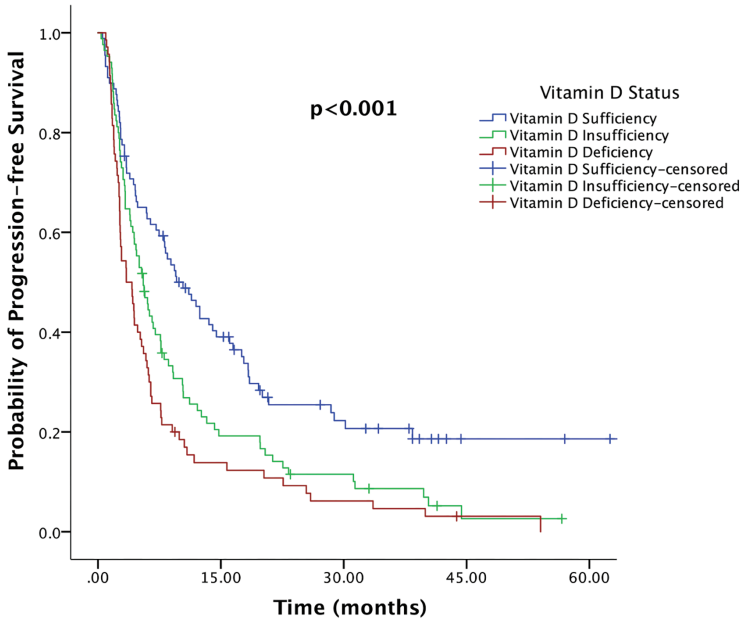

FIGURE 3: Progression-free survival of patients according to vitamin D status.

DISCUSSION

In this study, we observed that baseline serum vitamin D deficiency was independently associated with shorter PFS and OS in patients with advanced malignancies receiving ICIs. These results indicate that profound vitamin D deficiency may represent a clinically relevant biomarker of poor clinical outcomes in the immunotherapy setting, potentially reflecting impaired antitumor immunity and host nutritional-inflammatory status.

The prevalence of vitamin D deficiency varies across cancer populations but remains consistently high. In a prospective cohort of 77 patients with advanced NSCLC receiving ICIs, You et al.[18] reported vitamin D sufficiency (>20 ng/mL) in only 33.8% of patients, insufficiency (10-20 ng/mL) in 55.9%, and deficiency (<10 ng/mL) in 10.4%. In a recent cohort of 120 prostate cancer patients in a sun-rich climate, Hasan et al.[19] reported a median serum vitamin D level at diagnosis of 35.4 ng/mL (range: 7.8 to 120 ng/mL); vitamin D deficiency, defined as less than 20 ng/mL, was present in 12.5% of patients. In a cohort largely comprising patients with advanced disease and multiple prior lines of therapy, the observed prevalence of vitamin D deficiency (<12 ng/mL) was 28.7%. This exceeds rates reported in previous studies, implying that vitamin D deficiency may be especially common in heavily pretreated, advanced-stage patient groups and may hold prognostic importance.

Numerous investigations have focused on vitamin D's potential anticancer effects. Lower serum 25(OH)D is associated with higher incidence and mortality from lung cancer, according to two meta-analyses.[20,21] In another study, which included 4038 patients with 11 different malignancies and a median follow-up of 15.6 years, higher prediagnostic serum 25(OH)D concentrations were associated with improved OS (HR: 0.83, 95% CI: 0.70-0.98 for highest vs lowest quintile) and lung cancer-specific survival (HR: 0.63, 95% CI: 0.44-0.90).[22] However, evidence on the prognostic role of vitamin D in the immunotherapy era is limited. In advanced melanoma, Galus et al.[23] reported that patients who maintained normal vitamin D levels, either at baseline or through effective supplementation during anti-PD-1 therapy, achieved significantly higher objective response rates (56% vs. 36.2%, p=0.0111) and longer median PFS (11.25 vs. 5.75 months, p=0.0378) compared with those with persistently reduced levels, although no statistically significant difference in OS was observed (31.5 vs. 27 months, p=0.39). In a prospective NSCLC cohort, higher baseline 25(OH)D levels were associated with improved OS; the vitamin D-sufficient group demonstrated a significant benefit compared with the insufficient and deficient groups (HR: 0.45, 95% CI: 0.25-0.81). Median PFS was longer in vitamin D-sufficient patients (606 days vs. 326 and 308 days), although these differences were not statistically significant (p=0.12). Perhaps most compellingly, a large multi-center analysis of over 3,000 ICI-treated patients (across various tumor types) found that baseline vitamin D deficiency was independently associated with significantly shorter OS (HR: 2.06, 95% CI: 1.21-3.52), whereas pre-treatment vitamin D supplementation was

associated with improved survival outcomes (HR: 0.69, 95% CI: 0.52-0.92), regardless of the season of ICI initiation.[24] Our results are consistent with emerging evidence showing that baseline vitamin D deficiency independently predicted poorer OS, while both insufficient and deficient vitamin D levels predicted shorter PFS. Collectively, these findings suggest the potential prognostic value of baseline vitamin D status in patients receiving ICIs, highlighting that either insufficient or deficient levels may adversely affect survival outcomes.

The biological mechanisms underlying this association are an active area of research. Vitamin D inhibits tumor growth primarily by inducing cell-cycle arrest via upregulation of the CDK inhibitors p21 and p27 and downregulation of cyclins.[25] Vitamin D also promotes apoptosis by increasing pro-apoptotic BAX and decreasing anti-apoptotic BCL2 and BCLXL, suppresses angiogenesis by reducing vascular endothelial growth factor and other pro-angiogenic factors, and mitigates DNA damage by enhancing DNA repair.[26,27] Vitamin D also serves as a key immunomodulator in the antitumor immune response, enhancing the cytotoxic activity of macrophages, neutrophils, and NK cells, as well as modulating cytokine secretion to create a tumor-suppressive immune microenvironment. Vitamin D can also influence the gut microbiome, particularly the abundance and metabolic activity of Bacteroides fragilis, which have been linked to improved responses to ICIs.[14] The vitamin D receptor (VDR), expressed on most immune cells, regulates transcription of numerous target genes; a low VDR-related gene signature (vitamin D-VDR sign) has been associated with worse outcomes in multiple cancers.[28,29] Furthermore, vitamin D levels correlate with immune checkpoint regulation, as serum levels have been linked to PD-1 expression on $CD8^+$ T-cells in NSCLC, suggesting a potential mechanistic basis for its interaction with immunotherapy.[30]

Study Limitations

Despite the intriguing findings, our study has several important limitations. First, the retrospective and single-institution nature of our study may introduce selection biases and unmeasured confounding variables. Second, we used only one baseline measurement of 25(OH)D taken prior to ICI initiation, without serial monitoring. Vitamin D levels can fluctuate with seasonal exposure, supplementation, and acute-phase reactions; therefore, a single measurement may not reflect the patient's vitamin D status throughout therapy. Moreover, information regarding vitamin D supplementation during follow-up, including dose, duration, and adherence, was not systematically available and could not be analyzed. We also did not record the number of vitamin D-deficient patients who subsequently received vitamin D supplementation, which could have partially mitigated the deficiency during follow-up. Finally, we did not collect detailed data on other potential confounders, such as nutritional intake, body mass index, sarcopenia, systemic inflammation, and malnutrition, or on concurrent medications that could influence vitamin D levels. Furthermore, established predictive biomarkers for immunotherapy efficacy, such as PD-L1 expression, tumor mutational burden, and MSI status, were not routinely available and could not be incorporated into the analyses. Given these limitations, our findings should be considered hypothesis-generating and require additional validation in larger, prospective studies.

CONCLUSION

In conclusion, our study results suggest that baseline serum Vitamin D level may serve as a prognostic marker in ICI-treated patients. Given its potential influence on immune function and treatment outcomes, integrating vitamin D assessment into pretreatment evaluation may facilitate risk stratification and inform supportive care strategies. We think that the prognostic value of baseline serum Vitamin D levels as a candidate prognostic biomarker should be evaluated in prospective clinical studies.

Ethics

Ethics Committee Approval: The authors state that they have obtained Hacettepe University Health Sciences Research Ethics Committee approval (date: 26.08.2025, approval number: SBA 25/743).

Informed Consent: Retrospective study.

Footnotes

Authorship Contributions

Concept: T.K.Ş., S.A., B.Y.A., D.C.G., Design: T.K.Ş., D.C.G., Data Collection or Processing: T.K.Ş., O.B., G.K., N.G., F.Ş., S.A., Z.A., N.K., Ö.D., M.E., Ş.Y., S.A., B.Y.A., D.C.G., Analysis or Interpretation: T.K.Ş., B.Y.A., D.C.G., Literature Search: O.B., G.K., N.G., F.Ş., Writing: T.K.Ş., S.A., Z.A., N.K., Ö.D., M.E., Ş.Y., S.A., B.Y.A., D.C.G.

Conflict of Interest: Sercan Aksoy MD is editor-in-chief and Deniz Can Güven MD is section editor in Journal of Oncological Sciences. They had no involvement in the peer-review of this article and had no access to information regarding its peer-review.

Financial Disclosure: The authors declared that this study received no financial support.

REFERENCES

1. Shen KY, Zhu Y, Xie SZ, Qin LX. Immunosuppressive tumor microenvironment and immunotherapy of hepatocellular carcinoma: current status and prospectives. J Hematol Oncol. 2024;17(1):25. [Crossref] [PubMed] [PMC]
2. Almawash S. Revolutionary cancer therapy for personalization and improved efficacy: strategies to overcome resistance to immune checkpoint inhibitor therapy. Cancers (Basel). 2025;17(5):880. [Crossref] [PubMed] [PMC]

3. Shiravand Y, Khodadadi F, Kashani SMA, et al. Immune checkpoint inhibitors in cancer therapy. Curr Oncol. 2022;29(5):3044-3060. [Crossref] [PubMed] [PMC]
4. Tan S, Day D, Nicholls SJ, Segelov E. Immune checkpoint inhibitor therapy in oncology: current uses and future directions: JACC: CardioOncology state-of-the-art review. JACC CardioOncol. 2022;4(5):579-597. [Crossref] [PubMed] [PMC]
5. Zhang D, Zhao J, Zhang Y, Jiang H, Liu D. Revisiting immune checkpoint inhibitors: new strategies to enhance efficacy and reduce toxicity. Front Immunol. 2024;15:1490129. [Crossref] [PubMed] [PMC]
6. Jayathilaka B, Mian F, Franchini F, Au-Yeung G, IJzerman M. Cancer and treatment specific incidence rates of immune-related adverse events induced by immune checkpoint inhibitors: a systematic review. Br J Cancer. 2025;132(1):51-57. Erratum in: Br J Cancer. 2025;132(1):137. [Crossref] [PubMed] [PMC]
7. Yamaguchi H, Hsu JM, Sun L, Wang SC, Hung MC. Advances and prospects of biomarkers for immune checkpoint inhibitors. Cell Rep Med. 2024;5(7):101621. [Crossref] [PubMed] [PMC]
8. Muñoz A, Grant WB. Vitamin D and cancer: an historical overview of the epidemiology and mechanisms. Nutrients. 2022;14(7):1448. [Crossref] [PubMed] [PMC]
9. Veeresh PKM, Basavaraju CG, Dallavalasa S, et al. Vitamin D3 inhibits the viability of breast cancer cells in vitro and ehrlich ascites carcinomas in mice by promoting apoptosis and cell cycle arrest and by impeding tumor angiogenesis. Cancers (Basel). 2023;15(19):4833. [Crossref] [PubMed] [PMC]
10. Sherman MH, Yu RT, Engle DD, et al. Vitamin D receptor-mediated stromal reprogramming suppresses pancreatitis and enhances pancreatic cancer therapy. Cell. 2014;159(1):80-93. [Crossref] [PubMed] [PMC]
11. Kongsbak M, von Essen MR, Levring TB, et al. Vitamin D-binding protein controls T cell responses to vitamin D. BMC Immunol. 2014;15:35. [Crossref] [PubMed] [PMC]
12. Vanherwegen AS, Gysemans C, Mathieu C. Vitamin D endocrinology on the cross-road between immunity and metabolism. Mol Cell Endocrinol. 2017;453:52-67. [Crossref] [PubMed]
13. Stucci LS, D'Oronzo S, Tucci M, et al; Italian Melanoma Intergroup (IMI). Vitamin D in melanoma: controversies and potential role in combination with immune check-point inhibitors. Cancer Treat Rev. 2018;69:21-28. [Crossref] [PubMed]
14. Giampazolias E, Pereira da Costa M, Lam KC, et al. Vitamin D regulates microbiome-dependent cancer immunity. Science. 2024;384(6694):428-437. [Crossref] [PubMed] [PMC]
15. Gambichler T, Brown V, Steuke AK, Schmitz L, Stockfleth E, Susok L. Baseline laboratory parameters predicting clinical outcome in melanoma patients treated with ipilimumab: a single-centre analysis. J Eur Acad Dermatol Venereol. 2018;32(6):972-977. [Crossref] [PubMed]
16. Jiménez-Cortegana C, Sánchez-Martínez PM, Palazón-Carrión N, et al. Lower survival and increased circulating suppressor cells in patients with relapsed/refractory diffuse large B-cell lymphoma with deficit of vitamin D levels using R-GDP plus lenalidomide (R2-GDP): results from the R2-GDP-GOTEL trial. Cancers (Basel). 2021;13(18):4622. [Crossref]
17. Munns CF, Shaw N, Kiely M, et al. Global consensus recommendations on prevention and management of nutritional rickets. J Clin Endocrinol Metab. 2016;101(2):394-415. [Crossref] [PubMed] [PMC]
18. You W, Liu X, Tang H, et al. Vitamin D status is associated with immune checkpoint inhibitor efficacy and immune-related adverse event severity in lung cancer patients: a prospective cohort study. J Immunother. 2023;46(6):236-243. [Crossref] [PubMed]
19. Hasan N, Rafizadeh D, Gibson S, et al. Vitamin D deficiency in prostate cancer: prevalence in a sun-rich climate and influence of androgen deprivation therapy. World J Clin Oncol. 2025;16(6):108113. [Crossref] [PubMed] [PMC]
20. Feng Q, Zhang H, Dong Z, Zhou Y, Ma J. Circulating 25-hydroxyvitamin D and lung cancer risk and survival: a dose-response meta-analysis of prospective cohort studies. Medicine (Baltimore). 2017;96(45):e8613. [Crossref] [PubMed] [PMC]
21. Liu J, Dong Y, Lu C, et al. Meta-analysis of the correlation between vitamin D and lung cancer risk and outcomes. Oncotarget. 2017;8(46):81040-81051. [Crossref]
22. Weinstein SJ, Mondul AM, Layne TM, et al. Prediagnostic serum vitamin D, Vitamin D binding protein isoforms, and cancer survival. JNCI Cancer Spectr. 2022;6(2):pkac019. [Crossref] [PubMed] [PMC]
23. Galus Ł, Michalak M, Lorenz M, et al. Vitamin D supplementation increases objective response rate and prolongs progression-free time in patients with advanced melanoma undergoing anti-PD-1 therapy. Cancer. 2023;129(13):2047-2055. [Crossref] [PubMed]
24. Kennedy O, Ali N, Lee R, et al. Seasonal patterns in immunotherapy outcomes. J Clin Oncol. 2024;42(16_suppl):e14684-e14684. [Crossref]
25. Kawa S, Nikaido T, Aoki Y, et al. Vitamin D analogues up-regulate p21 and p27 during growth inhibition of pancreatic cancer cell lines. Br J Cancer. 1997;76(7):884-889. [Crossref] [PubMed] [PMC]
26. Kizildag S, Ates H, Kizildag S. Treatment of K562 cells with 1,25-dihydroxyvitamin D3 induces distinct alterations in the expression of apoptosis-related genes BCL2, BAX, BCLXL, and p21. Ann Hematol. 2010;89(1):1-7. [Crossref] [PubMed]
27. Jeon SM, Shin EA. Exploring vitamin D metabolism and function in cancer. Exp Mol Med. 2018;50(4):1-14. [Crossref] [PubMed] [PMC]
28. Anderson LN, Cotterchio M, Cole DE, Knight JA. Vitamin D-related genetic variants, interactions with vitamin D exposure, and breast cancer risk among Caucasian women in Ontario. Cancer Epidemiol Biomarkers Prev. 2011;20(8):1708-1717. Erratum in: Cancer Epidemiol Biomarkers Prev. 2014;23(7):1440-1442. [Crossref] [PubMed]
29. Slominski AT, Brożyna AA, Zmijewski MA, et al. Vitamin D signaling and melanoma: role of vitamin D and its receptors in melanoma progression and management. Lab Invest. 2017;97(6):706-724. [Crossref] [PubMed] [PMC]
30. Li P, Zhu X, Cao G, et al. 1α,25(OH)2D3 reverses exhaustion and enhances antitumor immunity of human cytotoxic T cells. J Immunother Cancer. 2022;10(3):e003477. [Crossref] [PubMed] [PMC]

ORIGINAL ARTICLE

DOI: 10.37047/jos.galenos.2026.2025-11-8

J Oncol Sci 2026;12(1):9-17

Survival Patterns in Early-onset Colorectal Cancer Receiving Adjuvant Capecitabine Based Therapy

Oğuzcan ÖZKAN[1], Aslı GEÇGEL[1], Zeynep Sıla GÖKDERE[1], Barış EMEKDAŞ[2], Hasan Çağrı YILDIRIM[1]

[1]Ege University Faculty of Medicine, Department of Medical Oncology, İzmir, Türkiye
[2]Ege University Faculty of Medicine, Department of Gastroenterology, İzmir, Türkiye

ABSTRACT

Objective: The incidence of early-onset colorectal cancer (EOCRC) is increasing worldwide, yet optimal adjuvant treatment strategies remain unclear. This study evaluated survival outcomes and prognostic factors in EOCRC patients treated with adjuvant capecitabine-based chemotherapy.

Material and Methods: This retrospective study included 51 patients aged younger than 50 years with high-risk stage II or stage III colorectal cancer who underwent curative surgery followed by capecitabine-based adjuvant therapy between 2017 and 2021. Overall survival (OS) and recurrence-free survival (RFS) were analyzed using Kaplan-Meier curves and Cox regression models.

Results: The median follow-up was 32 months. Stage III patients had significantly poorer OS and RFS than those of Stage II patients ($p<0.05$). In multivariate analysis, recurrence was the only independent predictor of OS [hazard ratio (HR)=12.45, p=0.002]. For RFS, nodal status remained an independent prognostic factor (HR=0.032, p=0.006). Among stage II patients, the XELOX regimen was associated with a significantly different recurrence risk compared to capecitabine monotherapy (HR=14.87, p=0.038).

Conclusion: In EOCRC, stage and nodal status are key prognostic determinants. Adjuvant therapy should be tailored to pathological risk rather than age alone, as XELOX may offer a recurrence benefit in selected stage II patients, whereas routine treatment intensification risks avoidable toxicity.

Keywords: Carly-onset colorectal cancer; adjuvant chemotherapy; capecitabine; survival analysis; prognostic factors; recurrence-free survival

INTRODUCTION

Colorectal cancer (CRC) is still a serious worldwide health issue, and in recent years a noticeable rise has been observed particularly among individuals younger than 50, a group classified as early-onset colorectal cancer (EOCRC).[1-4] Unlike late-onset CRC, EOCRC often presents with more advanced disease, distinct molecular profiles, and delays in diagnosis, as routine screening is not recommended for average-risk individuals younger than 50 years.[5-7]

While inherited conditions, such as Lynch syndrome and familial adenomatous polyposis, account for a subset of cases, most EOCRCs occur sporadically and are associated with lifestyle and metabolic factors, including obesity, diet, physical inactivity, and alterations in the gut microbiome.[8-11]

For individuals with high-risk stage II or stage III CRC, the recommended standard treatment involves adjuvant chemotherapy (ACT) based on fluoropyrimidines.[12,13] Younger patients are more frequently treated with multi-agent regimens such as capecitabine plus oxaliplatin (XELOX) and often receive higher cumulative doses and more intensive therapy than older patients.[13,14] However, evidence regarding the survival benefit of aggressive adjuvant therapy in EOCRC remains inconsistent. Several studies suggest that younger age is associated with higher recurrence rates, which may reflect more aggressive tumor biology, yet the benefit of intensified adjuvant therapy in low-risk stage II disease is unclear, and intensified adjuvant therapy may increase the risk of long-term treatment-related toxicity.[15-17]

Correspondence: Oğuzcan ÖZKAN MD,
Ege University Faculty of Medicine, Department of Medical Oncology, İzmir, Türkiye
E-mail: droguzcanozkan@yahoo.com
ORCID ID: orcid.org/0000-0002-4075-7775

Received: 24.11.2025 **Accepted:** 07.01.2026 **Epub:** 22.01.2026 **Publication Date:** 18.03.2026

Cite this article as: Özkan O, Geçgel A, Gökdere ZS, Emekdaş B, Yıldırım HÇ. Survival patterns in early-onset colorectal cancer receiving adjuvant capecitabine based therapy. J Oncol Sci. 2026;12(1):9-17

Available at journalofoncology.org

Given the rising incidence of EOCRC and ongoing uncertainty regarding optimal adjuvant treatment strategies, evaluating real-world treatment patterns and survival outcomes in this population is of clinical importance. This study aimed to investigate overall survival (OS), recurrence-free survival (RFS) and prognostic factors among patients with EOCRC who received capecitabine-based ACT following curative resection.

MATERIAL AND METHODS

Study Design and Patient Selection

Patients with high-risk stage II or stage III CRC who underwent curative surgical resection and received adjuvant capecitabine-based chemotherapy at our institution between January 2017 and December 2021 were included in this retrospective cohort analysis. Of the 190 eligible patients, 51 (26.8%) were younger than 50 years and were categorized as EOCRC. Patients were excluded if they (i) received adjuvant 5-fluorouracil-based regimens instead of capecitabine, (ii) had insufficient clinical or pathological data, or (iii) had evidence of metastatic disease at diagnosis. Clinical, pathological, and treatment-related data were obtained from electronic medical records.

Follow-up and Outcome Measures

The follow-up period was measured starting from the date of surgery. RFS was defined as the interval from surgery to the first documented radiologic or clinical recurrence, whereas OS was defined as the interval from surgery to death from any cause. Patients who did not experience an event were censored at their most recent follow-up, which extended through September 2025.

The authors state that they have obtained Ege University Medical Research Ethics Committee approval (date: 06.11.2025, approval number: 25-11T/76).

Statistical Analysis

Patient characteristics were summarized using descriptive statistics. Kaplan-Meier (KM) curves and log-rank tests were used for survival analysis, while Cox regression (CRA) was used to identify prognostic markers. Analyses were performed using SPSS v22; $p<0.05$ was considered statistically significant.

RESULTS

A total of 190 patients were screened, of whom 51 (26.8%) were identified as having EOCRC, defined as a diagnosis before the age of 50. The mean age at diagnosis in this cohort was 40.3±7.8 years, and the median age was 44 years [interquartile range (IQR) 35.5-46.0]. Of the included patients, 34 (66.7%) were male and 17 (33.3%) were female.

Regarding disease stage, 26 patients (51.0%) had stage II disease and 25 (49.0%) had stage III disease. Most tumors were classified as pT3-T4 at diagnosis, and nodal status was predominantly N0-N1. The median follow-up duration was 32 months (IQR, 24-45 months). Detailed clinicopathological characteristics of the study population are presented in Table 1.

A significant difference in gender distribution was observed between stage II and stage III patients ($p=0.022$); males were more common in stage III. The XELOX regimen was also used more frequently in stage III patients ($p=0.006$). No significant differences were found between the groups regarding pT stage, nodal status, histological grade, lymphovascular invasion (LVI), perineural invasion (PNI), microsatellite instability (MSI), mucinous component, or tumor localization ($p>0.05$ for all). Comparative clinicopathological data of patients with stage II and stage III disease are presented in Supplementary Table 1.

No significant association was observed between age at diagnosis and disease stage ($p=0.492$). In contrast, multiple clinicopathological variables, including sex, primary tumor (pT) stage, nodal status, tumor budding, tumor-infiltrating lymphocytes (TIL), histological grade, LVI, PNI, MSI status, mucinous histology, and human epidermal growth factor receptor 2 expression, showed significant associations with disease stage. In addition, recurrence status, number of metastatic sites, peritoneal involvement, baseline carcinoembryonic antigen (CEA) and carbohydrate antigen 19-9 levels, and adjuvant treatment regimen and duration were significantly associated with stage at diagnosis. These associations, evaluated using the chi-square test, are summarized in Table 2.

In the KM analysis, median OS was not reached for stage II patients, whereas it was 80.6 months for stage III patients. The difference in OS between the two groups was statistically significant (log-rank $p<0.05$). The estimated 2- and 5-year OS rates were 95% and 88%, respectively, in the stage II group, compared with 82% and 65% in the stage III group. KM OS curves by stage at diagnosis in patients with EOCRC receiving adjuvant capecitabine-based therapy are shown in Figure 1.

The median RFS was 95.2 months [95% confidence interval (CI): 85.8-104.5] in stage II patients and 70.4 months (95% CI: 51.2-89.7) in those with stage III disease. This difference was statistically significant (log-rank $p=0.005$), indicating that stage at diagnosis is an important prognostic factor for RFS. Based on KM estimates, the 2- and 5-year RFS rates were 92.0% and 82.5% for stage II patients and 83.8% and 63.4% for stage III patients, respectively. These findings demonstrate significantly better short- and long-term recurrence outcomes among patients with stage II disease. KM RFS curves stratified by stage at diagnosis in patients with

TABLE 1: Demographic and clinicopathological characteristics of patients at diagnosis.			
Variable	**Category**	**n**	**%**
Sex	Male	34	64.2%
	Female	17	32.1%
Stage at diagnosis	Stage II	26	49.1%
	Stage III	25	47.2%
pT	1	1	3.6%
	2	1	3.6%
	3	33	60.0%
	4	15	27.3%
pN	0	26	49.1%
	1	18	34.0%
	2	7	13.2%
Tumor budding	No	38	74.5%
	Yes	13	24.5%
TIL	No	41	80.3%
	Yes	3	19.7%
Positive surgical margin	No	50	98.1%
	Yes	1	1.9%
Grade	2	31	60.8%
	3	13	25.5%
	1	4	7.8%
LVI	0	31	63.3%
	1	16	32.7%
PNI	0	32	65.3%
	1	15	30.6%
MSI	Low	18	54.5%
	High	13	39.4%
Mucinous component	No	44	83.0%
	Yes	7	13.2%
Localization	Left	20	36.4%
	Rectum	14	25.5%
	Right	12	21.8%
	Multifocal	5	9.1%
Local therapies	No	42	79.2%
	Yes	9	17.0%
Recurrence	No	39	76.5%
	Yes	12	23.5%
Peritoneal carcinomatosis	No	48	90.6%
	Yes	3	5.7%
Baseline CEA	<5	41	77.4%
	>5	10	18.9%
Baseline CA19-9	<27	45	84.9%
	>27	6	11.3%

LVI: Lymphovascular invasion; PNI: Perineural invasion; MSI: Microsatellite instability; TIL: Tumor-infiltrating lymphocytes; CEA: Carcinoembryonic antigen; CA19-9: Carbohydrate antigen 19-9.

TABLE 2: Association between stage at diagnosis and clinicopathological variables.

Variable	P-value
Age	0.492
Sex	<0.001
pT	<0.001
N0	<0.001
Budding	<0.001
TIL	<0.001
Surgical margin	<0.001
Grade	<0.001
LVI	<0.001
PNI	<0.001
MSI	<0.001
Mucinous component	<0.001
HER2	<0.001
Localization	<0.001
Adjuvant therapy regimen	<0.001
Adjuvant therapy duration	<0.001
Recurrence (Yes/No)	0.007
Metastatic site number	0.028
Peritoneal carcinomatosis	<0.001
Baseline CEA	<0.001
Baseline CA19-9	<0.001
Local therapies	<0.001

Comparisons were performed using the chi-square test. LVI: Lymphovascular invasion; PNI: Perineural invasion; MSI: Microsatellite instability; CEA: Carcinoembryonic antigen; CA19-9: Carbohydrate antigen 19-9. P<0.05 was considered statistically significant.

EOCRC receiving adjuvant capecitabine-based therapy are presented in Figure 2.

In the univariate (UV) CRA for RFS, nodal status and baseline CEA levels emerged as significant prognostic factors. Patients with node-negative disease (N0) had a significantly lower recurrence risk [hazard ratio (HR)=0.076, 95% CI: 0.015-0.393; p=0.002], whereas elevated baseline CEA was associated with an increased recurrence risk (HR=5.192, 95% CI: 1.727-15.606; p=0.003). Higher pT stage (p=0.073) and node-positive disease (N+, p=0.087) showed borderline associations. Other clinicopathological variables, including age, sex, tumor grade, tumor budding, TIL, LVI, PNI, MSI status, mucinous histology, adjuvant regimen, and use of local therapies, were not significantly associated with RFS.

Variables with p<0.10 in the UV analysis (pT stage, nodal status, and baseline CEA), along with clinically relevant factors from the literature (MSI and LVI), were included in the multivariate (MV) model. In MV analysis, nodal status remained the only independent prognostic factor for RFS, with N0 status retaining its protective effect (HR=0.032; 95% CI, 0.003-0.371; p=0.006). Elevated baseline CEA (HR=4.418, 95% CI: 0.824-23.684, p=0.083) and MSI-high status (HR=0.193, 95% CI: 0.036-1.036, p=0.055) were of borderline statistical significance. pT stage, disease stage, and adjuvant regimen were not significant predictors in the adjusted model. The UV and MV CRA for RFS are shown in Table 3.

In the UV CRA for OS, the following were identified as significant prognostic factors: stage at diagnosis (HR=5.68, 95% CI: 1.24-26.1, p=0.025), nodal involvement (HR=2.45, 95%

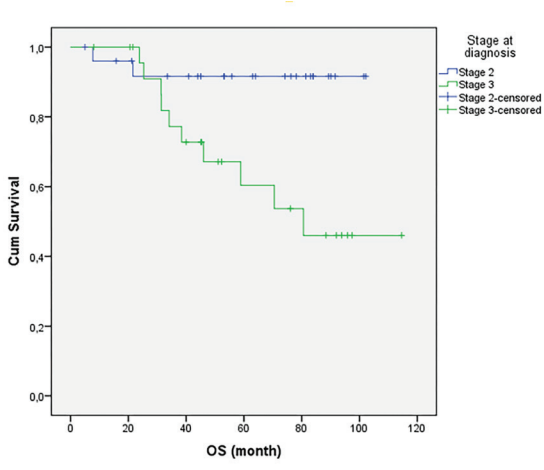

FIGURE 1: Kaplan-Meier OS curves according to stage at diagnosis in patients with EOCRC receiving adjuvant capecitabine-based therapy. Median OS was not reached in stage II patients, whereas it was 80.6 months in stage III patients. The difference between the groups was statistically significant (log-rank test, p<0.05).

EOCRC: Early-onset colorectal cancer; OS: Overall survival

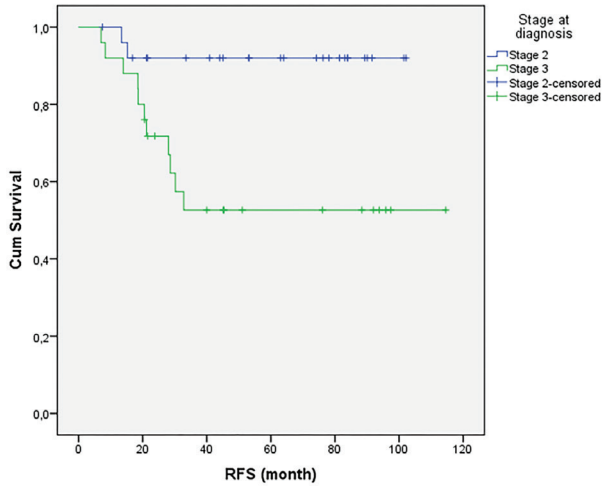

FIGURE 2: Kaplan-Meier RFS curves according to stage at diagnosis in patients with EOCRC receiving adjuvant capecitabine-based therapy. Stage II patients had a significantly longer RFS than stage III patients (median RFS: 95.2 vs. 70.4 months; log-rank p=0.005).

EOCRC: Early-onset colorectal cancer; RFS: Recurrence-free survival

CI: 1.17-5.15, p=0.018), presence of recurrence (HR=14.56, 95% CI: 3.72-57.0, p<0.001), and elevated baseline CEA at the time of metastasis (HR=3.19, 95% CI: 1.01-10.1, p=0.048). Other clinicopathological variables, including pT stage, tumor grade, LVI, PNI, MSI, mucinous histology, tumor localization, duration of adjuvant therapy, and TIL were not significantly associated with OS.

In the MV CRA, only the presence of recurrence remained an independent predictor of poorer OS (HR=12.45; 95% CI: 2.51-61.7; p=0.002). Stage at diagnosis, nodal involvement, and baseline CEA did not retain statistical significance after adjustment. These findings suggest that the limited number of survival events and potential intercorrelations between variables may have reduced the statistical power of the MV model. Table 4 shows the results of UV and MV CRA for the OS prognostic variables in EOCRC patients undergoing adjuvant capecitabine-based treatment.

When RFS was evaluated according to the adjuvant treatment regimen among stage II patients, the median RFS was 65.1 months (95% CI: 49.9-80.3) in the XELOX group and 69.0 months (95% CI: 46.0-91.9) in the capecitabine group, with no statistically significant difference (log-rank p=0.562). KM RFS curves by adjuvant treatment regimen (XELOX vs. capecitabine monotherapy) among patients with stage II EOCRC are shown in Figure 3.

In UV CRA, the type of adjuvant therapy did not show a significant association with RFS. Similarly, pT stage, lymphovascular invasion, tumor budding, mucinous histology, and nodal status were not significant predictors. However, MSI-high status (HR=0.24, 95% CI: 0.05-1.19, p=0.080) and N1 status (HR=0.17, 95% CI: 0.03-1.05, p=0.056) demonstrated borderline associations, suggesting potential prognostic relevance.

In the MV CRA, which included adjuvant therapy type, nodal status, and MSI due to clinical relevance and near-significant UV effects, the model was statistically significant overall (χ^2=11.221, p=0.024). Adjuvant therapy type emerged as an independent prognostic factor for RFS, with patients receiving capecitabine monotherapy having a significantly higher risk of recurrence compared to those receiving XELOX (HR=14.87, 95% CI: 1.16-191.39, p=0.038). Nodal status also retained independent prognostic significance, with N0 disease associated with a reduced recurrence risk (HR=0.065, 95% CI: 0.005-0.782, p=0.031). MSI-high status did not reach statistical significance in the adjusted model. UV and MV CRA of prognostic factors for RFS in stage II EOCRC patients are provided in Table 5.

TABLE 3: Univariate and multivariate Cox regression analyses for RFS.

Variable	Univariate HR (95% CI)	P-value	Multivariate HR (95% CI)	P-value
Age at diagnosis	1.007 (0.937-1.083)	0.843	-	-
Gender	1.116 (0.344-3.628)	0.855	-	-
Stage at diagnosis	0.439 (0.135-1.424)	0.170	1.561 (0.320-7.609)	0.581
pT	2.586 (0.914-7.314)	0.073	0.851 (0.267-2.707)	0.784
Nodal status (overall)	-	0.008	-	0.022
N0	0.076 (0.015-0.393)	0.002	0.032 (0.003-0.371)	0.006
N+	0.353 (0.107-1.162)	0.087	0.363 (0.078-1.691)	0.197
Tumor budding	1.395 (0.604-3.221)	0.435	-	-
TIL	1.259 (0.111-14.251)	0.853	-	-
Grade	0.666 (0.268-1.655)	0.381	-	-
LVI	1.073 (0.351-3.281)	0.902	-	-
PNI	1.266 (0.414-3.871)	0.679	-	-
MSI	0.393 (0.103-1.497)	0.171	0.193 (0.036-1.036)	0.055
Mucinous component	2.450 (0.673-8.916)	0.174	-	-
Localization	- (unstable model)	0.842	-	-
Adjuvant therapy	1.455 (0.476-4.449)	0.511	3.548 (0.704-17.877)	0.125
Local therapies	0.356 (0.050-2.940)	0.356	-	-
Baseline CEA	5.192 (1.727-15.606)	0.003	4.418 (0.824-23.684)	0.083

Variables with p<0.10 in univariate analysis and those considered clinically relevant were included in the multivariate model. HR: Hazard ratio; CI: Confidence interval; LVI: Lymphovascular invasion; PNI: Perineural invasion; MSI: Microsatellite instability; TIL: Tumor-infiltrating lymphocytes; CEA: Carcinoembryonic antigen; RFS: Recurrence-free survival. P<0.05 was considered statistically significant.

TABLE 4: Univariate and multivariate Cox regression analysis of prognostic factors for OS in patients with EOCRC receiving adjuvant capecitabine-based therapy.

Variable	P-value (univariate)	OS HR (univariate)	95% CI (min-max)	P-value (multivariate)	OS HR (multivariate)	95% CI (min-max)
Stage at diagnosis	0.025	5.684	1.242-26.022	0.560	2.123	0.182-24.77
pT	0.813	1.122	0.434-2.903	-	-	-
N0	0.018	2.453	1.164-5.164	0.884	0.898	0.217-3.70
TIL	0.950	1.080	0.096-12.177	-	-	-
Grade	0.672	0.818	0.322-2.075	-	-	-
LVI	0.860	1.109	0.351-3.503	-	-	-
PNI	0.564	1.402	0.445-4.422	-	-	-
MSI	0.123	0.289	0.060-1.396	0.476	0.554	0.121-2.54
Mucinous component	0.282	2.051	0.554-7.593	-	-	-
Localization	0.286	0.555	0.188-1.637	-	-	-
Duration of adjuvant therapy	0.242	2.184	0.591-8.071	-	-	-
Recurrence	<0.001	14.558	3.802-55.735	0.002	12.451	2.51-61.7
Baseline CEA1 at metastasis	0.048	3.190	1.012-10.060	0.683	0.762	0.205-2.83

Variables with p<0.10 in univariate analysis and those considered clinically relevant were included in the multivariate model. OS: Overall survival; HR: Hazard ratio; CI: Confidence interval; LVI: Lymphovascular invasion; PNI: Perineural invasion; MSI: Microsatellite instability; TIL: Tumor-infiltrating lymphocytes; CEA: Carcinoembryonic antigen; min-max: Minimum-maximum; EOCRC: Early-onset colorectal cancer. P<0.05 was considered statistically significant.

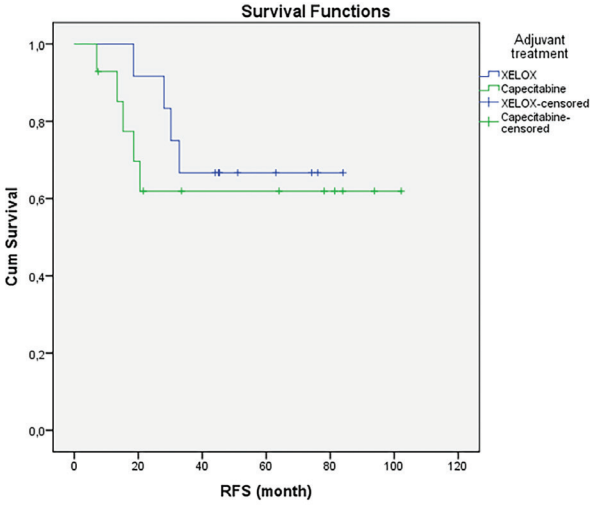

FIGURE 3: Kaplan-Meier RFS curves according to adjuvant treatment regimen (XELOX vs. capecitabine monotherapy) in stage II EOCRC patients. The XELOX regimen was associated with a significantly higher risk of recurrence compared to capecitabine alone (multivariate HR=14.87, p=0.038).

EOCRC: Early-onset colorectal cancer; RFS: Recurrence-free survival; HR: Hazard ratio

DISCUSSION

CRC continues to increase in prevalence among younger adults, and these patients are more likely to receive intensive ACT compared with older individuals. However, relying on age alone when making adjuvant therapy decisions may lead to overtreatment and unnecessary long-term toxicities. In a recent pooled analysis of six randomized trials from the IDEA collaboration, EOCRC patients demonstrated higher adherence to ACT, yet high-risk stage III (T4/N2) EOCRC patients had significantly lower 3-year RFS compared with older patients (54% vs. 64%, p<0.01), and younger age was identified as an independent adverse prognostic factor, supporting the concept of more aggressive tumor biology in EOCRC.[18]

Consistent with these findings, our study showed that patients with stage III EOCRC had significantly lower OS and RFS rates than those with stage II disease; nodal involvement emerged as an independent adverse prognostic factor. Similarly, a large cohort study evaluating the benefit of ACT in stage II EOCRC reported no significant survival advantage in most patients. Data from the XJCRC and SEER cohorts (n>3.500) showed no meaningful improvement in OS with adjuvant therapy

TABLE 5: Univariate and multivariate Cox regression analysis of prognostic factors for RFS in stage II EOCRC patients.

Variable	Univariate HR	Univariate 95% CI	P-value univariate	Multivariate HR	Multivariate 95% CI	P-value multivariate
Adjuvant treatment (XELOX vs. capecitabine)	1.474	0.394-5.517	0.564	14.873	1.156-191.391	0.038
pT	2.100	0.636-6.930	0.223	-	-	-
N0	0.172	0.028-1.046	0.056	0.065	0.005-0.782	0.031
N+	0.622	0.137-2.818	0.538	3.163	0.301-33.257	0.337
MSI	0.236	0.047-1.191	0.080	0.335	0.064-1.756	0.196
Tumor budding	1.144	0.452-2.897	0.777	-	-	-
LVI	0.502	0.104-2.428	0.392	-	-	-
Mucinous component	1.346	0.168-10.805	0.780	-	-	-

Variables with p<0.10 in univariate analysis and those considered clinically relevant were included in the multivariate model. HR: Hazard ratio; CI: Confidence interval; LVI: Lymphovascular invasion; PNI: Perineural invasion; MSI: Microsatellite instability; TIL: Tumor-infiltrating lymphocytes; CEA: Carcinoembryonic antigen; EOCRC: Early-onset colorectal cancer; RFS: Recurrence-free survival. P<0.05 was considered statistically significant.

among the dMMR, pMMR, or T3 subgroups (p=0.48, p=0.07, p=0.83), whereas patients with T4 disease experienced a significant long-term survival benefit, particularly beginning in the third year post-treatment (p=0.007).[19] Together, these results indicate that the survival benefit of ACT in stage II EOCRC is limited for most patients and suggest that treatment decisions should prioritize pathological risk factors such as T4 stage and nodal involvement rather than age alone.

A nationwide, real-world study using the Flatiron Health database reported that patients with stage II EOCRC were substantially more likely than older patients to receive ACT, particularly in the stage IIA subgroup, suggesting a more aggressive age-driven treatment approach.[20] However, no significant differences in OS or time to metastatic progression were observed between younger and older patients, regardless of whether adjuvant therapy was administered. These findings emphasize that extending adjuvant treatment beyond guideline-based indications may expose young, low-risk stage II patients to unnecessary toxicity without a demonstrable survival benefit.

Consistent with this, our results showed no significant difference in median RFS between XELOX and capecitabine monotherapy in stage II EOCRC when evaluated by KM analysis. However, MV CRA demonstrated that XELOX was associated with a significantly lower recurrence risk (HR=14.87, p=0.038), and node-negative (N0) disease independently predicted a favorable prognosis. This suggests that the benefit of oxaliplatin-based therapy in stage II EOCRC is not uniform and may be more relevant in selected patients rather than applied broadly. Although XELOX was associated with a reduced recurrence risk compared to capecitabine monotherapy in stage II patients, the small sample size and wide confidence intervals limit the robustness of this finding, which should be regarded as hypothesis-generating.

Similarly, a large population-based cohort study from Alberta, Canada, evaluating stage II EOCRC found that although ACT was more commonly used in patients with T4 tumors and high-grade histology, treatment was not associated with a statistically significant survival advantage (HR for recurrence=0.79; HR for mortality=0.80).[21] The authors emphasized the need for caution in interpreting these findings due to sample size limitations but highlighted that potential benefit may exist in biologically high-risk subgroups. Taken together, the emerging evidence suggests that adjuvant therapy in stage II EOCRC should not be based on age alone; rather, treatment decisions should incorporate adverse pathological features such as T4 disease and nodal involvement, and consideration should be given to the potential benefit of XELOX in carefully selected node-negative patients. Zhou et al. conducted a retrospective cohort study between 2013 and 2018 examining ACT patterns and survival outcomes in patients with stage II colon cancer.[22] Younger patients (18-49 years) had fewer comorbidities but demonstrated higher rates of poor differentiation (p=0.017) and MSI-H tumors (21.5%). They were significantly more likely to receive ACT [odds ratio (OR)=4.19; 95% CI: 2.25-7.83] and combination regimens (OR=3.18; 95% CI: 1.26-8.06) compared with older patients. However, survival outcomes did not differ between age groups, indicating that more intensive treatment approaches in younger patients do not necessarily confer improved clinical benefits. Consistent with these findings, in our study, adjuvant treatment type was not associated with OS in stage II EOCRC.

Tashkandi et al.[23] reported that treatment intensity declines with advancing age, with older patients receiving less surgery and chemotherapy. Younger patients, on the other hand, typically receive more intense care, especially regimens based on oxaliplatin. But a recent review showed that oxaliplatin-

based adjuvant therapy in stage II - stage III colon cancer was linked to a higher long-term risk of secondary malignancies, emphasising the need to weigh the benefit of early recurrence against the risk of late toxicity.[24]

In a population-based Korean study, the addition of oxaliplatin improved survival in stage III patients younger than 70 years, but no benefit was observed in older individuals or in stage II disease.[25] Similarly, another retrospective analysis found that ACT improved 5-year disease-free survival and OS only in high-risk stage II patients, whereas MSI-high tumors had a favorable prognosis and derived limited benefit from 5-fluorouracil-based regimens.[26] Ambalathandi and Meenakshisundaram[27] reported that EOCRC accounted for 14.5% of diagnosed cases, with a median age of 34 years and an OS rate of 81.5% at 20 months for localized disease. In contrast, a single-center cohort analysis found no independent prognostic effect of age (≤50 vs. >50 years) on tumor stage, location, or OS.[28] Additionally, the combined assessment of KRAS and MSI status in early-stage CRC is essential for more accurate risk stratification and for more effective guidance of adjuvant treatment strategies.[29] Collectively, these findings reinforce that age alone does not dictate prognosis or response to adjuvant therapy and further support a treatment approach focused on pathological and molecular risk factors rather than chronological age.

Study Limitations

There are some limitations to this study. Because of its retrospective design, single-center setting, and modest sample size, the generalizability of the results may be limited. Second, the statistical power of the MV models may have been reduced due to the heterogeneity of adjuvant regimens and the low number of survival events. Accordingly, the wide confidence intervals observed in some Cox regression models likely reflect the limited number of events, which may have reduced statistical power and necessitate cautious interpretation of these findings. Third, because of the small subgroup size and a limited number of deaths, OS comparisons by adjuvant treatment type could not be reliably performed in patients with stage II disease. Fourth, we were unable to stratify stage II patients into high- and low-risk categories, which limits the interpretation of treatment benefit in specific subgroups. This limitation is particularly relevant when interpreting the apparent benefit of oxaliplatin-based adjuvant therapy, as treatment effects may vary substantially across unrecognized risk strata within the heterogeneous stage II population. Although MSI status was included in the analysis, the absence of other relevant molecular markers, such as KRAS and BRAF mutations, may have further limited the ability to risk stratification and influenced the interpretation of prognostic and treatment-related outcomes. Additionally, since all patients in our cohort received ACT, selection bias is likely, reflecting a population with higher-risk disease. Finally, the median follow-up duration of 32 months may not fully capture long-term outcomes. Larger, prospective, multi-institutional studies incorporating molecular stratification are needed to validate these results and refine adjuvant treatment strategies for EOCRC.

In summary, accumulating evidence indicates that treatment decisions in EOCRC should prioritize tumor biology and pathological risk factors—such as MSI status, nodal involvement, T4 disease, and other adverse histological markers—rather than age alone. Our findings support a personalized, risk-adapted approach in which ACT is selectively intensified for high-risk patients while avoiding unnecessary toxicity in low-risk stage II cases. Such a strategy may optimize treatment efficacy and improve long-term outcomes in this increasingly relevant patient population.

CONCLUSION

In this retrospective study of EOCRC patients receiving adjuvant capecitabine-based therapy, stage at diagnosis and nodal status were key prognostic determinants. Recurrence was the strongest independent predictor of poor OS, and patients with stage III disease exhibited significantly lower OS and RFS. Among stage II patients, oxaliplatin-based therapy was associated with a reduced risk of recurrence in MV analysis, suggesting potential benefit in selected cases, while nodal negativity emerged as an independent protective factor. These findings underscore the importance of tailoring adjuvant therapy in EOCRC according to pathological and molecular risk features rather than patient age alone to optimize therapeutic efficacy and minimize unnecessary toxicity in young low-risk individuals.

Ethics

Ethics Committee Approval: The authors state that they have obtained Ege University Medical Research Ethics Committee approval (date: 06.11.2025, approval number: 25-11T/76).

Informed Consent: Retrospective study.

Footnotes

Authorship Contributions

Concept: O.Ö., A.G., Design: O.Ö., A.G., Z.S.G., B.E., H.Ç.Y., Data Collection or Processing: O.Ö., A.G., Z.S.G., B.E., Analysis or Interpretation: O.Ö., A.G., Literature Search: O.Ö., A.G., Z.S.G., B.E., H.Ç.Y., Writing: O.Ö., A.G., H.Ç.Y.

Conflict of Interest: No conflict of interest was declared by the authors.

Financial Disclosure: The authors declared that this study received no financial support.

REFERENCES

1. Malvezzi M, Carioli G, Bertuccio P, et al. European cancer mortality predictions for the year 2018 with focus on colorectal cancer. Ann Oncol. 2018;29(4):1016-1022. [Crossref] [PubMed]
2. Stoffel EM, Murphy CC. Epidemiology and mechanisms of the increasing incidence of colon and rectal cancers in young adults. Gastroenterology. 2020;158(2):341-353. [Crossref] [PubMed] [PMC]
3. Akimoto N, Ugai T, Zhong R, et al. Rising incidence of early-onset colorectal cancer - a call to action. Nat Rev Clin Oncol. 2021;18(4):230-243. [Crossref] [PubMed] [PMC]
4. Vuik FER, Nieuwenburg SAV, Nagtegaal ID, Kuipers EJ, Spaander MCW. Clinicopathological characteristics of early onset colorectal cancer. Aliment Pharmacol Ther. 2021;54(11-12):1463-1471. [Crossref] [PubMed] [PMC]
5. Brenner DR, Ruan Y, Shaw E, De P, Heitman SJ, Hilsden RJ. Increasing colorectal cancer incidence trends among younger adults in Canada. Prev Med. 2017;105:345-349. [Crossref] [PubMed]
6. Spaander MCW, Zauber AG, Syngal S, et al. Young-onset colorectal cancer. Nat Rev Dis Primers. 2023;9(1):21. [Crossref] [PubMed] [PMC]
7. Chung RY, Tsoi KKF, Kyaw MH, Lui AR, Lai FTT, Sung JJ. A population-based age-period-cohort study of colorectal cancer incidence comparing Asia against the West. Cancer Epidemiol. 2019;59:29-36. [Crossref] [PubMed]
8. O'Neill OM, Coleman HG, Reid H. Referral challenges for early-onset colorectal cancer: a qualitative study in UK primary care. BJGP Open. 2023;7(4):BJGPO.2023.0123. [Crossref] [PubMed] [PMC]
9. Durhuus JA, Therkildsen C, Kallemose T, Nilbert M. Colorectal cancer in adolescents and young adults with Lynch syndrome: a Danish register-based study. BMJ Open. 2021;11(12):e053538. [Crossref] [PubMed] [PMC]
10. Saad El Din K, Loree JM, Sayre EC, et al. Trends in the epidemiology of young-onset colorectal cancer: a worldwide systematic review. BMC Cancer. 2020;20(1):288. [Crossref] [PubMed] [PMC]
11. Ramadan M, Alsiary RA, Aboalola DA. Mortality-to-incidence ratio of early-onset colorectal cancer in high-income Asian and Middle Eastern countries: a systemic analysis of the Global Burden of Diseases Study 2019. Cancer Med. 2023;12(21):20604-20616. [Crossref] [PubMed] [PMC]
12. Araghi M, Soerjomataram I, Bardot A, et al. Changes in colorectal cancer incidence in seven high-income countries: a population-based study. Lancet Gastroenterol Hepatol. 2019;4(7):511-518. Erratum in: Lancet Gastroenterol Hepatol. 2019;4(8):e8. [Crossref] [PubMed] [PMC]
13. Nakagawa H, Ito H, Hosono S, et al. Changes in trends in colorectal cancer incidence rate by anatomic site between 1978 and 2004 in Japan. Eur J Cancer Prev. 2017;26(4):269-276. [Crossref] [PubMed]
14. Anugwom C, Braimoh G, Sultan A, Johnson WM, Debes JD, Mohammed A. Epidemiology and genetics of early onset colorectal cancer-African overview with a focus on Ethiopia. Semin Oncol. 2023;50(1-2):28-33. [Crossref] [PubMed]
15. Bailey CE, Hu CY, You YN, et al. Increasing disparities in the age-related incidences of colon and rectal cancers in the United States, 1975-2010. JAMA Surg. 2015;150(1):17-22. Erratum in: JAMA Surg. 2015;150(3):277. [Crossref] [PubMed] [PMC]
16. REACCT Collaborative; Zaborowski AM, Abdile A, Adamina M, et al. Characteristics of early-onset vs late-onset colorectal cancer: a review. JAMA Surg. 2021;156(9):865-874. Erratum in: JAMA Surg. 2021;156(9):894. [Crossref] [PubMed]
17. Siegel RL, Fedewa SA, Anderson WF, et al. Colorectal cancer incidence patterns in the United States, 1974-2013. J Natl Cancer Inst. 2017;109(8):djw322. [Crossref] [PubMed] [PMC]
18. Fontana E, Meyers JP, Sobrero AF, et al. Early-onset stage II/III colorectal adenocarcinoma in the IDEA database: Treatment adherence, toxicities, and outcomes from adjuvant fluoropyrimidine and oxaliplatin. Wolters Kluwer Health; 2021. [Crossref]
19. Cao S, Qiao Y, Wu L, et al. Postoperative adjuvant chemotherapy in patients with stage II early onset colorectal cancer: exploration and discovery using real-world data and the SEER database. Front Oncol. 2025;15:1566569. [Crossref] [PubMed] [PMC]
20. Leary JB, Hu J, Leal A, et al. Risk without reward: differing patterns of chemotherapy use do not improve outcomes in stage II early-onset colon cancer. JCO Oncol Pract. 2025;21(3):333-340. [Crossref] [PubMed] [PMC]
21. Basmadjian RB, O'Sullivan D, Jarada TN, et al. Adjuvant chemotherapy outcomes among patients with stage II early-onset colon cancer in Alberta. American Society of Clinical Oncology. 2025;43(Suppl 16). [Crossref]
22. Zhou Q, Zhou C, Zhang G, Xia X, Zhou X, Lang J. Age-related differences in adjuvant chemotherapy use and outcomes in stage II colon cancer: a retrospective cohort study. BMC Cancer. 2025;25(1):1527. [Crossref] [PubMed] [PMC]
23. Tashkandi E, Alghanmi HA, Almatari A, et al. Age-stratified insights in colorectal cancer: a four-tier analysis of presentation, treatment, and outcomes. 2025. [Crossref]
24. Buchler T, Ambrozova M, Majek O, Dianova T, Klika P, Dusek L. Risk of second primary malignancies after adjuvant chemotherapy for colon cancer. Cancer. 2025;131(20):e70116. [Crossref] [PubMed] [PMC]
25. Bong JW, Lee H, Jeong S, Kang S. Older age threshold for oxaliplatin benefit in stage II to III colorectal cancer. JAMA Netw Open. 2025;8(8):e2525660. [Crossref] [PubMed] [PMC]
26. Pina-Cabral T, Lobo-Martins S, Mansinho A, et al. 112P defining who benefits: adjuvant treatment patterns and survival outcomes in stage II colon cancer-a multicenter real-world analysis. Ann Oncol. 2025;36:S52. [Crossref]
27. Ambalathandi RC, Meenakshisundaram M. Carcinoma colon in young adults: an institutional experience. Journal of Dr NTR University of Health Sciences. 2025;14(2):149-152. [Crossref]
28. Alghanmi H, Tashkandi E, Almatari A, et al. 103P Characteristics of colon cancer in the comprehensive cancer center and overall survival of young versus old patients: single institute experience from 2015-2021. Ann Oncol. 2024;35:S1442. [Crossref]
29. Yildirim HC, Gunenc D, Almuradova E, Sutcuoglu O, Yalcin S. A narrative review of RAS mutations in early-stage colorectal cancer: mechanisms and clinical implications. Medicina (Kaunas). 2025;61(3):408. [Crossref] [PubMed] [PMC]

Click the link to access Supplementary Table 1: https://d2v96fxpocvxx.cloudfront.net/a5223c9c-50f0-490d-b293-6a74c2af8d3b/content-images/4a39d809-4fb6-4e6f-a5aa-c87ff3666751.pdf

ORIGINAL ARTICLE

DOI: 10.37047/jos.galenos.2026.2025-5-2
J Oncol Sci 2026;12(1):18-31

Bacoside A - A Potent Phytomedicine Attenuates Epithelial - Mesenchymal Transition in HCT 116 Colon Cancer Cells

Bhagavathy SIVATHANU

Department of Biomedical Sciences, Sri Ramachandra Institute of Higher Education and Research, Chennai, India

ABSTRACT

Objective: Epithelial mesenchymal transition (EMT) is the one of the significant events in the cancer metastasis. The active compounds Bacoside A from *Bacopa monnieri* good in antioxidant, anti-inflammatory, neuroprotective and anticancer properties. The present study focuses to check the efficiency of Bacoside A on EMT in HCT 116 colon cancer cell lines and to explore its potential cancer therapeutics.

Material and Methods: An *in vitro* study was designed with HCT 116 colon cancer cell lines. The cytotoxic effect of Bacoside A was carried out with the different concentrations ranges from 0-50 µg/mL. The free radical scavenging activity, the membrane stability assay, lipid peroxidation assay, protein denaturation assay and metal chelating activity were assessed. Cell migration and colony forming capacity was assessed with different concentrations of Bacoside A. Cell apoptosis was checked with Acrydine Orange - Propidium Iodide staining. The gene expression was performed with epitehlial markers and mesenchymal markers E-Cadherin, Snail and Vimentin.

Results: The results of the present work states that the Bacoside A potentially inhibit the cancer cell proliferation and the IC_{50} value was found be 32 µg/mL. Further investigation on membrane stability the lipid peroxidation and protein denaturation, concentration dependent inhibition was found upon Bacoside A treatment. Migration assay results conclude that the higher concentration inhibits cell growth and the lower concentration slows down the cell migration. The results of colony forming units by HCT 116 colon cancer cells were effectively inhibited by Bacoside A treatment. The EMT induction studies indicates the EMT was attenuated on Bacoside A treatment. The results of apoptosis study clearly indicate the Bacoside A treatment induced cancer cell death. The gene expression analysis further confirms that the epithelial protein markers E-Cadherin was upregulated and intermediary protein -snail and mesenchymal marker - vimentin were down regulated.

Conclusion: The results of present work clearly states that phyto compound Bacoside A had a potent anticancer and anti-metastatic activity for HCT 116 colon cancer cell lines tested *in vitro*. Bacoside A effectively inhibits cell viability, colony formation, cell migration and induced apoptotic cell death in colon cancer cell lines.

Keywords: *Bacopa monnieri*; Bacoside A; cancer diagnosis and treatments; E-cadherin; EMT; M-cadherin

INTRODUCTION

Colorectal cancer (CRC) ranks as the second leading cause of cancer death overall in both males and females, and it is the most commonly observed cancer in individuals younger than 50 years. The risk factors and causes of CRC include lifestyle factors such as an unhealthy diet, high alcohol intake, smoking, reduced physical activity, and excess body weight.[1] The CRC metastasis includes various mechanisms in which different intrinsic, factors, such as heterogeneity of tumour cells, genetic abnormalities, and epithelial mesenchymal transition (EMT), are involved. All initiate the metastatic process and lead to cancer invasion and spread.[2] In EMT, cells lose their epithelial characteristics, such as cellular integrity and cell-cell attachment; gain mesenchymal properties, such as increased cell motility; and become associated with an invasive or metastatic phenotype.[3] EMT is a key event in understanding cancer progression, development, and pathogenesis. More attention has been focused on EMT as a target in cancer therapy. During EMT, epithelial cells are transformed into

Correspondence: Bhagavathy SIVATHANU Ph.D.
Department of Biomedical Sciences, Sri Ramachandra Institute of Higher Education and Research, Chennai, India
E-mail: drbhagavathy@sriramachandra.edu.in
ORCID ID: orcid.org/0000-0002-9273-2887

Received: 06.05.2025 **Accepted:** 07.01.2026 **Epub:** 22.01.2026 **Publication Date:** 18.03.2026

Cite this article as: Bhagavathy S. Bacoside A - a potent phytomedicine attenuates epithelial - mesenchymal transition in HCT 116 colon cancer cells. J Oncol Sci. 2026;12(1):18-31

Available at journalofoncology.org

mesenchymal cells, changing from stationary, polarized cells to motile, spindle-shaped cells. This transition is believed to be a significant mechanism underlying cancer metastasis. Once these cells have disseminated to different sites, cancer cells tend to regain epithelial properties through the reversal of EMT, termed mesenchymal-epithelial transition (MET).[4] The process EMT expresses the intermediate filaments, changes the intracellular junctional composition, and alters cell morphology. Other important markers of EMT include membrane-bound E-cadherins, transcription factors, and epithelial-specific markers. The important mesenchymal markers include fibronectin, N-cadherin, and vimentin. Upregulation of epithelial markers and downregulation of mesenchymal markers are considered significant controlling events in cancer metastasis.[5] The transcription factors Snail 1, Snail 2, Twist, and ZEB1 are involved in the epigenetic expression of epithelial markers, transcription activation of matrix metalloproteins and cytoskeleton remodelling. EMT confers metastatic potential to cancer cells. EMT as a target in cancer therapeutics is considered a meaningful approach to preventing cancer progression.[6] Researchers are focusing on discovering and developing medications to combat cancer. The limitations of anticancer drugs include non-specificity, wide biological distribution, short half-life, and toxicity.[7] Several anticancer drugs have been identified from natural compounds of plant, animal, and microbial origin. There has been increasing interest in identifying medications derived from natural resources to treat CRC by acting on various specific targets. The benefits of medicinal herbs for CRC prevention include induction of apoptosis, cell-cycle arrest at various stages, and alteration of multiple cell-signalling pathways.[8] *Bacopa monnieri (B. monnieri)* is a medicinal herb found in India, commonly used in the Ayurvedic system of medicine for various treatments because of its pharmacological activities, such as neuroprotective, antioxidant, anti-ulcer, antimicrobial, analgesic, and anticancer properties.[9] Bacoside A is an amphiphilic mixture found in *B. monnieri*, consisting of both sterol and sugar moieties and including different saponin glycosides, namely bacopaside II, bacopaside X, Bacoside A3, and bacopasaponin C. Bacoside A possesses anti-cancer properties and effectively inhibits the growth of breast, colon, and liver cancers, as well as glioblastoma, as demonstrated by various studies.[10] Bacoside A can effectively interact with various signaling pathways, such as epidermal growth factor receptor/Ras/Raf/mitogen-activated protein kinase, Notch signaling, and Wnt/β-catenin signaling, as demonstrated by gene expression analysis and molecular docking studies in neuroblastoma cells.[11]

Bacoside I and II, reported to have tumour-suppressive effects specifically block transmembrane proteins, alter tumour cell migration, and affect metastasis in colon and breast cancer cells. Drugs targeting transmembrane alter cell migration, invasion, and growth of cancer cells.[12] Bacoside A significantly arrests the cell cycle and induces apoptosis in glioblastoma cells, which are highly metastatic and malignant, and for which temozolomide is insufficient to improve patient outcomes and survival.[13] Transmembrane proteins play a crucial role in cancer metastasis by influencing cell-cell adhesion, migration, and invasion. They act as signaling receptors, adhesion molecules, and transporters. Different transcriptomic and proteomic studies have attempted to elucidate their role in cancer metastasis.[14] Certain proteins, such as E-cadherin, M-cadherin, vimentin, Snail1, Snail2, and fibronectin are considered good indicators because they are directly involved in cancer metastasis through EMT.[15] Several external and internal factors can activate these proteins, stimulate the process of EMT, and lead to cancer metastasis. Recently, membrane proteins have increasingly been targeted by phytochemicals for cancer therapy to overcome chemoresistance. Most membrane-bound proteins possess receptors with subunits that receive signals; these proteins regulate the basal surface of cancer cells and lead to changes in cytoskeletal organization.[16]

Based on the above findings, the present study aimed to assess the potential of the phytocompound Bacoside A to modulate genes regulating EMT through *in vitro* gene expression analysis in HCT 116 colon cancer cell line. This preliminary study was aimed to identify the anti-inflammatory, apoptosis and EMT expression analysis and could be opening the way to recognize the therapeutic activity of phyto ccompound Bacoside A to treat against cancer spreading, invasion and the associated problems during the course of disease.

MATERIAL AND METHODS

Cell line maintenance: The human colon cancer cell line HCT 116 was propagated in Dulbecco's Modified Eagle Medium (DMEM) (Himedia) with glucose, supplemented with 10% fetal bovine serum and 1% penicillin-streptomycin; cultures were maintained in a 5% CO_2 incubator at 37°C. Cell counts were performed using a hemocytometer, and a density of 5.0×10^3 cells/well was used for the cytotoxicity assay. Sri Ramachandra Institute of Higher Education and Research Ethics Committee approval was obtained for conducting the cell line studies (approval number: IEC-NI/22/JUL/83/85, date: 14.10.2022).

Cytotoxic Assay: Cytotoxicity was evaluated using the MTT assay in the HCT 116 colon cancer cell line. MTT enters mitochondria of viable cells and is reduced to insoluble purple formazan crystals. The cells were solubilized with dimethyl sulfoxide, and the released formazan reagent was measured

spectrophotometrically at 570 nm. Different concentrations (5, 10, 20, 40, 80, 160, 320 µg/mL) of Bacoside A (Natural remedies, Bangalore, India) were dissolved in methanol and used to treat HCT 116 cells for a cytotoxicity assay. The optical density was measured at 570 nm on a microplate reader. The fifty percent inhibitory concentration (IC_{50}) of the drug was calculated from the dose-response curves.

Free Radical Scavenging Assay

DPPH Assay: Different concentrations of Bacoside A were mixed thoroughly with 1 mL of methanol and 0.1 mM DPPH, allowed to stand for 30 min in the dark, and the optical density was measured at 523 nm using a ultraviolet (UV)/visible (VIS) spectrophotometer. The standard and the blank were processed simultaneously.[17] The scavenging activity was calculated using the following formula:

$$\% \text{ Scavenging Activity} = (A_{control} - A_{sample})/A_{control} \times 100$$

were A_{sample} is the absorbance of the test sample

$A_{control}$ is the absorbance of the control.

Hydroxyl Radical Scavenging Activity: Assessment of hydroxyl radical scavenging activity was carried out with the reaction mixture contains, 1 mL of ferric chloride, 1 mL of hydrogen peroxide and 1 mL of ethylene diamine tetra acetic acid and 1 mL of stock solution of salicylic acid. Bacoside A at different concentrations (25-200 µg/mL) were added along with the reaction mixture allowed for the incubation at 37 °C for 1 hour. 1 mL of 2.8% sodium hydroxide was added to arrest the reaction and the optical density were measured at 510 nm using a UV-VIS spectrophotometer.[18] The percentage of scavenging activity of the sample was calculated by following formula:

$$\% \text{ Scavenging activity} = [(A_{control} - A_{sample})/A_{control}] \times 100$$

FRAP Assay: A working solution of 2,4,6-Tripyridyl-s-triazine (TPTZ) was prepared in acetate buffer. TPTZ solution and ferric chloride stock solution were mixed in a 1:1 ratio to prepare the Ferric reducing antioxidant power (FRAP) reagent. The test solution, Bacoside A, at concentrations of 25-200 µg/mL, was mixed thoroughly with FRAP reagent and incubated at room temperature for 30 minutes. The absorbance was measured at 593 nm using a spectrophotometer.[19] The antioxidant capacity of Bacoside A was calculated using the following formula:

$$\text{Antioxidant capacity} = (A_{sample} - A_{control})/\text{Slope}$$

In vitro membrane stability Assay

Lipid Peroxidation Assay: The lipid peroxidation assay, the cells were treated with different concentration (25-200 µg/mL) of Bacoside A, 20 µL of 2 mM ascorbic acid and 4 mM Fe_2SO_4 were added to the mixed solution and incubated for 60 min at 37 °C. Subsequently, 200 µL of TBARS reagent (40% trichloroacetic acid, 1.4% thiobarbituric acid, and 8% HCl) was added to the mixture, which was then incubated at 90 °C for 60 min. At the end of incubation, the mixture was allowed to stand at room temperature and was centrifuged at 10,000 rpm for 5 min at 4 °C. The supernatant was then collected and measured at 530 nm using a microplate reader. The lipid peroxidation status was calculated relative to the control.[20] The peroxidation status was assessed using the following formula:

$$\text{Concentration of MDA (nmol/mL)} = (S_A/S_V) \times DF$$

S_A = Amount of MDA in sample (nmol)

S_V = Sample volume (mL)

DF = Sample dilution factor

Protein Denaturation Assay: Protein denaturation assay was performed using Bacoside A at concentrations of 10-50 µg/mL with 0.5 mL of 1.5 mg/mL bovine serum albumin, followed by incubation at 37 °C for 20 min. This reaction mixture was further heated for 3 min at 57 °C. Added 250 µL of 0.5 M phosphate buffer (pH=6.3). 100 µL of each mixture was transferred into separate test tubes; alkaline copper reagent and 1% Folin-Ciocalteu reagent were added in the same proportion. After 10 min of incubation at 55 °C, absorbance was measured at 650 nm using a spectrophotometer.[21]

Metal Chelating Assay: Metal chelating assay measures the ability of test samples to chelate free ferrous ions in solution thereby inhibiting Fe(II) binding to ferrozine which generates a highly colored complex. EDTA acts as a positive control, capable of chelating ferrous ions in a dose-dependent manner.[22]

$$\text{Metal chelation (\%)} = (A_{control} - A_{Sample})/A_{Control} \times 100$$

Cell Migration Assay: Cells grown in DMEM medium with 10% FBS were seeded in a 6-well tissue culture plate. After 24 hours, the cells reached 80% confluence, forming a monolayer. The monolayer was scratched across the center of the well using a 10 µL tip, with the axis of the tip perpendicular to the bottom of the well. The cells were viewed under a phase-contrast microscope. The culture dish was placed in an incubator, and an image was captured every 12 hrs. 100,000 cells were incubated for 12 hours in a 5% CO_2 incubator at 37 °C. After 24 hours, cells were treated with the drug at the respective concentrations. A scratch was made in all wells using a sterile 10 µL pipette tip. The images were observed under a fluorescence microscope, and photographs of each well were captured and labeled at 0, 12, 24, and 36 hours, respectively.[23] The percentage of wound closure area was calculated using the following formula:

$$\% \text{ Wound Closure Area} = \frac{A(0) - A(t)}{A(0)} \times 100$$

Where A(t) - Wound area at time t, A(0) - Initial wound area

Clonogenic Assay: Mono layered cultured cells in six-well plates in a range of 5×10^6 cells/well and allowed to adhere. The cell culture medium was refreshed (2 mL/well), and cells were treated with Bacoside A. Depending on the proliferation rate, cells were then incubated at 37 °C for 36 hours; cell growth in all six-well plates was stopped by fixation and staining with 80% ethanol containing 8% methylene blue. Colonies of ≥50 cells were counted under the microscope. Based on the colony size and cell morphology, the magnification was adjusted.[24]

% Plating Efficiency (PE) % = No. of colonies formed/No.of colonies seeded X100

% Survival Fraction (SF) = No. of colonies formed after treatment/No.of colonies seeded X PE X100

EMT induction Analysis : The induction assay was performed with the warm culture media at 37 °C. All other parameters will be the same as in the standard culture protocols. Cells (1×10^6 per well) in a 6-well plate and were then treated with the IC_{50} concentration of Bacoside A. The treated plates were incubated at 37 °C in a carbon dioxide incubator, and the cell morphology was monitored at 0, 24, 36, and 48 h by inverted light microscopy.[25]

Cell apoptosis Assay: Cell apoptosis analysis was carried out using a combination of the fluorescent dyes acridine orange (AO) and propidium iodide (PI). When using the AO-PI mixture, it will stain the cells: live cells emit green fluorescence, and dead cells emit reddish-orange when exposed to an appropriate light source. HCT 116 cells were seeded at a density of 1×10^6 cells per well in a 35-mm dish and incubated for 24 hours. The cells were treated with 10 µg/mL, 20 µg/mL, and 30 µg/mL of Bacoside A. After incubation, the medium was removed and 100 µL of AO/PI stain was added to the plate. The viability of the cells were determined based on the emission of the fluorescent colour using an inverted fluorescent microscope.[26]

RNA Isolation, cDNA Synthesis and Quantitative Polymerase Chain Reaction (qPCR) Analysis: HCT 116 colon cancer cell lines ($3x10^5$ cells) were treated with control and Bacoside A inhibitory concentration (IC_{50}) for 48 hours. Every 12 hrs during the treatment, RNA was extracted using the Trizol method. The quantity and purity of RNA were assessed using a NanoDrop spectrophotometer. Reverse transcription reactions for the production of cDNA were carried out using the RevertAid First Strand cDNA Synthesis Kit. Genes specific for epithelial characteristics (E-cadherin), mesenchymal characteristics (vimentin), and the transcription factor (Snail - 1) were selected for expression analysis. Quantitative RT-PCR reactions were performed with High ROX Amplicon SYBR Green Master Mix and specific primers for target genes. Gene-specific forward and reverse primers are designed for the gene amplification reaction. Expression values for qPCR products were processed using the housekeeping gene β-actin as a reference, and ratios relative to untreated samples were calculated. The relative expression fold change was calculated by the 2-ΔΔCt method. The primer sequences used are as follows.

Primers	Forward Primer (5′-3′)	Reverse Primer (5′-3′)
E-Cadherin	CGACAAAGGACAGCCTATTT	AGTTGGGAAATGTGAGCAAT
Snail	ATACCACAACCAGAGATCCTCA	GACTCACTCGCCCCAAAGATG
Vimentin	GCTCGTCGTCGACAACGGCT	CATTTCACGCATCTGGCGTTC
β-actin	GCTCGTCGTCGACAACGGCT	CAAACATGATCTGGGTCATCTTCTC

By the comparative Ct method, the qPCR data were analysed, and the expression of target genes was normalized to that of β-actin. A 1.2% agarose gel was used to visualize the PCR products.

Western Blot Analysis: Proteins were extracted from the control and Bacoside A-treated groups after 48 hours. The PBS-washed cells were scraped off with a cell scalpel in 1 mL of cold PBS and centrifuged for 5 min at 4 °C and 5,000 g. Total protein was extracted from the supernatant using RIPA buffer. The protease and phosphatase inhibitors were added, and the proteins were kept on ice for 15 min. Then the lysates were centrifuged at 12,000 × g for 10 min. The supernatants were collected and used for total protein determination. The extracted proteins were separated by 10% gel electrophoresis and subsequently transferred to PVDF membranes (EMD Millipore). The membranes were blocked in 5% skim milk for 1 h at room temperature. Antibodies against β-actin, E-cadherin, vimentin, and Snail1 were incubated overnight at 4 °C. The secondary antibodies were added at a dilution of 1:1,000 and incubated for 2 h at 25 °C. The enhanced chemiluminescent substrate reagent (ECL) was applied to the film, and the film was analyzed on a Quant LAS 4010 imaging system (Ultra-Violet Products Ltd.).

Statistical Analysis

All the experiments were done in triplicates. Statistical analysis were performed using SPSS 16.0. Data were expressed as mean ± standard error of the mean. Chi-square test was used to assess associations between EMT-related gene expression and other parameters. An independent t-test was used to analyze differences between two unrelated groups. Statistical significance was accepted if $p<0.05$.

RESULTS

Cytotoxicity Assay: Cytotoxicity studies were performed using the MTT assay, which measures cell viability. The viable

cells capable of reducing MTT to purple formazan crystals were quantified. This is the most representative and sensitive method for assessing cell proliferation and growth. Percent growth inhibition at different concentrations of Bacoside A was observed in HCT 116 colon cancer cell lines. At concentrations up to 20 µg/mL, there was little growth inhibition, and above that concentration there was a marked decline in the growth of cancer cells. The cytotoxicity results showed that cell death was concentration-dependent. From the cytotoxicity linear curve, the fifty-percent IC_{50} was determined to be 32 µg/mL (Table 1, Figure 1).

***In vitro* free-radical scavenging activity:** A dose-dependent scavenging response of Bacoside A against free-radical generation was assessed. Bacoside A showed the strongest percentage inhibition and radical scavenging activity compared with the reference standard, gallic acid. In the DPPH assay, scavenging activity exceeded 60% at 40 µg/mL of Bacoside A. Results of the hydroxyl radical scavenging assay showed that Bacoside A exhibited 98% scavenging activity at a concentration of 50 µg/mL, which is almost equal to that of the potential standard free radical scavenger, gallic acid. Similarly, the ability to reduce ferric ions was determined by the FRAP assay, which indicates concentration-dependent linearity in the percentage reduction of ferric ions. At a concentration of 50 µg/mL, Bacoside A reduced ferric ions by 90% (Figure 2).

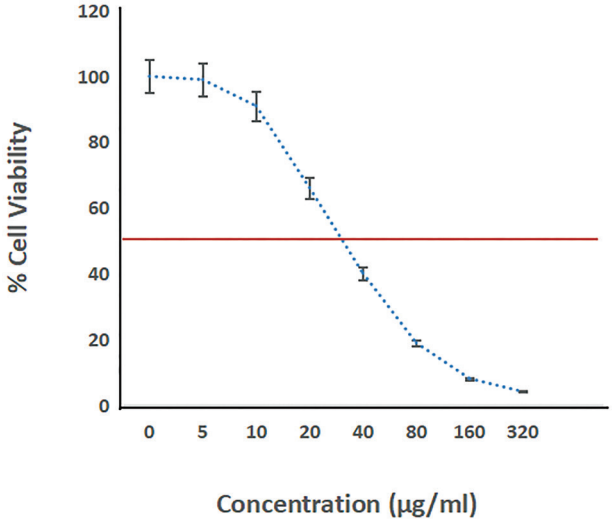

FIGURE 1: Cytotoxicity assay.
Values are mean ± standard error of the mean of triplicates (n=3).

TABLE 1: Cytotoxicity assay.

No.	Concentration (µg/mL)	% of viable cells
1	Control	100 ±0.01
2	5	99.01±0.02
3	10	91.92±0.04
4	20	66.11±0.003
5	40	40.11±0.002
6	80	18.89±0.003
7	160	8.04±0.002
8	320	4.04±0.003

Values are mean ± standard error of the mean of triplicates (n=3).

The HCT 116 cancer cells were further tested for the radical generation, and the scavenging role of Bacoside A at different concentrations were also tested using the above-mentioned assay. The results confirm that the phytomedicine Bacoside A is a potential radical scavenger that shows 15-35% radical-scavenging activity across all tested methods. This decrease may be due to continued rapid proliferation of cancer cells, which was also significantly inhibited ($p<0.05$) by Bacoside A at concentrations above 50 µg/mL (Figure 3).

***In vitro* Membrane Stability Assay:** Oxidation of macromolecules is a common process in cancer cells due the increase in the cellular deterioration by various mechanism. Thereby it is valid to analyse the molecular stability in the presence of Bacoside A, the results clearly proves that the Bacoside A effectively inhibit lipid peroxidation, significant ($p<0.05$) suppression of malondialdehyde levels were identified in dose dependent manner. Figure 4 shows that concentrations of Bacoside A higher than 50 µg/mL have a greater inhibitory effect on lipid peroxidation in colon cancer cell lines. Inhibition of protein denaturation also gradually increases with increasing concentrations of Bacoside A, reaching 80% inhibition at 50 µg/mL in bovine serum albumin. The generation of free ions has been the main cause of peroxidation in biological systems, and the metal-chelating activity was also tested on HCT 116 colon cancer cell lines, both with and without Bacoside A. A linear graph was observed, indicating that Bacoside A exhibited strong chelating activity with values above 85% and 50% in the absence and presence of HCT 116 colon cancer cell lines, at concentrations of 50 µg/mL and 200 µg/mL, respectively (Figure 4).

***In vitro* cell migration activity:** Cell migration was assessed using a scratch-wound assay and observed under an inverted phase-contrast microscope. Compared with the control, cell migration was observed in the treated group, but faster and maximal migration was observed in the control group at 24 hrs and 36 hrs. Wound closure in the test group was calculated to assess cancer cell migration at Bacoside A concentrations of 10 µg/mL and 32 µg/mL. The images clearly showed the rapid migration of the cancer cells in the Bacoside A-treated groups at the lower concentration. Almost 80% of the scratched area was covered by cells within 12 hrs, and complete closure was observed within 24 hrs. Cells treated

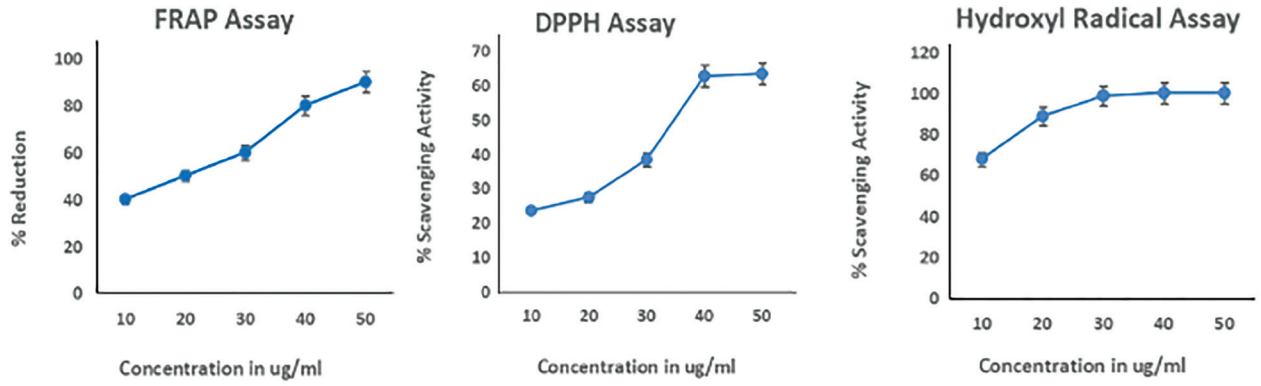

FIGURE 2*: In vitro* free radical scavenging assay.
Values are mean ± standard error of the mean of triplicates (n=3).

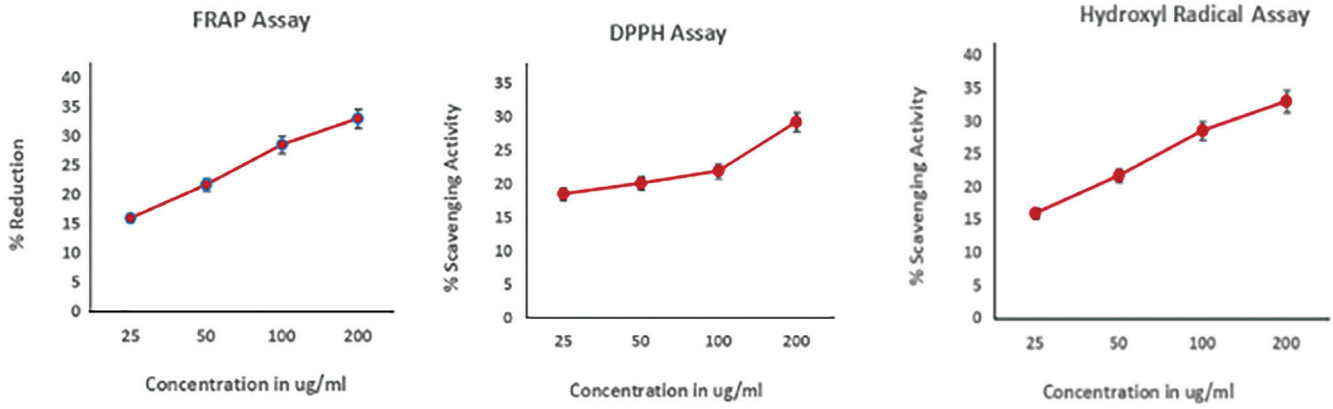

FIGURE 3: Free radical scavenging assay by Bacoside A on HCT 116 cell lines.
Values are mean ± standard error of the mean of triplicates (n=3).

with the lower concentration (10 µg/mL) covered 60% of the scratched area within 12 hours ($p<0.01$), indicating that the concentration used was insufficient to stop migration completely. In contrast to this result, the IC_{50} value of Bacoside A demonstrates a significant inhibitory effect ($p<0.001$) on cancer cell migration; only about 20% of cells were observed in the scratched area within 12 hrs of treatment (Table 2, Figure 5).

***In vitro* Clonogenic Assay:** The effect of Bacoside A on colony forming capacity of HCT 116 was carried out, the cancer cells usually grows in colonies by communicating with the neighbouring cells. Multiple proteins are involved in colony formation with adjacent cells. The results of the clonogenic assay show that treatment with Bacoside A at concentrations of 10-50 µg/mL significantly ($p<0.001$) reduces the colony-forming potential of cancer cells compared with the untreated control group. Calculation of colony-forming units (50 cells) after Bacoside A treatment showed that colony formation decreased gradually between 10 and 30 µg/mL, whereas concentrations of 40 and 50 µg/mL caused a rapid reduction to approximately one-fifth of the control (Figure 6). The surviving fraction calculation also correlates with this result and shows a significant decline as the concentration of Bacoside A increases above the IC_{50} values (Figure 7).

***In vitro* Epithelial - Mesenchymal transition induction Assay:** The EMT inducing cell culture conditions were applied to check the status of the epithelial to mesenchymal transition on Bacoside A treatment. Observations under phase-contrast microscopy demonstrated that cells lost their classical epithelial morphology and acquired a mesenchymal, spindle-shaped morphology over time. At 0 hr, both the induced and uninduced groups exhibited densely packed, spindle-shaped cells. EMT-induced cells treated with Bacoside A appeared less densely packed and exhibited a variant, spindle-shaped morphology and the number of cells also declined at 24 and 36 hours of observation. The results clearly indicate that the

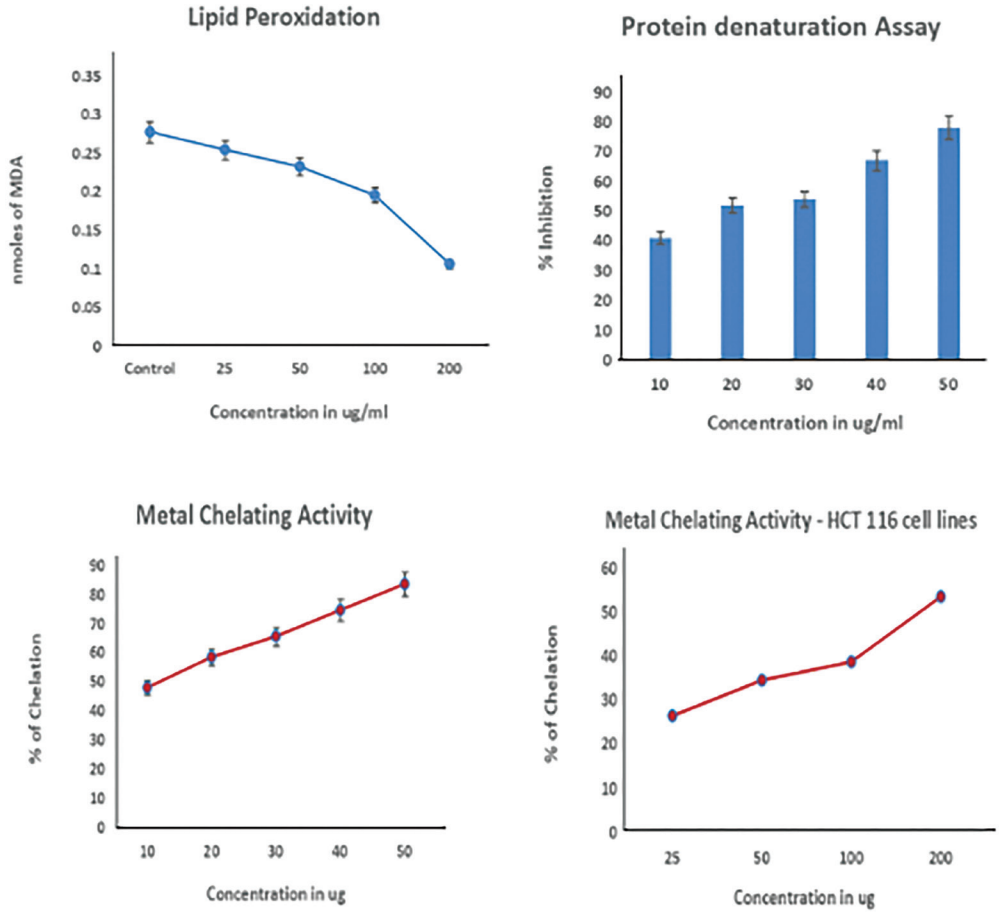

FIGURE 4: *In vitro* membrane stability assay.

Values are mean ± standard error of the mean of triplicates (n=3).

TABLE 2: ***In vitro*** **cell migration activity.**

Time (hrs)	Concentration					
	Control		10 (µg/mL)		32 (µg/mL)	
	Wound distance (mm)	Wound closure (%)	Wound distance (mm)	Wound closure (%)	Wound distance (mm)	Wound closure (%)
0	30.37±0.002	-	28.04±0.001	-	30.75±0.030	-
12	5.94±0.002	80.44	10.85±0.004	61.30**	23.95±0.002	22.11***
24	-	100	7.84±0.004	72.03**	20.74±0.003	32.55***
36	-	100	3.84±0.003	86.30*	18.73±0.001	39.08***

The values are mean ± standard error of the mean (n=3); ***p<0.001, **p<0.01, *p<0.05 statistically Significant compared with control.

cancer cell may have transitioned from the epithelial to the mesenchymal state by losing its intercellular integrity and converting into a loosely distributed form, suggesting that Bacoside A can effectively act on cancer cells and induce cell death (Figure 8).

Apoptosis Assay: The apoptotic assay was done with double staining of AO/PI in which the live and dead cells were identified based on the emission of green and reddish orange fluorescence. As shown in Figure 9, the untreated HCT 116 cancer cells appeared healthy and green, with intact nuclei. Treatment with Bacoside A at different concentrations (10-30 µg/mL), followed by incubation for 24 hours, resulted in an increased number of dead cells observed under a fluorescent microscope. Apoptotic results show that Bacoside A-treated cells at concentrations of 30 µg/mL and above exhibited increased late apoptotic features, with a reddish-orange

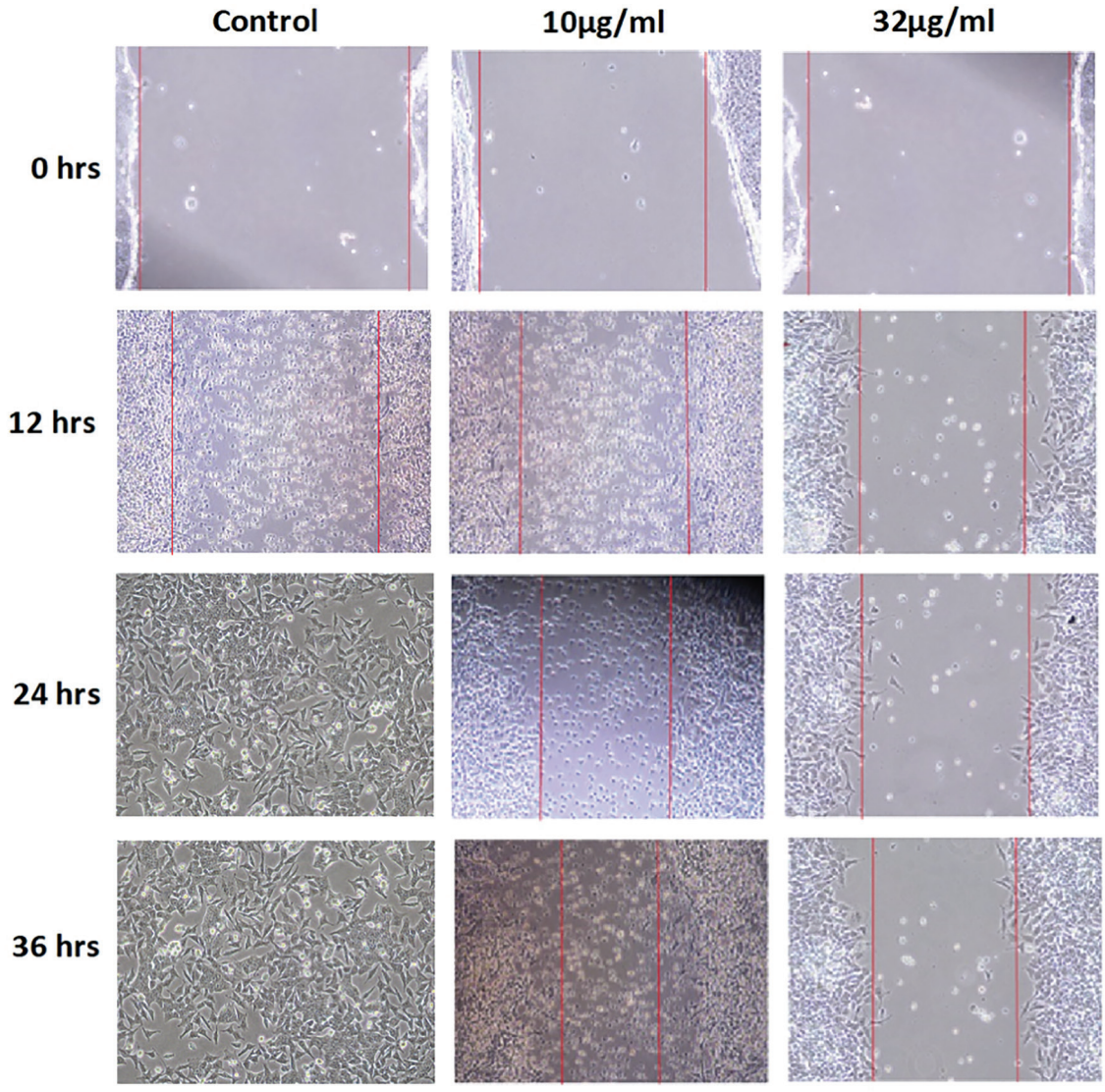

FIGURE 5*: In vitro* cell migration activity.

appearance attributable to PI-positive staining of denatured DNA within 12-24 hours. Lower concentrations (10 µg/mL and 20 µg/mL) can also induce apoptosis in cancer cells, as indicated by the relatively early apoptotic appearance of yellowish-orange fluorescence. Prolonged incubation induces the cellular necrosis observed in HCT 116 cells double-stained with AO/PI.

RNA Isolation, cDNA Synthesis and qPCR Analysis: The real time PCR analysis was carried out to analyse the expression pattern responsible genes involved in EMT mechanism and the changes observed under the treatment of IC_{50} dose of Bacoside A on HCT 116 cancer cells. The gene expression profile was evaluated using the epithelial marker E-cadherin, the EMT transcription factor Snail1, and the mesenchymal marker vimentin. The qPCR analysis of mRNA expression showed that the mRNA level of the epithelial marker E-cadherin was high and was up-regulated by Bacoside A during 48 hrs of treatment. The results further confirm that the mRNA expression levels of the mesenchymal marker vimentin and the transcription factor Snail1 were decreased and their gene expression was downregulated (Table 3, Figures 10, 11).

DISCUSSION

Cancer development from primary cancer cells involves several molecular mechanisms in our system. Metastasis is the ability of cancer cells to move away from the site of origin. Metastasis of cancer cells is the major cause for failure of therapy and disease management. The molecular mechanism of metastasis being poorly understood. EMT is one of the significant events that lead to invasion, stress resistance, and dissemination. Various *in vitro* and *in vivo* studies have demonstrated that EMT is associated with cancer metastasis.[27]

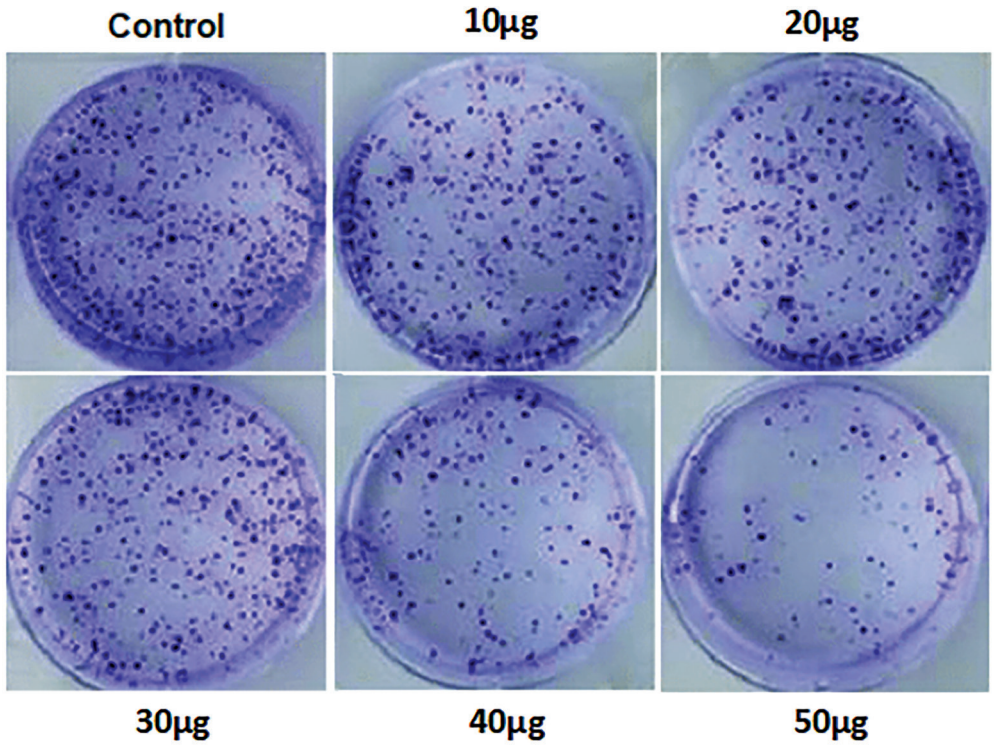

FIGURE 6: *In vitro* clonogenic assay.

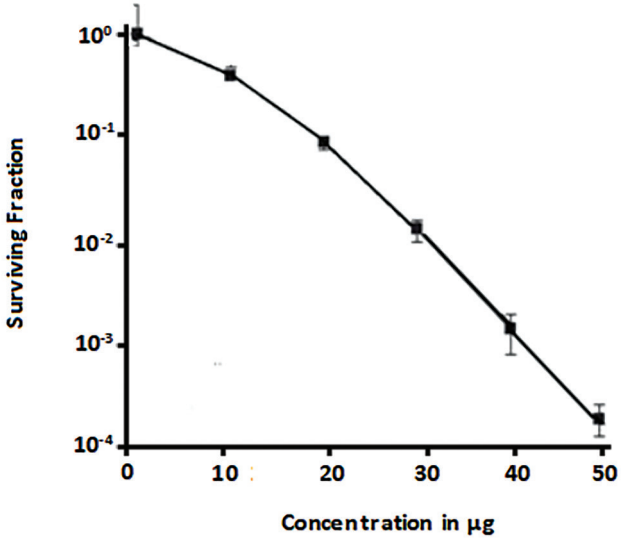

FIGURE 7: Percent survival fractions of colonies.
Values are mean ± standard error of the mean of triplicates (n=3).

In the present *in vitro* study, the effect of Bacoside A on EMT and the prevention of cancer metastasis was evaluated. Bacoside A demonstrated cytotoxicity against HCT 116 colon cancer cells, indicating that it is a promising anticancer agent. Similar studies on Bacoside A have demonstrated its cytotoxic effect via induction of apoptosis against various cancers, such as oral squamous cell carcinoma,[28] and its ability to inhibit cellular proliferation in C6 glioma cells.[29]

The study also finds the beneficiary effect of Bacoside A on free radical generation during cancer progression. The results of the present investigation clearly indicate that Bacoside A possesses substantial potential to inhibit the production of various types of free radicals. The hydroxyl radical produced in the body is highly reactive and is one of the most potent oxidizing agents; it reacts with almost all biomolecules in living cells at a high rate. It is involved in many pathological processes. A similar identification was also made for free-radical scavenging and antioxidant roles of bacosides against liver and nerve cells.[30] Another finding indicates that Bacoside A acts as an effective antioxidant, has a therapeutic role and is a potential anticancer, and analgesic agent.[31]

Cell membrane integrity maintains cellular stability. The results support that chronic inflammation accompanied by protein denaturation, is mainly caused by the loss of bonding interactions, especially hydrogen and disulphide bonds. When assessing membrane stability, the results of a lipid peroxidation and protein degradation study support that Bacoside A suppresses lipid peroxidation, effectively inhibits protein denaturation, and exerts a membrane-strengthening effect under inflammatory and disease conditions. It is

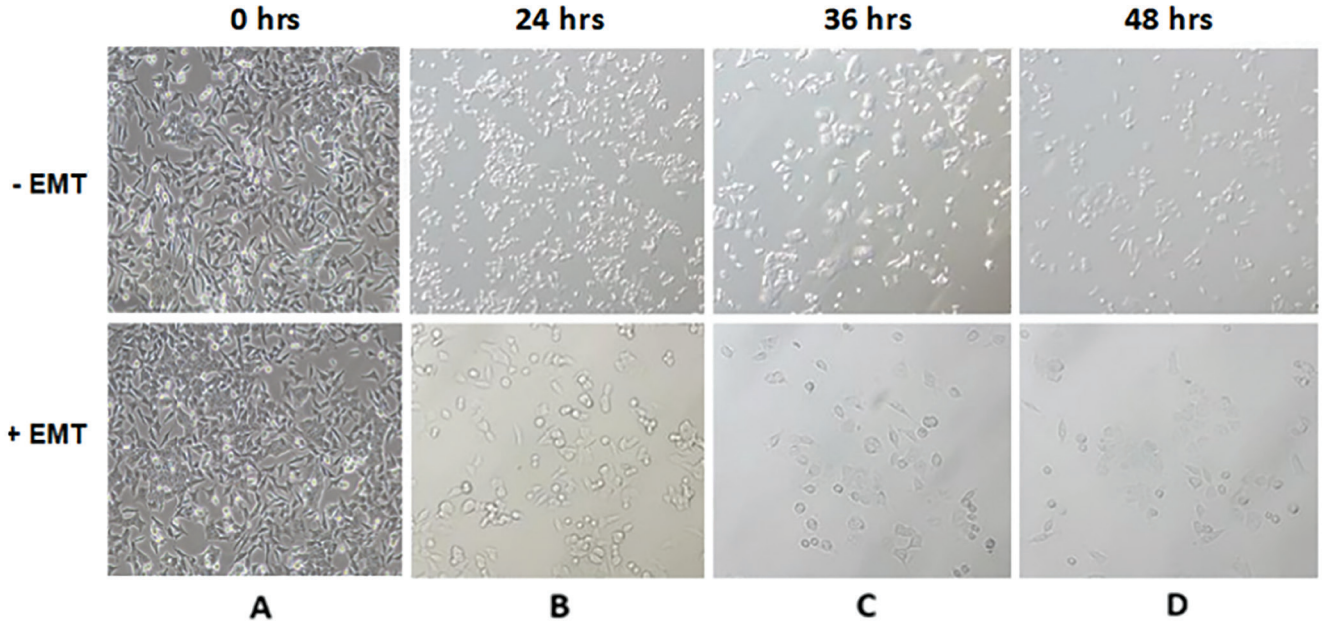

FIGURE 8: *In vitro* epithelial - mesenchymal transition induction assay.

Epithelial mesenchymal transition (EMT) induction on treatment of Bacoside A in HCT 116 colon cancer cells (A) Untreated cells showed viable cells with epithelial morphology (B) Lost on epithelial morphology and dead cells were observed in with less density (C, D) Structurally disrupted and dead cells were identified on EMT induction within 24 hours of bacoside A treatment.

TABLE 3: Fold changes in the gene expression analysis.

Genes	Time (hrs)	Average CT	ΔCT	ΔΔCT	$2^{-\Delta\Delta CT}$
E-Cadherin	0	35.85	17.18	-0.0183333	1.012788761
	12	34.74	16.21	-0.9883333	1.98389174
	24	33.73	15.065	-2.1333333	4.38729982
	36	32.64	14.09	-3.1083333	8.62385727
	48	32.23	13.85	-3.3483333	10.1847121
Snail1	0	32.615	13.945	-3.1117	8.644005559
	12	31.925	13.395	-2.5617	5.904029787
	24	30.92	12.255	-1.4217	2.679010062
	36	29.6	11.05	-0.2167	1.162072436
	48	28.605	10.225	0.6083	0.655969208
Vimentin	0	24.78	6.11	-1.1633333	2.239743156
	12	25.385	6.855	-0.4183333	1.133638278
	24	26.355	7.69	0.4166667	0.749153521
	36	26.385	7.835	0.5616667	0.0677519
	48	26.655	8.275	1.0016667	0.449422699

CT: Computed tomography.

therefore expected that the free radicals are scavenged by Bacoside A and that their attack on the macromolecules such as lipids, proteins, and nucleic acids is also mimicked. Research findings also support the present work, in an *in vivo* study in which dichlorvos induced oxidative stress and membrane instability, these effects were reversed by Bacoside A. research findings with the combinations of bacosides treatment proved they have the ability of membrane stabilization and give significant protection of cell membranes against injurious substances and thereby exhibit anti-inflammatory activity. These findings correlated with compounds inferred to stabilize lysosomal membranes, one of the mechanisms by

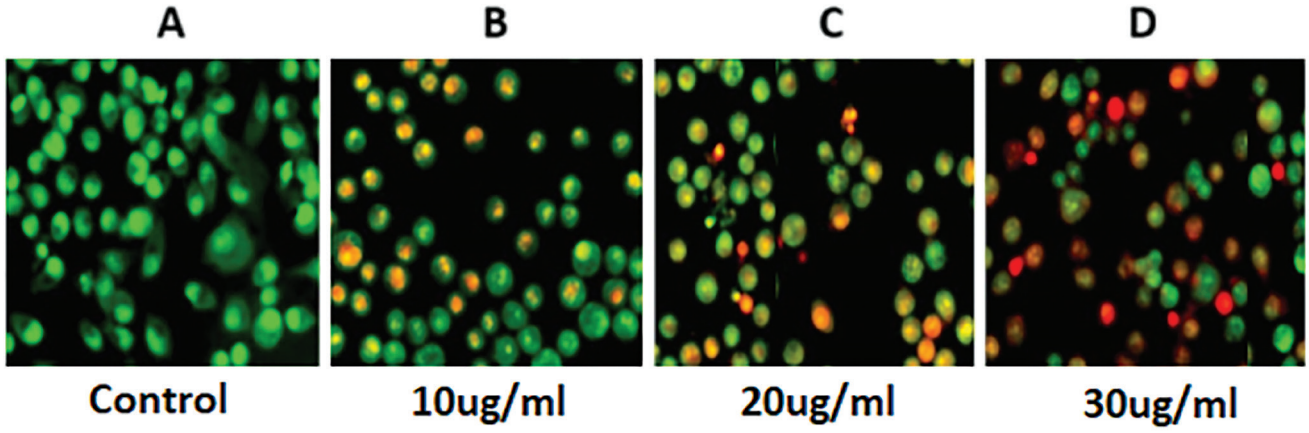

FIGURE 9: Apoptosis assay.

Apoptotic characteristics on treatment of Bacoside A in HCT 116 colon cancer were observed on 24 hours of treatment (A) Viable cells indicated by green fluorescence, (B, C) Early apoptosis features, namely, blebbing and chromatin condensation as well as late apoptotic cells were detected after 24 hours of treatment with bacoside A indicated by orange fluorescence, (D) Late apoptosis and cell necrosis were observed after 24 hours of Bacoside A shown by red fluorescence.

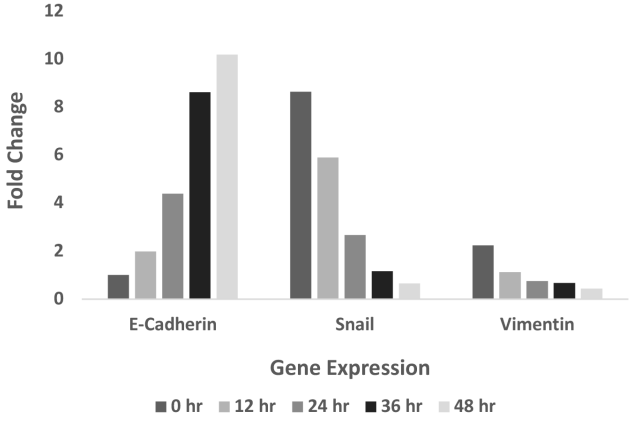

FIGURE 10: mRNA expression analysis.

which the test herb mediates its anti-inflammatory action.[32] Another study supports the present investigation states that the Bacoside A is a high potential compound that maintains the membrane potential and strengthen the molecular stability in colon cancer, mammary cancer, pancreatic cancer and in other illness such as Alzheimer's disease and Parkinson's disease.[10]

The membrane-bound proteins play an important role in maintaining membrane stability and integrity in cancer cells. In colon cancer, the ECM of the cell increases stiffness and gains the ability to hold the cells together and to communicate biochemical signals and information for its action. Alterations in this mechanism lead to variations in structure and function. Such proteins—MMPs, cadherins, integrins, fibronectin, and laminin—may be affected by oncogenic activation of canonical signalling pathways primarily involved in

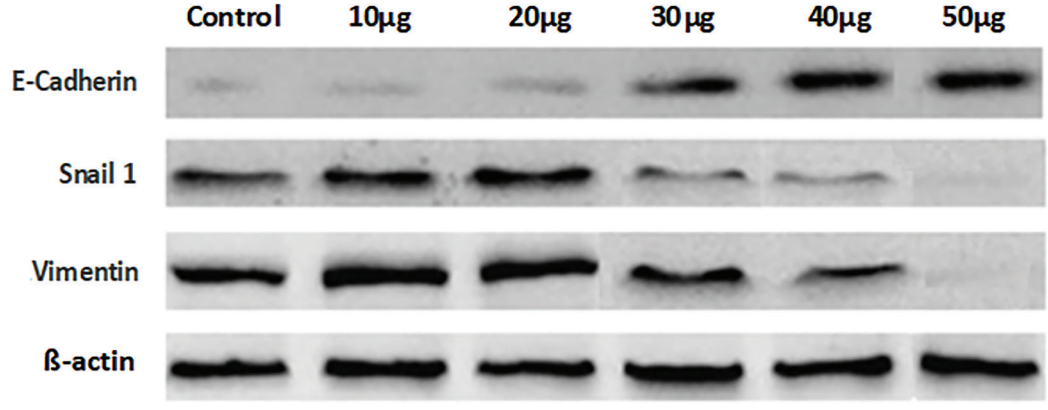

FIGURE 11: mRNA expression analysis.

cytoskeletal modification during adhesion and migration. The results of the present study's cell migration analysis indicate that rapid migrations observed in cancer cells may be due to disturbances in cell adhesion proteins, which effectively promote cancer cell mobility and lead to metastasis. Bacoside A effectively reverses this process by up to 75% at concentrations above 32 µg/mL. Studies conducted by Hai-Yun Liu (2024) reported that Bacoside A inhibits migration-associated matrix metalloproteinases MMP2 and MMP9.[12] Another study supports that combined doses of bacopside I and II possess a synergistic action in inhibiting endothelial migration and inducing apoptosis in CRC cells.[33]

The present study clearly demonstrates the inhibitory effect of Bacoside A on the colony-forming capacity of cancer cells. Colony formation is the capacity of individual cancer cells to form large colonies in which they exist as undifferentiated cancer stem cells. During treatment with Bacoside A at IC_{50} and above, the number of colony-forming units of cancer cells is effectively reduced. This may be due to increased cell death induced by Bacoside A treatment, which reduces cell integrity and disrupts the coordinating actions of related proteins required for colony formation. Studies using 3D clonogenic assays can facilitate understanding of the mechanisms underlying CSC stemness, notably drug resistance, pro- and anti-apoptotic mechanisms, and pathways involved in self-renewal. Cancer cells protease activity improve its invading capacity to other tissues by degrading the basement membrane and the surrounding ECM.[34] The studies conducted by Ishikawa et al.[35] state that clonogenic assays evaluate the ability of single cells to proliferate and form colonies.

The EMT induction assay was performed to assess the ability of the cancer cells: How they can separate from each other, adapt, and migrate to other areas. Signals from the tumor microenvironment stimulate cancer cells to undergo EMT and adopt an invasive phenotype. In the present study, lower-concentration Bacoside A-treated groups showed comparatively higher cell counts, whereas higher-concentration groups had significantly fewer cells, although individual cells were still observed. This indicates that Bacoside A can effectively reduce the number of cancer cells, and its effects on cell migration and invasion may be due to altered signaling pathways. A Literature review also supports that the study conducted in lung cancer provides promising evidence that certain drugs can induce changes in epithelial characteristics and mesenchymal conversion, which are involved in a wide variety of processes such as invasion, metastasis, and drug resistance in cancer cells.[36] Another noteworthy finding from the analysis of the EMT transition in breast cancer cells reveals that the combinatorial involvement of collagen and pro-inflammatory cytokines plays an important role in the phenotypic changes.[37]

The apoptotic studies in the present investigations clearly show that Bacoside A is an effective agent that destroys cancer cells and induces apoptosis. At lower concentrations, cell death is minimal, whereas at the IC_{50} a greater number of dead cells was observed. Several reports have suggested that the anticancer potential of plant-based chemotherapeutic agents triggers apoptosis by inducing functional changes in mitochondrial energy transfer in cancer cells through alterations in various signalling and cell-cycle arrest pathways. Further supporting evidence indicates that the aqueous fraction of the ethanolic extract of B. monneri inhibits cell viability, colony formation, cell migration , and induces apoptotic cell death in Cal33 and FaDu cells.[28]

EMT is induced during cancer progression and contributes to the formation of metastatic colonies. It is the process by which epithelial cells lose their differentiated characteristics and acquire mesenchymal traits. In this process, cancer cells acquire metastatic properties by increasing their mobility, invasiveness, and resistance to apoptosis. Furthermore, EMT-derived tumor cells acquire stem cell characteristics and become resistant to therapy. Protein expression levels related to migration, apoptosis, and autophagy were assessed by Western blotting. Findings revealed that, in the untreated group, the epithelial marker E-cadherin was downregulated, while the transcription factor Snail1 and the mesenchymal marker vimentin were upregulated; however, the expression of these proteins was modified during Bacoside A treatment. Here, the reciprocal interference between an altering tumor microenvironment and the EMT phenotype was investigated *in vitro*, suggesting that Bacoside A can promote the expression of epithelial markers such as E-cadherin, which is often down-regulated in EMT, thereby helping to maintain cell-cell adhesion and prevent cell migration. The anti-EMT effects of Bacoside A are thought to involve modulation of signaling pathways such as the Wnt/β-catenin pathway, which plays a crucial role in regulating EMT. Studies support that the EMT program is activated by autocrine and paracrine signals from the tumor microenvironment, which include a variety of cytokines, interleukins, and growth factors that stimulate signaling pathways in tumor cells and converge on the activation of a set of transcription factors. In addition to EMT-TF regulation of genes associated with epithelial and mesenchymal states, other regulatory mechanisms contribute to the control of these cell states.[38]

The overall finding of the present study clearly demonstrates the efficacy of Bacoside A against cancer cell migration. In addition, suppression of other transcriptional markers that support mesenchymal expression, such as Snail, Slug, and ZEB1, should be assessed. The extension studies related to the significant pathways that regulate the process of cancer metastasis in other cancers, such as liver and pancreatic cancers, in combination with the evaluation of the efficacy of Bacoside A administration

in the cancer-induced liver models, need to be analyzed. Further analysis of hypoxia-mediated arrest of cell migration can also be performed to strengthen the present findings.

CONCLUSION

EMT is recognized as playing a key role in cancer development, metastasis, and chemotherapy resistance, and its crucial roles throughout cancer progression have recently been investigated. Although there is still debate about whether EMT causes cancer metastasis, its importance in cancer chemoresistance is becoming more widely recognized, with many EMT-related signaling pathways implicated in cancer chemoresistance. Targeted cancer treatment has been an emerging field over the past decade. Several monoclonal antibody therapies and small-molecule compounds, particularly kinase inhibitors, have been discovered or synthesized and are undergoing clinical trials, demonstrating improved anticancer efficacy. While many targeted therapies demonstrated encouraging preliminary clinical outcomes, such as improved overall survival, a significant proportion of patients who received targeted therapies developed drug resistance after long-term treatment.

Ethics

Ethics Committee Approval: Sri Ramachandra Institute of Higher Education and Research Ethics Committee approval was obtained for conducting the cell line studies (approval number: IEC-NI/22/JUL/83/85, date: 14.10.2022).

Informed Consent: Retrospective study.

Footnotes

Conflict of Interest: No conflict of interest was declared by the author.

Financial Disclosure: The author declared that this study recieved financial support from Sri Ramachandra Institute of Higher Education and Resaerch, under GATE project (reference number: 34/DOF/2022)

REFERENCES

1. Siegel RL, Wagle NS, Cercek A, Smith RA, Jemal A. Colorectal cancer statistics, 2023. CA Cancer J Clin. 2023;73(3):233-254. [Crossref] [PubMed]
2. Shin AE, Giancotti FG, Rustgi AK. Metastatic colorectal cancer: mechanisms and emerging therapeutics. Trends Pharmacol Sci. 2023;44(4):222-236. [Crossref] [PubMed] [PMC]
3. Vu T, Datta PK. Regulation of EMT in colorectal cancer: a culprit in metastasis. Cancers (Basel). 2017;9(12):171. [Crossref] [PubMed] [PMC]
4. Pavlič A, Urh K, Štajer K, Boštjančič E, Zidar N. Epithelial-mesenchymal transition in colorectal carcinoma: comparison between primary tumor, lymph node and liver metastases. Front Oncol. 2021;11:662806. [Crossref] [PubMed] [PMC]
5. Ribatti D, Tamma R, Annese T. Epithelial-mesenchymal transition in cancer: a historical overview. Transl Oncol. 2020;13(6):100773. [Crossref] [PubMed] [PMC]
6. Huang Z, Zhang Z, Zhou C, Liu L, Huang C. Epithelial-mesenchymal transition: the history, regulatory mechanism, and cancer therapeutic opportunities. MedComm (2020). 2022;3(2):e144. [Crossref] [PubMed] [PMC]
7. Sapio L, Naviglio S. Innovation through tradition: the current challenges in cancer treatment. Int J Mol Sci. 2022;23(10):5296. [Crossref] [PubMed] [PMC]
8. Islam MR, Akash S, Rahman MM, et al. Colon cancer and colorectal cancer: prevention and treatment by potential natural products. Chem Biol Interact. 2022;368:110170. [Crossref] [PubMed]
9. Ghosh S, Khanam R, Acharya Chowdhury A. The evolving roles of *Bacopa monnieri* as potential anti-cancer agent: a review. Nutr Cancer. 2176-2166:(12-11)73;2021. [Crossref] [PubMed]
10. Roy D, Mullick R, Das D, Samanta D, Ganguli S. A review on the potential of bacosides as *therapeutic lead* molecules, International Research Journal of Plant Science. 2021;12(4):1-10. [Crossref]
11. Vishnupriya P, Saikia S, Kumar GS, Viswanadha VP, Molecular docking analysis of bacoside a with selected signalling factors involved in glioblastoma. Journal of Pharmaceutical Research International. 2022;34(32B):35-55. [Crossref]
12. Palethorpe HM, Smith E, Tomita Y, et al. Bacopasides I and II act in synergy to inhibit the growth, migration and invasion of breast cancer cell lines. Molecules. 2019;24(19):3539. [Crossref] [PubMed] [PMC]
13. Kim YZ, Kim CY, Lim J, et al; KSNO Guideline Working Group. The Korean society for neuro-oncology (KSNO) guideline for glioblastomas: version 2018.01. Brain Tumor Res Treat. 2019;7(1):1-9. [Crossref] [PubMed] [PMC]
14. Herrera-Quiterio GA, Encarnación-Guevara S. The transmembrane proteins (TMEM) and their role in cell proliferation, migration, invasion, and epithelial-mesenchymal transition in cancer. Front Oncol. 2023;13:1244740. [Crossref] [PubMed] [PMC]
15. Kaufhold S, Bonavida B. Central role of Snail1 in the regulation of EMT and resistance in cancer: a target for therapeutic intervention. J Exp Clin Cancer Res. 2014;33(1):62. [Crossref] [PubMed] [PMC]
16. Banerjee S, Lo WC, Majumder P, et al. Multiple roles for basement membrane proteins in cancer progression and EMT. Eur J Cell Biol. 2022;101(2):151220. [Crossref] [PubMed]
17. Valko M, Leibfritz D, Moncol J, Cronin MT, Mazur M, Telser J. Free radicals and antioxidants in normal physiological functions and human disease. Int J Biochem Cell Biol. 2007;39(1):44-84. [Crossref] [PubMed]
18. Leong LP, ShuiG. An investigation of antioxidant capacity of fruits in Singapore markets. Food Chemistry. 2002;76:69-75. [Crossref]
19. Benzie IF, Strain JJ. Ferric reducing/antioxidant power assay: direct measure of total antioxidant activity of biological fluids and modified version for simultaneous measurement of total antioxidant power and ascorbic acid concentration. Methods Enzymol. 1999;299:15-27. [Crossref] [PubMed]
20. Aguilar Diaz De Leon J, Borges CR. Evaluation of oxidative stress in biological samples using the thiobarbituric acid reactive substances assay. J Vis Exp. 2020;(159):10.3791/61122. [Crossref] [PubMed] [PMC]
21. Das P, Ghosal K, Jana NK, Mukherjee A, Basak P. Green synthesis and characterization of silver nanoparticles using belladonna mother tincture and its efficacy as a potential antibacterial and anti-inflammatory agent, Materials Chemistry and Physics. 2019;228:310-317. [Crossref]

22. Carter P. Spectrophotometric determination of serum iron at the submicrogram level with a new reagent (ferrozine). Anal Biochem. 1971;40(2):450-458. [Crossref] [PubMed]
23. Bobadilla AVP, Arévalo J, Sarró E, et al. In vitro cell migration quantification method for scratch assays. J R Soc Interface. 2019;16(151):20180709. [Crossref] [PubMed] [PMC]
24. Franken NA, Rodermond HM, Stap J, Haveman J, van Bree C. Clonogenic assay of cells in vitro. Nat Protoc. 2006;1(5):2315-2319. [Crossref] [PubMed]
25. Tang Y, Herr G, Johnson W, Resnik E, Aho J. Induction and analysis of epithelial to mesenchymal transition. J Vis Exp. 2013;(78):50478. [Crossref] [PubMed] [PMC]
26. Mascotti K, McCullough J, Burger SR. HPC viability measurement: trypan blue versus acridine orange and propidium iodide. Transfusion. 2000;40(6):693-696. [Crossref] [PubMed]
27. Fares J, Fares MY, Khachfe HH, Salhab HA, Fares Y. Molecular principles of metastasis: a hallmark of cancer revisited. Signal Transduct Target Ther. 2020;5(1):28. [Crossref] [PubMed] [PMC]
28. Mishra SR, Behera BP, Singh VK, et al. Anticancer activity of *Bacopa monnieri* through apoptosis induction and mitophagy-dependent NLRP3 inflammasome inhibition in oral squamous cell carcinoma. Phytomedicine. 2024;123:155157. [Crossref] [PubMed]
29. Sekhar VC, Viswanathan G, Baby S. Bacopaside II nanoparticles inhibit proliferation of C6 glioma cells, Phytomedicine. 2021;1(3):100040. [Crossref]
30. Sekhar VC, Viswanathan G, Baby S. Insights Into the molecular aspects of neuroprotective bacoside a and bacopaside I. Curr Neuropharmacol. 2019;17(5):438-446. [Crossref] [PubMed] [PMC]
31. Fatima U, Roy S, Ahmad S, et al. Investigating neuroprotective roles of *Bacopa monnieri* extracts: mechanistic insights and therapeutic implications. Biomed Pharmacother. 2022;153:113469. [Crossref] [PubMed]
32. Bist R, Chaudhary B, Bhatt DK. Defensive proclivity of bacoside A and bromelain against oxidative stress and AChE gene expression induced by dichlorvos in the brain of Mus musculus. Sci Rep. 2021;11(1):3668. [Crossref] [PubMed] [PMC]
33. Liu HY, Ji YL, Du H, Chen SH, Wang DP, Lv QL. Bacoside a inhibits the growth of glioma by promoting apoptosis and autophagy in U251 and U87 cells. Naunyn Schmiedebergs Arch Pharmacol. 2024;397(4):2105-2120. [Crossref] [PubMed]
34. Gomes NP, Frederick B, Jacobsen JR, Chapnick D, Su TT. A high throughput screen with a clonogenic endpoint to identify radiation modulators of cancer. Radiat Res. 2023;199(2):132-147. [Crossref] [PubMed] [PMC]
35. Ishikawa H, Menju T, Toyazaki T, et al. A novel cell-based assay for the high-throughput screening of epithelial-mesenchymal transition inhibitors: identification of approved and investigational drugs that inhibit epithelial-mesenchymal transition. Lung Cancer. 2023;175:36-46. [Crossref] [PubMed]
36. Isert L, Mehta A, Loiudice G, Oliva A, Roidl A, Merkel OM. An in vitro approach to model EMT in breast cancer. Int J Mol Sci. 2023;24(9):7757. [Crossref] [PubMed] [PMC]
37. Chaudhry GE, Md Akim A, Sung YY, Sifzizul TMT. Cancer and apoptosis: the apoptotic activity of plant and marine natural products and their potential as targeted cancer therapeutics. Front Pharmacol. 2022;13:842376. [Crossref] [PubMed] [PMC]
38. Morgado-Diaz JA, Wagner MS, Sousa-Squiavinato ACM, et al. Epithelial-mesenchymal transition in metastatic colorectal cancer. In: Morgado-Diaz JA, editor. Gastrointestinal Cancers [Internet]. Brisbane (AU): Exon Publications; 2022 Sep 30. Chapter 3. [Crossref]

ORIGINAL ARTICLE

DOI: 10.37047/jos.galenos.2026.2025-10-12

J Oncol Sci 2026;12(1):32-40

Scottish Inflammatory Prognostic Score Predicts Survival in Metastatic Non-Small-Cell Lung Cancer Treated with Immune Checkpoint Inhibitors

Caner ACAR, Haydar Çağatay YÜKSEL, Gökhan ŞAHİN, Fatma Pınar AÇAR, Erdem GÖKER

Ege University Faculty of Medicine, Department of Internal Medicine, Division of Medical Oncology, İzmir, Türkiye

ABSTRACT

Objective: The Scottish Inflammatory Prognostic Score (SIPS)—based on serum albumin and neutrophil count—has prognostic value in programmed death-ligand 1 (PD-L1)-high non-small-cell lung cancer (NSCLC), but its performance in broader real-world populations is uncertain.

Material and Methods: We conducted a single-centre, retrospective study of patients with metastatic NSCLC who were treated with immune-checkpoint inhibitors between June 2016 and January 2025. SIPS was calculated pre-treatment (albumin 3.5 g/dL=1; neutrophils >7,500/μL=1). Progression-free survival (PFS) and overall survival (OS) were estimated using the Kaplan-Meier method and compared using the log-rank test. Cox regression was performed to estimate hazard ratios (HRs) and account for potential confounding.

Results: Among 178 patients, the median age was 64.9 years, 80.3% were male, and 55 (30.9%) were classified as SIPS high-risk. High-risk was associated with shorter PFS (median 3.13 months, 95% confidence interval (CI) 2.27-3.70 vs. 4.27 months, 95% CI: 3.63-6.47; p<0.001) and shorter OS (median 4.73 months, 95% CI: 3.23-7.07 vs. 15.23 months, 95% CI: 12.23-23.90; p<0.001). In multivariable analyses, SIPS high-risk predicted inferior PFS (HR: 1.72, 95% CI: 1.18-2.52; p=0.005) and OS (HR: 2.21, 95% CI: 1.48-3.31; p<0.001). Effects were consistent across PD-L1 strata, treatment regimens, and lines of therapy; no significant interactions were detected.

Conclusion: In a real-world NSCLC cohort, SIPS independently stratified PFS and OS, and may complement routine clinical variables in baseline risk discussions. Prospective multi-centre studies should validate SIPS, assess longitudinal applications, and determine whether SIPS-guided strategies improve patient-centred outcomes.

Keywords: Cancer diagnosis and treatments; immunotherapy; lung cancer; medical oncology; oncology

INTRODUCTION

Lung cancer is the leading cause of cancer mortality globally, with 2.5 million new cases and 1.8 million deaths, according to GLOBOCAN 2022 estimates.[1] Non-small-cell lung cancer (NSCLC) accounts for approximately 85% of lung cancer cases.[2] Over the last decade, immune checkpoint inhibitors (ICIs) have transformed the treatment of solid tumors, resulting in substantial improvements in survival outcomes.[3] Since nivolumab was approved in 2015, ICIs have become a cornerstone of NSCLC therapy, either as monotherapy or in combination with platinum-based chemotherapy.[4] In a population-based analysis using the SEER database, Wang et al.[5] reported that the 5-year cancer-specific survival rate in NSCLC improved from 9.0% in the pre-immunotherapy era (2010-2014) to 14.3% in the immunotherapy era (2015-2020), thereby confirming the real-world survival benefit of ICIs in lung cancer. Despite these advances, both primary and acquired resistance to ICIs remain common, thereby limiting the durable benefit for a significant proportion of patients.[6] Accordingly, there is a critical need for reliable biomarkers to refine patient selection for ICIs.

Correspondence: Caner ACAR MD,
Ege University Faculty of Medicine, Department of Internal Medicine, Division of Medical Oncology, İzmir, Türkiye

E-mail: acar.caner@yahoo.com

ORCID ID: orcid.org/0000-0002-9782-6807

Received: 24.10.2025 **Accepted:** 01.02.2026 **Epub:** 09.03.2026 **Publication Date:** 18.03.2026

Cite this article as: Acar C, Yüksel HÇ, Şahin G, Açar FP, Göker E. Scottish inflammatory prognostic score predicts survival in metastatic non-small-cell lung cancer treated with immune checkpoint inhibitors. J Oncol Sci. 2026;12(1):32-40

Available at journalofoncology.org

Currently, programmed death-ligand 1 (PD-L1) expression and tumor mutational burden (TMB) are the most commonly used biomarkers to guide ICI therapy in NSCLC.[7] Although clinically useful, PD-L1 is an imperfect predictor: high expression does not guarantee benefit, and some patients with low expression still respond to treatment. Moreover, PD-L1 testing is affected by inter-assay variability and intratumoral heterogeneity, which reduces its predictive reliability at clinically relevant thresholds.[8] Following the phase II KEYNOTE-158 trial, pembrolizumab was approved to treat pembrolizumab to treat TMB-high tumors in previously treated patients across cancer types.[9] Nevertheless, assay and bioinformatic non-uniformity—together with variable cut-points—complicate its translation into practice.[10] Somatic genomic alterations also shape ICI response; for instance, in KRAS-mutant NSCLC, co-mutations in STK11 or KEAP1 are strongly associated with reduced benefit from PD-L1 blockade.[11] Accordingly, there is a need for complementary biomarkers that are robust, clinically practical, and amenable to serial, non-invasive assessment.

Peripheral blood biomarkers have recently attracted attention due to their accessibility, low cost, and reproducibility. Systemic inflammation can impair antitumor immunity by suppressing T-cell responses in the tumor microenvironment;[12] malnutrition has consistently been linked to poor prognosis across multiple cancer types.[13] Composite inflammatory and nutritional indices—such as the neutrophil-to-lymphocyte ratio, platelet-to-lymphocyte ratio, modified Glasgow prognostic score, and prognostic nutritional index—have demonstrated prognostic utility not only in lung cancer but also in various other malignancies.[14-16] Recently, Stares et al.[17] proposed the Scottish Inflammatory Prognostic Score (SIPS), a simple score based on serum albumin and neutrophil count, for patients with PD-L1 ≥50% NSCLC treated with first-line pembrolizumab, and showed that it effectively stratified survival outcomes. Subsequent external validations in PD-L1-high NSCLC confirmed its prognostic relevance.[18] Nevertheless, the performance of SIPS across broader patient populations—including different treatment lines and varying PD-L1 strata—remains uncertain. Therefore, we investigated the prognostic utility of SIPS in patients with metastatic NSCLC treated with ICIs and examined whether its effect was reproducible across clinical strata.

MATERIAL AND METHODS

This retrospective single-center study enrolled patients treated at the Department of Medical Oncology, Ege University, between June 1, 2016, and January 1, 2025. Eligible participants had metastatic NSCLC and were treated with ICIs. We excluded patients who lacked laboratory data or follow-up information necessary for survival analyses. The study adhered to Good Clinical Practice and to the ethical principles of the Declaration of Helsinki, and was approved by the Ege University Institutional Review Board (approval no: 25-10.1T/23, date: 16.10.2025).

Data were abstracted from electronic records and included demographics; Eastern Cooperative Oncology Group performance status (ECOG PS); histologic subtype; PD-L1 level; metastatic sites and their count; ICI treatment line; receipt of chemoimmunotherapy; and the laboratory variables required to compute the SIPS (serum albumin and absolute neutrophil count). SIPS was derived by awarding one point for albumin <3.5 g/dL and one point for neutrophils >7,500/μL. Although the original scheme defines low (0), intermediate (1), and high (2) risk, we merged the intermediate and high categories—given the small number of high-risk cases (n=9)—into a single "high-risk" group (scores 1-2), and low-risk corresponded to a score of 0. Progression-free survival (PFS) was defined as the interval from ICI initiation to documented progression or death, and overall survival (OS) was defined as the interval from ICI initiation to death from any cause.

Statistical Analysis

Categorical variables are presented as n (%), whereas continuous variables are summarized as medians and interquartile ranges (IQR). Baseline group comparisons (SIPS low vs. high) were conducted using the chi-square test or Fisher's exact test for categorical variables and the Mann-Whitney U test for continuous variables. PFS and OS were analyzed with Kaplan-Meier estimates and compared using the log-rank test. Associations with PFS and OS were explored using Cox proportional hazards models in both univariable and multivariable forms. To limit residual confounding, covariates with univariable $p<0.20$ were entered into the multivariable models. All analyses were performed in Jamovi 2.3.28 and R 4.2.2. Two-sided p-values <0.05 were considered statistically significant.

RESULTS

Baseline Characteristics

In total, 178 patients were eligible. Baseline variables are detailed in Table 1. The median age was 64.9 years (IQR: 54.6-75.2), with 143 males (80.3%). Non-squamous histology was the most common subtype (67.4%). Fifteen patients (8.4%) received chemoimmunotherapy, whereas 163 (91.6%) received PD-1/PD-L1 monotherapy. ICI was given as first-line treatment to 31 patients (17.4%) and as second- or later-line treatment to 147 patients (82.6%).

SIPS was calculated from pretreatment albumin and neutrophil counts. The SIPS low-risk (0 points) and high-risk

(1-2 points) groups consisted of 123 (69.1%) and 55 (30.9%) patients, respectively. The comparison of patients' baseline characteristics by SIPS risk groups is shown in Table 1. As expected, the high-risk group had lower albumin and higher neutrophil counts (both p<0.001). ECOG PS ≥2 was more frequent in the high-risk group (30.9% vs. 7.3%; p<0.001), whereas other baseline features did not differ significantly between the risk groups (p>0.05 for each variable).

TABLE 1: Baseline clinicopathological characteristics of patients according to SIPS risk groups.

Variables	SIPS low-risk (n=123)	SIPS high-risk (n=55)	Total (n=178)	p
Age, years				
<65	63 (51.2)	27 (49.1)	90 (50.6)	0.920
≥65	60 (48.8)	28 (50.9)	88 (49.4)	
Sex				
Male	97 (78.9)	46 (83.6)	143 (80.3)	0.592
Female	26 (21.1)	9 (16.4)	35 (19.7)	
ECOG PS				
0-1	114 (92.7)	38 (69.1)	152 (85.4)	<0.001
≥2	9 (7.3)	17 (30.9)	26 (14.6)	
Histology				
Squamous	41 (33.3)	17 (30.9)	58 (32.6)	0.884
Non-squamous	82 (66.7)	38 (69.1)	120 (67.4)	
PD-L1				
Negative	42 (34.1)	12 (21.8)	54 (30.3)	0.370
1-49%	17 (13.8)	8 (14.5)	25 (14.0)	
≥50	33 (26.8)	20 (36.4)	53 (29.8)	
Unknown	31 (25.2)	15 (27.3)	46 (25.8)	
Brain metastasis				
No	94 (77.0)	44 (80.0)	138 (78.0)	0.808
Yes	28 (23.0)	11 (20.0)	39 (22.0)	
Liver metastasis				
No	110 (90.2)	45 (81.8)	155 (87.6)	0.190
Yes	12 (9.8)	10 (18.2)	22 (12.4)	
Bone metastasis				
No	78 (63.4)	32 (58.2)	110 (61.8)	0.619
Yes	45 (36.6)	23 (41.8)	68 (38.2)	
Number of metastatic sites				
<3	57 (46.3)	19 (34.5)	76 (42.7)	0.191
≥3	66 (53.7)	36 (65.5)	102 (57.3)	
Chemotherapy combination				
No	115 (93.5)	48 (87.3)	163 (91.6)	0.276
Yes	8 (6.5)	7 (12.7)	15 (8.4)	
ICI treatment line				
First	21 (17.1)	10 (18.2)	31 (17.4)	1.000
Second and later	102 (82.9)	45 (81.8)	147 (82.6)	
Albumin, g/dL	4.1 (3.9, 4.3)	3.4 (3.0, 3.8)	4.0 (3.6, 4.2)	<0.001
Neutrophil/μL	4500 (3650, 5660)	7970 (5665, 11150)	5015 (3910, 6747)	<0.001

SIPS: Scottish Inflammatory Prognostic Score; ECOG PS: Eastern Cooperative Oncology Group performance status; PD-L1: Programmed death-ligand 1; ICI: Immune checkpoint inhibitor.
Data are presented as n (%) for categorical variables and as medians (IQR) for continuous variables.

Kaplan-Meier Estimates and Cox Proportional Hazards Analyses

Kaplan-Meier estimates showed significantly worse outcomes for the SIPS high-risk group (Figure 1). Median PFS was 3.13 months [95% confidence interval (CI): 2.27-3.70] in the high-risk group versus 4.27 months (95% CI: 3.63-6.47) in the low-risk group (p<0.001). Median OS was 4.73 months (95% CI: 3.23-7.07) for the high-risk group versus 15.23 months (95% CI: 12.23-23.90) for the low-risk group (p<0.001).

Cox regression results for PFS are shown in Table 2. For PFS, univariable Cox models identified the following significant risk factors: ECOG PS ≥2 [hazard ratio (HR): 2.47 (95% CI: 1.61-3.80)], liver metastasis [HR: 2.36 95% CI: 1.47-3.77]), bone metastasis [HR: 1.42 (95% CI: 1.02-1.97)], number of metastatic sites ≥3 [HR: 2.03 (95% CI: 1.45-2.83)], and SIPS high-risk [HR: 1.85 (95% CI: 1.32-2.61)]. Variables with univariable p<0.20 were included in the multivariable analysis. SIPS high-risk status remained independently associated with shorter PFS (HR: 1.72; 95% CI: 1.18-2.52; p=0.005). ECOG PS ≥2 (HR: 1.70, 95% CI: 1.05-2.75), liver metastasis (HR: 1.66, 95% CI: 1.01-2.75), and ≥3 metastatic sites (HR: 1.98, 95% CI: 1.31-2.98) were also independent risk factors.

The Cox regression results for OS are presented in Table 3. Univariable analyses identified ECOG PS ≥2 [HR: 3.36 (95% CI: 2.14-5.26)], liver metastasis [HR: 2.44 (95% CI: 1.49-4.01)], bone metastasis [HR: 1.69 (95% CI: 1.19-2.42)], ≥3 metastatic sites [HR: 2.80 (95% CI: 1.90-4.13)], and SIPS high-risk [HR: 2.53 (95% CI: 1.74-3.67)] as significant risk factors for shorter OS. Variables with univariable p<0.20 were included in the multivariable analysis. SIPS high-risk remained an independent predictor of worse OS [HR: 2.21 (95% CI: 1.48-3.31); p<0.001], together with ≥3 metastatic sites [HR: 2.52 (95% CI: 1.57-4.03)] and ECOG PS ≥2 [HR: 2.05 (95% CI: 1.20-3.51)].

Subgroup and Interaction Analyses

To examine the consistency of effects, we fitted Cox models including an interaction term between SIPS and each prespecified subgroup (age, sex, ECOG, histological subgroups, PD-L1 level, brain, liver, or bone metastases, number of metastatic sites, receipt of chemoimmunotherapy, and treatment line). Forest plots for OS and PFS (Figure 2) showed a uniformly adverse association of high SIPS risk across all subgroups, and no significant interactions were detected (all P-interaction >0.05), indicating that the prognostic effect of SIPS was consistent across clinically relevant patient subgroups.

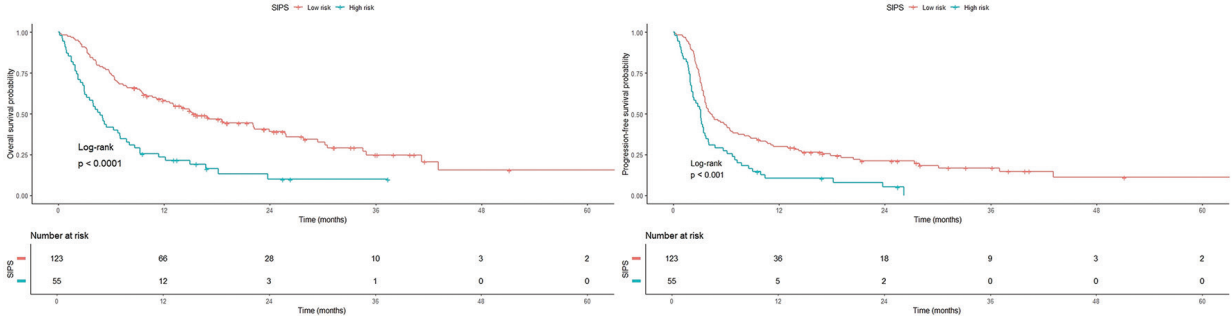

FIGURE 1: Kaplan-Meier curves for overall survival and progression-free survival and by SIPS risk groups.

SIPS: Scottish Inflammatory Prognostic Score

TABLE 2: Univariate and multivariate cox regression analyses for PFS.

Variables	Univariable analysis, HR (95% CI)	p	Multivariable analysis HR (95% CI)	p
Age, years				
<65				
≥65	1.15 (0.84-1.59)	0.382		
Sex				
Male				
Female	1.12 (0.75-1.66)	0.577		
ECOG PS				
0-1				
≥2	2.47 (1.61-3.80)	<0.001	1.70 (1.05-2.75)	0.032

TABLE 2: Continued

Variables	Univariable analysis, HR (95% CI)	p	Multivariable analysis HR (95% CI)	p
Histology				
Squamous				
Non-squamous	0.88 (0.63-1.23)	0.457		
PD-L1				
Negative				
1-49%	0.75 (0.45-1.27)	0.284	0.74 (0.44-1.27)	0.277
≥50	0.72 (0.48-1.08)	0.111	0.66 (0.43-1.01)	0.054
Unknown	1.03 (0.67-1.57)	0.902	0.99 (0.64-1.54)	0.980
Brain metastasis				
No				
Yes	1.16 (0.79-1.71)	0.453		
Liver metastasis				
No				
Yes	2.36 (1.47-3.77)	<0.001	1.66 (1.01-2.75)	0.048
Bone metastasis				
No				
Yes	1.42 (1.02-1.97)	0.035	0.84 (0.57-1.25)	0.397
Number of metastatic sites				
<3				
≥3	2.03 (1.45-2.83)	<0.001	1.98 (1.31-2.98)	0.001
Chemotherapy combination				
No				
Yes	1.12 (0.63-1.98)	0.697		
ICI treatment line				
First				
Second and later	1.18 (0.77-1.80)	0.439		
SIPS				
Low-risk				
High-risk	1.85 (1.32-2.61)	<0.001	1.72 (1.18-2.52)	0.005

SIPS: Scottish Inflammatory Prognostic Score; ECOG PS: Eastern Cooperative Oncology Group performance status; PD-L1: Programmed death-ligand 1; ICI: Immune checkpoint inhibitor; HR: Hazard ratio; CI: Confidence interval; PFS: Progression-free survival.

TABLE 3: Univariate and multivariate cox regression analyses for OS.

Variables	Univariable analysis, HR (95% CI)	p	Multivariable analysis HR (95% CI)	p
Age, years				
<65				
≥65	1.27 (0.89-1.81)	0.184	1.10 (0.75-1.62)	0.621
Sex				
Male				
Female	0.80 (0.50-1.28)	0.346		
ECOG PS				
0-1				
≥2	3.36 (2.14-5.26)	<0.001	2.05 (1.20-3.51)	0.009

TABLE 3: Continued				
Variables	**Univariable analysis, HR (95% CI)**	**p**	**Multivariable analysis HR (95% CI)**	**p**
Histology				
Squamous				
Non-squamous	0.85 (0.59-1.22)	0.369		
PD-L1				
Negative				
1-49%	0.93 (0.53-1.64)	0.812		
≥50	0.83 (0.52-1.31)	0.417		
Unknown	1.17 (0.74-1.86)	0.497		
Brain metastasis				
No				
Yes	1.36 (0.90-2.06)	0.139	1.13 (0.72-1.78)	0.594
Liver metastasis				
No				
Yes	2.44 (1.49-4.01)	<0.001	1.39 (0.80-2.39)	0.238
Bone metastasis				
No				
Yes	1.69 (1.19-2.42)	0.004	0.85 (0.54-1.34)	0.485
Number of metastatic sites				
<3				
≥3	2.80 (1.90-4.13)	<0.001	2.52 (1.57-4.03)	<0.001
Chemotherapy combination				
No				
Yes	0.86 (0.45-1.64)	0.640		
ICI treatment line				
First				
Second and later	1.47 (0.90-2.40)	0.123	1.40 (0.82-2.39)	0.215
SIPS				
Low-risk				
High-risk	2.53 (1.74-3.67)	<0.001	2.21 (1.48-3.31)	<0.001

SIPS: Scottish Inflammatory Prognostic Score; ECOG PS: Eastern Cooperative Oncology Group performance status; PD-L1: Programmed death-ligand 1; ICI: Immune checkpoint inhibitor; HR: Hazard ratio; CI: Confidence interval; OS: Overall survival.

DISCUSSION

In this study of patients with NSCLC treated with ICIs, the SIPS high-risk group was associated with shorter PFS and OS. These associations remained significant after adjustment for established covariates—including ECOG PS, metastatic burden, and PD-L1 expression—underscoring the independent prognostic value of SIPS. In addition, having ≥3 metastatic sites and an ECOG PS ≥2 were identified as adverse factors in multivariable analyses.

Our findings are consistent with, and extend, prior literature. Since SIPS was first introduced by Stares et al.[17] in 2022 as a novel prognostic score for patients with PD-L1 ≥50% NSCLC treated with pembrolizumab, Gomez-Randulfe et al.[18] externally validated SIPS in patients with PD-L1 ≥50% NSCLC, confirming robust survival stratification. In a post-progression analysis following pembrolizumab, Stares et al.[19] again showed that SIPS tracked survival and suggested its utility in identifying patients who may benefit from best supportive care and earlier referral to palliative care. Among patients with cancer of unknown primary, SIPS effectively stratified survival across favorable- and poor-risk groups defined by clinicopathologic features.[20] Evidence from other tumors further supports generalizability: in patients with

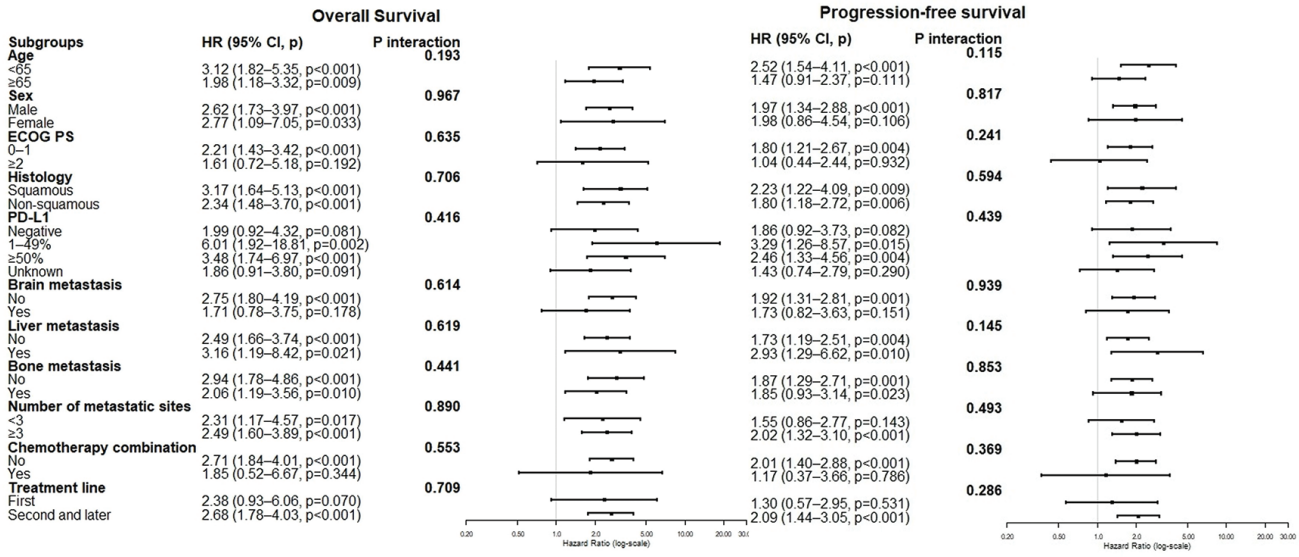

FIGURE 2: Subgroup analyses and interaction tests for SIPS high-risk with overall survival and progression-free survival.

SIPS: Scottish Inflammatory Prognostic Score

esophageal squamous cell carcinoma receiving neoadjuvant chemoimmunotherapy, pretreatment SIPS predicted 3-year disease-free survival (DFS),[21] and in patients with hepatocellular carcinoma after hepatectomy, SIPS provided meaningful DFS risk stratification.[22] Notably, Raynes et al.[23] reported higher irAE incidence in SIPS low-risk patients with lung cancer, implying that SIPS—by indexing systemic inflammation—may also identify patient subsets at increased risk of immune-related toxicity. Beyond oncology settings, Taş et al.[24] linked SIPS to in-hospital mortality among patients with acute heart failure, suggesting broader applicability of SIPS as an inflammation-based risk score. Beyond corroborating prior reports, our study adds to the generalizability by showing that in a real-world NSCLC cohort spanning all PD-L1 strata (<1%, 1-49%, ≥50%), including patients treated with chemoimmunotherapy, ICI monotherapy, and those receiving ICI beyond first-line, SIPS consistently stratified risk for both PFS and OS. Notably, efficacy associations were stable across these subgroups, and we detected no statistically significant interactions.

The biological plausibility of SIPS as a composite marker is strong. By combining neutrophilia and hypoalbuminemia, SIPS captures systemic inflammation and nutritional status in a single score. Neutrophils are the front-line defenders against pathogens; however, accumulating evidence shows they also promote tumor progression and can modulate responses to anticancer therapies. Elevated neutrophil counts—often reflective of a pro-inflammatory milieu—are associated with poorer outcomes and reduced benefit from ICI in lung cancer.[25] Mechanistically, neutrophils can reshape the tumor microenvironment, attenuating T-cell and macrophage antitumor functions,[26] fostering angiogenesis and extracellular matrix remodeling, and facilitating circulating tumor cell survival and metastatic seeding.[27] Hypoalbuminemia is an established prognostic biomarker in NSCLC.[28] As a negative acute-phase reactant largely driven by interleukin-6, serum albumin predominantly reflects chronic inflammation. Hypoalbuminemia is also frequently observed in patients with malnutrition and cancer cachexia. Prior studies indicate that poor nutritional status and persistent inflammation undermine adaptive immune responses and contribute to disease progression during ICI therapy.[26] From a pharmacokinetic perspective, low albumin may increase clearance of therapeutic monoclonal antibodies, reducing systemic exposure and the time that drug concentrations remain above efficacious level.[29]

Although our results establish SIPS as a prognostic marker in NSCLC, whether it predicts benefit from specific ICI strategies remains unresolved and warrants prospective evaluation. If validated for clinical use, SIPS could support personalized care—informing decisions about treatment escalation (e.g., combination immunotherapy or chemoimmunotherapy) or de-escalation (e.g., ICI monotherapy in suitable patients), prompting earlier supportive and palliative interventions, and guiding the intensity of follow-up and toxicity monitoring. Future work should (i) prospectively test SIPS-guided stratification as a decision aid for individualized treatment selection and supportive-care timing; (ii) assess its prognostic utility and generalizability across malignancies beyond NSCLC; (iii) evaluate longitudinal use—tracking baseline and

on-treatment changes in neutrophils and albumin—to enable dynamic risk updating for response and survival; (iv) clarify the biological and pharmacokinetic rationale in translational studies; and (v) perform head-to-head comparative studies against established indices.

Study Limitations

Several limitations should be noted. The retrospective, single-center design may introduce selection bias and leave residual confounding even after adjustment. Treatment heterogeneity (different agents, limited chemoimmunotherapy exposure, and a predominance of later-line ICI) and small subgroup sizes reduce the statistical power for interaction testing and may also limit generalizability. Importantly, ICI was administered across different treatment lines, with the majority of patients receiving ICI monotherapy as later-line treatment, which may have influenced prognostic performance and may limit extrapolation of the findings to first-line or combination settings. Because the original SIPS high-risk group was small, we merged the intermediate- and high-risk groups, precluding assessment of a three-tier gradient. Finally, SIPS was derived from a single pretreatment measurement; the absence of longitudinal assessments may reduce prognostic precision.

CONCLUSION

In this single-center cohort of metastatic NSCLC treated with ICIs, SIPS was consistently associated with shorter PFS and OS, independent of ECOG PS, metastatic burden, and PD-L1 expression. The association was stable across PD-L1 strata, treatment regimens, and lines of therapy, supporting its generalizability in real-world practice. Given its simplicity and low cost, SIPS can complement standard clinical variables to refine baseline risk discussions. Validation in multicenter cohorts is warranted to corroborate our findings and to define how SIPS should be used clinically.

Ethics

Ethics Committee Approval: The study adhered to Good Clinical Practice and to the ethical principles of the Declaration of Helsinki, and was approved by the Ege University Institutional Review Board (approval no: 25-10.1T/23, date: 16.10.2025).

Informed Consent: Retrospective study.

Footnotes

Authorship Contributions

Surgical and Medical Practices: C.A., H.Ç.Y., G.Ş., F.P.A., E.G., Concept: C.A., H.Ç.Y., Design: C.A., H.Ç.Y., Data Collection or Processing: C.A., G.Ş., F.P.A., Analysis or Interpretation: C.A., E.G., Literature Search: C.A., G.Ş., Writing: C.A.

Conflict of Interest: No conflict of interest was declared by the authors.

Financial Disclosure: The authors declared that this study received no financial support.

REFERENCES

1. Bray F, Laversanne M, Sung H, et al. Global cancer statistics 2022: GLOBOCAN estimates of incidence and mortality worldwide for 36 cancers in 185 countries. CA Cancer J Clin. 2024;74(3):229-263. [Crossref] [PubMed]
2. Herbst RS, Morgensztern D, Boshoff C. The biology and management of non-small cell lung cancer. Nature. 2018;553(7689):446-454. [Crossref] [PubMed]
3. Robert C. A decade of immune-checkpoint inhibitors in cancer therapy. Nat Commun. 2020;11(1):3801. [Crossref] [PubMed] [PMC]
4. Borghaei H, Paz-Ares L, Horn L, et al. Nivolumab versus docetaxel in advanced nonsquamous non-small-cell lung cancer. N Engl J Med. 2015;373(17):1627-1639. [Crossref] [PubMed] [PMC]
5. Wang Y, Kondrat K, Adhikari J, Nguyen Q, Yu Q, Uprety D. Survival trends among patients with metastatic non-small cell lung cancer before and after the approval of immunotherapy in the United States: a surveillance, epidemiology, and end results database-based study. Cancer. 2025;131(1):e35476. [Crossref] [PubMed]
6. Zhou S, Yang H. Immunotherapy resistance in non-small-cell lung cancer: from mechanism to clinical strategies. Front Immunol. 2023;14:1129465. [Crossref] [PubMed] [PMC]
7. Rother C, John T, Wong A. Biomarkers for immunotherapy resistance in non-small cell lung cancer. Front Oncol. 2024;14:1489977. [Crossref] [PubMed] [PMC]
8. Ngo P, Cooper WA, Wade S, et al. Why PD-L1 expression varies between studies of lung cancer: results from a Bayesian meta-analysis. Sci Rep. 2025;15(1):4166. [Crossref] [PubMed] [PMC]
9. Marabelle A, Fakih M, Lopez J, et al. Association of tumour mutational burden with outcomes in patients with advanced solid tumours treated with pembrolizumab: prospective biomarker analysis of the multicohort, open-label, phase 2 KEYNOTE-158 study. Lancet Oncol. 2020;21(10):1353-1365. [Crossref] [PubMed]
10. Esposito Abate R, Pasquale R, Sacco A, et al. Harmonization of tumor mutation burden testing with comprehensive genomic profiling assays: an IQN path initiative. J Immunother Cancer. 2024;12(2):e007800. [Crossref] [PubMed] [PMC]
11. Ricciuti B, Arbour KC, Lin JJ, et al. Diminished efficacy of programmed death-(ligand)1 inhibition in STK11- and KEAP1-mutant lung adenocarcinoma is affected by KRAS mutation status. J Thorac Oncol. 2022;17(3):399-410. [Crossref] [PubMed] [PMC]
12. Sui Q, Zhang X, Chen C, et al. Inflammation promotes resistance to immune checkpoint inhibitors in high microsatellite instability colorectal cancer. Nat Commun. 2022;13(1):7316. [Crossref] [PubMed] [PMC]
13. Johannet P, Sawyers A, Qian Y, al. Baseline prognostic nutritional index and changes in pretreatment body mass index associate with immunotherapy response in patients with advanced cancer. J Immunother Cancer. 2020;8(2):e001674. Erratum in: J Immunother Cancer. 2021;9(9):e001674corr1. [Crossref] [PubMed] [PMC]
14. Wang H, Yang R, Cheng C, Wang S, Liu D, Li W. Prognostic value of the Glasgow prognostic score in non-small cell lung cancer patients receiving immunotherapy: a meta-analysis. Nutr Cancer. 2024;76(2):187-195. [Crossref] [PubMed]
15. Tsai YT, Schlom J, Donahue RN. Blood-based biomarkers in patients with non-small cell lung cancer treated with immune checkpoint blockade. J Exp Clin Cancer Res. 2024;43(1):82. [Crossref] [PubMed] [PMC]

16. Chen G, Bao B, Ye Y, Hu A, Sun J, Liu W. Prognostic value of the systemic immune-inflammation index in non-small cell lung cancer patients treated with immune checkpoint inhibitors: a systematic review and meta-analysis. Front Oncol. 2025;15:1532343. [Crossref] [PubMed] [PMC]
17. Stares M, Ding TE, Stratton C, et al. Biomarkers of systemic inflammation predict survival with first-line immune checkpoint inhibitors in non-small-cell lung cancer. ESMO Open. 2022;7(2):100445. [Crossref] [PubMed] [PMC]
18. Gomez-Randulfe I, Gomes F, MacKean M, Phillips I, Stares M. Validation of the Scottish inflammatory prognostic score (SIPS) in NSCLC patients treated with first-line pembrolizumab. Cancers (Basel). 2024;16(22):3833. [Crossref] [PubMed] [PMC]
19. Stares M, Doyle E, Chapple S, et al. Prognostic value of the Scottish inflammatory prognostic score in patients with NSCLC expressing PD-L1 ≥ 50 % progressing on first-line pembrolizumab. Lung Cancer. 2024;189:107497. [Crossref] [PubMed]
20. Harvey S, Stares M, Scott JA, et al. Biomarkers of systemic inflammation provide additional prognostic stratification in cancers of unknown primary. Cancer Med. 2024;13(3):e6988. [Crossref] [PubMed] [PMC]
21. Zhao Q, Wang L, Yang X, Feng J, Chen Q. Association of the Scottish inflammatory prognostic score with treatment-related adverse events and prognosis in esophageal cancer receiving neoadjuvant immunochemotherapy. Front Immunol. 2024;15:1418286. [Crossref] [PubMed] [PMC]
22. Shen S, Qiu X, Yang C, et al. Prognostic importance of the Scottish inflammatory prognostic score in patients with hepatocellular carcinoma after hepatectomy: a retrospective cohort study. BMC Cancer. 2024;24(1):1393. [Crossref] [PubMed] [PMC]
23. Raynes G, Stares M, Low S, et al. Immune-related adverse events, biomarkers of systemic inflammation, and survival outcomes in patients receiving pembrolizumab for non-small-cell lung cancer. Cancers (Basel). 2023;15(23):5502. [Crossref] [PubMed] [PMC]
24. Taş A, Tunca Ç, Tanık VO, Özlek B. The Scottish inflammatory prognostic score: a novel biomarker for predicting in-hospital mortality in acute heart failure with reduced ejection fraction. Heart Lung. 2025;74:291-299. [Crossref] [PubMed]
25. Zer A, Sung MR, Walia P, et al. Correlation of neutrophil to lymphocyte ratio and absolute neutrophil count with outcomes with PD-1 axis inhibitors in patients with advanced non-small-cell lung cancer. Clin Lung Cancer. 2018;19(5):426-434.e1. [Crossref] [PubMed]
26. Zhu M, Jia R, Zhang X, Xu P. The success of the tumor immunotherapy: neutrophils from bench to beside. Front Immunol. 2025;16:1524038. [Crossref] [PubMed] [PMC]
27. Szczerba BM, Castro-Giner F, Vetter M, et al. Neutrophils escort circulating tumour cells to enable cell cycle progression. Nature. 2019;566(7745):553-557. [Crossref] [PubMed]
28. Guven DC, Sahin TK, Erul E, et al. The association between albumin levels and survival in patients treated with immune checkpoint inhibitors: a systematic review and meta-analysis. Front Mol Biosci. 2022;9:1039121. [Crossref] [PubMed] [PMC]
29. Bajaj G, Suryawanshi S, Roy A, Gupta M. Evaluation of covariate effects on pharmacokinetics of monoclonal antibodies in oncology. Br J Clin Pharmacol. 2019;85(9):2045-2058. [Crossref] [PubMed] [PMC]

ORIGINAL ARTICLE

DOI: 10.37047/jos.galenos.2026.2025-10-1

J Oncol Sci 2026;12(1):41-50

Incidence and Patterns of Second Primary Malignancies in Genitourinary Cancer Survivors: A 20-Year Single-Center Experience

İmdat EROĞLU[1], Hatice AVŞAR[2], Osman SÜTÇÜOĞLU[1], Gözde SAVAŞ[1], Fatih GÜRLER[1], Uğur COŞKUN[1], Aytuğ ÜNER[1], Ozan YAZICI[1], Ahmet ÖZET[1], Nuriye ÖZDEMİR[1]

[1]Gazi University Faculty of Medicine, Department of Medical Oncology, Ankara, Türkiye
[2]Gazi University Faculty of Medicine, Department of Internal Medicine, Ankara, Türkiye

ABSTRACT

Objective: Genitourinary (GU) cancers represent a major global cancer burden. With improved survival, second primary malignancies (SPMs) have become an important challenge in survivorship care. However, data specific to GU cancer survivors are limited.

Material and Methods: We conducted a retrospective cohort study of patients with GU cancers diagnosed at Gazi University between 2004 and 2024. Patients with prior malignancies were excluded. Demographic and clinical data were retrieved from medical records. SPMs were defined as synchronous (≤6 months) or metachronous (>6 months).

Results: Among 1,628 patients, 57 developed an SPM, yielding an overall incidence of 3.5%. Incidence rates by subgroup were as follows: prostate cancer, 5.1% (28/548); bladder cancer, 2.7% (12/445); renal cell carcinoma (RCC), 2.9% (11/385); and testicular cancer, 2.4% (6/250). Overall, 26.3% of SPMs were synchronous and 73.7% were metachronous. The most common SPMs were lung cancers (22.8%) and secondary GU cancers (22.8%), followed by gastrointestinal cancers (15.8%) and skin cancers (14.0%). Subgroup analysis showed distinct patterns: in prostate cancer survivors, lung cancers (25.0%) and bladder cancers (17.8%) were most frequent; in bladder cancer survivors, gastrointestinal cancers (33.3%) and lung cancers (25.0%) predominated; in RCC patients, lung cancers were most common (27.3%); and in testicular cancer survivors, secondary urogenital tumors predominated (50.0%). The median interval to SPM diagnosis was 25.9 months, with the longest latency observed in testicular cancer survivors (76.4 months).

Conclusion: The incidence of SPMs in GU cancers was lower than that reported in population-based studies, but the distribution patterns were consistent, with lung and urogenital tumors predominating. These results emphasize the need for tailored, long-term surveillance in GU cancer survivors.

Keywords: Cancer diagnosis and treatments; genitourinary; kidney tumors; prostate cancer

INTRODUCTION

Genitourinary (GU) cancers constitute a heterogeneous group of malignancies with a significant global impact, and data from the most recent Global Burden of Disease Study demonstrate that these malignancies represent an increasing proportion of the global cancer burden.[1,2] Over the past two decades, advancements in therapeutic strategies have contributed to a decline in mortality rates for prostate, bladder, and kidney cancers, whereas mortality for testicular cancer has remained relatively stable.[3] As survival outcomes improve, survivorship care has become increasingly important, particularly in addressing not only long-term physical and psychosocial sequelae, but also the heightened risk of developing second primary malignancies (SPMs) in this patient population.

The development of SPMs represents a serious and growing concern, particularly in patients with GU cancers who may be exposed to various carcinogenic therapies, such as radiotherapy (RT), chemotherapy, and hormone

Correspondence: İmdat EROĞLU MD,
Gazi University Faculty of Medicine, Department of Medical Oncology, Ankara, Türkiye
E-mail: i.eroglu.1903@gmail.com

ORCID ID: orcid.org/0000-0001-6619-4141

Received: 03.10.2025 **Accepted:** 01.02.2026 **Epub:** 12.03.2026 **Publication Date:** 18.03.2026

Cite this article as: Eroğlu İ, Avşar H, Sütçüoğlu O, et al. Incidence and patterns of second primary malignancies in genitourinary cancer survivors: a 20-year single-center experience. J Oncol Sci. 2026;12(1):41-50

Available at journalofoncology.org

treatments.[4-6] These secondary cancers can significantly impact morbidity, mortality, and healthcare burden, yet they remain understudied in this patient population.

Although previous studies have explored SPMs in cancer survivors more broadly,[7,8] data specific to GU malignancies are limited. Better understanding of the incidence patterns and timing of SPM development in this group is needed to inform tailored survivorship care strategies. In this study, we investigate the incidence and distribution of SPMs among patients with prostate, bladder, kidney, and testicular cancers.

MATERIAL AND METHODS

Study Design and Patient Population

This study is a single-center, retrospective cohort analysis of patients diagnosed with GU cancers who presented to the Department of Medical Oncology at Gazi University School of Medicine between 2004 and 2024. Initial patient identification was conducted using ICD-10 diagnostic codes corresponding to GU malignancies, specifically: C61.0-C61.9 (prostate cancer), C62.0-C62.9 (testicular cancer), C64.0-C64.9 (kidney cancer), and C67.0-C67.9 (bladder cancer). For the purposes of this study, cancers classified as C65.0-C65.9 (renal pelvis) and C66.0-C66.9 (ureter) were grouped with bladder cancer (C67.0-C67.9) due to their anatomical proximity and similar clinical management. Within this cohort, patients who developed a SPM after the initial diagnosis of a GU cancer were identified. All primary and secondary malignancies were subsequently confirmed by histopathological examination, and diagnoses were validated using pathology reports to ensure that SPMs represented independent primary tumors rather than recurrences or metastases. Patients with a history of primary malignancy before diagnosis of GU cancer were excluded from the analysis to ensure that the GU tumor was the index cancer. This study was conducted in accordance with the Declaration of Helsinki, and ethical approval was obtained from the Ethics Committee of Gazi University (research code: 2025-1570, date: 22.09.2025).

Data Collection and Endpoints

Data collection was performed retrospectively through a review of electronic medical records and patients' files. Demographic variables, including age at diagnosis and gender, were extracted from patients' medical records. Detailed clinical information was collected, encompassing the histological types of both the primary GU cancer and any subsequent SPMs. Treatment modalities received for the primary tumor, such as surgery, chemotherapy, RT, and hormonal therapy, were recorded. Tumor staging data at the time of diagnosis were obtained for both the primary and secondary malignancies. The stage of the primary tumor when the secondary malignancy was diagnosed was also documented to assess disease status during follow-up. The interval between the initial diagnosis of the primary GU cancer and the diagnosis of the SPM was calculated to evaluate temporal patterns in the development of secondary malignancies. Cancers detected within six months of the initial primary tumor are classified as synchronous, while those that appear more than six months after the first primary tumor are considered metachronous.[9] The primary endpoint of the study was the incidence and classification of SPMs. The secondary endpoint was defined as the time interval between the diagnoses of the primary and secondary malignancies.

Statistical Analysis

Statistical analyses were performed with IBM SPSS software version 25.0 (S.P.S.S. Inc., Chicago, IL, U.S.A.). Categorical variables are presented as counts and percentages. Means and standard deviations for normally distributed variables, and medians and interquartile ranges (IQRs) (25^{th}-75^{th} percentiles) for non-normally distributed variables were reported. Normality was evaluated using the Kolmogorov-Smirnov test. The incidence of SPMs was calculated as the proportion of patients who developed an SPM following the diagnosis of a primary GU cancer. Subgroup analyses were performed based on the type of primary GU cancer (prostate, kidney, bladder, testicular) and the type of SPM. The incidence of SPMs and of their subtypes was calculated for the overall cohort and for each primary cancer type. The median follow-up time was calculated using the reverse Kaplan-Meier method. The time interval between the diagnosis of the primary GU cancer and the SPM was calculated in months.

RESULTS

Study Population, Follow-up and Frequency of SPMs

A total of 1,628 patients with primary GU cancers were included. The most common primary malignancies were prostate cancer (33.7%), bladder cancer (27.3%), renal cell carcinoma (RCC) (23.6%), and testicular cancer (15.4%). During follow-up, 57 patients developed an SPM, yielding an overall incidence of 3.5%. The highest SPM rate was observed in prostate cancer (n=28, 5.1%), followed by RCC (n=11, 2.9%), bladder cancer (n=12, 2.7%), and testicular cancer (n=6, 2.4%). Overall, 26.3% of SPMs were synchronous and 73.7% were metachronous, with synchronous SPM rates of 28.6% for prostate cancer, 16.7% for bladder cancer, 36.4% for RCC, and 16.7% testicular cancer.

The median follow-up for the overall cohort was 140.8 months [95% confidence interval (CI): 101.7-179.9]. Median follow-up for each primary tumor type was as follows: 186.9 months (95% CI: 84.3-289.6) for prostate cancer, 140.8 months

(95% CI: 77.1-204.5) for testicular cancer, 135.4 months (95% CI: 102.7-168.1) for RCC, and 51.6 months (95% CI: 44.8-58.5) for bladder cancer.

Among prostate cancer patients, eight synchronous SPMs were identified: lung cancer (n=3); gastrointestinal cancer (n=2; both colon); urogenital cancer (n=2; low-grade bladder cancer and RCC); and head and neck cancer (n=1; larynx). In bladder cancer patients, the two synchronous tumors were a gastrointestinal stromal tumor (GIST) and testicular cancer. In patients with RCC, the four synchronous tumors were colon, ovarian, pancreatic neuroendocrine, and prostate cancers. Among testicular cancer patients, only one case of a synchronous tumor was observed: thyroid cancer.

Patient Characteristics of Cases with Second Primary Malignancies

Subsequent analyses were restricted to the 57 patients who developed an SPM. All patients were male, except three female patients with RCC. The median age at primary tumor diagnosis was 66.1 years for prostate cancer, 69.1 years for bladder cancer, 58.8 years for RCC, and 34.7 years for testicular cancer. Median ages at SPM diagnosis were 72.9, 70.1, 61.6, and 42.3 years, respectively. At the time of primary diagnosis, metastatic disease was present in 44.4% of prostate cancer patients, 8.3% of bladder cancer patients, 18.2% of RCC patients, and 16.6% of testicular cancer patients. At the time of SPM diagnosis, metastases were observed in 35.7% of prostate cancer patients (n=10), 45.5% of bladder cancer patients (n=5), and 9.0% of RCC patients (n=1), whereas no metastatic SPM was detected in testicular cancer patients.

Among prostate cancer patients with metastatic SPM, the most frequent sites were the colon (n=2), the lung (n=2), and cancers of unknown primary (n=2), followed by bladder cancer, medullary thyroid carcinoma, GIST, and lymphoma (n=1 each). Metastatic SPMs in bladder cancer included lung cancer (n=2), gastric cancer (n=2), and pancreatic cancer (n=1). The only metastatic SPM observed in patients with RCC was pancreatic cancer. At the time of SPM diagnosis, the primary tumor remained metastatic in 35.7% of patients with prostate cancer, 25.0% of patients with bladder cancer, and 27.3% of patients with RCC; all patients with testicular cancer were in remission. Baseline demographic and clinical characteristics are summarized in Table 1.

Distribution of SPMs According to Primary GU Cancer

The most frequent SPM types observed among the 57 patients were lung cancer (n=13, 22.8%) and GU cancers other than the primary index tumor (n=13, 22.8%). These were followed by gastrointestinal cancers (n=9, 15.8%) and skin cancers (n=8, 14.0%). Less common SPM types included endocrine cancers (n=4, 7.0%), hematological malignancies (n=2, 3.5%), gynecological cancers (n=1, 1.8%), head and neck cancers (n=2, 3.5%), cancers of unknown primary (n=2, 3.5%), and GISTs (n=3, 5.3%).

The distribution of SPM types varied according to the primary GU cancer. The most frequent subsequent cancers among patients with prostate cancer were lung cancer (n=7) and secondary GU cancers (n=7). In bladder cancer survivors, gastrointestinal cancers (n=4) and skin and lung cancers (n=3 each) were predominant. Among RCC patients, lung cancer (n=3) was the most common. Testicular cancer survivors most frequently developed urogenital malignancies (n=3) The overall distribution is illustrated in Figure 1, while the specific SPM subtypes for each primary tumor type are detailed in Figure 2.

Among prostate cancer patients who developed bladder cancer (n=5), all cases were low-grade urothelial carcinomas, and four patients had a history of primary RT for prostate cancer.Among prostate cancer patients who developed lung cancer (n=7), all cases were non-small-cell lung carcinoma; 5 patients (71.4%) had a history of smoking.

Interval Between Primary and Second Primary Malignancies

The median interval between the diagnosis of the primary GU cancer and the development of SPM was 25.9 months (IQR: 5.4-86.8) for the overall cohort of 57 patients. When stratified by primary cancer type, the median intervals were 25 months (IQR: 3.5-102.3) for prostate cancer, 21.1 months (IQR: 12.5-38.1) for bladder cancer, 19.3 months (IQR: 4-71.8) for RCC, and 76.4 months (IQR: 40.6-173) for testicular cancer. In the overall cohort, the shortest median intervals to SPM development were observed for gynecological (5.4 months), endocrine (7.5 months), and gastrointestinal (11.5 months) cancers.

DISCUSSION

In this study, we evaluated the timing and distribution of SPMs in patients with primary GU cancers. Across all groups, the most frequently observed SPMs were lung, urogenital, gastrointestinal, and skin cancers. We found that approximately one-quarter of all SPMs were synchronous, while the majority were metachronous. The shortest median intervals to development of SPMs were observed in secondary gynecological, endocrine, and gastrointestinal malignancies, whereas the longest were observed for SPMs of unknown primary site and for SPMs at certain urogenital sites. These findings align with previous population-based studies reporting substantial variability in SPM latency across tumor types, likely reflecting differences in carcinogenic exposures, tumor biology, and surveillance intensity.

Although there are several reports addressing the

TABLE 1: Clinicopathological features of patients.					
Variable	**Whole cohort (n=57)**	**Prostate cancer (n=28)**	**Bladder cancer (n=12)**	**Kidney cancer (n=11)**	**Testicular cancer (n=6)**
Age at diagnosis of primary malignancy (years, median; min-max)	64.6 (26.4-89.7)	66.1 (53.6-80.9)	69.1 (32.1-89.7)	58.8 (49.1-70.6)	34.7 (26.2-64)
Age at diagnosis of secondary malignancy (median; min-max)	68.4 (29.6-90.7)	72.9 (54.3-82.9)	70.7 (43.7-90.7)	61.6 (49.6-75.2)	42.3 (29.6-67.7)
Gender					
Female	3 (5.3%)	0 (0%)	0 (0%)	3 (27.3%)	0 (0%)
Male	54 (94.7%)	28 (100%)	12 (100%)	8 (72.7%)	6 (100%)
Smoking history					
None	25 (43.9%)	12 (42.9%)	5 (41.7%)	5 (45.5%)	3 (50%)
Active-smoker	13 (22.8%)	7 (25%)	3 (25%)	1 (9.1%)	2 (33.3%)
Ex-smoker	19 (33.3%)	9 (32.1%)	4 (33.3%)	5 (45.5%)	1 (16.7%)
Histology of the PT					
-Adenocarcinoma	28	28	-	-	-
-High-grade urothelial	7	-	7	-	-
-Low-grade urothelial	3	-	3	-	-
-Squamous cell	2	-	2	-	-
-Clear cell RCC	8	-	-	8	-
-Papillary RCC	2	-	-	2	-
-Chromofobe RCC	1	-	-	1	-
-Seminoma	4	-	-	-	4
-Non-seminoma	2	-	-	-	2
Stage of PT at diagnosis					
Stage 0-2	27 (47.4%)	11 (39.3%)	5 (41.7%)	7 (63.6%)	4 (66.6%)
Stage 3	14 (24.6%)	4 (14.3%)	6 (50%)	2 (18.2%)	2 (33.3%)
Stage 4	16 (28.1%)	13 (46.4%)	1 (8.3%)	2 (18.2%)	-
Stage of SPM at diagnosis					
Stage 0-2	33 (57.9%)	15 (53.6%)	5 (41.7%)	7 (63.6%)	6 (100%)
Stage 3	7 (12.3%)	3 (10.7%)	2 (16.6%)	2 (18.2%)	-
Stage 4	17 (29.8%)	10 (35.7%)	5 (41.7%)	2 (18.2%)	-
Stage of PT at diagnosis of SPM					
Remission	32 (56.1%)	14 (50%)	8 (72.7%)	6 (54.5%)	4 (66.6%)
Under treatment for non-metastaic disease	9 (15.8%)	4 (14.3%)	1 (9.1%)	2 (18.2%)	2 (33.3%)
Metastatic	16 (28.1%)	10 (35.7%)	3 (27.3%)	3 (27.2%)	-
Previous treatment for PT					
Chemotherapy	22	7	8	1	6
ADT	19	19	-	-	-
ARPI	2	2	-	-	-
TKI	5	-	-	5	-
Radiotherapy for primary	11	10	-	1	-
Intravesical treatment	3	-	3	-	-
Immunotherapy	1	-	-	1	-
Survival					
Alive	28 (47.4%)	11 (39.3%)	5 (45.5%)	6 (54.5%)	6 (100%)
Exitus	29 (52.6%)	17 (60.7%)	6 (54.5%)	5 (45.5%)	-

ADT: Androgen-deprivation treatment; ARPI: Androgen receptor pathway inhibitor; PT: Primary tumor; RCC: Renal cell carcinoma; SPM: Second primary tumor; min: Minimum; max: Maximum; TKI: Tyrosine kinase inhibitor.

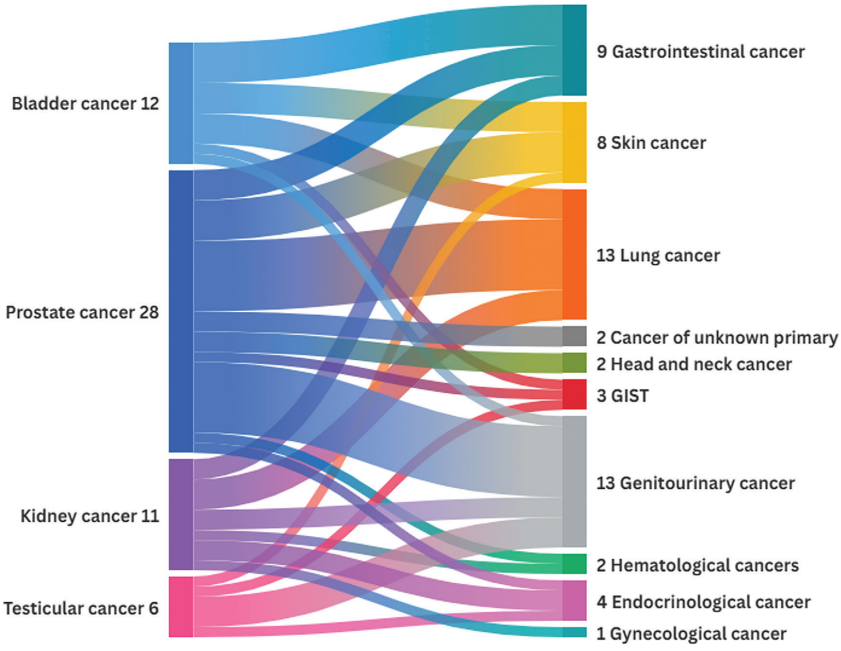

FIGURE 1: General distribution of second primary tumors.

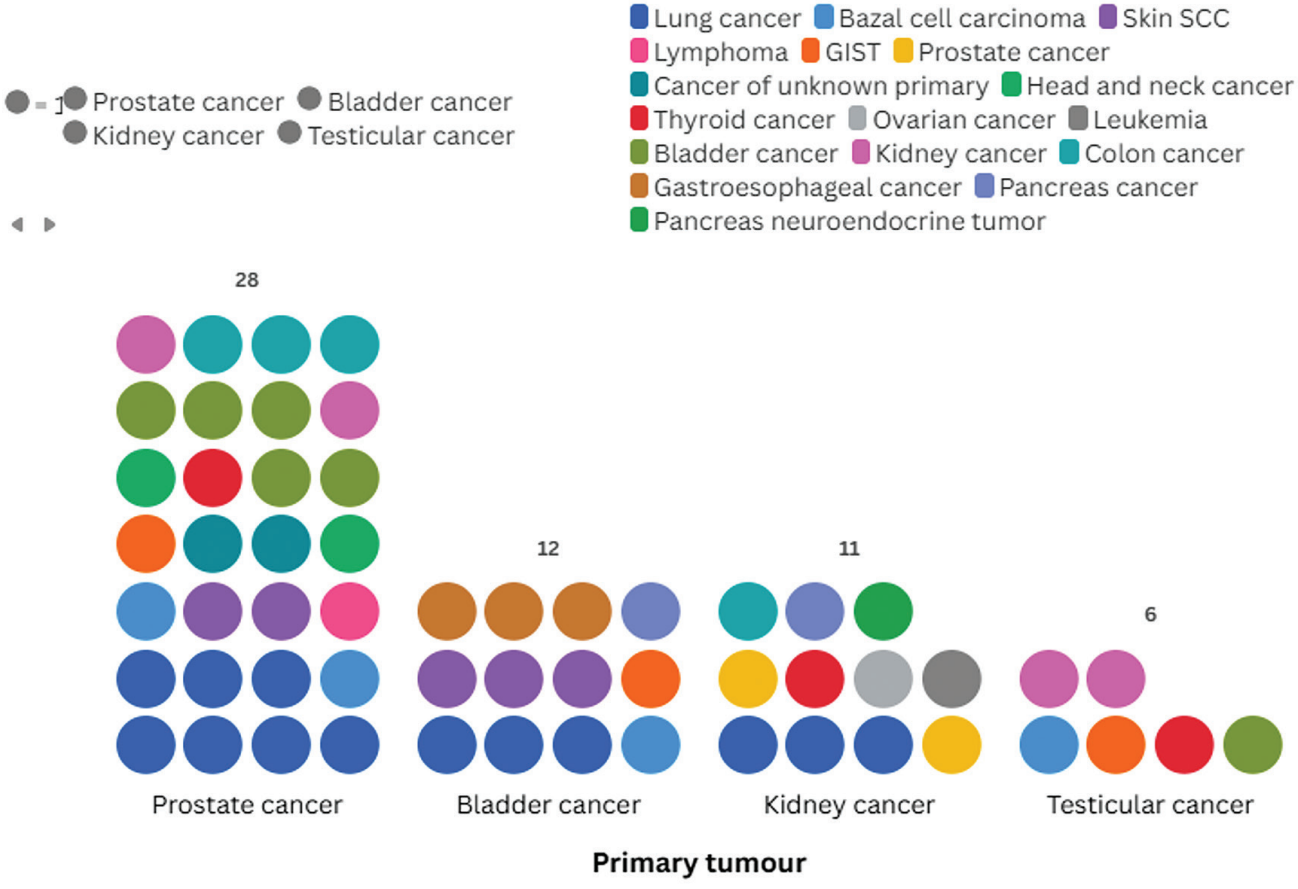

FIGURE 2: Detailed distribution of secondary malignancies in each genitourinary cancer.

development of SPMs in individual GU cancers, particularly in the prostate and bladder, data on SPM occurrence across all GU malignancies remain limited. In a study using the Surveillance, Epidemiology, and End Results Program (SEER) database that included 1,041,217 patients with GU cancers, the overall incidence of SPMs was 11%, with a higher incidence observed in endocrine system cancers and urinary system cancers. These findings highlight the need for careful long-term surveillance in patients with GU cancer and suggest that certain subgroups may be at increased risk for developing secondary malignancies.[10] On the other hand, a more recent analysis of the SEER database, including 140,620 patients with GU cancers, reported an SPM incidence of 23.9%, with respiratory and urogenital tumors being the most frequently observed.[11] Interestingly, in our cohort, the incidence of SPMs was 3.5%, which is considerably lower than the rates reported in other studies. This difference may be related to sample size, country-specific patterns, or heterogeneity of SPM incidence among GU cancers. Additionally, the relatively low incidence of SPMs observed in our cohort may be partly explained by methodological and cohort-specific factors. Although the overall median follow-up duration was substantial, its length varied considerably across subgroups, with notably shorter follow-up in certain cancer types, which may have limited detection of late-occurring SPMs. In addition, the retrospective, oncology department-based design of the study may have resulted in incomplete capture of SPMs that were diagnosed and managed outside the medical oncology setting, such as those followed primarily in surgical or other specialty clinics. Patients with early-stage disease who did not require prolonged oncologic follow-up may therefore be underrepresented. Furthermore, SPMs diagnosed at external institutions may not have been consistently recorded in the institutional database. Collectively, these factors may have contributed to an underestimation of the true incidence of SPMs in our cohort. Consistent with the literature, lung and GU cancers were the most common SPMs in our dataset, underscoring the importance of vigilant surveillance for lung and secondary GU malignancies in patients with a primary GU cancer.

In our cohort, prostate cancer constituted the largest proportion of cases, and these patients exhibited a higher incidence of SPMs compared with both the overall cohort and patients with other malignancies. In a SEER-based analysis of 284,738 patients, the incidence of SPMs in prostate cancer was reported as 5.3%,[12] which is comparable to the rate observed in our cohort (5.1%), indicating consistency with previously published data. In the same study, age at prostate cancer diagnosis, histological grade, tumor grade, history of RT, and prior surgery were all associated with the development of SPMs.[12] Although we cannot establish causality in our analysis, since only patients with SPMs were included, it is noteworthy that the overall incidence of SPMs in our cohort was substantially lower than that reported in the literature, whereas the incidence among prostate cancer patients was comparable to previous studies. Although prostate cancer patients represented the subgroup with the highest incidence of SPMs in our cohort, a large US population-based study has reported that prostate cancer survivors have a lower overall risk of developing SPMs compared with the general population, including a reduced risk of lung cancer. In contrast, these studies consistently demonstrated an increased risk of bladder, kidney, soft-tissue, and endocrine malignancies.[13] However, in our cohort, lung and GU cancers were the most frequently observed SPMs, suggesting potential geographic or cohort-specific differences and underscoring the heterogeneity of SPM risk among prostate cancer patients. However, since our study did not include a direct comparison with the general population, no conclusions can be drawn regarding relative risk in this context. In contrast, a Swiss cohort study of 20,000 patients reported that prostate cancer survivors had a lower risk of developing an SPM than the general population during the first four years after diagnosis, but this risk subsequently increased in a stepwise manner. Notably, consistent with our findings, the three most common SPM types in that study were lung, GU, and colorectal cancers. Moreover, treatment modality was shown to influence the type of SPM that developed.[14] These observations suggest that our results are consistent with international data and highlight the potential impact of treatment-related factors on SPM patterns.

One of the most well-documented findings in the literature is an increased risk of SPMs among prostate cancer patients who received RT. Compared with patients who did not undergo RT, those treated with RT have been shown to be at higher risk of developing SPMs, particularly bladder cancer, colorectal cancers (including colon and anus), hematologic malignancies, and lung cancer.[15-17] Numerous studies have demonstrated that prostate cancer patients receiving RT exhibit an increased risk of developing pelvic malignancies, particularly bladder cancer.[15,18,19] Furthermore, a meta-analysis indicated that all RT modalities are associated with an increased risk of secondary bladder cancer; secondary bladder cancers requiring cystectomy have a poorer prognosis than primary bladder cancers.[20] Current evidence suggests that stereotactic body RT may be safer than other RT modalities in this regard.[21] In our cohort, five patients with prostate cancer developed secondary bladder cancer, making secondary bladder cancer the second most frequent SPM after lung cancer. Four of these five patients had a history of prostate RT.

Although some studies have reported that secondary bladder cancers following prostate RT tend to be more aggressive and high-grade,[22] all tumors in our patients were low-grade. These findings underscore the importance of vigilant surveillance for bladder cancer in prostate cancer patients who have received RT.

The development of SPMs in bladder cancer patients is among the most extensively studied topics within GU malignancies. In a SEER-based study involving 238,358 patients with bladder cancer, the incidence of SPMs was 19.7%, which was significantly higher than in the general population. In that study, the most frequent SPMs were hypopharyngeal, esophageal, hepatic, and lung cancers.[23] In another U.S.-based study, the incidence of SPMs among patients who underwent radical cystectomy was 12.3%, with lung and colorectal cancers being the most commonly observed.[24] In a study from Türkiye analyzing data from 2,334 patients in a 38-year cohort, the incidence of SPMs among patients with urothelial carcinoma was 11.1%, with lung cancer the most frequently observed SPM.[25] In our cohort, the incidence of SPMs in bladder cancer patients was lower than in these large population-based studies; this can be explained by a smaller sample size and shorter follow-up duration. However, consistent with the literature, lung cancer emerged as one of the most frequent secondary malignancies. Moreover, similar to the SEER data, gastroesophageal tumors were among the most common SPMs observed in our cohort.

The development of SPMs in RCC patients has been investigated in multiple cohorts, which have reported an increased incidence of SPMs in these patients compared with the general population. In a SEER database study of 43,477 patients with RCC, the incidence of SPMs was 13.6%; the five most common cancer types were brain, pancreas, liver, lung, and prostate.[26] In a population-based study conducted in Taiwan, the incidence of SPMs among patients with RCC was reported as 11.6% in the local cohort, whereas the nationwide incidence was 4.68%. The most common cancer subtypes observed were bladder cancer, liver cancer, colon cancer, lung cancer, and prostate cancer.[27] In a Danish cohort, it was demonstrated that the risk of developing SPMs increased with time after an RCC diagnosis; the incidence rose from 2.8% in the first year to 17.8% in the twentieth year.[28] Furthermore, Rabbani et al.[29] showed that the histological subtype of RCC may influence the development of SPMs, with a particularly increased risk of bladder and prostate cancers observed in patients with papillary RCC. In our cohort, the overall incidence of SPMs was lower than in previous reports. However, consistent with the literature, lung and prostate cancers were among the most frequently observed subtypes. The lower incidence in our study may be attributable to ethnic differences as well as the relatively shorter follow-up period. Moreover, because the majority of our patients had clear-cell RCC, we could not assess the potential impact of histological subtype on the development of SPMs.

In patients with testicular cancer, the risk of developing SPMs is increased due to both the younger age at diagnosis and the use of RT and chemotherapeutic agents such as etoposide, which are associated with a higher likelihood of secondary cancers, especially hematological malignancies.[30,31] In a cohort study of 40,575 patients, the incidence of SPMs among testicular cancer survivors was 5.6%. Notably, malignant mesothelioma showed the greatest relative increase in risk (relative risk: 3.4), while other cancers with elevated risk included esophageal, lung, colon, bladder, pancreatic, and gastric cancers. The overall pattern was similar between the seminoma and non-seminoma groups, although younger patients exhibited a higher risk. In a meta-analysis comprising 88,683 patients, the incidence of SPMs was found to be 5.8; while surgery alone did not increase the risk, RT, chemotherapy, or their combination were associated with an elevated risk. In particular, subdiaphragmatic RT has been identified as a significantly stronger risk factor for the development of SPMs.[32] In our cohort, the incidence of SPMs was 2.4%, which is lower than that reported in the literature. None of the patients had a history of RT; notably, two of the six patients who developed SPMs were diagnosed with RCC. Although this association is not commonly reported in the literature,[33] it was observed in our cohort. Additionally, were no hematological malignancies among patients with testicular cancer. This result might be related to a short follow-up time. The relatively small sample size may have influenced this finding.

Among patients with urogenital cancers in our cohort, the most frequently observed SPMs were lung cancers, other urogenital cancers, gastrointestinal cancers, and skin cancers. Several interrelated mechanisms likely contribute to this pattern. First, shared environmental and lifestyle exposures such as smoking, alcohol consumption, dietary factors, and ultraviolet radiation, all of which are well-known carcinogens, may predispose survivors to multiple malignancies, including lung and GI tumors, due to widespread systemic effects.[34] Second, treatment-related modalities, namely RT and chemotherapy, have been shown to induce DNA damage and epigenetic changes, thereby elevating the risk of SPMs across different organ systems. This is particularly relevant for skin and GI tumors following pelvic or abdominal irradiation.[35] Third, the concept of field cancerization explains how widespread pre-neoplastic changes in epithelial tissues, potentially driven by chronic exposure to carcinogens, can lead to multifocal tumor development in anatomically adjacent regions (e.g.,

urogenital and GI tracts).[36,37]

Beyond describing incidence patterns, several findings from our cohort have potential clinical implications. Notably, RCC was observed as an SPM among testicular cancer survivors. Although this association has been infrequently reported in the literature, it may reflect shared genetic susceptibility, treatment-related effects, or increased imaging surveillance in this relatively young patient population. Testicular cancer survivors often undergo long-term radiological follow-up, which may facilitate earlier detection of incidental renal tumors.[38-41] Additionally, systemic therapies and an underlying predisposition to malignancy cannot be excluded. This observation underscores the importance of long-term surveillance of testicular cancer survivors, even in the absence of traditional risk factors or prior exposure to RT. From a clinical perspective, the predominance of lung and secondary GU malignancies as SPMs in our cohort has important implications for survivorship care. These findings suggest that follow-up strategies in GU cancer survivors should extend beyond recurrence surveillance and incorporate risk-adapted screening for common SPMs. In particular, attention to respiratory symptoms, smoking history, and appropriate thoracic imaging may be warranted, especially in patients with known tobacco exposure. Similarly, vigilance for secondary GU tumors is crucial, particularly among prostate cancer survivors with a history of pelvic RT. Collectively, these observations support a more individualized and long-term surveillance approach, tailored to the primary tumor type, treatment exposure, and patient-specific risk factors.

Study Limitations

This study has some limitations. The relatively small sample size and shorter follow-up period may have led to an underestimation of the true incidence of SPMs. Detailed information on lifestyle factors and treatment modalities was limited. Due to the limited number of patients who developed SPM and incomplete data on certain clinical and lifestyle factors, such as smoking history and RT exposure, formal univariate risk factor analyses could not be performed reliably. The single-center nature of this study may limit the generalizability of the findings, and larger multicenter cohorts are needed to more accurately estimate the incidence of SPMs. In addition, the lack of routinely available genetic and molecular data precluded evaluation of inherited susceptibility or treatment-related genomic alterations. Prospective multicenter studies incorporating molecular profiling are warranted.In addition, the potential impact of histological subtypes could not be assessed due to the small sample size. Finally, the retrospective design is subject to inherent biases. On the other hand, this study provides one of the few analyses of SPMs in GU cancers in our population, offering valuable local data that complement international findings. The single-center design ensured consistency in diagnosis and follow-up, reducing heterogeneity in data collection.

CONCLUSION

In conclusion, our findings indicate that the incidence and distribution of SPMs among patients with urogenital cancers in our cohort were generally lower than those reported in the literature. However, lung, prostate, and other urogenital tumors remained the most frequent sites, consistent with previous studies. These results underscore the multifactorial etiology of SPMs, involving environmental exposures, treatment-related effects, and genetic predispositions. Importantly, our data emphasize the need for long-term, tailored surveillance strategies for GU cancer survivors. Prospective studies with larger sample sizes and extended follow-up are warranted to further elucidate risk factors and guide personalized monitoring and preventive interventions.

Ethics

Ethics Committee Approval: This study was conducted in accordance with the Declaration of Helsinki, and ethical approval was obtained from the Ethics Committee of Gazi University (research code: 2025-1570, date: 22.09.2025).

Informed Consent: Retrospective cohort study.

Footnotes

Authorship Contributions

Surgical and Medical Practices: İ.E., H.A., O.S., G.S., F.G., U.C., A.Ü., O.Y., A.Ö., N.Ö., Concept: İ.E., F.G., N.Ö., Design: İ.E., Data Collection or Processing: İ.E., H.A., U.C., A.Ü., O.Y., A.Ö., N.Ö., Analysis or Interpretation: İ.E., H.A., O.S., G.S., F.G., Literature Search: İ.E., Writing: İ.E., O.S., N.Ö.

Conflict of Interest: No conflict of interest was declared by the authors.

Financial Disclosure: The authors declared that this study received no financial support.

REFERENCES

1. Bray F, Laversanne M, Sung H, et al. Global cancer statistics 2022: GLOBOCAN estimates of incidence and mortality worldwide for 36 cancers in 185 countries. CA Cancer J Clin. 2024;74(3):229-263. [Crossref] [PubMed]
2. Zhang Z, Xie Y, Liu L, et al. Global, regional, and national burden of genitourinary cancers in 204 countries and territories, 1990-2021: a systematic analysis for the global burden of disease study 2021. J Natl Cancer Cent. 2025;5(3):330-345. [Crossref] [PubMed] [PMC]
3. Ghazwani Y, Alghafees M, Suheb MK, et al. Trends in genitourinary cancer mortality in the United States: analysis of the CDC-WONDER database 1999-2020. Front Public Health. 2024;12:1354663. [Crossref] [PubMed] [PMC]
4. Murray L, Henry A, Hoskin P, Siebert FA, Venselaar J; PROBATE group of GEC ESTRO. Second primary cancers after radiation for prostate cancer: a systematic review of the clinical data and impact

of treatment technique. Radiother Oncol. 2014;110(2):213-28. [Crossref] [PubMed] [PMC]

5. Scailteux LM, Bezin J, Gundelwein M, et al. Second primary cancers and hormonal therapies for prostate cancer: a nested case-control study. Fundam Clin Pharmacol. 2025;39(2):e70004. [Crossref] [PubMed] [PMC]
6. Boffetta P, Kaldor JM. Secondary malignancies following cancer chemotherapy. Acta Oncol. 1994;33(6):591-598. [Crossref] [PubMed]
7. Kjaer TK, Andersen EAW, Ursin G, et al. Cumulative incidence of second primary cancers in a large nationwide cohort of Danish cancer survivors: a population-based retrospective cohort study. Lancet Oncol. 2024;25(1):126-136. [Crossref] [PubMed]
8. Morton LM, Onel K, Curtis RE, Hungate EA, Armstrong GT. The rising incidence of second cancers: patterns of occurrence and identification of risk factors for children and adults. Am Soc Clin Oncol Educ Book. 2014:e57-e67. [Crossref] [PubMed]
9. Moertel CG. Multiple primary malignant neoplasms: historical perspectives. Cancer. 1977;40(4 Suppl):1786-1792. [Crossref] [PubMed]
10. Tripathi N, Ayaz A, Naqvi SAA, et al. Secondary primary malignancies among patients with GU cancer. J Clin Oncol 2024;42. [Crossref]
11. Fazal F, Ur Rehman ME, Khokhar AA, et al. Second primary malignancies and their associations with age, gender, and latency periods in urogenital cancers: a retrospective cohort study. Cureus. 2025;17(8):e90017. [Crossref] [PubMed] [PMC]
12. Shou J, Wo Q. Risk of second primary malignancies for prostate cancer: a surveillance, epidemiology, and end results population-based study. Asian Journal of Urology. 2025. [Crossref]
13. Davis EJ, Beebe-Dimmer JL, Yee CL, Cooney KA. Risk of second primary tumors in men diagnosed with prostate cancer: a population-based cohort study. Cancer. 2014;120(17):2735-2741. [Crossref] [PubMed] [PMC]
14. Van Hemelrijck M, Feller A, Garmo H, et al. Incidence of second malignancies for prostate cancer. PLoS One. 2014;9(7):e102596. [Crossref] [PubMed] [PMC]
15. Bagshaw HP, Arnow KD, Trickey AW, Leppert JT, Wren SM, Morris AM. Assessment of second primary cancer risk among men receiving primary radiotherapy vs surgery for the treatment of prostate cancer. JAMA Netw Open. 2022;5(7):e2223025. [Crossref] [PubMed] [PMC]
16. Wu Y, Li Y, Han C, et al. Risk of second primary malignancies associated with radiotherapy in prostate cancer patients: competing risk analysis. Future Oncol. 2022;18(4):445-455. [Crossref] [PubMed]
17. Wallis CJ, Mahar AL, Choo R, et al. Second malignancies after radiotherapy for prostate cancer: systematic review and meta-analysis. BMJ. 2016;352:i851. [Crossref] [PubMed] [PMC]
18. St-Laurent MP, Acland G, Hamilton SN, et al. Long-term second malignancies in prostate cancer patients treated with low-dose-rate brachytherapy and radical prostatectomy. J Urol. 2024;212(1):63-73. [Crossref] [PubMed]
19. Abern MR, Dude AM, Tsivian M, Coogan CL. The characteristics of bladder cancer after radiotherapy for prostate cancer. Urol Oncol. 2013;31(8):1628-1634. [Crossref] [PubMed]
20. Matsukawa A, Yanagisawa T, Miszczyk M, et al. Incidence and outcomes of secondary bladder cancer following radiation therapy for prostate cancer: a systematic review and meta-analysis. Eur Urol Focus. 2025;11(3):471-481. [Crossref] [PubMed]
21. Dee EC, Muralidhar V, King MT, et al. Second malignancy probabilities in prostate cancer patients treated with SBRT and other contemporary radiation techniques. Radiother Oncol. 2021;161:241-250. [Crossref] [PubMed]
22. Suriano F, Altobelli E, Sergi F, Buscarini M. Bladder cancer after radiotherapy for prostate cancer. Rev Urol. 2013;15(3):108-112. [Crossref] [PubMed] [PMC]
23. Ogedegbe OJ, Bai S, Ntukidem OL, et al. Second primary malignancy in bladder cancer: a retrospective population-based analysis. J Clin Oncol. 2025;42(Suppl 5):676. [Crossref]
24. Hensley PJ, Duan Z, Bree K, et al. Competing mortality risk from second primary malignancy in bladder cancer patients following radical cystectomy: implications for survivorship. Urol Oncol. 2023;41(2):108.e11-108.e17. [Crossref] [PubMed]
25. Şahin AF, Altok M, Akdeniz F, Yıldız G, Divrik RT. Second primary cancers in patients with urothelial cancers. Investig Clin Urol. 335-330:(5)57;2016. [Crossref] [PubMed] [PMC]
26. Ntukidem OL, Ogedegbe OJ, Olafimihan AG, et al. Updated trends in second primary malignancy in patients with renal cell carcinoma: a retrospective population-based analysis. J Clin Oncol. 2025;43(16_suppl):e16546. [Crossref]
27. Lu Y-C, Tsai Y-C, Chow P-M, et al. The risk of subsequent malignancies in patients with renal cell carcinoma: a nationwide, population-based study. Urological Science. 2022;33(3):124-129. [Crossref]
28. Bengtsen MB, Farkas DK, Sørensen HT, Nørgaard M. Renal cell carcinoma and risk of second primary cancer: a Danish nationwide cohort study. Cancer Med. 2024;13(11):e7237. [Crossref] [PubMed] [PMC]
29. Rabbani F, Reuter VE, Katz J, Russo P. Second primary malignancies associated with renal cell carcinoma: influence of histologic type. Urology. 2000;56(3):399-403. [Crossref] [PubMed]
30. Zhang W, Gou P, Dupret JM, Chomienne C, Rodrigues-Lima F. Etoposide, an anticancer drug involved in therapy-related secondary leukemia: enzymes at play. Transl Oncol. 2021;14(10):101169. [Crossref] [PubMed] [PMC]
31. Curreri SA, Fung C, Beard CJ. Secondary malignant neoplasms in testicular cancer survivors. Urol Oncol. 2015;33(9):392-398. [Crossref] [PubMed]
32. van den Belt-Dusebout AW, de Wit R, Gietema JA, et al. Treatment-specific risks of second malignancies and cardiovascular disease in 5-year survivors of testicular cancer. J Clin Oncol. 2007;25(28):4370-4378. [Crossref] [PubMed]
33. Auskalnis S, Janciauskiene R, Rimsaite U, Alksnyte A, Ugenskiene R. Correction: Auskalnis et al. synchronous seminoma of testis and renal cell carcinoma: a rare case report. *Medicina* 2024, *60*, 1553. Medicina (Kaunas). 2024;60(12):2042. Erratum for: Medicina (Kaunas). 2024;60(9):1553. [Crossref] [PubMed] [PMC]
34. Phua ZJ, MacInnis RJ, Jayasekara H. Cigarette smoking and risk of second primary cancer: a systematic review and meta-analysis. Cancer Epidemiol. 2022;78:102160. [Crossref] [PubMed]
35. Dracham CB, Shankar A, Madan R. Radiation induced secondary malignancies: a review article. Radiat Oncol J. 2018;36(2):85-94. [Crossref] [PubMed] [PMC]
36. Torezan LA, Festa-Neto C. Cutaneous field cancerization: clinical, histopathological and therapeutic aspects. An Bras Dermatol. 2013;88(5):775-786. [Crossref] [PubMed] [PMC]
37. Dakubo GD, Jakupciak JP, Birch-Machin MA, Parr RL. Clinical implications and utility of field cancerization. Cancer Cell Int. 2007;7:2. [Crossref] [PubMed] [PMC]

38. Travis LB, Beard C, Allan JM, et al. Testicular cancer survivorship: research strategies and recommendations. J Natl Cancer Inst. 2010;102(15):1114-30. [Crossref] [PubMed] [PMC]
39. Fung C, Fossa SD, Milano MT, Oldenburg J, Travis LB. Solid tumors after chemotherapy or surgery for testicular nonseminoma: a population-based study. J Clin Oncol. 2013;31(30):3807-3814. [Crossref] [PubMed] [PMC]
40. Welch HG, Black WC. Overdiagnosis in cancer. J Natl Cancer Inst. 2010;102(9):605-613. [Crossref] [PubMed]
41. Hollingsworth JM, Miller DC, Daignault S, Hollenbeck BK. Rising incidence of small renal masses: a need to reassess treatment effect. J Natl Cancer Inst. 2006;98(18):1331-1334. [Crossref] [PubMed]

ORIGINAL ARTICLE

DOI: 10.37047/jos.galenos.2026.2025-11-9

J Oncol Sci 2026;12(1):51-58

Survival Outcomes and Prognostic Factors in Head and Neck Adenoid Cystic Carcinoma Following Curative Surgery

Hatice BÖLEK[1], Mehmet KAYAALP[1], Taha Koray ŞAHİN[2], Osman Talha DOĞAN[3], Seher YÜKSEL[4], Sümeyra Duru BİRGİ[5], İbrahim Halil GÜLLÜ[2], Mustafa Kürşat GÖKCAN[6], Sercan AKSOY[2], Hatime Arzu YAŞAR[1]

[1]Ankara University Faculty of Medicine, Department of Medical Oncology, Ankara, Türkiye
[2]Hacettepe University Faculty of Medicine, Department of Medical Oncology, Ankara, Türkiye
[3]Hacettepe University Faculty of Medicine, Department of Internal Medicine, Ankara, Türkiye
[4]Ankara University Faculty of Medicine, Department of Pathology, Ankara, Türkiye
[5]Ankara University Faculty of Medicine, Department of Radiation Oncology, Ankara, Türkiye
[6]Ankara University Faculty of Medicine, Department of Otorhinolaryngology, Ankara, Türkiye

ABSTRACT

Objective: Adenoid cystic carcinoma (ACC) is a rare malignancy characterized by indolent progression and a high-risk of local recurrence and distant metastasis. This study aimed to identify predictors of recurrence, distant metastasis, and survival among patients with head and neck ACC who underwent primary curative surgery.

Material and Methods: We conducted a retrospective analysis of patients with head and neck ACC diagnosed between January 2005 and December 2023. The clinical and pathological parameters were assessed to identify prognostic factors.

Results: Among the 125 patients included in the study, recurrence occurred in 73 patients (58.4%) and distant metastasis was detected in 46 patients (36.8%). The estimated 5-year, 10-year, and 15-year recurrence-free survival (RFS) rates were 49%, 27%, and 19%, respectively. The estimated overall survival rates at 5, 10, and 15 years were 86%, 78%, and 55%, respectively. Multivariate analysis revealed that male gender was an independent poor prognostic factor for RFS [hazard ratio (HR): 2.11, 95% confidence interval (CI): 1.15-3.86] and for distant-metastasis-free survival (HR: 2.79, 95% CI: 1.41-5.56). Despite aggressive treatment, more than one-third of patients experience distant recurrence during follow-up.

Conclusion: Our study identified male gender as an independent predictor of poor prognosis in patients who underwent primary curative surgery.

Keywords: Adenoid cystic carcinoma; head and neck cancer; male gender; prognostic factors; recurrence; salivary gland tumors

INTRODUCTION

Adenoid cystic carcinoma (ACC) is a rare tumor that originates in secretory glands. ACC is the most common malignant tumor of the minor salivary glands (30%) and the second most common in the major salivary glands (10%).[1] However, ACC may originate from other sites in the head and neck region. ACC predominantly affects women, accounting for approximately 60-70% of cases and being most common in the 5th or 6th decades of life.[2] ACC shows a slow growth pattern, often demonstrating extensive local infiltration and perineural invasion. Most of the time, the symptoms are vague and caused by the mass effect of the primary tumor. Because the tumor grows slowly, diagnosis is often delayed and challenging.

The initial treatment of ACC is surgery; however, achieving clear surgical margins is relatively difficult as the true extent

Correspondence: Hatime Arzu YAŞAR MD;
Ankara University Faculty of Medicine, Department of Medical Oncology, Ankara, Türkiye
E-mail: arzuyasar@gmail.com
ORCID ID: orcid.org/0000-0002-0545-1383

Received: 25.11.2025 **Accepted:** 08.03.2026 **Epub:** 12.03.2026 **Publication Date:** 18.03.2026

Cite this article as: Bölek H, Kayaalp M, Şahin TK, et al. Survival outcomes and prognostic factors in head and neck adenoid cystic carcinoma following curative surgery. J Oncol Sci. 2026;12(1):51-58

Available at journalofoncology.org

of ACC tumors is often underestimated.[3] Surgery is generally followed by external radiation therapy, as ACC appears to be sensitive to radiotherapy (RT), with postoperative RT increased the local control rates.[3,4] Despite aggressive local therapy, typically involving surgery and RT, the majority of ACC patients eventually develop recurrent or metastatic disease. In some studies, the 10-year recurrence rate exceeds 60%.[5,6] Chemotherapy is generally the first-line treatment in the metastatic setting for patients without a targetable mutation who need systemic therapy. Upon disease progression, anti-vascular endothelial growth factor tyrosine kinase inhibitors may be considered.[7-9] The long-term prognoses remain poor, with an estimated overall survival (OS) rate of less than 70% over a 10-year period.[10-12] The rarity of ACC, along with its tendency for late recurrence and the need for prolonged follow-up periods, makes the identification of prognostic markers particularly challenging. In this study, we aimed to evaluate survival outcomes and prognostic factors in patients with head and neck ACC who underwent primary surgery.

MATERIAL AND METHODS

We conducted a retrospective cohort study involving patients diagnosed with ACC of the head and neck who were treated and followed up at two tertiary hospitals in Ankara, Türkiye, between January 2005 and December 2023. The study included patients who had a diagnosis of ACC of the head and neck, were older than 18 years of age, and underwent primary curative surgery. The study excluded patients with metastatic disease at diagnosis and those with incomplete data required for survival analysis.

We extracted demographic information (e.g., age, gender), Eastern Cooperative Oncology Group (ECOG) performance status, pathological characteristics (e.g., histological subtype, perineural invasion), presence of adjuvant treatment, date of recurrence, date of the last follow-up, and mortality status. Surgical margin positivity is defined as the presence of tumor cells at the resected margin or within ≤5 mm. The primary endpoints of the study were recurrence-free survival (RFS) and factors affecting RFS. Secondary endpoints were distant metastasis-free survival (DMFS) and OS. RFS was defined as the time from surgery to recurrence or death. DMFS was defined as the time from surgery to the date of distant metastasis or death. OS was defined as the time from surgery to the date of death.

The study was approved by the Ankara University Faculty Ethics Committee (date: 10/02/2025, application number: 2025000051-2) and it was carried out in accordance with the Code of Ethics of the World Medical Association also known as a declaration of Helsinki.

Statistical Analysis

All statistical analyses were conducted using IBM SPSS Statistics for Mac, version 24.0 (IBM Corp., Armonk, NY). Continuous variables were expressed as medians with interquartile ranges, while categorical variables were presented as percentages. Categorical variables were compared using the chi-square test, and continuous variables were compared using either the Mann-Whitney U test or the Student's t-test. Survival outcomes were estimated using the Kaplan-Meier method. Multivariate analyses were performed using variables with a p-value of ≤0.10 in the univariate analyses. Multivariable Cox regression analysis was employed to calculate hazard ratios (HRs) with 95% confidence intervals (CIs). All p-values were two-sided, with statistical significance defined as $p<0.05$.

RESULTS

A total of 152 patients with ACC of the head and neck were identified. Among them, 22 patients were excluded due to metastatic disease at diagnosis, and 5 were excluded due to lack of follow-up and incomplete data for survival analysis. A total of 125 patients were included in the study. The median age was 47 years (range, 19.8-79.8 years). Among the patients, 72 (57.6%) were female, and 77 (63.1%) had an ECOG performance status of 0. Of the primary tumor sites, 40 (32%) originated from the major salivary glands, 40 (32%) from the oral cavity and hypopharynx, and 19 (15.2%) from the nasal sinuses. Other tumor locations are detailed in Table 1. The most common histologic types were cribriform (41.4%) and mixed (41.4%). Among the 114 patients with available clinical T stage data, 16 (14.0%) had T1 disease, 39 (34.2%) had T2, 37 (32.5%) had T3, and 22 (19.3%) had T4. Regarding nodal status (n=115), 97 patients (84.3%) were node-negative, while 18 (15.7%) were node-positive. Only 24 patients (20.9%) underwent surgery resulting in negative surgical margins. A total of 99 patients (79.2%) received adjuvant treatment, of whom 69 (69.7%) underwent RT and 30 (30.3%) received chemoradiotherapy (CRT). Among the 30 patients treated with CRT, 23 received concurrent cisplatin, 2 received carboplatin, and 1 received doxorubicin; the concurrent chemotherapy agent was unknown for the remaining 4 patients.

The median follow-up time was 71.7 months (95% CI: 54.5-88.9). Recurrence occurred in 73 patients (58.4%). Median RFS was 59.9 months (95% CI: 44.4-75.5) (Figure 1A). The 5-year, 10-year, and 15-year RFS were 49%, 27%, and 19%, respectively. By recurrence type, 35 patients (47.9%) experienced only locoregional recurrence, 27 (37.0%) experienced distant recurrence, and 11 (15.1%) experienced both locoregional and distant recurrence. Treatment for the first recurrence is given in Table 2. Multivariate Cox regression analysis showed

TABLE 1: Baseline characteristics of patients.		
Variables		**n=125**
Age, years (median, range)		47.01 (19.8-79.8)
Age, years (n=125)	<55	88 (70.4)
	≥55	37 (29.6)
Gender (n=125)	Female	72 (57.6)
	Male	53 (42.4)
ECOG-PS (n=122)	0	77 (63.1)
	1	42 (34.4)
	2	3 (2.5)
Primary location (n=125)	Parotid	16 (12.8)
	Submandibular-sublingual gland	24 (19.2)
	Oral cavity-hypopharynx	40 (32)
	Nasopharynx	7 (5.6)
	Nasal sinuses	19 (15.2)
	Maxilla	9 (7.2)
	Mandibula	1 (0.8)
	Orbital	4 (3.2)
	Larynx	5 (4)
Histologic subtype (n=70)	Tubular	5 (7.1)
	Cribriform	29 (41.4)
	Solid	7 (10)
	Mixed	29 (41.4)
T stage (n=114)	1	16 (14)
	2	39 (34.2)
	3	37 (32.5)
	4	22 (19.3)
Nodal status (n=115)	N -	97 (84.3)
	N +	18 (15.7)
Surgical margin (n=113)	Negative	24 (20.9)
	Positive	91 (79.1)
Solid component (n=80)	No	47 (58.8)
	Yes	33 (41.3)
PNI (n=93)	No	20 (21.5)
	Yes	73 (78.5)
Adjuvant treatment (n=125)	No	26 (20.8)
	Yes	99 (79.2)
Type of adjuvant treatment (n =99)	RT	69 (69.7)
	CRT	30 (30.3)

CRT: Chemoradiotherapy; ECOG: Eastern Cooperative Oncology Group; PNI: Perineural invasion; PS: Performance status; RT: Radiotherapy.

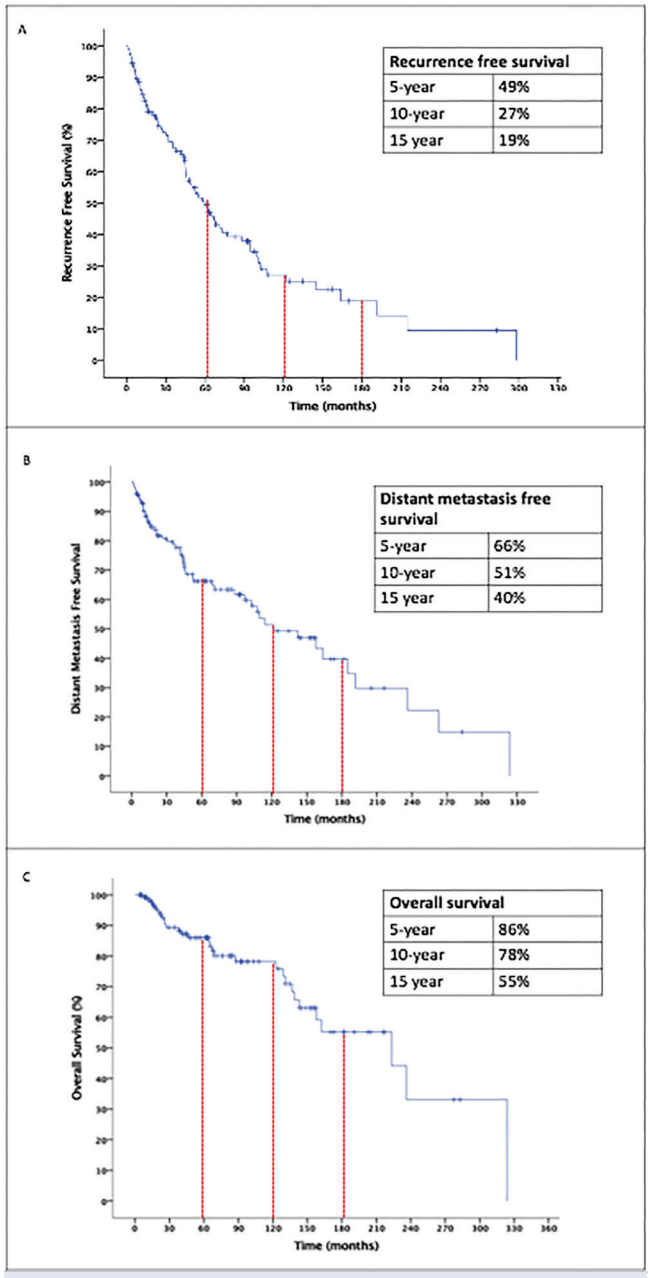

FIGURE 1: Kaplan-Meier curve for recurrence free survival (A), distant metastasis free survival (B) and overall survival (C).

that male gender was an independent predictor of RFS (male vs. female HR: 2.11, 95% CI: 1.15-3.86; p=0.016) after adjusting for confounding factors such as primary tumor location, T stage, nodal status, surgical margin, and type of adjuvant treatment (Table 3).

Distant metastasis occurred in 46 (36.8%) patients. The median DMFS was 121.4 months (95% CI: 72.9-169.9) (Figure 1B). Five-year, 10-year, and 15-year DMFS rates were 66%, 51%, and 40%, respectively. The most common metastatic site was the lung (82.6%), followed by non-regional lymph nodes (41.3%), bone (19.6%), and liver (13%) (Table 4). Multivariate

Cox regression analysis showed that male gender was an independent predictor of DMFS (male vs. female HR: 2.79, 95% CI: 1.41-5.56; p=0.003) after adjustment for confounding factors such as primary tumor location, surgical margin, and type of adjuvant treatment (Table 5).

TABLE 2: Characteristics of first recurrence (n=73).

Type of recurrence	Locoregional	35 (47.9)
	Distant	27 (37)
	Locoregional + distant	11 (15.1)
Type of treatment	Surgery	21 (28.8)
	Surgery + RT	8 (10.9)
	Surgery + CRT	4 (5.5)
	RT	6 (8.2)
	CRT	3 (4.1)
	Systemic treatment	19 (26)
	No treatment	12 (16.4)

CRT: Chemoradiotherapy; RT: Radiotherapy.

Thirty (24%) patients died during follow-up. The median OS was 223.3 months (95% CI: 96.6-349.9) (Figure 1C). The 5-year, 10-year, and 15-year OS rates were 86%, 78%, and 55%, respectively. No variables were found to be predictors of OS in the univariate analysis; therefore, multivariate analysis was not performed (Supplementary Table 1).

DISCUSSION

ACC accounts for only about 1% of all head and neck cancers, and its rarity has limited the availability of high-quality clinical evidence. Because of this, research on ACC is limited. Its prolonged clinical course, initially slow growth, and subsequent progression pose clinical challenges. Due to these factors, real-world data on this disease is generally limited. In our study, we report patient characteristics and prognostic factors associated with this disease, based on a relatively large patient cohort. Our study demonstrated that male gender was an independent prognostic factor for the RFS and DMFS, but did not impact the OS. The 5-year RFS, DMFS, and OS rates were 49%, 66%, and 86%, respectively, while the 15-year RFS,

TABLE 3: Univariate and multivariate analyses for recurrence free survival.

Variable		Univariate		Multivariate	
		HR (95% CI)	p	HR (95% CI)	p
Age	<55	1		-	
	≥55	1.12 (0.67-1.91)	0.642	-	-
Gender	Female	1		1	
	Male	1.58 (0.99-2.51)	0.054	2.11 (1.15-3.86)	**0.016**
ECOG-PS	0	1		-	
	1	1.33 (0.82-2.16)	0.247	-	-
Primary location	Major salivary gland	1		1	
	Other	2.07 (1.21-3.56)	**0.008**	1.17 (0.80-3.65)	0.166
T stage	T1-2	1		1	
	T3-4	1.56 (0.94-2,58)	0.083	0.97 (0.50-1.86)	0.917
Nodal status	N -	1		1	
	N +	2.02 (1.11-3.66)	**0.021**	1.74 (0.87-3.48)	0.116
Surgical margin	Negative	1		-	
	Positive	1.66 (0.93-2.62)	0.085	1.75 (0.79-3.85)	0.165
Solid component	No	1		-	
	Yes	1.05 (0.57-1.92)	0.883	-	-
PNI	No	1		-	
	Yes	0.87 (0.43-1.75)	0.694	-	-
Adjuvant treatment	No	1		-	
	Yes	0.79 (0.45-1.41)	0.434	-	-
Type of adjuvant treatment	RT	1		1	
	CRT	1.35 (1.02-1.79)	**0.037**	1.28 (0.67-2.42)	0.455

CI: Confidence interval; CRT: Chemoradiotherapy; ECOG: Eastern Cooperative Oncology Group; HR: Hazard ratio; PNI: Perineural invasion; PS: Performance status; RT: Radiotherapy.

DMFS, and OS rates were 19%, 40%, and 55%, respectively. These findings support the indolent but persistent nature of ACC, with a high tendency for late recurrence and metastasis.

RFS, DMFS, and OS rates at landmark time points vary across different studies.[1,10,13,14] A Swedish study involving 142 patients treated with curative intent reported the following survival outcomes: 5-year disease free survival (DFS) of 64.9%, 10-year DFS of 49.6%, and 15-year RFS of 37.7%, while 5-year OS was 83.5%, 10-year OS was 59.4%, and 15-year OS was 42.5%.[15] The study demonstrated that adjuvant treatment prolonged both RFS and OS; however, no significant difference was observed between RT and CRT. The percentage use of adjuvant therapy and the types of adjuvant therapy were similar to those in our study. However, compared with this study, our study observed lower RFS rates but higher OS rates. On the other hand, a large surveillance, epidemiology, and end results program (SEER) database study including 1555 patients diagnosed between 1993 and 2007—including metastatic patients—found 5-year, 10-year, and 15-year OS rates of 85%, 73%, and 67%, respectively.[12] The variability in survival rates across studies is likely attributable to differences in patient demographics, disease stage, histopathological characteristics, and treatment strategies.

In our study, male sex was the only independent poor prognostic factor for recurrence and distant metastasis; however, it was not prognostic for OS. SEER database analysis,

TABLE 4: Characteristics of distant metastasis (n=46).

Metastasis sites	Non-regional LN	19 (41.3)
	Lung	38 (82.6)
	Liver	6 (13)
	Bone	9 (19.6)
	CNS	5 (10.9)
	Kidney	1 (2.2)
	Adrenal gland	1 (2.2)
Type of treatment	Surgery	5 (10.9)
	Systemic treatment	30 (65.2)
	No treatment	11 (23.9)

LN: Lymph node.

TABLE 5: Univariate and multivariate analyses for distant metastasis free survival.

Variable		Univariate		Multivariate	
		HR (95% CI)	p	HR (95% CI)	p
Age	<55	1		-	
	≥55	1.63 (0.88-2.99)	0.118	-	-
Gender	Female	1		1	
	Male	2.20 (1.24-3.91)	**0.007**	2.79 (1.41-5.56)	**0.003**
ECOG-PS	0	1			
	1	1.23 (0.72-2.09)	0.443	-	-
Primary location	Major salivary gland	1		1	-
	Other	1.97 (1.02-1.97)	**0.045**	1.19 (0.88-4.42)	0.098
T stage	T1-2	1		-	
	T3-4	1.38 (0.75-2.53)	0.303	-	-
Nodal status	N -	1		-	
	N +	1.54 (0.73-3.22)	0.257	-	-
Surgical margin	Negative	1		1	
	Positive	2.34 (1.08-5.07)	**0.030**	1.44 (0.64-3.26)	0.376
Solid component	No	1		-	
	Yes	1.36 (0.64-2.92)	0.425	-	-
PNI	No	1		-	
	Yes	2.62 (0.79-8.63)	0.113	-	-
Adjuvant treatment	No	1		-	
	Yes	1.91 (0.76-4.82)	0.171	-	-
Type of adjuvant treatment	RT	1		1	
	CRT	1.49 (1.08-2.07)	**0.014**	1.51 (0.73-3.09)	0.266

CI: Confidence interval; CRT: Chemoradiotherapy; ECOG: Eastern Cooperative Oncology Group; HR: Hazard ratio; PNI: Perineural invasion; PS: Performance status; RT: Radiotherapy.

including more than 3000 patients, showed OS significantly shorter in male patients with head and neck ACC (HR: 0.73; 95% CI: 0.65-0.8[2]).[12] Also, another SEER database analysis by Lloyd et al.[10] demonstrated that overall and cancer specific survival was shorter in male patients. Furthermore, a recent meta-analysis including 17.497 patients showed that male gender was associated with poor DMFS and OS.[16] Although these results suggest a potential hormonal influence on the biological behavior of ACC, the prognostic impact of male gender remains uncertain, as studies have yielded conflicting results.[17,18] Estrogen receptor β expression has been demonstrated in ACC, and experimental data suggest that estrogen signalling may impact differentiation; however, the clinical relevance of these observations remains uncertain, and any sex-related hormonal contribution to outcomes should be considered hypothesis-generating.[19,20] Additional, possible explanations for the observed female advantage include greater health and body awareness, which may facilitate earlier symptom recognition, timelier presentation to care, and consequently earlier diagnosis.[21]

In univariate analysis, tumor location other than the major salivary gland was associated with shorter RFS and DMFS. Tumors originated from major salivary glands, especially from the parotid gland, and a more favorable prognosis was found in patients who were treated with curative intent.[2] While some cohorts have shown similar findings, not all studies have reported a significant impact of the subsite on disease prognosis.[1,10,13,22,23] ACCs located in the nasal sinuses or nasal cavity are often diagnosed at a later stage than those in the major salivary glands, which may adversely affect prognosis. Although study results are conflicting, considering several studies have indicated, prognosis may worsen with advancing T stage.[1,2,6,24] In our cohort, 91 patients (79.1%) had positive surgical margins. Even in early-stage ACC patients, positive surgical margins are common, and tumor size, location, and the surgeon can influence the likelihood of positive surgical margins. ACC arising near the skull base (nasopharynx, nasal cavity, and paranasal sinuses) is associated with a higher risk of local recurrence, largely because clear margins are difficult to achieve due to involvement of critical structures such as the skull base, dura, cranial nerves, and carotid artery, which limits the extent of resection.[3] Even within the same anatomic location, positive surgical margins are more frequent in ACC than in other histologic types, potentially owing to its marked tendency for perineural spread and infiltrative growth. Positive surgical margin and perineural invasion are other factors that have been identified as predictors of poor outcomes in head and neck ACC.[3,23,25] However, findings regarding prognostic markers remain conflicting, with studies yielding inconsistent results.[26] Moreover, the interrelationships among these defined prognostic markers further complicate their interpretation.

In our cohort, neither the receipt of adjuvant therapy nor the adjuvant modality was associated with survival outcomes. This may be attributable to the vast majority of patients receiving adjuvant treatment, thereby limiting meaningful between-group comparisons. Although postoperative RT with or without concurrent chemotherapy is commonly recommended after resection for head and neck ACC, there are no randomized or prospective trials definitively establishing its benefit. In a retrospective study of 319 patients with non-metastatic head and neck ACC, postoperative RT was associated with improved local recurrence–free survival, but not with DMFS, DFS, or OS.[27] These results align with several other studies showing that postoperative RT primarily impacts local control.[28-30] Since these studies are retrospective, treatment allocation was likely influenced by baseline risk factors, which should be taken into account when interpreting the findings, given the potential for selection bias and confounding by indication.

Study Limitations

Our study has several limitations. First, its retrospective design is subject to inherent biases, including selection bias and missing data, which may have influenced the outcomes; in particular, several pathological variables were not consistently available across all cases, including histologic subtype, presence of a solid component, PNI, exact surgical margin distance. Second, the relatively low number of death events limited the statistical power of OS analyses, potentially reducing our ability to detect prognostic associations and precluding robust multivariable modeling for OS. Additionally, there are no standardized guidelines for adjuvant treatment in ACC, and treatment approaches are heterogeneous, potentially influencing survival outcomes. Lastly, the impact of molecular biomarkers on prognosis could not be assessed, as molecular testing data were not available for this cohort.

CONCLUSION

ACC is a rare head and neck tumor characterized by late relapses. Despite aggressive treatment, more than one-third of patients experience distant recurrence during follow-up. Our study identified male gender as an independent poor prognostic factor in patients who underwent primary curative surgery. In the future, prospective multi-institutional studies with larger sample sizes, extended follow-up periods, and molecular marker integration will be needed to further elucidate the prognostic factors for ACC.

Ethics

Ethics Committee Approval: The study was approved by the Ankara University Faculty Ethics Committee (date: 10/02/2025, application number: 2025000051-2) and it was carried out in accordance with the Code of Ethics of the World Medical Association also known as a declaration of Helsinki.

Informed Consent: Retrospective study.

Footnotes

Authorship Contributions

Surgical and Medical Practices: H.B., S.Y., S.D.B., İ.H.G., M.K.G., S.A., H.A.Y., Concept: H.B., S.A., H.A.Y., Design: H.B., H.A.Y., Data Collection or Processing: H.B., M.K., T.K.Ş., O.T.D., H.A.Y., Analysis or Interpretation: H.B., H.A.Y., Literature Search: H.B., H.A.Y., Writing: H.B., M.K., T.K.Ş., O.T.D., S.Y., S.D.B., İ.H.G., M.K.G., S.A., H.A.Y.

Conflict of Interest: Sercan Aksoy MD is editor-in-chief in Journal of Oncological Sciences. He had no involvement in the peer-review of this article and had no access to information regarding its peer-review.

Financial Disclosure: The author declared that this study received no financial support.

REFERENCES

1. Ouyang DQ, Liang LZ, Zheng GS, et al. Risk factors and prognosis for salivary gland adenoid cystic carcinoma in southern china: a 25-year retrospective study. Medicine (Baltimore). 2017;96(5):e5964. [Crossref] [PubMed] [PMC]
2. Zupancic M, Näsman A, Friesland S, Dalianis T. Adenoid cystic carcinoma, clinical presentation, current treatment and approaches towards novel therapies. Anticancer Res. 2024;44(4):1325-1334. [Crossref] [PubMed]
3. Garden AS, Weber RS, Morrison WH, Ang KK, Peters LJ. The influence of positive margins and nerve invasion in adenoid cystic carcinoma of the head and neck treated with surgery and radiation. Int J Radiat Oncol Biol Phys. 1995;32(3):619-626. [Crossref] [PubMed]
4. Miglianico L, Eschwege F, Marandas P, Wibault P. Cervico-facial adenoid cystic carcinoma: study of 102 cases. Influence of radiation therapy. Int J Radiat Oncol Biol Phys. 1987;13(5):673-678. [Crossref] [PubMed]
5. Balamucki CJ, Amdur RJ, Werning JW, et al. Adenoid cystic carcinoma of the head and neck. Am J Otolaryngol. 2012;33(5):510-518. [Crossref] [PubMed]
6. Atallah S, Casiraghi O, Fakhry N, et al. A prospective multicentre REFCOR study of 470 cases of head and neck adenoid cystic carcinoma: epidemiology and prognostic factors. Eur J Cancer. 2020;130:241-249. [Crossref] [PubMed]
7. Tchekmedyian V, Sherman EJ, Dunn L, et al. Phase II study of lenvatinib in patients with progressive, recurrent or metastatic adenoid cystic carcinoma. J Clin Oncol. 2019;37(18):1529-1537. [Crossref] [PubMed] [PMC]
8. Locati LD, Galbiati D, Calareso G, et al. Patients with adenoid cystic carcinomas of the salivary glands treated with lenvatinib: activity and quality of life. Cancer. 2020;126(9):1888-1894. [Crossref] [PubMed]
9. Kang EJ, Ahn MJ, Ock CY, et al. Randomized phase II study of axitinib versus observation in patients with recurred or metastatic adenoid cystic carcinoma. Clin Cancer Res. 2021;27(19):5272-5279. [Crossref] [PubMed]
10. Lloyd S, Yu JB, Wilson LD, Decker RH. Determinants and patterns of survival in adenoid cystic carcinoma of the head and neck, including an analysis of adjuvant radiation therapy. Am J Clin Oncol. 2011;34(1):76-81. [Crossref] [PubMed]
11. Bjørndal K, Krogdahl A, Therkildsen MH, et al. Salivary adenoid cystic carcinoma in Denmark 1990-2005: outcome and independent prognostic factors including the benefit of radiotherapy. Results of the Danish Head and Neck Cancer Group (DAHANCA). Oral Oncol. 2015;51(12):1138-1142. [Crossref] [PubMed]
12. Ellington CL, Goodman M, Kono SA, et al. Adenoid cystic carcinoma of the head and neck: incidence and survival trends based on 1973-2007 surveillance, epidemiology, and end results data. Cancer. 2012;118(18):4444-5441. Erratum in: Cancer. 2012;118(21):5448-5449. [Crossref] [PubMed]
13. Cheng Y, Xu L, Chen Z, et al. Prognosis of adenoid cystic carcinoma in head and neck region treated with different regimens-a single-centre study. Cancer Med. 2023;12(3):2368-2377. [Crossref] [PubMed] [PMC]
14. Ciccolallo L, Licitra L, Cantú G, Gatta G; EUROCARE working group. Survival from salivary glands adenoid cystic carcinoma in European populations. Oral Oncol. 2009;45(8):669-674. [Crossref] [PubMed]
15. Zupancic M, Näsman A, Berglund A, Dalianis T, Friesland S. Adenoid cystic carcinoma (AdCC): a clinical survey of a large patient cohort. Cancers (Basel). 2023;15(5):1499. [Crossref] [PubMed] [PMC]
16. Lavareze L, Kimura TC, Cacita N, et al. Survival outcomes in adenoid cystic carcinoma of the head and neck: a systematic review of 17 497 cases and meta-analysis. Head Neck. 2025;47(5):1541-1553. [Crossref] [PubMed]
17. Oplatek A, Ozer E, Agrawal A, Bapna S, Schuller DE. Patterns of recurrence and survival of head and neck adenoid cystic carcinoma after definitive resection. Laryngoscope. 2010;120(1):65-70. [Crossref] [PubMed]
18. Ko JJ, Siever JE, Hao D, Simpson R, Lau HY. Adenoid cystic carcinoma of head and neck: clinical predictors of outcome from a Canadian centre. Curr Oncol. 2016;23(1):26-33. [Crossref] [PubMed] [PMC]
19. Marques YM, Giudice FS, Freitas VM, et al. Oestrogen receptor β in adenoid cystic carcinoma of salivary glands. Histopathology. 2012;60(4):609-616. [Crossref] [PubMed]
20. Mujtaba H, Ahmad S, Khan ZA, et al. Immunohistochemical expression of estrogen receptor-β in adenoid cystic carcinoma of salivary gland–a descriptive study. Journal of Cancer Research and Therapeutics. 2024;20(6):1872-1877. [Crossref]
21. Micheli A, Mariotto A, Giorgi Rossi A, Gatta G, Muti P. The prognostic role of gender in survival of adult cancer patients. EUROCARE working group. Eur J Cancer. 1998;34(14 Spec No):2271-2278. [Crossref] [PubMed]
22. Tasoulas J, Divaris K, Theocharis S, et al. Impact of tumor site and adjuvant radiotherapy on survival of patients with adenoid cystic carcinoma: a SEER database analysis. Cancers (Basel). 2021;13(4):589. [Crossref] [PubMed] [PMC]
23. de Morais EF, da Silva LP, Moreira DGL, et al. Prognostic factors and survival in adenoid cystic carcinoma of the head and neck: a retrospective clinical and histopathological analysis of patients seen at a cancer center. Head Neck Pathol. 2021;15(2):416-424. [Crossref] [PubMed] [PMC]
24. Zhang CY, Xia RH, Han J, et al. Adenoid cystic carcinoma of the head and neck: clinicopathologic analysis of 218 cases in a Chinese population. Oral Surg Oral Med Oral Pathol Oral Radiol. 2013;115(3):368-375. [Crossref] [PubMed]

25. Amit M, Na'ara S, Trejo-Leider L, et al. Defining the surgical margins of adenoid cystic carcinoma and their impact on outcome: an international collaborative study. Head Neck. 2017;39(5):1008-1014. [Crossref] [PubMed] [PMC]
26. Morse E, Fujiwara RJT, Judson B, Prasad ML, Mehra S. Positive surgical margins in parotid malignancies: institutional variation and survival association. Laryngoscope. 2019;129(1):129-137. [Crossref] [PubMed]
27. Chen Y, Zheng ZQ, Chen FP, et al. Role of postoperative radiotherapy in nonmetastatic head and neck adenoid cystic carcinoma. J Natl Compr Canc Netw. 2020;18(11):1476-1484. [Crossref] [PubMed]
28. Choi SH, Yang AJ, Yoon SO, et al. Role of postoperative radiotherapy in resected adenoid cystic carcinoma of the head and neck. Radiat Oncol. 2022;17(1):197. [Crossref] [PubMed] [PMC]
29. Ali S, Palmer FL, Katabi N, et al. Long-term local control rates of patients with adenoid cystic carcinoma of the head and neck managed by surgery and postoperative radiation. Laryngoscope. 2017;127(10):2265-2269. [Crossref] [PubMed] [PMC]
30. Chen AM, Bucci MK, Weinberg V, et al. Adenoid cystic carcinoma of the head and neck treated by surgery with or without postoperative radiation therapy: prognostic features of recurrence. Int J Radiat Oncol Biol Phys. 2006;66(1):152-159. [Crossref] [PubMed]

Click the link to access Supplementary Table 1: https://d2v96fxpocvxx.cloudfront.net/080b1dc9-b5e8-4382-b356-1411b16f2612/content-images/45e7313c-430c-478e-b8e9-313c6e475d29.pdf

ORIGINAL ARTICLE

DOI: 10.37047/jos.galenos.2026.2026-1-1

J Oncol Sci 2026;12(1):59-66

Real-world Efficacy and Safety of Trastuzumab Deruxtecan in HER2-positive Metastatic Breast Cancer: A Multicenter Retrospective Study from Türkiye

Harun MUĞLU[1], Erdem SÜNGER[1], Lamia ŞEKER CAN[2], Özgür HAN[3], Bünyamin GÜNEY[3], Jamshid HAMDARD[1], Burçin ÇAKAN DEMİREL[1], Özgür AÇIKGÖZ[1], Ömer Fatih ÖLMEZ[1], Mesut ŞEKER[2], Ahmet BİLİCİ[1]

[1]İstanbul Medipol University Faculty of Medicine, Department of Medical Oncology, İstanbul, Türkiye
[2]Bezmialem Vakıf University Faculty of Medicine, Department of Medical Oncology, İstanbul, Türkiye
[3]University of Health Sciences Türkiye, İstanbul Training and Research Hospital, Department of Medical Oncology, İstanbul, Türkiye

ABSTRACT

Objective: Trastuzumab deruxtecan (T-DXd) is a novel human epidermal growth factor receptor 2 (HER2)-directed antibody-drug conjugate that has demonstrated significant clinical activity in patients with HER2-positive metastatic breast cancer (mBC) in multiple pivotal trials. However, data regarding its effectiveness and safety in real-world settings, particularly from underrepresented regions such as Türkiye, remain limited.

Material and Methods: This retrospective, multicenter observational study included HER2-positive mBC patients [immunohistochemistry (IHC) score of 3+, or IHC score of 2+ with *in situ* hybridization-positive gene amplification] who received T-DXd after at least one prior line of systemic therapy. Clinical outcomes, including objective response rate (ORR), disease control rate (DCR), progression-free survival (PFS), and overall survival (OS), were evaluated. Subgroup and univariate Cox regression analyses were conducted to assess prognostic factors. Adverse events (AEs) were recorded and graded according to the Common Terminology Criteria for AEs version 5.0 (CTCAE v5.0).

Results: A total of 39 patients were included. The ORR was 89.7%, and the DCR was 100%. Median PFS and median OS were not reached at the time of analysis. In univariate analysis, a better Eastern Cooperative Oncology Group performance status and receipt of T-DXd in earlier treatment lines were associated with improved survival outcomes. AEs were generally manageable; grade ≥3 toxicity occurred in 15.4% of patients. Interstitial lung disease (ILD) was observed in 7.7% of patients, leading to treatment discontinuation in one patient.

Conclusion: T-DXd demonstrated high clinical efficacy and manageable toxicity in a real-world cohort of Turkish patients with HER2-positive mBC. These results are consistent with those reported in clinical trials and support the use of T-DXd as an effective treatment option in routine clinical practice. Our findings also highlight the importance of early identification and management of treatment-related AEs, particularly ILD.

Keywords: Trastuzumab deruxtecan; HER2-positive breast cancer; metastatic breast cancer; real-world evidence; antibody-drug conjugate; interstitial lung disease; progression-free survival

INTRODUCTION

Human epidermal growth factor receptor 2 (HER2) is overexpressed in approximately 15-20% of breast cancers and is associated with increased tumor proliferation, aggressive clinical behavior, and a historically poor prognosis in the absence of targeted therapies.[1,2] The introduction of HER2-directed agents such as trastuzumab, pertuzumab, and trastuzumab emtansine (T-DM1) has revolutionized the management of HER2-positive metastatic breast cancer (mBC), significantly improving survival outcomes in both early-stage and advanced disease.[3-5] Nonetheless, treatment resistance frequently develops, and a substantial proportion of patients ultimately progress after two or more lines of HER2-targeted therapies, highlighting the need for more effective agents in later lines of therapy.[6]

Correspondence: Harun MUĞLU MD;
İstanbul Medipol University Faculty of Medicine, Department of Medical Oncology, İstanbul, Türkiye
E-mail: hm1635@hotmail.com
ORCID ID: orcid.org/0000-0001-9584-0827

Received: 05.01.2026 **Accepted:** 08.03.2026 **Epub:** 12.03.2026 **Publication Date:** 18.03.2026

Cite this article as: Muğlu H, Sünger E, Şeker Can L, et al. Real-world efficacy and safety of trastuzumab deruxtecan in HER2-positive metastatic breast cancer: a multicenter retrospective study from Türkiye. J Oncol Sci. 2026;12(1):59-66

Available at journalofoncology.org

Trastuzumab deruxtecan (T-DXd) is a novel antibody-drug conjugate (ADC) comprising a humanized anti-HER2 monoclonal antibody conjugated to a topoisomerase I inhibitor payload via a cleavable linker.[7] Unlike earlier ADCs, T-DXd possesses a high drug-to-antibody ratio (~8:1) and exhibits a potent bystander killing effect, which enables it to target both HER2-overexpressing and neighboring low-HER2-expressing tumor cells.[8] These pharmacological advantages have translated into favorable clinical outcomes across multiple trials. Although randomized clinical trials provide high-quality evidence under controlled conditions, their strict eligibility criteria may limit generalizability to routine clinical practice. Patients enrolled in pivotal trials often represent selected populations, whereas real-world patients are typically more heterogeneous in terms of age, performance status (PS), comorbidities, prior treatment exposure, and disease burden, including the presence of brain metastases. Consequently, real-world evidence (RWE) is crucial to validate the effectiveness and safety of T-DXd in broader and more representative patient populations.[9]

The clinical activity of T-DXd has been demonstrated in multiple pivotal trials. The phase II DESTINY-Breast01 study established its efficacy in heavily pretreated patients, while the phase III DESTINY-Breast03 trial confirmed its superiority over T-DM1 in the second-line setting. More recently, DESTINY-Breast02 further supported its benefit in patients previously treated with T-DM1, consolidating its role across multiple lines of therapy.[10-12]

Several observational studies have evaluated the real-world use of trastuzumab deruxtecan, supporting its effectiveness and manageable safety profile outside clinical trial settings. However, these reports originate primarily from Western European cohorts, and data from other geographic regions remain limited.[13-16]

Nevertheless, real-world data from Türkiye remain scarce, and no national-level study to date has reported the use of T-DXd in routine practice. Given the regional differences in treatment accessibility, sequencing strategies, and patient characteristics, it is essential to generate local data to inform clinicians and guide therapeutic decisions.

In this retrospective, multicenter study, we aimed to evaluate the real-world clinical outcomes of T-DXd in patients with HER2-positive mBC treated in Türkiye. Specifically, we assessed objective response rate (ORR), disease control rate (DCR), progression-free survival (PFS), overall survival (OS), and treatment-related adverse events (AEs), including interstitial lung disease (ILD). Additionally, we investigated potential prognostic factors for survival outcomes in routine clinical practice. By providing multicenter data from an underrepresented population, this study contributes region-specific evidence to the growing body of real-world literature on T-DXd.

MATERIAL AND METHODS

This retrospective multicenter observational study was conducted at three oncology centers in Türkiye between November 2025 and January 2026 to evaluate the real-world effectiveness and safety of T-DXd in patients with HER2-positive mBC. The study included adult patients (≥18 years) with histologically confirmed HER2-positive disease, defined as immunohistochemistry (IHC) 3+ or IHC 2+ with *in situ* hybridization (ISH) positivity, who had received at least one prior line of systemic therapy for metastatic disease. Patients were identified via electronic medical records, and treatment with T-DXd was administered in accordance with standard clinical practice. Patients were excluded if they had HER2-negative or HER2-low disease (i.e., IHC 0, 1+, or 2+ with ISH-negative), were enrolled in interventional clinical trials during T-DXd treatment, or had incomplete clinical documentation. T-DXd was administered intravenously at a starting dose of 5.4 mg/kg every three weeks (q3w), in accordance with standard clinical practice and the prescribing information. Dose reductions were implemented when clinically indicated, with the first dose reduction to 4.4 mg/kg and a second reduction to 3.2 mg/kg. Further dose reduction beyond 3.2 mg/kg led to treatment discontinuation. Treatment interruptions, dose adjustments, and permanent discontinuations were performed at the discretion of the treating physician based on toxicity severity and established safety recommendations. Treatment was continued until disease progression, unacceptable toxicity, or physician's decision.

Only patients with active brain metastases (defined as untreated lesions or lesions with radiological progression at the time of T-DXd initiation) were recorded as having central nervous system (CNS) involvement. Patients with previously treated and radiologically stable brain metastases were not included in this category.

Demographic and clinical data, including age, hormone receptor status, Eastern Cooperative Oncology Group (ECOG) PS, number and type of prior therapies, and presence of brain metastases, were collected at baseline. Treatment responses were assessed by the treating investigators at each participating center, based on radiological evaluations performed according to the Response Evaluation Criteria in Solid Tumors version 1.1. Radiological assessments were performed approximately every 8-12 weeks according to institutional practice. Given the retrospective, real-world design of the study, response assessments were not centrally reviewed or blinded. The primary outcome

measures included ORR and DCR. The secondary endpoints were PFS and OS. PFS was defined as the time from initiation of T-DXd to documented disease progression or death from any cause, whichever occurred first. OS was defined as the time from initiation of T-DXd to death from any cause. AEs were retrospectively collected through systematic review of electronic medical records, including physician notes, laboratory results, and imaging reports. ILD was defined based on the presence of new pulmonary symptoms and/or radiological findings suggestive of drug-related pneumonitis, as documented in medical records. Alternative causes such as infection, pulmonary embolism, or disease progression were excluded based on clinical and radiological evaluation where applicable. ILD severity was graded according to Common Terminology Criteria for Adverse Events (CTCAE) version 5.0.[17] Other toxicities were also graded according to the CTCAE, version 5.0.[17] No prospective active safety monitoring was performed due to the retrospective design of the study.

Statistical Analysis

Statistical analysis was performed using IBM SPSS Statistics version 25.0. Categorical variables were presented as frequencies and percentages, while continuous variables were reported as medians and ranges. Survival analyses (PFS and OS) were conducted using the Kaplan-Meier method, and subgroup comparisons were performed using the log-rank test. Associations between categorical variables were examined using the chi-square test or Fisher's exact test, where appropriate. A p-value <0.05 was considered statistically significant. Patients without documented progression or death at the time of data cut-off were censored on the date of their last follow-up. Because of the limited sample size and the small number of outcome events, multivariable modeling was not performed to avoid overfitting. Therefore, exploratory univariate Cox regression analyses were conducted. Data completeness was assessed prior to statistical analysis. A small proportion of missing data was identified for certain baseline variables. Therefore, analyses were performed using a complete-case approach without imputation.

The data cut-off date for survival analyses was January 31, 2026. Median follow-up time was calculated from the date of initiation of T-DXd to the date of last follow-up or death, whichever occurred first.

The study protocol was reviewed and approved by the Non-Interventional Clinical Research Ethics Committee of İstanbul Medipol University (approval no: 1322, date: 30.10.2025). All procedures were performed in accordance with the ethical standards of the institutional and national research committees and with the 1964 Declaration of Helsinki and its later amendments. Due to the retrospective nature of the study, the requirement for informed consent was waived.

RESULTS

A total of 39 patients with HER2-positive breast cancer who received T-DXd were included in this real-world analysis. Baseline clinicopathological characteristics are summarized in Table 1. The median age at diagnosis was 46 years (range, 24-66). Most patients had a good PS, with 97.4% having an ECOG PS of 0-1.

The majority of tumors (97.4%) were invasive ductal carcinomas, and hormone receptor positivity was observed in 64.1% of patients. *De novo* metastatic disease was present in 30.8% of cases. Visceral metastases were observed in 64.1% of patients, including liver metastases in 33.3% of patients; active (untreated or radiologically progressing) brain metastases were present in 35.9% of patients at the time of T-DXd initiation.

All patients had previously received trastuzumab, and most had been treated with pertuzumab (89.7%) and T-DM1 (87.2%). T-DXd was most commonly administered in the third-line setting (53.8%), followed by ≥4th line (35.9%). All patients received T-DXd at a starting dose of 5.4 mg/kg. The median number of treatment cycles was 12 (range, 3-71). At the data cut-off (January 31, 2026), the median follow-up from T-DXd initiation was 11.3 months (range, 2.2-28.2 months).

The best overall responses to T-DXd were complete response in 30.8% of patients, partial response in 59.0%, and stable disease in 10.3%. Accordingly, the ORR was 89.7%, and the DCR was 100%. At the time of analysis, disease progression was observed in 6 patients (15.4%). Median PFS was not reached. Kaplan-Meier estimates for PFS are shown in Figure 1.

During the follow-up period, 9 deaths (23.1%) were recorded. When OS was calculated from the time of metastatic diagnosis,

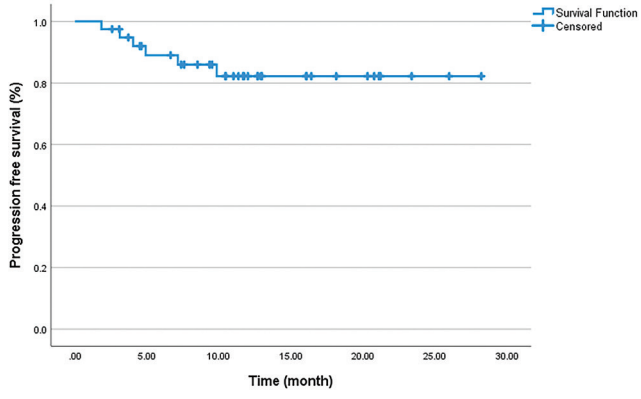

FIGURE 1: Kaplan-Meier curve for progression-free survival.

the median OS was not reached. OS from the initiation of T-DXd therapy was also evaluated. Median OS from T-DXd initiation was not reached. Kaplan-Meier curves for OS from metastatic diagnosis and from T-DXd initiation are presented in Figures 2 and 3, respectively.

TABLE 1: Baseline clinicopathological characteristics of patients with HER2-positive breast cancer treated with T-DXd in a real-world setting (n=39).

Variable	Total (n=39)
Age at diagnosis, years, median (range)	46 (24-66)
Menopausal status, n (%)	
Premenopausal	23 (59.0)
Postmenopausal	16 (41.0)
ECOG performance status, n (%)	
0	30 (76.9)
1	8 (20.5)
≥2	1 (2.6)
Histology, n (%)	
Invasive ductal carcinoma	38 (97.4)
Other	1 (2.6)
Hormone receptor status, n (%)	
ER-positive	25 (64.1)
PR-positive	16 (41.0)
HER2 status before T-DXd, n (%)	
IHC 3+	26 (66.7)
IHC 2+/ISH+	11 (28.2)
De novo metastatic disease, n (%)	12 (30.8)
Metastatic sites at baseline, n (%)	
Visceral metastasis (any)	25 (64.1)
Liver metastasis	13 (33.3)
Bone metastasis	19 (48.7)
Active (untreated/progressing) brain metastasis	14 (35.9)
Prior systemic treatments, n (%)	
Trastuzumab	39 (100)
Pertuzumab	35 (89.7)
Taxane	39 (100)
T-DM1	34 (87.2)
Capecitabine	12 (30.8)
Lapatinib	8 (21.1)
Line of T-DXd therapy, n (%)	
2nd line	4 (10.3)
3rd line	21 (53.8)
≥4th line	14 (35.9)
T-DXd dose	5.4 mg/kg (100%)

ECOG: Eastern Cooperative Oncology Group; ER: Estrogen receptor; HER2: Human epidermal growth factor receptor 2; HR: Hormone receptor; IHC: immunohistochemistry; ISH: *In situ* hybridization; PR: Progesterone receptor; T-DM1: Trastuzumab emtansine; T-DXd: Trastuzumab deruxtecan.

Univariate analyses for PFS and OS are summarized in Tables 2A and 2B, respectively. For PFS, no baseline clinical or treatment-related variables demonstrated a statistically significant association.

Several variables were significantly associated with OS in univariate analysis, including ECOG PS (p=0.03), prior exposure to T-DM1 (p=0.02), prior exposure to capecitabine (p=0.023), line of T-DXd therapy (p=0.049), and receipt of subsequent therapy after T-DXd (p=0.032). Other clinicopathological characteristics, such as comorbidity status, menopausal status, metastatic status at diagnosis, hormone receptor status, and metastatic site involvement, were not significantly associated with survival outcomes.

Treatment-related AEs are summarized in Table 3. Overall, T-DXd was well tolerated. The most frequently observed AEs of any grade were alopecia (74.4%), nausea (66.7%), leukopenia (56.4%), anemia (51.3%), and neutropenia (48.7%). Grade 3-4 AEs occurred in 15.4% of patients, with neutropenia,

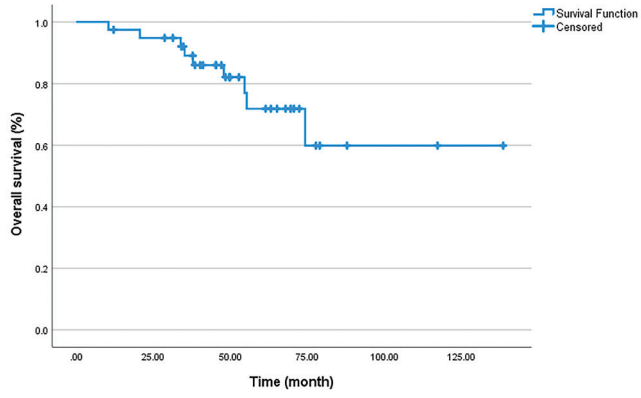

FIGURE 2: Kaplan-Meier curve for overall survival from metastatic diagnosis.

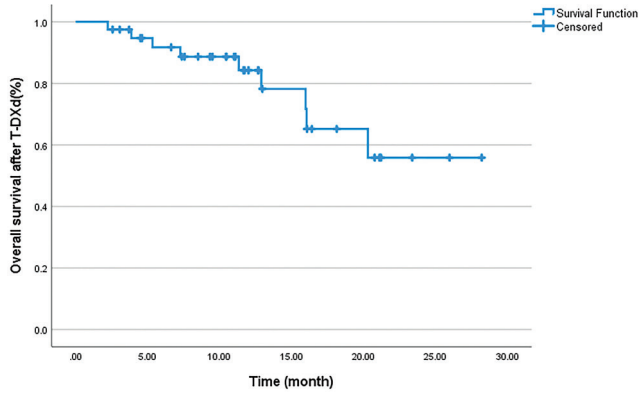

FIGURE 3: Kaplan-Meier curve for overall survival from trastuzumab deruxtecan initiation.

T-DXd: Trastuzumab deruxtecan.

leukopenia, anemia, thrombocytopenia, nausea, and ILD being the most common severe toxicities. Dose reductions due to treatment-related toxicity were required in 33.3% of patients, while treatment interruptions and permanent treatment discontinuations occurred in 17.9% and 5.1% of patients, respectively. ILD was observed in 7.7% of patients and led to treatment discontinuation in one patient. No treatment-related deaths were recorded.

TABLE 2A: Univariate analysis for progression-free survival.

Variable	p-value for PFS
Comorbidity (yes vs. no)	0.333
Menopausal status	0.622
Metastatic status at diagnosis (*de novo* vs. recurrent)	0.640
ECOG performance status	0.413
Prior pertuzumab exposure (yes vs. no)	0.781
Prior T-DM1 exposure (yes vs. no)	0.05
Prior capecitabine exposure (yes vs. no)	0.341
Prior lapatinib exposure (yes vs. no)	0.836
Hormone receptor status (positive vs. negative)	0.535
Line of T-DXd therapy	0.187
Liver metastasis	0.423
Lung metastasis	0.914
Bone metastasis	0.375
Active (untreated/progressing) brain metastasis	0.207

PFS: Progression-free survival; ECOG: Eastern Cooperative Oncology Group; T-DM1: Trastuzumab emtansine; T-DXd: Trastuzumab deruxtecan.

TABLE 2B: Univariate analysis for overall survival.

Variable	p-value for OS
Comorbidity (yes vs. no)	0.302
Menopausal status	0.949
Metastatic status at diagnosis (*de novo* vs. recurrent)	0.800
ECOG performance status	0.03
Prior pertuzumab exposure (yes vs. no)	0.781
Prior T-DM1 exposure (yes vs. no)	0.02
Prior capecitabine exposure (yes vs. no)	0.023
Prior lapatinib exposure (yes vs. no)	0.242
Hormone receptor status (positive vs negative)	0.602
Line of T-DXd therapy	0.049
Liver metastasis	0.668
Lung metastasis	0.911
Bone metastasis	0.732
Active (untreated/progressing) brain metastasis	0.244
Subsequent therapy after T-DXd (yes vs. no)	0.032

OS: Overall survival; ECOG: Eastern Cooperative Oncology Group: T-DM1, Trastuzumab emtansine; T-DXd: Trastuzumab deruxtecan.

DISCUSSION

The high response rates observed in our cohort are consistent with those reported in pivotal DESTINY trials and emerging real-world studies.[10,11] However, the ORR in our study appears numerically higher than in some controlled settings, which may reflect differences in patient selection, follow-up duration, and retrospective assessment.[13,18,19]

The relatively short median follow-up duration and a limited number of progression and death events may have influenced survival estimates. Median PFS and OS were not reached at the time of analysis; therefore, long-term survival outcomes should be interpreted cautiously. The small sample size (n=39) further limits statistical precision and generalizability.

In our real-world cohort, median PFS was not reached at the time of analysis and appeared comparable to that reported in controlled trials, despite the inclusion of patients with a broad range of prior therapies and varying ECOG PS. This real-world effectiveness corroborates existing observational studies, including the DE-REAL study, which also reported meaningful clinical activity of T-DXd in routine practice albeit with somewhat lower median PFS and ORR than in trials.[13]

Real-world studies from France and Greece, as well as from multinational cohorts further support the generalizability of T-DXd efficacy across diverse populations and healthcare systems. These findings demonstrate that T-DXd maintains

TABLE 3: Trastuzumab deruxtecan-related adverse events (n=39).

Adverse event	Any grade n (%)	Grade 3-4 n (%)
Anemia	20 (51.3)	1 (2.6)
Leukopenia	22 (56.4)	2 (5.1)
Neutropenia	19 (48.7)	1 (2.6)
Thrombocytopenia	14 (35.9)	2 (5.1)
Nausea	26 (66.7)	5 (12.8)
Vomiting	12 (30.8)	1 (2.6)
Diarrhea	11 (28.2)	0
Transaminase elevation	14 (35.9)	0
Alopecia	29 (74.4)	0
Interstitial lung disease	3 (7.7)	1 (2.6)
Any grade ≥3 adverse event	–	6 (15.4)
Dose reduction due to toxicity	–	13 (33.3)
Treatment interruption	–	7 (17.9)
Treatment discontinuation	–	2 (5.1)

high clinical utility beyond the controlled conditions of randomized clinical trials.[14,15,20-23]

In our univariate analyses, factors such as ECOG PS, the number of prior therapies, and the presence of brain metastases were associated with variations in survival outcomes. Specifically, patients with better PS and fewer prior lines of treatment tended to show longer PFS and OS. These findings are consistent with other analyses showing that earlier integration of T-DXd in the treatment sequence may enhance outcomes, particularly in second-line settings as highlighted by DESTINYBreast03.[11]

Although several associations were observed in univariate analysis, these findings should be interpreted with caution given the limited sample size and number of outcome events.[19] Notably, the receipt of subsequent lines of therapy after T-DXd was associated with improved survival outcomes, suggesting that T-DXd can serve as a therapeutic bridge, enabling further treatment options. However, this finding should be interpreted cautiously due to the potential for time-dependent bias inherent in retrospective analyses.

Brain metastases represent a challenging clinical subgroup with a poorer prognosis. While DESTINY trials and pooled analyses have shown that T-DXd provides intracranial responses, albeit with lower magnitudes than extracranial disease, our cohort's outcomes in patients with baseline CNS involvement were acceptable and generally aligned with these observations.[16] RWE increasingly recognizes the need for more focused studies on CNS disease management with ADCs, a priority area given the historical limitations of systemic therapies in controlling brain metastases.[24]

Safety outcomes in our study were consistent with the known toxicity spectrum of T-DXd. Most AEs were low-grade and manageable, with grade ≥3 events observed in 15.4% of patients. This aligns with real-world and clinical trial safety data showing manageable toxicity profiles when appropriate monitoring and supportive care are provided.[10,11,13] Dose reductions were required in a proportion of patients, reflecting clinical practice adjustments to ameliorate side effects while maintaining therapeutic effectiveness.

Of particular interest is the incidence of ILD/pneumonitis, a well-documented and potentially serious AE associated with T-DXd. Clinical trial data indicate ILD incidence ranging from 10-15% in some cohorts, with rare fatal outcomes.[10,11,25] Meta-analyses also report ILD rates of approximately 11.7% across breast cancer patients treated with T-DXd, with higher risk potentially linked to dose intensity and patient characteristics.[20,25] In our cohort, ILD occurred at a frequency consistent with these reports, confirming the necessity of vigilant pulmonary monitoring and early intervention protocols in routine care. Additional real-world studies emphasize that while ILD remains a toxicity of concern, it is often manageable when recognized promptly, underlining the importance of multicenter experience and multidisciplinary approaches to toxicity management.[18,20,26,27]

Cardiotoxicity and other ADC-related toxicities appear to be infrequent but are also under active investigation, with pooled analyses suggesting a low but measurable incidence that warrants clinical awareness and baseline cardiac assessment. Real-world safety data increasingly contribute to refining guidelines for dose modifications and supportive care to improve tolerability without compromising efficacy.[28,29]

The accumulation of RWE, including this study and other international cohorts, complements phase III evidence by demonstrating the reproducibility of T-DXd's efficacy and safety in broader, everyday clinical settings. Narrative reviews of real-world studies underscore consistent activity of T-DXd and emphasize its favorable safety profile, while also identifying areas where evidence is limited — such as older patients, those with comorbidities, and HR-negative subgroups. Additionally, ongoing research explores T-DXd's potential in combination regimens, novel sequencing strategies, and emerging indications such as first-line treatment in combination with other targeted agents.[13,30]

As ADC-based therapy continues to evolve, prospective registry studies and larger real-world databases will be crucial to optimize patient selection, mitigate toxicity, and determine sequencing strategies that maximize both survival and quality of life. Integrating molecular biomarkers and longitudinal patient-reported outcomes may further enhance the clinical applicability of these findings.

Study Limitations

Our study's retrospective design, relatively small sample size, and short follow-up duration represent important limitations. The limited number of outcome events reduces statistical power and precludes robust prognostic modeling. Additionally, the absence of centralized radiological review and the potential heterogeneity across participating centers may have influenced the outcome assessment. Therefore, the findings should be interpreted as exploratory and hypothesis-generating rather than definitive. Furthermore, while real-world data provide valuable insights, they are subject to potential confounding factors and heterogeneity in clinical practice. Despite these limitations, our findings add to a growing body of RWE that reinforces the role of T-DXd as a potent therapeutic agent for HER2-positive mBC in routine clinical settings. Given the limited sample size and number of outcome events, multivariable analyses were not performed

to avoid model overfitting; therefore, prognostic findings are exploratory in nature.

CONCLUSION

In this real-world multicenter study from Türkiye, T-DXd demonstrated substantial clinical benefit in patients with HER2-positive mBC who had previously received at least one line of systemic therapy. The high ORR and DCR, together with favorable PFS, are consistent with efficacy reported in randomized clinical trials and other real-world cohorts. Although certain clinical variables such as ECOG PS and treatment line were associated with survival outcomes in univariate analysis, these findings should be interpreted cautiously due to the limited sample size and number of events.

Importantly, the safety profile of T-DXd was manageable, with AEs comparable to those observed in larger studies, including a relatively low but clinically relevant incidence of ILD. Our study contributes valuable real-world data from an underrepresented population and supports the integration of T-DXd into standard care pathways for HER2-positive mBC. Further large-scale and prospective studies are warranted to refine patient selection, optimize treatment sequencing, and enhance the safe use of this potent therapeutic agent in diverse clinical settings.

Ethics

Ethics Committee Approval: The study protocol was reviewed and approved by the Non-Interventional Clinical Research Ethics Committee of İstanbul Medipol University (approval no: 1322, date: 30.10.2025).

Informed Consent: Retrospective study.

Footnotes

Author Contributions

Surgical and Medical Practices: H.M., E.S., L.Ş.C., Ö.H., Ö.F.Ö., M.Ş., Concept: H.M., B.G., J.H., A.B., Design: H.M., B.Ç.D., Ö.A., A.B., Data Collection or Processing: H.M., E.S., L.Ş.C., Ö.H., B.Ç.D., Ö.A., Ö.F.Ö., M.Ş., Analysis or Interpretation: H.M., A.B., Literature Search: H.M., B.G., J.H., A.B., Writing: H.M.

Conflict of Interest: No conflict of interest was declared by the authors.

Financial Disclosure: The authors declared that this study received no financial support.

REFERENCES

1. Slamon DJ, Clark GM, Wong SG, Levin WJ, Ullrich A, McGuire WL. Human breast cancer: correlation of relapse and survival with amplification of the HER-2/neu oncogene. Science. 1987;235(4785):177-182. [Crossref] [PubMed]
2. Wolff AC, Hammond MEH, Allison KH, et al. Human epidermal growth factor receptor 2 testing in breast cancer: American Society of Clinical Oncology/College of American Pathologists Clinical Practice Guideline focused update. J Clin Oncol. 2018;36(20):2105-2122. [Crossref] [PubMed]
3. Swain SM, Baselga J, Kim SB, et al; CLEOPATRA Study Group. Pertuzumab, trastuzumab, and docetaxel in HER2-positive metastatic breast cancer. N Engl J Med. 2015;372(8):724-734. [Crossref] [PubMed] [PMC]
4. Verma S, Miles D, Gianni L, et al; EMILIA Study Group. Trastuzumab emtansine for HER2-positive advanced breast cancer. N Engl J Med. 2012;367(19):1783-1791. Erratum in: N Engl J Med. 2013;368(25):2442. [Crossref] [PubMed] [PMC]
5. Baselga J, Cortés J, Kim SB, et al; CLEOPATRA Study Group. Pertuzumab plus trastuzumab plus docetaxel for metastatic breast cancer. N Engl J Med. 2012;366(2):109-119. [Crossref] [PubMed] [PMC]
6. Krop IE, Suter TM, Dang CT, et al. Feasibility and cardiac safety of trastuzumab emtansine after anthracycline-based chemotherapy as (neo)adjuvant therapy for human epidermal growth factor receptor 2-positive early-stage breast cancer. J Clin Oncol. 2015;33(10):1136-1142. [Crossref] [PubMed] [PMC]
7. Ogitani Y, Aida T, Hagihara K, et al. DS-8201a, A novel HER2-targeting ADC with a novel DNA topoisomerase I inhibitor, demonstrates a promising antitumor efficacy with differentiation from T-DM1. Clin Cancer Res. 2016;22(20):5097-5108. [Crossref] [PubMed]
8. Nakada T, Sugihara K, Jikoh T, Abe Y, Agatsuma T. The latest research and development into the antibody-drug conjugate, [fam-] trastuzumab deruxtecan (DS-8201a), for HER2 cancer therapy. Chem Pharm Bull (Tokyo). 2019;67(3):173-185. [Crossref] [PubMed]
9. Khozin S, Blumenthal GM, Pazdur R. Real-world data for clinical evidence generation in oncology. J Natl Cancer Inst. 2017;109(11). [Crossref] [PubMed]
10. Modi S, Saura C, Yamashita T, et al; DESTINY-Breast01 Investigators. Trastuzumab deruxtecan in previously treated HER2-positive breast cancer. N Engl J Med. 2020;382(7):610-621. [Crossref] [PubMed] [PMC]
11. Cortés J, Kim SB, Chung WP, et al; DESTINY-Breast03 Trial Investigators. Trastuzumab deruxtecan versus trastuzumab emtansine for breast cancer. N Engl J Med. 2022;386(12):1143-1154. [Crossref] [PubMed]
12. André F, Hee Park Y, Kim SB, et al. Trastuzumab deruxtecan versus treatment of physician's choice in patients with HER2-positive metastatic breast cancer (DESTINY-Breast02): a randomised, open-label, multicentre, phase 3 trial. Lancet. 2023;401(10390):1773-1785. Erratum in: Lancet. 2023;402(10418):2196. Erratum in: Lancet. 2024;403(10430):912. [Crossref] [PubMed]
13. Botticelli A, Caputo R, Scagnoli S, et al. Real-world outcomes of trastuzumab deruxtecan in patients with HER2+ metastatic breast cancer: the DE-REAL study. Oncologist. 2024;29(4):303-310. [Crossref] [PubMed] [PMC]
14. Kotteas E, Panagiotou E, Grammoustianou M, et al. Real-world safety and efficacy of trastuzumab deruxtecan (T-DXd) in patients with HER2-positive/HER2-low metastatic breast cancer: a multicenter retrospective cohort study. Future Oncol. 2025;21(24):3189-3196. [Crossref] [PubMed] [PMC]
15. Jourdain H, Di Meglio A, Mansouri I, Desplas D, Zureik M, Haddy N. Use and outcomes of trastuzumab deruxtecan in HER2-positive and HER2-low metastatic breast cancer in a real-world setting: a nationwide cohort study. ESMO Open. 2024;9(12):104083. [Crossref] [PubMed] [PMC]
16. Harbeck N, Ciruelos E, Jerusalem G, et al; DESTINY-Breast12 study group. Trastuzumab deruxtecan in HER2-positive advanced breast cancer with or without brain metastases: a phase 3b/4 trial. Nat Med. 2024;30(12):3717-3727. Erratum in: Nat Med. 2024;30(12):3780. [Crossref] [PubMed] [PMC]

17. Freites-Martinez A, Santana N, Arias-Santiago S, Viera A. Using the common terminology criteria for adverse events (CTCAE - Version 5.0) to evaluate the severity of adverse events of anticancer therapies. Actas Dermosifiliogr (Engl Ed). 2021;112(1):90-92. English, Spanish. [Crossref] [PubMed]
18. Antonarelli G, Milano M, Andreon C, et al. Real-world safety and efficacy profiles of trastuzumab deruxtecan in patients with advanced breast cancer. ESMO Open. 2025;10(11):105847. [Crossref] [PubMed] [PMC]
19. Lazaratos AM, Dankner M, Hamouda A, et al. The real-world clinical outcomes of heavily pretreated HER2+ and HER2-low metastatic breast cancer patients treated with trastuzumab deruxtecan at a single centre. Curr Oncol. 2024;32(1):1. [Crossref] [PubMed] [PMC]
20. Xue C, Liao Q, Huang R, et al. Prognostic index for predicting outcomes of trastuzumab deruxtecan in HER2 expressing metastatic breast cancer: a real-world multicenter study. Oncologist. 2025;30(8):oyaf174. [Crossref] [PubMed] [PMC]
21. Pierga J-Y Asselain B, Teixeira L, et al. 190P French real-world safety and effectiveness of trastuzumab deruxtecan (T-DXd) in the treatment of patients (pts) with HER2+ metastatic or unresectable breast cancer (m/u BC): First results of REALITY-01 ambispective study. ESMO Open. 2024;9. [Crossref]
22. Petit T, Hajjaji N, Antoine EC, et al. Trastuzumab deruxtecan in previously treated HER2-positive metastatic or unresectable breast cancer: real-life data from the temporary use authorization program in France. Cancer Med. 2024;13(9):e7168. [Crossref] [PubMed] [PMC]
23. Saura C, Wildiers H, Bianchini G, et al. European experience of patients with HER2-positive advanced/metastatic breast cancer accessing trastuzumab deruxtecan through a named patient program: the EUROPA T-DXd study. Front Oncol. 2025;15:1650981. [Crossref] [PubMed] [PMC]
24. Khatri VM, Mestres-Villanueva MA, Yarlagadda S, et al. Multi-institutional report of trastuzumab deruxtecan and stereotactic radiosurgery for HER2 positive and HER2-low breast cancer brain metastases. NPJ Breast Cancer. 2024;10(1):100. [Crossref] [PubMed] [PMC]
25. Powell CA, Modi S, Iwata H, et al. Pooled analysis of drug-related interstitial lung disease and/or pneumonitis in nine trastuzumab deruxtecan monotherapy studies. ESMO Open. 2022;7(4):100554. [Crossref] [PubMed] [PMC]
26. Swain SM, Nishino M, Lancaster LH, et al. Multidisciplinary clinical guidance on trastuzumab deruxtecan (T-DXd)-related interstitial lung disease/pneumonitis-focus on proactive monitoring, diagnosis, and management. Cancer Treat Rev. 2022;106:102378. [Crossref] [PubMed]
27. Kawakami H, Uchino K, Hashimoto W, Muro K. Real-world evaluation of interstitial lung disease/pneumonitis in patients treated with trastuzumab deruxtecan for HER2-positive advanced or recurrent gastric cancer: a postmarketing surveillance study in Japan. ESMO Open. 2025;10(12):105914. [Crossref] [PubMed] [PMC]
28. Seth L, Bhave A, Kollapaneni S, et al. Cardiotoxic effects of antibody drug conjugates vs standard chemotherapy in ERBB2-positive advanced breast cancer: a systematic review and meta-analysis. JAMA Netw Open. 2025;8(11):e2540336. [Crossref] [PubMed] [PMC]
29. Soares LR, Vilbert M, Rosa VDL, Oliveira JL, Deus MM, Freitas-Junior R. Incidence of interstitial lung disease and cardiotoxicity with trastuzumab deruxtecan in breast cancer patients: a systematic review and single-arm meta-analysis. ESMO Open. 2023;8(4):101613. [Crossref] [PubMed] [PMC]
30. Quaquarini E, Luelli F, Lasagna A, et al. Trastuzumab-deruxtecan for the treatment of metastatic breast cancer patients: data from real world studies. Cancers (Basel). 2025;17(21):3505. [Crossref] [PubMed] [PMC]

ORIGINAL ARTICLE

DOI: 10.37047/jos.galenos.2026.2025-8-9

J Oncol Sci 2026;12(1):67-73

Vascular FDG Uptake on PET/CT in Patients Receiving Immune Checkpoint Inhibitors

Ali Kaan GÜREN[1], Kevser ÖKSÜZOĞLU[2], Erkam KOCAASLAN[1], Şerife ÇETİN[2], Taylan KAPLAN[3], Nazım Can DEMİRCAN[1], Murat SARI[1], Salih ÖZGÜVEN[2], Tunç ÖNEŞ[2], İbrahim Vedat BAYOĞLU[1], Osman KÖSTEK[1]

[1]Marmara University Faculty of Medicine, Department of Internal Medicine, Division of Medical Oncology, İstanbul, Türkiye
[2]Marmara University Faculty of Medicine, Department of Nuclear Medicine, İstanbul, Türkiye
[3]Marmara University Faculty of Medicine, Department of Internal Medicine, Division of Rheumatology, İstanbul, Türkiye

ABSTRACT

Objective: Numerous drug-related adverse effects are difficult to distinguish because they emerge concurrently with disease progression. Aside from case reports and case reviews, there is a paucity of publications providing detailed analyses of immune checkpoint inhibitors (ICIs) in relation to increased vascular FDG Uptake on positron emission tomography/computed tomography (PET/CT).

Material and Methods: The study comprised patients with histopathologically diagnosed cancer who were treated with ICIs. We analysed pre- and post-treatment PET/CT images to calculate the PET vascular activity score (PETVAS) for 15 vascular areas. We specifically examined patients with greater uptake compared with baseline. Patients with non-small cell lung cancer (NSCLC) were categorised based on an increase in uptake; progression-free survival (PFS) and overall survival (OS) were compared.

Results: One hundred forty eight patients were included in the study. A total of 482 PET/CT images were examined. Patients received five different ICIs across 13 cancer types. Ten (6.7%) patients exhibited increased 18F-fluorodeoxyglucose (FDG) uptake relative to pretreatment. Two of them (1.3%) had grade 2 or higher uptake. Among 68 NSCLC patients, higher uptake did not significantly affect PFS or OS (p=0.73 for PFS and p=0.37 for OS; both p>0.05).

Conclusion: Clinical and biochemical manifestations of underlying malignancy may obscure ICI-related arteritis. In patients presenting with unexplained constitutional symptoms and elevated acute-phase reactants, the PETVAS score may support the identification of clinically relevant vascular FDG uptake and help guide further diagnostic evaluation.

Keywords: Immune checkpoint inhibitors; immune-related adverse events; arteritis; ICI related arteritis; PETVAS score

INTRODUCTION

Immune checkpoint inhibitors (ICIs) are monoclonal antibodies structured as immunoglobulin G1 and immunoglobulin G4, employed in the treatment of various cancers by targeting specific molecules, including programmed cell death receptor-1 (PD-1), programmed cell death ligand-1 (PD-L1), and cytotoxic T lymphocyte-associated antigen-4 (CTLA-4).[1] Currently, they are utilised independently, in conjunction with traditional chemotherapies, or in combination with one another (against PD-1 or anti PDL-1 and CTLA-4) for the treatment of various malignancies.[2] Alongside offering considerable survival benefits in numerous cancer types, numerous immune-related adverse events (irAEs) such as pneumonitis, colitis, hepatitis, hypophysitis, thyroiditis, nephritis, and rash have been documented.[3,4] In addition to these clearly delineated irAEs, numerous case reports indicate that these medications can induce vasculitis with diverse presentations, encompassing both large-vessel vasculitis and anti-neutrophil cytoplasmic antibody (ANCA)-associated vasculitis. Nonetheless, there is no definitive consensus about the mechanism of ICI-related vasculitis.[5]

Correspondence: Ali Kaan GÜREN MD;
Marmara University Faculty of Medicine, Department of Internal Medicine, Division of Medical Oncology, İstanbul, Türkiye
E-mail: alikaanguren@gmail.com
ORCID ID: orcid.org/0000-0002-3562-5006

Received: 26.08.2025 **Accepted:** 08.03.2026 **Epub:** 12.03.2026 **Publication Date:** 18.03.2026

Cite this article as: Güren AK, Öksüzoğlu K, Kocaaslan E, et al. Vascular FDG uptake on PET/CT in patients receiving immune checkpoint inhibitors. J Oncol Sci. 2026;12(1):67-73

Available at journalofoncology.org

Arteritis encompasses a diverse array of disorders characterised by inflammation of the vessel wall. While it results in varying clinical manifestations depending on the affected organ, constitutional symptoms, such as malaise and fatigue, are present in nearly all cases of arteritis. Diagnosis is based on laboratory findings, clinical observations, imaging techniques, and, where feasible, histological analysis.[6,7] Laboratory results and systemic symptoms resemble the clinical manifestations observed in cancer patients, particularly during the metastatic phase. In cancer patients, The common constitutional symptoms such as malaise, fatigue, muscle pain, and elevated acute-phase reactants are often associated with the primary disease itself. Many side effects develop concurrently with disease progression and therefore cannot be clearly defined.

Positron emission tomography-computed tomography (PET/CT) has long been used in the diagnosis and follow-up of arteritis.[8] The primary advantages encompass its non-invasive nature, early identification of inflammation, and concurrent visualization of multiple vascular regions.[9] The PET vascular activity score (PETVAS), calculated from 18F-fluorodeoxyglucose (FDG) uptake across 15 vascular areas, has been shown to be effective in diagnosing and monitoring large artery vasculitis. Despite debates over its sensitivity and specificity, extensive research exists on its application in patients diagnosed with and monitored for arteritis.[10-12]

Although the diagnosis of arteritis is established through a combination of clinical, laboratory, radiological, and histopathological findings, documenting this retrospectively, particularly in a cohort of cancer patients, is challenging. In this context, the present study aims to examine the frequency of increased FDG uptake — which may assist in the diagnosis of arteritis — in patients receiving ICIs, and to evaluate the association between this increased FDG uptake and survival in patients with non-small cell lung cancer (NSCLC).

MATERIAL AND METHODS

Study Population

Patients who received treatment at the Marmara University Pendik Training and Research Hospital, Medical Oncology Clinic between January 1, 2018, and December 31, 2023 were included in the study. They had to have been diagnosed with cancer by histopathological examination and to have received any ICI as part of their treatment. Patients treated with ICI for less than 3 months; patients with a diagnosis of rheumatologic disease; patients with chronic arterial disease (including atherosclerosis); patients receiving statins for any indication; and patients who received radiotherapy within the last 1 year were excluded from the study.

Data Collection and Study Design

The patients' data were retrospectively analysed using patient files and the hospital electronic information system. For PET/CT imaging, scans were performed in 3D mode from the head to below the knee. The acquired images were reconstructed in cross-sectional, coronal, and sagittal planes. A low-dose CT scan was performed to provide attenuation correction and anatomical orientation. Imaging was performed one hour after FDG injection. Four independent nuclear medicine physicians interpreted the images, unaware of the clinical data. A total of 15 arterial regions were evaluated: ascending aorta, aortic arch, descending thoracic aorta, abdominal aorta, innominate artery, carotid arteries, subclavian arteries, axillary arteries, iliac arteries, and femoral arteries. PETVAS was calculated. Arterial regions were graded according to FDG uptake on a 0-3 scale: Grade 0 — no uptake; Grade 1 — less uptake than the liver; Grade 2 — uptake equal to the liver; Grade 3 — greater uptake than the liver. Patients' treatment responses were evaluated according to the Response Evaluation Criteria in Solid Tumours version 1.1.

PET/CTs performed within 1 month before the ICIs' start date, at 3 months post-treatment, and at 6 months, 1 year, 2 years, and 3 years (for patients who continued treatment) were analysed, and PETVAS scores were calculated. Since the largest patient group comprised patients with NSCLC, this group was analysed in more detail with respect to the relationship between PETVAS score and survival. All patients in the NSCLC group were at the metastatic stage and had received at least one line of chemotherapy. All patients had received ICI alone in the 2nd or subsequent lines. Patients with no increase in FDG uptake after treatment were assigned to Group 1, and those with increased uptake were assigned to Group 2. Progression-free survival (PFS) and overall survival (OS) were compared between groups.

Statistical Analysis

All statistical analyses were performed using SPSS version 22.0 (IBM Corp.). PFS was calculated as the time in months from the first treatment dose to disease progression, death (if the patient died during treatment), or the day of the last visit (if the patient was still receiving treatment). OS was calculated as the time in months from the first treatment dose to the date of death or to the date of the last visit, if the patient was still alive. Categorical variables were analyzed using the chi-square test. 95% confidence intervals (CIs) were calculated using the Brookmeyer and Crowley method. When the study data were evaluated, the conformity of the parameters to a normal distribution was assessed by the Shapiro-Wilk test. An

independent-samples t-test was used to compare normally distributed parameters, and the Mann-Whitney U test was used to compare non-normally distributed parameters. Survival differences between the groups were compared using the log-rank test. Significance was evaluated at the $p<0.05$ level.

Ethics Statements

This study was conducted in accordance with the principles of the Declaration of Helsinki. Approval was granted by Marmara University Faculty of Medicine, İstanbul, Türkiye, number: 09.2024.911, date: 19.07.2024.

RESULTS

We evaluated 207 patients who received ICIs. Thirty four patients were excluded because they received ICIs for less than three months; 16 patients were excluded because they did not have baseline or control PET/CT scans; and 9 patients were excluded because the data were incomplete. A total of 148 participants took part in the trial. A total of 482 PET/CT scans were assessed: 148 prior to therapy, 148 at three months, 102 at six months, 44 at one year, 22 at two years, and 18 at three years.

The average age of the patients was 63.2 years, with a range from 31 to 88 years. There were 113 male and 35 female patients. The patients were diagnosed with SCLC, NSCLC, renal cell carcinoma (RCC), malignant melanoma, bladder carcinoma, hepatocellular carcinoma, esophageal carcinoma, head and neck cancers, breast carcinoma, endometrial carcinoma, rectal carcinoma, and Merkel cell carcinoma. One hundred forty six patients presented with metastatic disease, whereas 2 patients presented with stage 3 disease. We used nivolumab, the combination of nivolumab and ipilimumab, atezolizumab, pembrolizumab, and avelumab as ICIs. Table 1 delineates the characteristics of the patients and the distribution of these characteristics.

A total of 148 patients received ICI treatment. A total of 136 patients received immunotherapy alone, while 12 patients received treatment in combination with chemotherapy. Among 136 patients, 13 had received tyrosine kinase inhibitors (patients diagnosed with hepatocellular carcinoma and RCC). In previous series, chemotherapy was used in 123 patients. Chemotherapy agents received were cisplatin, carboplatin, gemcitabine, pemetrexed, docetaxel, paclitaxel, vinorelbine, 5-fluorouracil, irinotecan, and oxaliplatin.

Pre-treatment PET/CT scans of 128 patients showed no increased FDG uptake in any region. Increased uptake with a total score of 1 or more was observed in 20 patients. Scores of patients with uptake ranged from 1 to 8, and none of the patients had an uptake of 2 points or more in any region. Five patients had uptake in 1 region, 10 patients had uptake in 2 regions, 3 patients had uptake in 3 regions, 1 patient had uptake in 7 regions, and 1 patient had uptake in 8 regions.

On post-treatment PET/CTs, no change was observed in 120 (81%) patients who had no uptake at baseline. On PET/CT, among 20 (13.5%) patients who had uptake at baseline, uptake continued at the same level in 9 (6%) patients, decreased but persisted in 5 (3.4%) patients, disappeared completely in 4 (2.6%) patients, and increased in 2 (1.3%) patients. In 8 (5.4%) patients who initially had no uptake, increased uptake was observed after treatment. In total, 10 (6.7%) patients showed increased uptake compared to pre-treatment PET/CT. In 2 of these patients (1.3%), 2 or more uptakes were detected in any region. These findings are summarised in Table 2.

TABLE 1: Basic characteristics of patients.

	Total patiens (n=148)
Age (minimum-maximum)	63.2 (31-88)
Gender (%)	
Male	113 (76.4)
Female	35 (23.6)
Types of cancer (%)	
Lung cancer (LC)	79 (53.3)
Small cell LC	7 (4.7)
Non-small cell LC	72 (48.6)
Renal cell cancer	29 (19.5)
Malign melanoma	14 (9.4)
Bladder cancer	7 (4.7)
Hepatocellular cancer	4 (2.7)
Esophageal cancer	4 (2.7)
Mesothelioma	4 (2.7)
Head and neck cancers	3 (2)
Breast cancer	1 (0.6)
Endometrial carcinoma	1 (0.6)
Rectal cancer	1 (0.6)
Merkel cell carcinoma	1 (0.6)
Stage (%)	
Metastatic stage	146 (98.6)
Non-metastatic stage	2 (1.3)
ICIs (%)	
Nivolumab	120 (81)
Nivolumab + Ipilimumab	5 (3.3)
Atezolizumab	11 (7.4)
Pembrolizumab	8 (5.4)
Avelumab	4 (2.7)

ICIs: Immune checkpoint inhibitors.

Of the 10 patients with increased involvement, 5 had NSCLC, 2 had RCC, 2 had bladder cancer, and 1 had SCLC. Five patients received nivolumab, 2 received pembrolizumab, 2 received atezolizumab, and 1 received avelumab; these findings are shown in Table 3.

One of the patients with grade 2 or higher uptake, a 68-year-old male with SLCL, was treated with carboplatin, etoposide, and atezolizumab for 3 months, and PET/CT showed increased uptake in 5 regions. Grade 3 uptake was observed in the left subclavian artery, whereas grade 2 uptake was observed in the right subclavian and right axillary arteries. In addition, grade 1 uptake was observed in the left axillary and right brachiocephalic arteries. Figure 1 displays the patient's pre- and post-treatment PET/C scans. Another patient exhibiting increased uptake was a 65-year-old male with NSCLC. The patient received 5 lines of conventional chemotherapy, followed by single-agent nivolumab as 6th-line therapy. PET/CT at the 6th month of treatment showed almost complete regression, while PET/CT at the 9th month of treatment showed grade 2 involvement in the left carotid and right brachiocephalic arteries, and grade 1 involvement in the right carotid and left brachiocephalic arteries. No increased involvement was observed in any of the previous scans. Table 4 summarises the involved regions and the maximum scores for the remaining patients. Increased involvement was found in 5 patients at the 3rd month follow-up, in 3 patients at the 6th month follow-up, and in 2 patients at the 9th month follow-up. The mean time to the development of uptake was 5.1 months.

TABLE 2: The distribution of patients before and after treatment according to PETVAS score.

	Total patients (n=148)
Pre-treatment (%)	
PETVAS =0	128 (86.4)
PETVAS ≥1	20 (13.5)
Post-treatment (%)	
Always negative	120 (81)
Stable while positive	9 (6)
Decreasing while positive	9 (6)
Increasing while positive	2 (1.3)
Increasing while negative	8 (5.4)
Total increasing	10 (6.7)
≥2 in any artery	2 (1.3)

PETVAS: Positron emission tomography vascular activity score.

TABLE 3: Characteristics of patients with increased uptake, ICIs used and time until increased uptake.

	Total patiens (n=10)
Types of cancer (%)	
Non-small cell lung cancer (LC)	5 (50)
Renal cell cancer	2 (20)
Bladder cancer	2 (20)
Small cell LC	1 (10)
Stage (%)	
Metastatic stage	10 (100)
ICIs (%)	
Nivolumab	5 (50)
Pembrolizumab	2 (20)
Atezolizumab	2 (20)
Avelumab	1 (10)
Time until increased uptake (%)	
3 months	5 (50)
6 months	3 (30)
9 months	2 (20)

ICIs: Immune checkpoint inhibitors.

Seventy-two patients with NSCLC received immunotherapy treatment. Survival data for 69 patients were calculated. While 64 patients (Group 1) had no significant increase in PET/CT uptake after treatment, 5 patients (Group 2) had increased uptake compared with pre-treatment PET/CTs. Table 5 describes the main characteristics of the groups. Median PFS was 6.26 months (95% CI: 5.21-7.32) in Group 1; 7.2 months (95% CI: 1.92-12.47) in Group 2; and 6.33 months (95% CI: 5.29-7.37) in all patients. When the groups were compared, the p-value was 0.73, indicating that the difference was not statistically significant (p>0.05). Median OS was 9.40 months (95% CI: 8.13-10.67) for Group 1, 11.4 months (95% CI: 5.56-17.23) for Group 2, and 9.55 months (95% CI: 8.30-10.79) overall. When the groups were compared, the p-value was 0.37, which is not statistically significant (p>0.05).

DISCUSSION

ICIs were associated with increased FDG uptake of at least grade 1 in 6.7% of our patients and of grade 2 or higher in 1.3%. This increased uptake was evaluated specifically in NSCLC patients; no difference in survival was observed between those with and without increased uptake. Furthermore, during the follow-up period, none of our patients were suspected of having arteritis; the data were analyzed retrospectively.

There are many comprehensive studies demonstrating that patients with irAEs who receive ICIs have longer survival compared to those without irAEs.[13,14] Accordingly, we grouped patients diagnosed with NSCLC into two groups: those with an increase in PETVAS score after ICIs and those without. When we compared the PFS and OS of the two groups, there was a numerical difference between them, but it was not

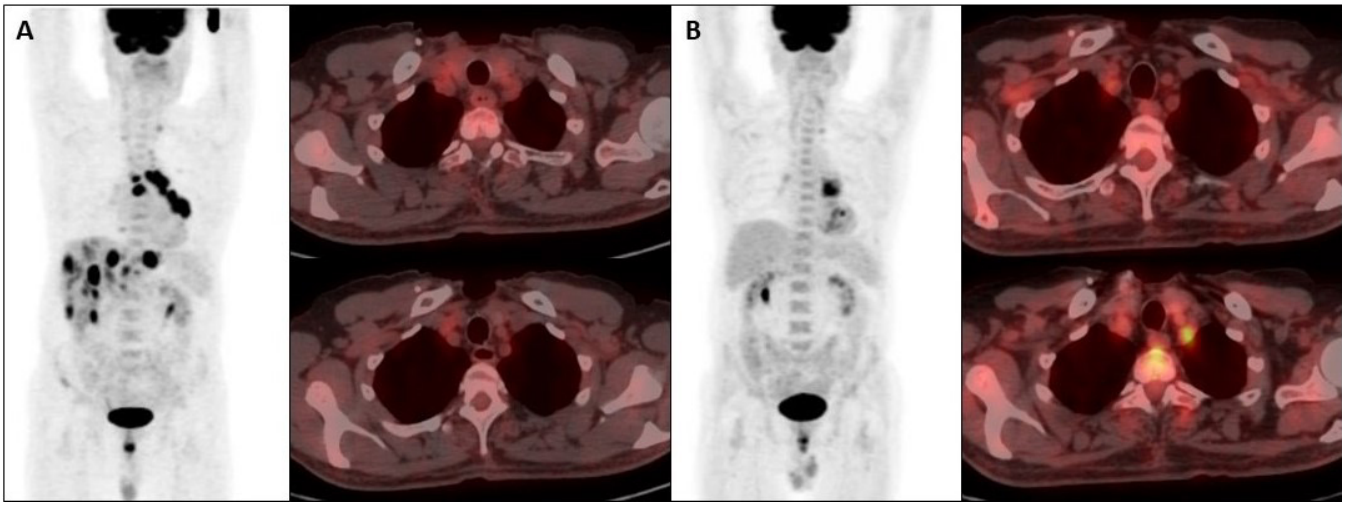

FIGURE 1: A) PET/CT sections before treatment B) PET/CT sections after treatment.

PET: Positron emission tomography; CT: Computed tomography.

TABLE 4: Distribution of patients with increased PETVAS score according to the number of involved arteries and PETVAS score.

Number of patients (%)	Number of arteries	Maximum score	Total score
1 (10)	1	1	1
4 (40)	2	1	2
1 (10)	3	1	3
2 (20)	4	1	4
1 (10)	3	2	5
1 (10)	5	3	9

PETVAS: Positron emission tomography vascular activity score.

statistically significant. Considering the insufficient number of patients and the unequal distribution of patients among the groups, we believe larger studies are needed to ensure statistical reliability.

In the review by Daxini et al.[5], the median time from the initiation of treatment until vasculitis developed was 3 months.[6] Of our two patients with grade 2 or higher uptake, one had increased uptake at the 3rd-month follow-up, whereas the other had increased uptake on PET/CT performed at the 9th month. The mean time course for all patients with increased uptake was 5.1 months, indicating that increased uptake may occur at a later stage than reported in previous studies.

ICI-associated vasculitis may lead to heterogeneous involvement ranging from cerebral vasculitis to ANCA-associated vasculitis, from systemic vasculitis to large vessel vasculitis.[15-18] Although tissue biopsy is the gold standard for diagnosing vasculitis, it is not always possible in large-vessel vasculitis. In the diagnosis of large vessel vasculitis, magnetic resonance imaging and PET/CT come to the forefront in patients in whom biopsy cannot be performed and are accepted as the standard approach.[19] In our study, we examined large-vessel involvement because we evaluated only PET/CT scans from patients assessed retrospectively, in whom vasculitis was not suspected and was therefore not adequately investigated. The PETVAS score, which is used to define, grade, and standardise arterial involvement status, indicated arterial involvement that varied according to the timing of treatment initiation. Because that we frequently use PET/CT in disease follow-up, we consider that the evaluation of the PETVAS score by nuclear medicine specialists in patients with suspected vasculitis, without the need for additional examinations and costs will contribute to the diagnosis and follow-up.

ICIs has been primarily administered in the treatment of malignant melanoma.[20] Therefore, like many irAEs, ICI-related vasculitis was first observed in patients diagnosed with malignant melanoma.[6] As ICIs began to be administered in other malignancies, ICIs-related vasculitis was reported in cancer types such as lung cancer and RCC.[4] Our study revealed increased FDG uptake in patients with NSCLC, SCLC, RCC, and bladder cancer. In addition to ICIs used in the first reported cases, such as nivolumab, ipilimumab, and pembrolizumab, increased involvement was also found in our patients treated with atezolizumab and avelumab. Considering all of the above, we think that ICI-related vasculitis can be expected in all cancer patients treated with ICIs, regardless of the primary cancer and the type of ICI used.

PETVAS has emerged as a valuable tool for quantitatively assessing vascular FDG uptake and detecting vascular inflammation. Elevated PETVAS scores are generally associated with active arteritis and reflect increased metabolic activity due to inflammatory cell infiltration in the vessel

TABLE 5: Baseline characteristics of patients with metastatic non-SCLC, medication used and PFS and OS times.				
	Group 1 (n=64)	Group 2 (n=5)	Total patients (n=69)	p
Age (minimum-maximum)	64.2 (42-82)	67 (56-79)	64.9 (42-82)	0.23
Gender (%)				
Male	54 (84.3)	5 (100)	59 (85.5)	0.33
Female	10 (15.6)	0 (0)	10 (14.4)	
ICIs (%)				
Nivolumab	61 (95.3)	4 (80)	65 (94.2)	0.15
Pembrolizumab	3 (4.6)	1 (20)	4 (5.7)	
PFS median (95% CI)	6.26 (5.21-7.32)	7.20 (1.92-12.47)	6.33 (5.29-7.37)	0.73
OS median (95% CI)	9.40 (8.13-10.67)	11.4 (5.56-17.23)	9.55 (8.30-10.79)	0.37
SCLC: Small cell lung cancer; PFS: Progression-free survival; OS: Overall survival; CI: Confidence interval.				

wall.[21] However, high PETVAS scores can also be observed in advanced age, atherosclerotic plaques, and systemic inflammation.[12] In our study, patients were categorized as having increased PETVAS uptake if uptake increased compared with baseline imaging; patients with persistent uptake at baseline without an increase were not included in the increased FDG uptake group.

Study Limitations

The absence of a control group of cancer patients not treated with ICIs is a key limitation. It prevents us from determining whether the observed vascular FDG uptake is attributable to ICI therapy itself or to other factors that are common in advanced cancer, such as atherosclerosis or systemic inflammation. Therefore, our findings suggest an association but cannot establish causality. Furthermore, we were unable to evaluate laboratory data because of missing values and discrepancies in acute-phase reactants caused by frequent intercurrent infectious conditions and acute pathologies. Detailed physical examination findings could not be documented because the systemic evaluations performed during patient examinations focused on the primary disease.

CONCLUSION

Increased vascular FDG uptake may represent an underrecognized imaging finding in patients receiving ICIs. As ICIs are increasingly used across disease stages, such findings may be encountered more frequently in routine clinical practice. In patients with unexplained systemic symptoms and elevated inflammatory markers, PET-based vascular assessment using the PETVAS score may provide a practical tool to support clinical decision-making and guide further evaluation. These imaging findings may prompt consideration of immune-mediated arteritis in the appropriate clinical context.

Ethics

Ethics Committee Approval: This study was conducted in accordance with the principles of the Declaration of Helsinki. Approval was granted by Marmara University Faculty of Medicine, İstanbul, Türkiye, number: 09.2024.911, date: 19.07.2024.

Informed Consent: Retrospective study.

Footnotes

Authorship Contributions

Surgical and Medical Practices: A.K.G., K.Ö., N.C.D., M.S., S.Ö., T.Ö., İ.V.B., O.K., Concept: A.K.G., M.S., Design: A.K.G., E.K., T.K., T.Ö., İ.V.B., O.K., Data Collection or Processing: A.K.G., E.K., T.Ö., İ.V.B., Analysis or Interpretation: K.Ö., Ş.Ç., S.Ö., T.Ö., İ.V.B., O.K., Literature Search: Ş.Ç., T.K., İ.V.B., O.K., Writing: A.K.G., O.K.

Conflict of Interest: No conflict of interest was declared by the authors.

Financial Disclosure: The authors declared that this study received no financial support.

REFERENCES

1. Pavan A, Attili I, Pasello G, Guarneri V, Conte PF, Bonanno L. Immunotherapy in small-cell lung cancer: from molecular promises to clinical challenges. J Immunother Cancer. 2019;7(1):205. [Crossref] [PubMed] [PMC]
2. Shitara K, Ajani JA, Moehler M, et al. Nivolumab plus chemotherapy or ipilimumab in gastro-oesophageal cancer. Nature. 2022;603(7903):942-948. [Crossref] [PubMed] [PMC].
3. Naidoo J, Murphy C, Atkins MB, et al. Society for Immunotherapy of Cancer (SITC) consensus definitions for immune checkpoint inhibitor-associated immune-related adverse events (irAEs) terminology. J Immunother Cancer. 2023;11(3):e006398. [Crossref] [PubMed] [PMC]
4. Lee CM, Wang M, Rajkumar A, Calabrese C, Calabrese L. A scoping review of vasculitis as an immune-related adverse event from checkpoint inhibitor therapy of cancer: unraveling the complexities at the intersection of immunology and vascular pathology. Semin Arthritis Rheum. 2024;66:152440. [Crossref] [PubMed]
5. Daxini A, Cronin K, Sreih AG. Vasculitis associated with immune checkpoint inhibitors-a systematic review. Clin Rheumatol. 2018;37(9):2579-2584. [Crossref] [PubMed]
6. Saadoun D, Vautier M, Cacoub P. Medium- and large-vessel vasculitis. Circulation. 2021;143(3):267-282. [Crossref] [PubMed]

7. Maz M, Chung SA, Abril A, et al. 2021 American College of Rheumatology/vasculitis foundation guideline for the management of giant cell arteritis and takayasu arteritis. Arthritis Rheumatol. 2021;73(8):1349-1365. [Crossref] [PubMed] [PMC]
8. Salvarani C, Soriano A, Muratore F, Shoenfeld Y, Blockmans D. Is PET/CT essential in the diagnosis and follow-up of temporal arteritis? Autoimmun Rev. 2017;16(11):1125-1130. [Crossref] [PubMed]
9. Dejaco C, Ramiro S, Duftner C, et al. EULAR recommendations for the use of imaging in large vessel vasculitis in clinical practice. Ann Rheum Dis. 2018;77(5):636-643. [Crossref] [PubMed]
10. Galli E, Muratore F, Mancuso P, et al. The role of PET/CT in disease activity assessment in patients with large vessel vasculitis. Rheumatology (Oxford). 2022;61(12):4809-4816. [Crossref] [PubMed] [PMC]
11. Grayson PC, Alehashemi S, Bagheri AA, et al. ^{18}F-fluorodeoxyglucose-positron emission tomography as an imaging biomarker in a prospective, longitudinal cohort of patients with large vessel vasculitis. Arthritis Rheumatol. 2018;70(3):439-449. [Crossref] [PubMed] [PMC]
12. Dashora HR, Rosenblum JS, Quinn KA, et al. Comparing semiquantitative and qualitative methods of vascular ^{18}F-FDG PET activity measurement in large-vessel vasculitis. J Nucl Med. 2022;63(2):280-286. [Crossref] [PubMed] [PMC]
13. Zhang Q, Wang W, Yuan Q, et al. Correlation between immune-related adverse events and the efficacy of PD-1/PD-L1 inhibitors in the treatment of non-small cell lung cancer: systematic review and meta-analysis. Cancer Chemother Pharmacol. 2022;89(1):1-9. [Crossref] [PubMed] [PMC]
14. Zhou X, Yao Z, Yang H, Liang N, Zhang X, Zhang F. Are immune-related adverse events associated with the efficacy of immune checkpoint inhibitors in patients with cancer? A systematic review and meta-analysis. BMC Med. 2020;18(1):87. [Crossref] [PubMed] [PMC]
15. Läubli H, Balmelli C, Kaufmann L, et al. Influenza vaccination of cancer patients during PD-1 blockade induces serological protection but may raise the risk for immune-related adverse events. J Immunother Cancer. 2018;6(1):40. [Crossref] [PubMed] [PMC]
16. Laamech R, Terrec F, Emprou C, et al. Efficacy of plasmapheresis in nivolumab-associated ANCA glomerulonephritis: a case report and pathophysiology discussion. Case Rep Nephrol Dial. 2021;11(3):376-383. [Crossref] [PubMed] [PMC]
17. Betrains AE, Blockmans DE. Immune checkpoint inhibitor-associated polymyalgia rheumatica/giant cell arteritis occurring in a patient after treatment with nivolumab. J Clin Rheumatol. 2021;27(8S):S555-S556. [Crossref] [PubMed]
18. Kang A, Yuen M, Lee DJ. Nivolumab-induced systemic vasculitis. JAAD Case Rep. 2018;4(6):606-608. [Crossref] [PubMed] [PMC]
19. Dejaco C, Ramiro S, Bond M, et al. EULAR recommendations for the use of imaging in large vessel vasculitis in clinical practice: 2023 update. Ann Rheum Dis. 2024;83(6):741-751. [Crossref] [PubMed]
20. Larkin J, Chiarion-Sileni V, Gonzalez R, et al. Combined nivolumab and ipilimumab or monotherapy in untreated melanoma. N Engl J Med. 2015;373(1):23-34. Erratum in: N Engl J Med. 2018;379(22):2185. [Crossref] [PubMed] [PMC]
21. Kang F, Han Q, Zhou X, et al. Performance of the PET vascular activity score (PETVAS) for qualitative and quantitative assessment of inflammatory activity in Takayasu's arteritis patients. Eur J Nucl Med Mol Imaging. 2020;47(13):3107-3117. [Crossref] [PubMed]

ORIGINAL ARTICLE

DOI: 10.37047/jos.galenos.2026.2026-2-3

J Oncol Sci 2026;12(1):74-81

The Prognostic Value of a Composite Score in Predicting Mortality Among Metastatic Castration-resistant Prostate Cancer Patients Treated with Enzalutamide

İlker Nihat ÖKTEN[1], Tuba BAYDAŞ[1], İbrahim ÇİL[2], Mehmet BEŞİROĞLU[1], Sinan KOCA[1]

[1]Göztepe Prof. Dr. Süleyman Yalçın City Hospital, Clinic of Medical Oncology, İstanbul, Türkiye
[2]University of Health Sciences Türkiye, Ümraniye Training and Research Hospital, Department of Medical Oncology, Ümraniye, İstanbul, Türkiye

ABSTRACT

Objective: This study aimed to develop a composite prognostic score using prostate-specific antigen (PSA) elimination rate, lactate dehydrogenase (LDH), alkaline phosphatase (ALP), and albumin derived from routine blood biochemistry tests in patients with castration-resistant prostate cancer and to evaluate the prognostic value of this index for overall survival.

Material and Methods: This multicenter retrospective cohort study included 173 patients receiving enzalutamide treatment. The performance of PSA elimination rate, albumin/ALP ratio, and LDH/ALP ratio in mortality classification was evaluated using receiver operating characteristic analysis. The composite prognostic score was created by summing indices with significant area under the curve values. An increase in the score was interpreted as an increased mortality risk. The role of the composite score in predicting mortality was investigated.

Results: The mean age of the patients included in the study was 68.61±8.57 years (range: 43-87). PSA elimination rate, LDH/ALP ratio, and albumin/ALP ratio were found to be lower in the mortality group. The 10-year survival rate was 16.3% for patients with a composite prognostic score of 3, 32.3% for those with a score of 2, 46.5% for those with a score of 1, and 70.4% for those with a score of 0. The mean overall survival was 64.6 months for score 3, 99.6 months for score 2, 134.4 months for score 1, and 205 months for score 0 ($p<0.001$). Mortality risk was 2.85-fold lower in patients with a score of 1 [hazard ratio (HR): 0.35, $p=0.001$] and 2.56-fold lower in those with a score of 0 (HR: 0.39, $p=0.036$). In the Fagan nomogram, the post-test probability for the combined prognostic score was calculated as 68.1%.

Conclusion: Based on our findings, the developed composite prognostic score demonstrated significant potential for predicting mortality. The combined use of PSA elimination rate, LDH/ALP ratio, and albumin/ALP ratio improved mortality prediction accuracy. This composite prognostic score may assist clinicians in decision-making regarding treatment strategies.

Keywords: Prostate cancer; enzalutamide; biomarker

INTRODUCTION

Prostate cancer is the most common cancer in men and the second leading cause of cancer-related mortality. Approximately 27% of all new annual cancer cases and 11% of cancer-associated deaths in men are attributed to prostate cancer.[1] While the five-year survival rate exceeds 90% in localized prostate cancer, it decreases to 31% in advanced and metastatic stages.[2] Androgen deprivation therapy (ADT) forms the basis of prostate cancer treatment. Currently, chemotherapy (docetaxel) and androgen receptor-targeted agents such as abiraterone acetate, enzalutamide, apalutamide, and darolutamide are used in combination with ADT.[3] However, many patients eventually develop metastatic castration-resistant prostate cancer (mCRPC), which is associated with a poorer prognosis. Although most patients initially respond to ADT, progression to castration-resistant disease is common.[4] Patients with high tumor burden

Correspondence: İlker Nihat ÖKTEN MD;
Göztepe Prof. Dr. Süleyman Yalçın City Hospital, Clinic of Medical Oncology, İstanbul, Türkiye
E-mail: ilkernihat@gmail.com
ORCID ID: orcid.org/0000-0003-2360-3392

Received: 06.02.2026 **Accepted:** 08.03.2026 **Epub:** 12.03.2026 **Publication Date:** 18.03.2026

Cite this article as: Ökten İN, Baydaş T, Çil İ, Beşiroğlu M, Koca S. The prognostic value of a composite score in predicting mortality among metastatic castration-resistant prostate cancer patients treated with enzalutamide. J Oncol Sci. 2026;12(1):74-81

Available at journalofoncology.org

progress more rapidly to castration-resistant prostate cancer and have lower survival rates.[5] Prognostic variables such as Gleason score or clinical stage may be used in mCRPC, but reliable and accurate prediction tools are still lacking.[6]

Recent studies have shown that routinely used diagnostic biomarkers such as serum alkaline phosphatase (ALP), lactate dehydrogenase (LDH), and albumin have prognostic value in several cancer types.[7-10] These markers are readily obtained from routine blood biochemistry tests and are currently evaluated as standard parameters for some cancer patients. Serum ALP is primarily secreted by osteoblasts, kidneys, the gastrointestinal tract, and other organs, and is considered an important indicator of bone metastases in cancer patients.[11] Serum albumin functions in maintaining plasma colloid osmotic pressure, nutrient transport, and antioxidant activity.[12] Studies have demonstrated that malnutrition may promote tumor growth and progression and negatively affect treatment response and survival. Reduced serum albumin levels are closely associated with poor prognosis in malignancies.[13,14] LDH is an enzyme responsible for converting pyruvate to lactate during glycolysis. LDH levels are increased in tumor cells as a result of a metabolic shift toward anaerobic glycolysis and an adaptation to hypoxic conditions. Additionally, cancer cells rely on glucose to produce metabolites required for growth, invasion, angiogenesis, and metastasis. These mechanisms contribute to elevated serum LDH levels, making LDH a potential prognostic marker for tumor progression.[15]

Although these biomarkers have been widely investigated in malignant tumors, their prognostic value in castration-resistant prostate cancer has not been adequately explored.[16] The aim of this study was to develop a composite prognostic score based on LDH, ALP, and albumin derived from routine blood biochemistry tests in patients with castration-resistant prostate cancer and to evaluate its prognostic significance for overall survival.

MATERIAL AND METHODS

This multicenter retrospective cohort study was conducted among patients receiving enzalutamide treatment for metastatic prostate cancer between 2017 and 2021 across twelve tertiary healthcare centers.

In the sample size analysis, assuming a Type I error of 0.05, a power of 95%, and an effect size d=0.5 with N2/N1=1, the minimum sample sizes required were calculated as N1: 88 and N2: 88, totaling 176 participants. Because no reference study was available for direct comparison in the literature, the effect size was considered moderate (0.5) according to Cohen's guidelines. During the study period, 320 patients with prostate cancer were screened across 12 centers; 173 who met the inclusion and exclusion criteria were enrolled (Figure 1).

Inclusion criteria were as follows:

- Patients aged ≥18 years with histopathologically confirmed prostate adenocarcinoma.
- Patients meeting the diagnostic criteria for mCRPC, defined as biochemical and/or radiological progression despite continuous androgen suppression (luteinizing hormone-releasing hormon analog/antagonist or orchiectomy) with serum testosterone <20 ng/dL.
- Patients who received enzalutamide as first-line systemic therapy during the mCRPC stage.
- Eastern Cooperative Oncology Group (ECOG) performance status of 0-1 at treatment initiation.
- Availability of baseline prostate-specific antigen (PSA), Gleason score, complete blood count, ALP and LDH values, and adequate follow-up data for survival analysis at the start of enzalutamide therapy.

Exclusion criteria were as follows:

- Non-metastatic disease or non-nmCRPC prior to developing castration resistance.
- Prior treatment during the mCRPC stage with second-generation androgen receptor pathway inhibitors (e.g., abiraterone, apalutamide, darolutamide) or chemotherapy before starting enzalutamide.

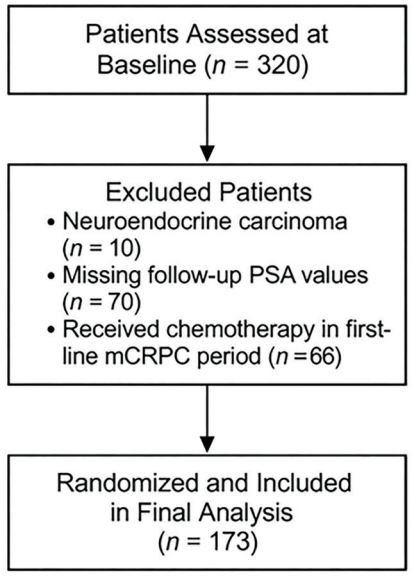

FIGURE 1: Consort diagram.

PSA: Prostate-specific antigen; mCRPC: Metastatic castration-resistant prostate cancer.

- Presence of small-cell/neuroendocrine morphology or dominant neuroendocrine component on pathology.
- History of another active malignancy (excluding non-melanoma skin cancers and appropriately treated *in situ* cancers with no recurrence).
- Missing baseline laboratory or follow-up data required for enzalutamide initiation, insufficient follow-up duration to allow survival evaluation, or restricted access to patient files.

The demographic and clinical characteristics of each patient were recorded retrospectively, including age, dates of diagnosis and metastasis, Gleason score, metastatic sites, ECOG performance status, treatment response, progression status, and survival outcomes. Laboratory parameters were obtained from measurements performed within 14 days prior to initiation of enzalutamide therapy. Baseline PSA, PSA nadir, LDH, ALP, and serum albumin levels were evaluated in all patients. Three biochemical indices—PSA ratio (baseline PSA/nadir PSA), albumin/ALP ratio, and LDH/ALP ratio—were calculated and used in prognostic analyses. The primary endpoint of the study was overall survival. Secondary endpoints included progression-free survival, treatment response, and the prognostic impact of the composite score. All data were anonymized, and the study was conducted in accordance with the Declaration of Helsinki after approval was granted by Marmara University Faculty of Medicine, İstanbul, Türkiye, number: 09.2024.911, date: 19.07.2024. Treatment protocol: Enzalutamide was administered orally at a dose of 160 mg daily.

Histopathological grading of prostate adenocarcinoma was performed using the Gleason scoring system, which is accepted as the gold standard for assessing tumor biology and prognosis. Specimens from all patients, obtained by biopsy or radical prostatectomy, were reviewed by experienced genitourinary pathologists. In the Gleason system, tumor architecture is classified into histological patterns graded from 1 to 5 based on their deviation from normal glandular architecture. For each case, the primary pattern, representing the most dominant tumor area, and the secondary pattern, representing the next most prevalent component, were identified. The Gleason score was calculated by summing these two grades (e.g., 3+4=7). In the presence of high-grade components (grade 4 or 5), these were incorporated into scoring even if not predominant, in accordance with the International Society of Urological Pathology recommendations.

Gleason scores were further categorized according to widely accepted literature classifications:

- 6 (3+3): low-grade tumor
- 7 (3+4 or 4+3): intermediate-grade tumor, with prognostic differences depending on pattern distribution
- 8-10: high-grade tumors with aggressive biological behavior

Patients were considered to have mCRPC if biochemical and/or radiological progression occurred while maintaining serum testosterone levels below 20 ng/dL under continuous androgen suppression.[17]

PSA progression: At least three consecutive PSA elevations (measured ≥1 week apart) with an increase of ≥2 ng/mL

Radiological progression: Appearance of new lesions or enlargement of existing metastases

In the receiver operating characteristic (ROC) analysis evaluating the performance of PSA elimination rate (calculated as the ratio of baseline to nadir PSA), albumin/ALP ratio, and LDH/ALP ratio for mortality classification, all three indices demonstrated statistically significant area under curve (AUC) values, though with modest discriminatory power. The optimal cut-off values were determined to be 6.94 for PSA ratio (sensitivity 60%, specificity 73%, AUC: 0.688), 0.03 for albumin/ALP ratio (sensitivity 65%, specificity 74%, AUC: 0.703), and 1.95 for LDH/ALP ratio (sensitivity 60%, specificity 73%, AUC: 0.634). Values below these thresholds were associated with higher mortality risk (Table 1, Figure 2).

The composite score was generated by summing the indices that showed significant AUC values. For each marker, values below the determined cut-off were assigned 1 point (indicating higher mortality risk), whereas values above the cut-off were assigned 0 points. The total composite score ranged from 0 to 3. Higher scores reflected a greater mortality risk (Table 2).

TABLE 1: ROC analysis.

	Cut-point	Sensitivity (%)	Specificity (%)	PPV (%)	NPV (%)	Youden's index	AUC	p	DeLong test
1. PSA elimination ratio	<6.94	60	72.73	68	65.31	0.327	0.688	<0.001	1 vs. 2 p=0.785
2. Albumin/ALP	<0.03	64.71	73.86	70.51	68.42	0.386	0.703	<0.001	1 vs. 3 p=0.352
3. LDH/ALP	<1.95	62.35	61.36	60.92	62.79	0.237	0.634	<0.001	2 vs. 3 p=0.006

ROC: Receiver operating characteristic; PSA: Prostate-specific antigen; PPV: Positive predictive value; NPV: Negative predictive value; AUC: Area under the curve; ALP: Alkaline phosphatase; LDH: Lactate dehydrogenase.

Statistical Analysis

Statistical analyses were performed using JAMOVI software (version 2.6.17). Normality was assessed using the Kolmogorov-Smirnov test. Pearson chi-square test, Fisher's exact test, t-test, Kaplan-Meier survival analysis, and Cox regression analysis were used to evaluate the data. ROC analysis was used to assess the mortality classification performance of the indices, and the optimal cut-off value was determined using the Youden index and AUC. The DeLong test was applied to compare AUC values. A p-value <0.05 was considered statistically significant.

RESULTS

The mean age of patients included in the study was 68.61±8.57 years (range: 43-87). The proportion of patients with disease progression and the proportion of those without pathological response were significantly higher in the deceased group. When index values were compared by survival status, baseline PSA, nadir PSA, and neutrophil-to-lymphocyte ratio were higher in the mortality group, whereas the baseline PSA/nadir PSA ratio, LDH/ALP ratio, and albumin/ALP ratio were lower (Table 3).

Analysis of survival durations and 1-, 3-, 5-, and 10-year survival rates, stratified by composite scores, revealed statistically significant differences between groups. Patients with a score of 3 had significantly shorter mean survival than those with scores of 0 and 1, and patients with a score of 2 had shorter mean survival than those with a score of 0. Ten-year survival rates were 16.3% for score 3, 32.3% for score 2, 46.5% for score 1, and 70.4% for score 0. Mean overall survival times were 64.6, 99.6, 134.4, and 205 months for scores 3, 2, 1, and 0, respectively (Table 4, Figure 3).

A Cox regression analysis created to predict mortality was statistically significant (p<0.001). Variables found to be significant in the model included Gleason score, composite score, and presence of progression. Patients with a Gleason score of 9-10 had a 1.69-fold higher mortality risk, while those with progression had a 4.69-fold higher mortality risk. Mortality risk was 65% lower in patients with a composite score of 1 [hazard ratio (HR): 0.35] and 61% lower in those with a score of 0 (HR: 0.39). In the Fagan nomogram, the post-test probability for the combined prognostic score was calculated as 68.1%. The pre-test mortality probability of 49% increased to 68.1% following the application of the model (Table 5, Figure 4).

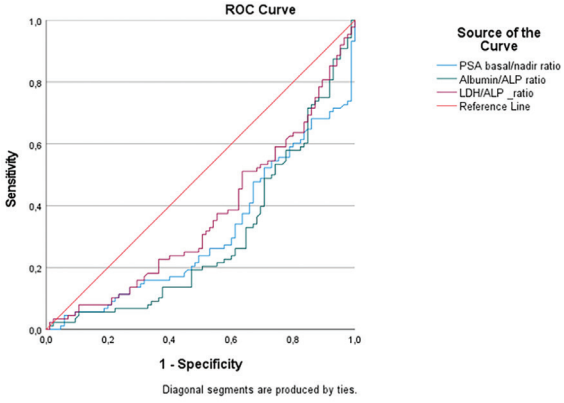

FIGURE 2: ROC analysis.

ROC: Receiver operating characteristic; LDH: Lactate dehydrogenase; ALP: Alkaline phosphatase; PSA: Prostate-specific antigen.

TABLE 2: Composite score calculation.

Composite score	If value is below cut-off → score 1, If value is above cut-off → score 0		Score
PSA elimination ratio	<6.94 = 1 point	>6.94 = 0 points	
Albumin/ALP	<0.03 = 1 point	>0.03 = 0 points	
LDH/ALP	<1.95 = 1 point	>1.95 = 0 points	
			Total

PSA: Prostate-specific antigen; ALP: Alkaline phosphatase; LDH: Lactate dehydrogenase.

TABLE 3: Sociodemographic and clinical characteristics according to survival status.

	Mortality Mean ± SD or median (IQR) or n (%)		
	Absent (n=85)	Present (n=88)	
Age	67.33±8.57	69.85±8.44	0.053
PSA (baseline)	27 (79.34)	52.09 (155.35)	**<0.001**
PSA (nadir)	3 (17.96)	46.57 (60.05)	**0.001**
PSA elimination ratio	10.41 (29.69)	2.72 (9.40)	**<0.001**
NLR	2.91 (1.97)	3.49 (3.02)	**0.027**
LDH/ALP ratio	2.37 (2.15)	1.70 (1.49)	**0.002**
Albümin/ALP ratio	0.038 (0.04)	0.022 (0.02)	**<0.001**

TABLE 3: Continued			
	Mortality Mean ± SD or median (IQR) or n (%)		
	Absent (n=85)	Present (n=88)	
Gleason score			
6-8	43 (50.6)	40 (45.5)	0.499
9-10	42 (49.4)	48 (54.5)	
Metastasis			
Bone	40 (47.1)	28 (31.8)	0.087
Lymph node	4 (4.7)	3 (3.4)	
Bone + lymph node	41 (48.2)	57 (64.8)	
Visceral metastasis			
Absent	66 (77.6)	67 (76.1)	0.954
Liver	9 (10.6)	10 (11.4)	
Lung	7 (8.2)	9 (10.2)	
Other	3 (3.5)	2 (2.3)	

PSA: Prostate-specific antigen; SD: Standard deviation; IQR: Interquartile range; NLR: Neutrophil-to-lymphocyte ratio; LDH: Lactate dehydrogenase; ALP: Alkaline phosphatase.

TABLE 4: 1-, 3-, 5-, and 10-year survival rates according to total composite score.

					95% confidence interval		
Score	Time (month)	Number at risk	Number of events	Survival (%)	Lower (%)	Upper (%)	Mean (month)
3	12	49	1	98.0	94.2	100.0	64.6
3	36	25	22	53.9	41.7	69.7	
3	60	15	7	37.7	26.0	54.7	
3	120	2	6	16.3	7.0	38.1	
2	12	43	0	100.0	100.0	100.0	99.6
2	36	30	10	76.1	64.2	90.2	
2	60	16	8	54.4	40.7	72.7	
2	120	6	5	32.3	18.5	56.5	
2	240	1	3	8.6	1.5	49.6	
1	12	43	0	100.0	100.0	100.0	134.4
1	36	34	5	87.9	78.4	98.4	
1	60	21	3	77.9	65.1	93.1	
1	120	7	6	46.5	28.6	75.6	
0	12	37	0	100.0	100.0	100.0	205.0
0	36	34	2	94.5	87.4	100.0	
0	60	17	3	84.1	71.8	98.5	
0	120	7	2	70.4	51.9	95.4	

TABLE 5: Multivariate survival analysis.

Dependent		All	HR (univariable)	HR (multivariable)
Gleason category	6-8	83 (48.0)	-	-
	9-10	90 (52.0)	1.94 (1.25-3.01, p=0.003)	1.69 (1.06-2.69, **p=0.026**)
Composite prognostic score	3	50 (28.9)	-	-
	2	43 (24.9)	0.56 (0.34-0.94, p=0.028)	0.63 (0.36-1.09, p=0.095)
	1	43 (24.9)	0.32 (0.18-0.57, p<0.001)	0.35 (0.19-0.66, **p=0.001**)
	0	37 (21.4)	0.15 (0.07-0.35, p<0.001)	0.39 (0.16-0.94, **p=0.036**)

TABLE 5: Continued				
Dependent		**All**	**HR (univariable)**	**HR (multivariable)**
Progression	No	74 (42.8)	-	-
	Yes	99 (57.2)	6.29 (3.34-11.85, p<0.001)	4.69 (2.34-9.38, **p<0.001**)
Bone-lymph node metastasis	Bone	68 (39.3)	-	-
	Lymph node	7 (4.0)	0.98 (0.30-3.23, p=0.975)	2.35 (0.67-8.25, p=0.183)
	Bone + lymph node	98 (56.6)	1.43 (0.90-2.25, p=0.126)	1.15 (0.71-1.88, p=0.567)
Visceral metastasis	No	133 (76.9)	-	-
	Liver	19 (11.0)	1.13 (0.58-2.20, p=0.720)	1.08 (0.53-2.23, p=0.826)
	Lung	16 (9.2)	1.18 (0.59-2.38, p=0.636)	0.75 (0.35-1.58, p=0.446)
	Other	5 (2.9)	0.96 (0.23-3.94, p=0.957)	1.10 (0.26-4.65, p=0.900)
HR: Hazard ratio				

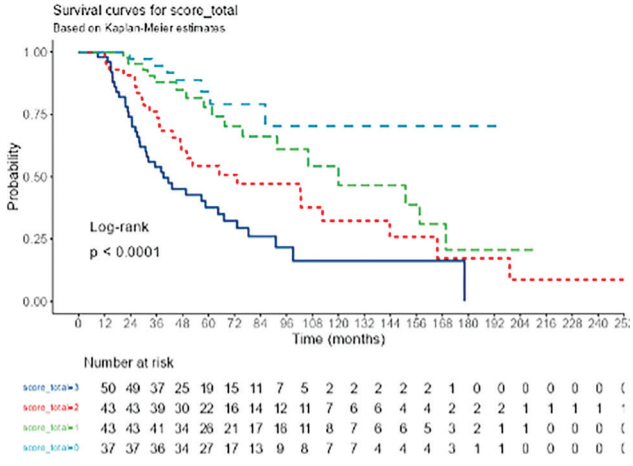

FIGURE 3: Overall survival by total composite score.

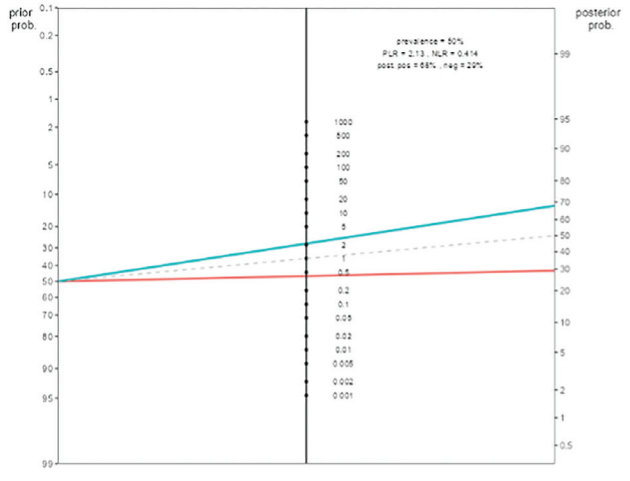

FIGURE 4: Fagan nomogram.

NLR: Neutrophil-to-lymphocyte ratio; PLR: Platelet-to-lymphocyte ratio.

DISCUSSION

Castration-resistant prostate cancer represents an advanced stage of prostate cancer characterized by disease progression despite ADT.[18] Owing to its distinct biological behavior, resistance mechanisms, and therapeutic limitations, its management requires a differentiated approach compared to hormone-sensitive disease.[18] Prognosis in castration-resistant prostate cancer is heterogeneous, and reliable prognostic biomarkers are needed to estimate survival risk more accurately. Despite the widespread use of biomarkers such as PSA and other clinical parameters, achieving high predictive accuracy in prognosis remains challenging.[19]

In our study, we evaluated the prognostic value of a composite score developed for castration-resistant prostate cancer with respect to survival. Gleason score, the composite index score, and the presence of progression were identified as independent predictors of mortality. When survival groups were compared, baseline PSA, nadir PSA, PSA elimination rate, LDH/ALP ratio, and albumin/ALP ratio were lower in patients who died than in those who survived. The 10-year survival rates were 16.3% for score 3, 32.3% for score 2, 46.5% for score 1, and 70.4% for score 0. Mortality risk was 2.85-fold lower in patients with a score of 1 (HR: 0.35) and 2.56-fold lower in those with a score of 0 (HR: 0.39).

In a study by Huo et al.[20], a cohort of 703 patients with mCRPC was evaluated using a comprehensive set of 41 clinical and demographic variables to predict 24-month mortality, and machine-learning models were compared. PSA, albumin, and LDH were among the identified predictive variables. These findings support the effective use of clinical markers in machine-learning-based mortality prediction. In our study, ROC analysis demonstrated that PSA elimination rate, albumin/ALP ratio, and LDH/ALP ratio each had significant AUC values and acceptable classification performance. The optimal cut-off values showed sensitivities of 60%, 65%, and

60% and specificities of 73%, 74%, and 73% for PSA ratio, albumin/ALP, and LDH/ALP, respectively. The composite score created from these markers was a significant predictor of mortality, increasing the estimated probability of mortality at presentation from 49% to 68%.

In a study by Chen et al.[21], factors associated with progression in castration-resistant prostate cancer were evaluated, and albumin, PSA, ALP, and LDH were identified as independent risk factors. A model incorporating albumin, PSA, ALP, LDH, Gleason score, and perineural invasion achieved a discrimination power of 77.82%. ROC analysis demonstrated strong predictive performance, with an AUC of 0.845 for predicting progression. The model was later validated in an external cohort, confirming high net clinical benefit. In a meta-analysis by Mori et al.[22], elevated LDH levels were associated with worse survival [HR: 2.07; 95% confidence interval (CI): 1.75-2.44] and increased progression risk (HR: 1.08; 95% CI: 1.01-1.16) in metastatic prostate cancer. Subgroup analyses in both castration-resistant and hormone-sensitive disease demonstrated that LDH remained prognostic (HR: 2.02 and HR: 2.25, respectively). High LDH levels were associated with an increased risk of mortality and disease progression. Researchers suggested that LDH may be incorporated into prognostic tools to guide treatment decision-making. Consistent with these findings, our study shows that combining LDH, albumin, and PSA into a composite score improves mortality prediction.

In a study by Whitney et al.[23], factors associated with mortality in non- mCRPC were evaluated, and PSA doubling time was found to be significant. Patients with PSA doubling time ≥9 months had a 50% lower mortality risk compared to those <9 months (HR: 0.5). Similarly, in our study, the PSA elimination rate was identified as a significant independent predictor of mortality in both univariate and multivariate analyses, with slower elimination associated with an increased risk.

In the study by Schlack et al.[24], the prognostic value of ALP-flare, LDH, PSA, and their combination after initiating enzalutamide was evaluated. More than 50% reduction in PSA, LDH normalization, and ALP flare were associated with longer median progression-free survival. When the combined dynamics of ALP-flare, LDH normalization, and PSA reduction were compared to PSA reduction alone, patients with all three favorable markers demonstrated significantly longer progression-free and overall survival. Consistent with these findings, our results show that combining biomarkers significantly enhances predictive performance and that favorable biomarker dynamics correlate with longer survival. Available evidence and our study indicate that LDH, albumin, and ALP are associated with progression and mortality and that combining them may improve risk stratification. These easily accessible parameters may alert clinicians to high-risk patients and contribute to clinical decision-making.

Study Limitations

The retrospective design of our study and the possibility of missing data may have introduced information bias, while the limited number of participating centers could have led to selection bias. Despite these limitations, the development of a new model by combining routinely available parameters is a key strength of our study.

CONCLUSION

Our findings demonstrate that the composite prognostic score, developed using PSA elimination rate, LDH/ALP ratio, and albumin/ALP ratio, has significant potential to predict mortality in castration-resistant prostate cancer. Combined evaluation of decreasing trends in these biomarkers improved the accuracy of mortality estimation. This composite score may aid in identifying high-risk patients and guiding treatment decisions. Further validation through prospective cohort studies is recommended.

Acknowledgements: We would like to thank Tuğba Akın Telli, Ayşe Demirci, Mustafa Karaağaç, Ahmet Küçükarda, Semiha Urvay, Sedat Tarık Fırat, Zeynep Oruç, Mehmet Murat Zerey, and Ezgi Çoban for their contributions.

Ethics

Ethics Committee Approval: This study was conducted in accordance with the principles of the Declaration of Helsinki. Approval was granted by Marmara University Faculty of Medicine, İstanbul, Türkiye, number: 09.2024.911, date: 19.07.2024.

Informed Consent: Retrospective study.

Footnotes

Authorship Contributions

Concept: İ.N.Ö., T.B., İ.Ç., M.B., S.K., Design: İ.N.Ö., S.K., Data Collection or Processing: İ.N.Ö., T.B., İ.Ç., M.B., S.K., Analysis or Interpretation: İ.N.Ö., T.B., İ.Ç., M.B., Literature Search: İ.N.Ö., T.B., Writing: İ.N.Ö., T.B.

Conflict of Interest: No conflict of interest was declared by the authors.

Financial Disclosure: The authors declared that this study received no financial support.

REFERENCES

1. Siegel RL, Miller KD, Fuchs HE, Jemal A. Cancer statistics, 2022. CA Cancer J Clin. 2022;72(1):7-33. [Crossref] [PubMed]
2. Bandini M, Pompe RS, Marchioni M, et al. Radical prostatectomy or radiotherapy reduce prostate cancer mortality in elderly patients: a population-based propensity score adjusted analysis. World J Urol. 2018;36(1):7-13. [Crossref] [PubMed]
3. Marchioni M, Di Nicola M, Primiceri G, et al. New antiandrogen compounds compared to docetaxel for metastatic hormone sensitive prostate cancer: results from a network meta-analysis. J Urol. 2020;203(4):751-759. [Crossref] [PubMed]

4. Hoffman KE, Penson DF, Zhao Z, et al. Patient-reported outcomes through 5 years for active surveillance, surgery, brachytherapy, or external beam radiation with or without androgen deprivation therapy for localized prostate cancer. JAMA. 2020;323(2):149-163. [Crossref] [PubMed] [PMC]
5. Das M. Androgen deprivation therapy for prostate cancer. Lancet Oncol. 2017;18(10):e567. [Crossref] [PubMed]
6. Cook GJ, Azad G, Padhani AR. Bone imaging in prostate cancer: the evolving roles of nuclear medicine and radiology. Clin Transl Imaging. 2016;4(6):439-447. [Crossref] [PubMed] [PMC]
7. Abu-Talib M, Brown LR. Albumin-to-alkaline phosphatase ratio as a novel prognostic indicator for patients undergoing minimally invasive lung cancer surgery: propensity score matching analysis using a prospective database. Int J Surg. 2019;69:152. [Crossref] [PubMed]
8. Xue X, Li JX, Wang JW, et al. Association between alkaline phosphatase/albumin ratio and the prognosis in patients with chronic kidney disease stages 1-4: results from a C-STRIDE prospective cohort study. Front Med (Lausanne). 2023;10:1215318. [Crossref] [PubMed] [PMC]
9. D'Agostino M, Cairns DA, Lahuerta JJ, et al. Second revision of the International Staging System (R2-ISS) for overall survival in multiple myeloma: a European Myeloma Network (EMN) report within the HARMONY project. J Clin Oncol. 2022;40(29):3406-3418. Erratum in: J Clin Oncol. 2022;40(34):4032. [Crossref] [PubMed]
10. Olszewski AJ, Jakobsen LH, Collins GP, et al. Burkitt lymphoma international prognostic index. J Clin Oncol. 2021;39(10):1129-1138. [Crossref] [PubMed] [PMC]
11. Martín-Ontiyuelo C, Sánchez-Font A, Gimeno E, Suárez-Piñera M, Curull V. Hypermetabolic bone on ^{18}F-FDG-PET/CT in a patient with lung cancer: is it always metastasis? Arch Bronconeumol (Engl Ed). 2020;56(1):51-52. English, Spanish. [Crossref] [PubMed]
12. Taverna M, Marie AL, Mira JP, Guidet B. Specific antioxidant properties of human serum albumin. Ann Intensive Care. 2013;3(1):4. [Crossref] [PubMed] [PMC]
13. Abe T, Nakata K, Kibe S, et al. Prognostic value of preoperative nutritional and immunological factors in patients with pancreatic ductal adenocarcinoma. Ann Surg Oncol. 2018;25(13):3996-4003. [Crossref] [PubMed]
14. Liu J, Jiang S, Yang X, Li X, Wang N. The significant value of preoperative prognostic nutritional index for survival in pancreatic cancers: a meta-analysis. Pancreas. 2018;47(7):793-799. [Crossref] [PubMed]
15. Chambers SK, Occhipinti S, Foley E, et al. Mindfulness-based cognitive therapy in advanced prostate cancer: a randomized controlled trial. J Clin Oncol. 2017;35(3):291-297. [Crossref] [PubMed]
16. Nadamuni M, D'Amico AV, Donovan JL, Hamdy FC. Decision making in prostate cancer. N Engl J Med. 2023;389(14):1335-1338. [Crossref] [PubMed]
17. Cornford P, van den Bergh RCN, Briers E, et al. EAU-EANM-ESTRO-ESUR-SIOG guidelines on prostate cancer. Part II-2020 update: treatment of relapsing and metastatic prostate cancer. Eur Urol. 2021;79(2):263-282. [Crossref] [PubMed]
18. Horak J, Petrausch U, Omlin A. Metastasiertes kastrationsresistentes prostatakarzinom: welche sequenzen sind am sinnvollsten? [Metastatic castration-resistant prostate cancer-what are rational sequential treatment options?]. Urologie. 2023;62(12):1295-1301. German. [Crossref] [PubMed] [PMC]
19. Davis ID. Combination therapy in metastatic hormone-sensitive prostate cancer: is three a crowd? Ther Adv Med Oncol. 2022;14:17588359221086827. [Crossref] [PubMed] [PMC]
20. Huo X, Kohli M, Finkelstein J. Machine learning approaches for predicting mortality in metastatic castration-resistant prostate cancer. Stud Health Technol Inform. 2025;328:26-30. [Crossref] [PubMed]
21. Chen W, Li J, A G, et al. Development of a predictive model for progression to castration-resistant prostate cancer in patients with high bone tumor burden. Am J Cancer Res. 2025;15(6):2719-2732. [Crossref] [PubMed] [PMC]
22. Mori K, Kimura S, Parizi MK, et al. Prognostic value of lactate dehydrogenase in metastatic prostate cancer: a systematic review and meta-analysis. Clin Genitourin Cancer. 2019;17(6):409-418. [Crossref] [PubMed]
23. Whitney CA, Howard LE, Freedland SJ, et al. Impact of age, comorbidity, and PSA doubling time on long-term competing risks for mortality among men with non-metastatic castration-resistant prostate cancer. Prostate Cancer Prostatic Dis. 2019;22(2):252-260. [Crossref] [PubMed]
24. Schlack K, Krabbe LM, Rahbar K, et al. ALP bouncing and LDH normalization in bone metastatic castration-resistant prostate cancer patients under therapy with enzalutamide: an exploratory analysis. Transl Androl Urol. 2021;10(10):3986-3999. [Crossref] [PubMed] [PMC]

REVIEW

DOI: 10.37047/jos.galenos.2026.2025-9-2
J Oncol Sci 2026;12(1):82-93

A Survey on Machine and Deep Learning Techniques for Breast Cancer Prediction

Pallavi JADHAV, Ajit S. PATIL

D. Y. Patil Education Society Deemed to be University, Kolhapur, India

ABSTRACT

Breast cancer is a leading cause of cancer-related mortality among women worldwide, making early and accurate diagnosis essential for effective treatment and improved patient outcomes. In recent years, machine learning (ML) and deep learning (DL) techniques have emerged as promising tools for predicting and classifying breast cancer using gene expression and clinical data. However, existing studies face several limitations. Many rely solely on ML or DL approaches, lack comprehensive strategies for feature selection or extraction, and demonstrate inconsistent performance across datasets. These gaps result in models that are insufficiently accurate, uninterpretable, or unable to generalize well to unseen data. This work aims to address these challenges by conducting a detailed literature survey of existing ML and DL models applied to breast cancer prediction. The objectives include identifying common datasets, performance metrics, model types, and feature-engineering techniques. A structured methodology was followed to analyze peer-reviewed studies and extract trends in performance and limitations. Findings show that, while DL models outperform traditional ML in terms of accuracy, they often lack transparency and robust feature engineering. In conclusion, a unified approach combining advanced feature selection and extraction methods with DL techniques is necessary to develop accurate, generalizable breast cancer prediction systems.

Keywords: Breast cancer; machine learning; deep learning; feature selection; feature extraction; prediction models

INTRODUCTION

Cancer is one of the leading causes of death worldwide and is characterized by the uncontrolled growth and spread of abnormal cells in the body. These cells can invade surrounding tissues and metastasize to distant organs, making the disease highly complex and difficult to treat in its advanced stages. Cancer originates from genetic mutations, which are often triggered by environmental factors, lifestyle choices, hereditary predispositions, or a combination of these.[1,2] As the disease progresses, it disrupts the normal functioning of vital organs and systems, ultimately resulting in significant morbidity and mortality. There are many different types of cancer, each named after the organ or tissue where it originates. The most common types include lung cancer, prostate cancer, breast cancer, colorectal cancer, and liver cancer. Others, such as pancreatic, ovarian, and brain cancers, are less common but often more aggressive. Each type of cancer has unique characteristics, progression patterns, and treatment protocols. Among these, breast cancer is the most commonly diagnosed cancer in women globally and is also a leading cause of cancer-related mortality in women.[3,4]

Breast cancer originates in the breast tissue, typically in the ducts or lobules. The disease begins when cells in the breast mutate and grow uncontrollably, forming a tumor. In many cases, these tumors can become malignant, meaning they have the potential to spread to other parts of the body. Factors contributing to the occurrence of breast cancer include age, genetic mutations (such as *BRCA1* and *BRCA2*), hormonal imbalances, lifestyle factors (e.g., alcohol consumption, obesity), and family history.[5] According to the World Health Organization (WHO), breast cancer has surpassed lung cancer as the most diagnosed cancer globally. In its 2021 report, WHO estimated that in 2020, 2.3 million women worldwide were diagnosed with breast cancer and 685,000 died from

Correspondence: Pallavi JADHAV MD,
D. Y. Patil Education Society Deemed to be University, Kolhapur, India
E-mail: pallavijadhav18@gmail.com
ORCID ID: orcid.org/0000-0001-5080-0813

Received: 16.09.2025 **Accepted:** 07.01.2026 **Epub:** 22.01.2026 **Publication Date:** 18.03.2026

Cite this article as: Jadhav P, Patil AS. A survey on machine and deep learning techniques for breast cancer prediction. J Oncol Sci. 2026;12(1):82-93

Available at journalofoncology.org

it.[6] These alarming statistics highlight the pressing need for improved diagnostic and prognostic tools for early detection and effective treatment planning. Moreover, breast cancer can be identified using various forms of data. Imaging techniques such as mammography, ultrasound, and magnetic resonance imaging are widely used in clinical settings for tumor detection and localization.[7] Recently, gene expression data have emerged as a powerful source for understanding the molecular mechanisms underlying breast cancer.[8] Gene expression profiling (GEP) offers a more granular view by identifying genes that are overexpressed or underexpressed, aiding early diagnosis, subtype classification, and survival prediction.

However, most current research is primarily focused on imaging-based analysis using machine learning (ML) and deep learning (DL).[8-10] In contrast, comparatively little attention has been given to gene expression data, despite its rich potential for molecular-level insights. Among the existing studies that utilize gene expression data, a significant proportion rely on traditional ML models such as support vector machines (SVM), random forests (RF), and Naïve Bayes (NB), with limited exploration of novel or hybrid approaches. Moreover, only a few studies have employed DL for gene expression-based breast cancer prediction or survival analysis, and those that have done so have not demonstrated consistently high performance or robustness. This gap indicates the need for a focused review and analysis of existing methods in this area. To address this, the present study conducts a comprehensive review of recent works published between 2024 and 2025, selected from a pool of 150 papers retrieved from IEEE, Google Scholar, Web of Science, and Scopus. After outdated and less relevant papers were discarded, 25 papers were chosen for in-depth analysis. The main goal of this work was to explore and evaluate current methodologies, datasets, performance metrics, and predictive accuracies in breast cancer detection and gene expression analysis. The contributions of this work are as follows:

- Conducts a comprehensive review of recent (2024-2025) literature focused on breast cancer detection using gene expression data.
- Twenty-five carefully selected papers were analyzed from an initial pool of 150 retrieved from reputable sources such as IEEE, Web of Science, Scopus, and Google Scholar.
- Highlights the research gap where most studies are focused on imaging data, while gene expression data remains underexplored.
- Demonstrates that existing gene expression studies largely use basic ML models with limited application of novel or advanced techniques.
- Shows that DL methods applied to gene expression have not achieved high predictive accuracy (ACC) or model robustness.
- Categorizes existing approaches based on datasets, performance metrics, and models used, offering clear insight into current research trends.
- Provides a foundation for future work, encouraging the development of novel DL architectures specifically designed for gene expression-based breast cancer prediction and survival analysis.

This manuscript is structured to provide a comprehensive analysis of ML and DL approaches in breast cancer prediction. Section II presents the literature review, covering existing methodologies and related work. Section III discusses the findings from the reviewed studies, divided into four subsections: 3.1 Literature Survey Findings, 3.2 Datasets Used, 3.3 Performance Metrics Used, and 3.4 ML and DL Models with Feature Extraction and Selection Approaches. Section IV highlights the issues and challenges identified in current research. Finally, section V concludes the study with a summary of insights.

Literature Survey

The literature survey explores recent advancements in breast cancer prediction, classification, and survival analysis using ML and DL approaches. Various studies utilized multi-omic datasets, such as the Molecular Taxonomy of Breast Cancer International Consortium (METABRIC) and The Cancer Genome Atlas-Breast Invasive Carcinoma (TCGA-BRCA), integrating clinical, genomic, and imaging data to enhance predictive ACC and personalize treatment. Various strategies were applied to feature selection, classification, and survival prediction. For instance, Mahmoud et al.[11] to develop an advanced genomics-based architecture for predicting breast cancer survival in order to address disease variability and complexity. In this study, the multi-omic METABRIC dataset,[12] which includes clinical data, somatic mutations, and gene expression from a large patient cohort, was integrated and pre-processed. This work employed DL approaches, including Graph-Convolutional Networks (GCN), Long Short-Term Memory (LSTM), and Variational Autoencoders (VAE), which were trained using a stochastic gradient descent optimization approach with an 80:20 train-test split. Evaluations were conducted using specificity, sensitivity/recall (REC), and ACC. The findings showed that among VAE, GCN, and LSTM, LSTM achieved 98.7% ACC. The findings show that integration of multi-omic data within an optimized DL approach improves the ACC of survival prediction and enables more effective, personalized treatment strategies.

Bharanidharan et al.[13], aimed at designing computational accurate/efficient system for cancer detection across five regions, i.e., renal (kidney), prostate, lung, liver and breast. For this study, the microarray dataset from 1027 patients, sourced from CuMiD,a[14] was considered. This work utilized Sparse Auto-Encoder, Independent Component Analysis and Principal Component Analysis (PCA) for dimensionality reduction of the dataset, and employed Remora-Optimization, guided by a local entropy-based fitness function, to enhance feature transformation and classification ACC. For classification, SVM, NB, decision tree (DT), and RF were utilized. For the evaluation of this study, six performance metrics, i.e., REC, balanced ACC score (BAC), F-score (FS), precision (PRE), Cohen's kappa coefficient (KAP), and Matthews correlation coefficient (MCC), were utilized. Results show that dimensionality was reduced from 36,805 to 80 features, with average balanced ACC improving to 93.4%, compared with 82.7% without the proposed approach. Kishore Khan et al.[15] aimed to develop an effective breast cancer classification approach using the METABRIC dataset.[12] This work included data preprocessing, dimensionality reduction using PCA, and MCC-based feature selection. Further, a deep neural network (DNN) was used; it was enhanced with dropout layers, and early stopping was applied during training on selected features using MCC. The performance was evaluated using ACC, PRE, REC, and FS, alongside gene expression visualization. Results show that dimensionality reduction provided a boost in classification performance, resulting in higher ACC.

Das et al.[16] focused on enhancing breast cancer staging and classification by integrating ML with bioinformatics analyses using gene expression data from TCGA-BRCA dataset.[17] The methodology of this work involved the identification of differentially expressed genes and their analysis using protein-protein interaction, regulatory-network, and signaling-pathway approaches to uncover potential therapeutic targets. The ML models used included RF, SVM, DT, Gaussian NB (GNB), K-Nearest Neighbors (KNN), and eXtreme Gradient Boosting (XGB) for classification of cancer stage and cancer subtype. For evaluation, ACC, PRE, REC, FS, and specificity were considered. Evaluations showed that RF and XGB achieved better results, reaching 97.19% and 95.23%, respectively. Findings show that key proteins and micro ribonucleic acids (miRNAs) are potential biomarkers, demonstrating the method's potential to advance personalized treatment approaches. Hu et al.[18], aimed at enhancing identification of cancer-driver genes by addressing limitation in existing approaches related to feature relationships and noise in protein-protein interaction (PPI) data. This work utilized a dynamic-incentive-model (DIM) to construct a hypergraph to minimize false positives in PPI networks. Gene importance within hyperedges was assessed using Network Functional score (NFS), and DIM integrates NFS with miRNA and messenger RNA (mRNA) differential expression scores. The DIM was evaluated on pan-cancer, prostate cancer, lung cancer, and breast cancer datasets. The evaluation was performed using the area under the receiver operating characteristic curve (AUC-ROC), with DIM outperforming existing approaches and demonstrating strong cross-cancer generalization, thereby improving targeted gene discovery.

Kurniadi and Saputri[19] aimed to investigate breast-cancer survivability using multi-modal data from the METABRIC dataset.[12] Because the dataset is high-dimensional, this work used XGB to select top-k features. This work further utilized ML classifiers (XGB, RF, SVM, and KNN) using selected features. The evaluation metrics used for the study included ACC, PRE, REC, and FS. Findings show that XGB and RF achieved the highest ACC (72.7%). Findings show that feature optimization is important for achieving good performance in survival prediction. Brahmatej Rupavath et al.[20] aimed to improve metastasis prediction in breast cancer by using a recursive neural network (RecNN) and the METABRIC dataset[12], which provides comprehensive genomic information. The approach included data preprocessing using named-entity recognition for structured classification and feature selection using Least Absolute Shrinkage and Selection Operator (LASSO). In this work, the RecNN was applied to predict metastasis on the basis of selected features. For evaluation, ACC, PRE, REC, and FS were considered; the RecNN achieved 98.69% ACC, outperforming approaches such as CNN.

Puttegowda et al.[21], aimed at improving breast-cancer and personalized treatment by predicting key-clinical attributes, i.e., cancer subtype, tumor stage and progesterone-receptor status utilizing ML. For this study, the METABRIC dataset was utilized, which provides extensive clinical and genomic information. In this study, classification was performed using logistic-regression (LR), SVM, RF, and an ensemble of these approaches. Evaluations were conducted with respect to ACC, with SVM-radial basis function achieving 99.79% ACC, SVM achieving 97.93% ACC, RF achieving 97.59% ACC, and LR achieving 89.45% ACC. Findings show the effectiveness of non-linear models in capturing complex patterns, achieving prognostic ACC, and supporting personalized cancer treatment planning. Ghosh et al.[22] focused on the identification of subtype-specific gene biomarkers for breast cancer, utilizing gene expression data to support precise treatment and classification. For this study, the TCGA-BRCA dataset[17] was utilized. The methodology involved feature selection using LASSO, which was combined with four ML approaches (i.e., NB, KNN, SVM, and RF) to determine the best approach, with SVM achieving the best performance.

Furthermore, a modified Compact Genetic Approach (mCGA) was employed to refine biomarker selection for subtypes [basal-like, human epidermal growth factor receptor 2 (HER2)-enriched, Luminal B, and Luminal A]. Evaluations showed AUC-ROC values of 100% for HER2 and Basal, 97.31%, and 98.78% for Luminal A. The pathway and enrichment analyses demonstrated biological relevance.

Turova et al.[23], aimed at improving breast-cancer subtyping by introducing breast-cancer classifier (BCC), a ML-based approach which utilizes RNA-sequence data for addressing limitation in current approaches like Immunohisto-Chemistry and PAM50, which are particularly focused in identifying HER2-low sub-type. In their study, data from TCGA-BRCA,[17] SCAN-B cohorts,[24] and METABRIC[12] were considered, from which the BCC was developed. The approach involved training BCC to classify breast-cancer subtypes, with a focus on distinguishing HER2-low as a unique group and reclassifying PAM50's normal subtype. Statistical analysis showed that BCC had high ACC. Findings show prognostic similarities between HER2-low and basal subtypes. Findings show that BCC's approach has potential to enhance treatment stratification and to deepen molecular understanding of breast cancer. Asfaw and Tegaw[25] aimed to compare survival outcomes of breast cancer patients undergoing mastectomy versus breast-conserving surgery (BCS) using ML approaches. This study utilized the METABRIC dataset,[12] which was first preprocessed using an imputation approach, then subjected to a Synthetic Minority Oversampling Technique (SMOTE)-based class-balancing approach, and finally underwent feature selection. For classification, DT, XGB, LR, GNB, RF, KNN, SVM, AdaBoost, and Gradient-Boosting (GB) were used; GB achieved 95.4% training and 86.4% testing ACC for mastectomy class. For the BCS class, GB achieved training and testing ACCs of 94.6% and 82.8%, respectively. The important features included age, the Nottingham Prognostic Index, and relapse-free status. Findings showed that younger patients derived greater benefit from BCS, supporting personalized treatment approaches.

Yaqoob and Verma[26] aimed to enhance breast cancer classification using gene-expression data by introducing a hybrid feature-selection approach that combined the Kashmiri-Apple Optimization Approach (KAO) and Armadillo-Optimization Approach (AOA), followed by an SVM classifier. The KAO was employed for global exploration of informative genes, while AOA performed local refinement to reduce redundancy and prevent premature convergence. The KAO-AOA-SVM was applied to breast cancer datasets, achieving 98.97% ACC using only 15 genes. The approach demonstrated consistent performance across gene subsets, indicating robustness and potential for clinical and cross-cancer applications. Kallah-Dagadu et al.[27], aimed at enhancing breast-cancer prediction by identification of key-genes using ML and explainable AI (XA) approaches. This study used the TCGA-BRCA[17] dataset, which contained 1,208 samples and 3,602 gene features. In this work, KNN, SVM, and RF were applied with feature selection. The XAI approaches included accumulated local effects, partial dependence plots, and SHapley Additive exPlanations (SHAP) values, which were used to interpret model outputs and assess gene importance. The leaving-one-covariate-in approach was used to identify the top ten predictive genes, with SVM and RF rankings closely aligned. The Findings showed the value of explainability in ML-driven cancer diagnosis for improving clinical decision-making.

Aliouane et al.[28] aimed to improve breast cancer classification by integrating a DL approach with SHAP to interpret gene expression data. The approach involved training a DL model and evaluating it using 5-fold cross-validation and ensemble learning on the ArrayExpress (E-MTAB-3732) dataset,[29] achieving a mean ACC of 99.64%. To assess generalizability, the CuMiDa dataset[14] was utilized; it comprises only three databases (GSE42568, GSE7904, and GSE45827), which achieved ACCs of 99.14%, 100%, and 98.67%, respectively. SHAP analysis identified key genes, including KRT5, ESR1, KRT19, and DSCAM-AS1. Further validation using the MalaCards[30] database demonstrated the relevance of genes, providing evidence of the method's effectiveness for biomarker interpretability and discovery. Li et al.[31] aimed to develop a stable and accurate approach for breast cancer prognosis that addressed data distribution shifts across diverse datasets; they presented a model called Deep-Global Balancing-Cox Regression (DGBCox), which integrated causal inference with DP. The gene-expression data were first transformed into latent representations using a deep autoencoder, and the resulting representations were then balanced using a causality-based approach. Causal features were selected using balanced representations for survival prediction. The DGBCox was evaluated on twelve breast cancer datasets, on which it outperformed existing benchmark approaches in both stability and predictive ACC, demonstrating effectiveness in heterogeneous data scenarios and improving prognostic reliability.

Rabah et al.[32] aimed to enhance noninvasive breast cancer subtype classification by developing a multi-modal DL approach that combined mammography images with clinical metadata. Utilizing the Chinese Mammography Database[33], which contains 4,056 mammography images from 1,775 patients, the approach classifies breast lesions into five classes: triple-negative, HER2-enriched, Luminal B, Luminal A, and benign. The approach integrated image

and clinical data, and its performance was evaluated using AUC, achieving 88.78% ACC. Sridharan and Ghosh[34] aimed to enhance breast cancer survival prediction by integrating GEP data with agent-based modelling (ABM). The approach first identified key genes involved in cancer progression using GEP, and then constructed a model representing how genes influence cellular behavior. These insights were incorporated into ABM to simulate tumor growth and treatment response under various conditions. The predictive performance of the GEP-ABM was validated using actual patient data and benchmarked against existing approaches using ACC-based metrics. Findings suggest that GEP-ABM integration improves survival predictions and supports more personalized, data-driven breast cancer treatment strategies.

Kunta and Lepakshi[35] aimed at developing ascalable, non-invasive solution for breast cancer detection using mRNA gene expression data. The approach involved transforming one-dimensional mRNA sequences into two-dimensional images to capture spatial information. After standard preprocessing and applying SMOTE for class balancing, features were extracted using AlexNet and ResNet101 to mitigate issues such as local feature dependence and vanishing gradients. These features were further combined and used to train an Ensemble-of-Ensemble classifier, which incorporated XGB, RF, AB, bagging, and extra-trees for consensus-based prediction. When evaluated on gene expression data, the model achieved 99.91% ACC, confirming its robustness and applicability. Li et al.[36] presented a novel bi-clustering approach, Bi-clustering differential-sparsity-constraints and dynamic-graph-regularization (BCDD), designed to enhance cancer subtype classification by addressing limitations in existing sparse singular-value decomposition (SVD)-based approaches. The approach incorporated differential sparsity constraints, applying an L1/2-norm to genes and an L1-norm to samples, to reflect the inherent sparsity imbalance in cancer gene expression data. Additionally, a dynamic graph regularization strategy was proposed, which enabled iterative updates to the graph adjacency matrix based on changes in SVD to avoid bias introduced by previously extracted biclusters. For evaluations, the five datasets from TCGA[37] were considered; these included the TCGA-BRCA dataset.[17] The BCDD demonstrated superior bi-clustering ACC and robustness compared to state-of-the-art methods, confirming its effectiveness in identifying biologically relevant gene modules.

Goidescu et al.[38], aimed at exploring contribution of moderate/low risk gene mutations for hereditary breast cancer using multi-gene panel testing. Next-generation sequencing was used to analyze 255 breast cancer patients who met clinical criteria for genetic testing. Among the 104 identified pathogenic variants, 21 were found in moderate-risk genes (notably CHEK2 and ATM), three were found in low-risk genes (MSH1 and MLH1), and eight were found in genes with insufficient evidence of risk. The analysis emphasized the clinical relevance of reporting less-penetrant mutations to enhance genetic risk assessment. Findings support expanding genetic screening to improve diagnostic precision, personalize treatment strategies, and refine breast cancer risk prediction models across populations. Rezaei et al.[39], aimed to evaluate role of AI in enhancing breast cancer diagnosis and management through transcriptomic data analysis. A systematic search across databases including PubMed, Scopus, WoS, Embase, and IEEE Xplore identified 7,287 studies, of which 54 were selected for final analysis: 24 focused on RNA sequencing and 30 on GEP. The methodology involved screening by multiple reviewers and extraction of data on AI models and molecular techniques. Common AI methods included RF, CNNs, SVMs, and LASSO. These approaches demonstrated high potential in biomarker identification, prognosis prediction, and drug response optimization, though further large-scale validation and interdisciplinary research are needed.

Thâalbi and Akhloufi[40] aimed at enhancing breast cancer gene expression prediction by introducing EMGP-Net, a novel DL architecture combining EfficientFormer and MambaVision. EMGP-Net was trained using a leave-one-patient-out method on the HER2+ dataset (8 patients)[41] and validated externally on the STNet dataset (23 patients),[42] with training alternating between the two datasets. The model integrated features from both architectures using attention mechanisms and dense layers to predict the expression of 250 selected genes. Evaluation using the Pearson correlation coefficient (PCC) showed superior performance, achieving a maximum PCC of 0.7903 for the *PTMA* gene. Chowdhury and Kamal[43] aimed to develop an interpretable ML framework for classifying BRCA subtypes using RNA-sequencing data. The approach utilized the TCGA transcriptomic dataset,[37] incorporating dimensionality reduction and performing hyperparameter tuning via grid search to optimize classification models. SHAP values were employed to identify significant transcriptomic markers relevant to subtype differentiation. The model's performance was evaluated using metrics such as ACC, PRE, and FS, thereby demonstrating enhanced classification ACC and interpretability compared with existing approaches. Additionally, gene set enrichment analysis revealed key molecular pathways linked to BRCA subtypes, highlighting the method's potential to support personalized prognosis and treatment planning in clinical settings.

Nasarudin et al.[44], focused on developing an interpretable DL model for predicting breast cancer survival using METABRIC dataset.[12] The approach integrated bidirectional (BiLSTM)

and CNN architectures with minimum redundancy maximum relevance (MRMR) for feature selection. Evaluations were conducted using METABRIC (n=1980) and TCGA-BRCA (n=1080) datasets, incorporating clinical data, copy number alterations, and gene expression profiles. Performance was assessed using ACC and AUC-ROC metrics. The model achieved 98% ACC on METABRIC and 96% on TCGA, outperforming existing methods. These findings suggest the model's robustness and potential to support personalized treatment decisions in breast cancer care. Maigari et al.[45] aimed to review advancements in multimodal DL approaches for breast cancer survival prediction, focusing on architectures that integrated imaging, genomic, and clinical data. A systematic literature review was conducted using databases and search engines such as Google Scholar, Web of Science, and Scopus, from which 19 relevant studies were selected. These studies employed DL methods, particularly CNNs, to handle high-dimensional, heterogeneous data. Evaluation metrics included predictive ACC and model interpretability. Findings revealed that CNNs and hybrid models, including Graph Neural Networks, significantly improved prognostic ACC. However, gaps remain in dynamic modeling, multimodal integration, and explainability, underscoring the need for robust and interpretable solutions in PRE oncology.

Findings

This section presents the key findings derived from an extensive review of recent research on breast cancer prediction using ML and DL techniques. The studies were analyzed based on their methodologies, datasets, performance metrics, and model architectures. Emphasis was placed on understanding how different approaches handle data preprocessing, feature selection, and model evaluation. The findings are categorized to clarify trends and limitations in the existing literature. By identifying common practices and shortcomings, this section lays the foundation for recognizing research gaps and justifying the need for more robust, interpretable, and generalizable DL-based frameworks.

Literature Survey Findings

This section presents and discusses key findings from the reviewed literature; these findings are systematically summarized in Table 1. The table summarizes outcomes of various studies on breast cancer prediction, classification, and survival analysis that employed ML, DL, and hybrid techniques. It highlights the use of diverse datasets, such as METABRIC and TCGA-BRCA, and advanced models, such as LSTM, XGB, and DNN. The findings provide insights into the performance of different approaches in terms of ACC, interpretability, feature selection, and into their potential for clinical application in personalized cancer treatment.

Datasets Used

The literature review reveals that METABRIC[12], TCGA-BRCA[17], and CuMiDa[14] are the most commonly used datasets for breast cancer research and analysis, as presented in Table 2. These datasets provide extensive genomic, transcriptomic, and clinical information, making them highly valuable for developing ML and DL models focused on prediction, classification, survival analysis, and personalized treatment planning.

The METABRIC[12], TCGA-BRCA[17], and CuMiDa[14] datasets are described in detail below.

• METABRIC[12]: METABRIC is a widely used breast cancer dataset that includes clinical and genomic data from approximately 2,000 patients. It provides gene expression profiles, somatic mutation data, copy number aberrations, and survival outcomes. The dataset is instrumental in building models for prognostic analysis, metastasis prediction, and clinical feature classification.

• TCGA-BRCA[17]: TCGA-BRCA dataset contains comprehensive multi-omic profiles, including mRNA expression, DNA methylation, copy number variations, and clinical annotations for over 1,000 breast cancer patients. It supports subtype classification, survival analysis, and biomarker discovery. It is a benchmark dataset for breast cancer ML/DL research because of its size, richness, and the availability of follow-up data.

• CuMiDa[14]: The Curated Microarray Database (CuMiDa) is a collection of microarray gene expression datasets covering various types of cancer, including breast, liver, lung, prostate, and kidney. It contains over 1,000 patient samples and is primarily used for multi-class classification, dimensionality reduction, and benchmarking optimization-based ML approaches.

Performance Metrics Used

Performance evaluation plays a crucial role in assessing the effectiveness of ML and DL models in breast cancer prediction and analysis. Various studies have employed a range of metrics depending on the problem type, data balance, and model objective. The most commonly used metrics include ACC, PRE, REC, and FS, particularly for classification tasks. Other metrics, such as balanced accuracy (BAC), kappa (KAP), MCC, and AUC-ROC, are used for imbalanced datasets and multiclass classification tasks. PCC was adopted for expression-level prediction. Table 3 summarizes the performance metrics used in the reviewed studies.

Below are common performance metrics used in the literature and how they are calculated:

ACC indicates the ratio of correctly predicted observations to total observations.

$$Accuracy = \frac{TP + TN}{TP + TN + FP + FN} \quad (1)$$

where *TP=True Postive, TN=True Negative, P=False Positive* and *N=False Negative.*

PRE: Measures how many of the positively predicted instances are actually positive.

$$Precision = \frac{TP}{TP + FP} \quad (2)$$

REC: Measures how many actual positive instances were correctly identified.

$$Recall = \frac{TP}{TP + FN} \quad (3)$$

FS: The harmonic mean of precision and recall, balancing both.

$$FS = 2 \times \frac{Precision \times Recall}{Precision + Recall} \quad (4)$$

Balanced Accuracy (BAC): Used when data is imbalanced. It is the average of sensitivity and specificity.

TABLE 1: Literature survey findings.

Reference	Findings
11	An LSTM model achieved 98.7% accuracy using the multi-omics METABRIC dataset for survival prediction.
13	Dimensionality was reduced from 36,805 to 80 features, and balanced accuracy improved to 93.4%.
15	PCA- and MCC-based feature selection with a DNN improved classification performance.
16	RF and XGB achieved accuracies of 97.19% and 95.23%, respectively, and identified key proteins and miRNAs.
18	DIM model improved cancer-driver gene identification with strong cross-cancer generalization.
19	XGB and RF models achieved 72.7% accuracy in survival prediction using selected METABRIC features.
20	RecNN achieved an accuracy of 98.69% in predicting metastasis using LASSO-selected features.
21	SVM-RBF achieved 99.79% accuracy in predicting key clinical attributes from METABRIC data.
22	SVM performed best, with subtype-specific AUC-ROC scores of up to 100% for HER2 and Basal subtypes.
23	BCC improved subtyping accuracy and reclassified HER2-low as a distinct subtype.
25	The Gradient Boosting model achieved 86.4% test accuracy for the mastectomy class; age and relapse were key predictors.
26	KAO-AOA-SVM achieved an accuracy of 98.97% using only 15 genes to classify breast cancer.
27	XAI methods, such as SHAP, helped identify the top predictive genes; SVM and RF showed concordant rankings.
28	DL with SHAP achieved up to 100% accuracy and validated key genes, including ESR1 and KRT5.
31	DGBCox improved prognostic reliability across 12 datasets by addressing distributional shifts in the data.
32	Multimodal DL using mammograms and clinical data achieved an accuracy of 88.78%.
34	Integration of GEP with ABM improved survival prediction and tumor simulation accuracy.
35	An E2E classifier using mRNA image features achieved 99.91% accuracy.
36	The BCDD biclustering approach outperformed traditional SVD for subtype classification.
38	Identified moderate/low-risk gene mutations, supporting extended genetic screening.
39	A systematic review confirmed ML's promise in diagnosis, biomarker discovery, and treatment prediction.
40	EMGP-net achieved high gene expression prediction accuracy, with a PCC of 0.7903 for PTMA.
43	An interpretable ML model using SHAP and enrichment analysis improved BRCA subtype classification.
44	BiLSTM-CNN with MRMR achieved accuracies of 98% (METABRIC) and 96% (TCGA).
45	The review identified CNNs and hybrid DL models as top performers in multimodal survival prediction.

METABRIC: The Molecular Taxonomy of Breast Cancer International Consortium; LSTM: Long short-term memory; PCA: Principal component analysis; MCC: Mathew's correlation coefficient; XGB: eXtreme gradient-boosting; RF: Random forest; DIM: Dynamic-incentive-model; LASSO: Least-absolute-shrinkage and selection-operator; RecNN: Recursive-neural-network; SVM: Support vector machines; RBF: Radial basis function; AUC-ROC: Area under curve-receiver operating characteristic; HER2: Human epidermal growth factor receptor 2; KAO: Kashmiri-Apple optimization approach; AOA: Armadillo-optimization approach; SHAP: SHapley Additive exPlanations; DL: Deep learning; DGBCox: Deep-global balancing-cox regression; GEP: Gene expression profiling; ABM: Agent-based modelling; E2E: Ensemble-of-ensemble; BCDD: Bi-clustering differential-sparsity-constraints and dynamic-graph-regularization; SVD: Singular-value decomposition; ML: Machine learning; BiLSTM: Bi-directional long short-term memory; CNN: Convolutional neural network; MRMR: Minimum redundancy maximum relevance; TCGA: The cancer genome atlas.

$$Balanced\ Accuracy = \frac{1}{2}\left(\frac{TP}{TP+FN} + \frac{TN}{TN+FP}\right) \quad (5)$$

Kappa Coefficient (KAP): Measures agreement between predicted and actual labels while considering chance agreement.

$$\kappa = \frac{P_0 - P_e}{1 - P_e} \quad (6)$$

where P_0 denotes observed accuracy, P_e denotes expected accuracy by chance.

MCC: Provides a balanced measure even for imbalanced datasets.

$$MCC = \frac{(TP \times TN) - (FP \times FN)}{\sqrt{(TP+FP)(TP+FN)(TN+FP)(TN+FN)}} \quad (7)$$

AUC-ROC (Area Under Curve - Receiver Operating Characteristic): Measures the ability of a classifier to distinguish between classes. Higher AUC indicates better model performance.

$$AUC - ROC = \int_0^1 TPR(FPR)dFPR \quad (8)$$

where PR=True Postive Rate, FPR=False Positive Rate.

The Pearson correlation coefficient (PCC) measures the linear correlation between predicted and true gene expression levels.

$$PCC = \frac{\sum(x_i - \bar{x})(y_i - \bar{y})}{\sqrt{\sum(x_i - \bar{x})^2 (y_i - \bar{y})^2}} \quad (9)$$

TABLE 2: Dataset used in existing works.

Reference	Dataset used
11,15, 19, 20, 21, 23, 25, 44	METABRIC[12]
13, 28	CuMiDa[14]
16, 22, 23, 27, 30, 36, 43, 44	TCGA-BRCA[17]
24	SCAN-B
32	CMMD[33]
31	12 breast cancer datasets
38	Custom gene panel sequencing
41, 42	HER2+, STNet
29	ArrayExpress (E-MTAB-3732)
37	TCGA (multiple, including BRCA)

METABRIC: The Molecular Taxonomy of Breast Cancer International Consortium; HER2: Human epidermal growth factor receptor 2; TCGA: The cancer genome atlas; BRCA: Breast invasive carcinoma; CuMiDa: The curated microarray database; CMMD: Chinese mammography database; SCAN-B: The Sweden Cancerome Analysis Network-Breast.

x_i where and y_i are predicted and actual values respectively.

ML and DL Models and Feature Extraction and Selection Approaches Used

ML and DL techniques have been widely adopted in breast cancer research for tasks such as classification, survival prediction, and biomarker identification. These models are often complemented with feature selection and feature extraction methods to enhance performance, reduce dimensionality, and improve interpretability. Feature selection techniques, such as LASSO, MCC, and MRMR, help identify the most relevant variables, whereas extraction methods, such as PCA and autoencoders transform raw data into meaningful representations. Table 4 provides a comprehensive overview of the reviewed studies, highlighting the use of ML, DL, feature selection, and feature extraction techniques across different research efforts in this domain.

Issues and Challenges

This section discusses the issues and challenges. Table 5 summarizes the key issues and challenges identified in existing ML and DL approaches for breast cancer prediction and analysis. While many studies have demonstrated high performance, they often exhibit limitations, such as the exclusive use of ML or DL without cross-paradigm validation. Additionally, several works rely on basic or outdated feature selection methods, which may not adequately capture complex biological interactions. In some studies, feature extraction methods such as PCA or VAE, though effective for dimensionality reduction, can lead to a loss of interpretability or of biologically relevant information. Another significant issue across studies is the limited generalizability and lack of external validation, particularly when using small datasets or omics-specific models. Furthermore, imbalanced datasets, overfitting, and inconsistent benchmarking between ML and DL approaches affect the deployment of robust models in clinical settings.

TABLE 3: Performance metrics used in reviewed studies.

Reference	Performance metrics used
11, 15, 16, 19-22,25-28, 43, 44	Accuracy, precision, recall, F1-score
13	Balanced accuracy score, F1-score, precision, recall, kappa, Matthews correlation coefficient
23, 36	Area under the curve-receiver operating characteristic
31, 34, 38, 39	Custom metrics, statistical validation, interpretability-based assessments
40	Pearson correlation coefficient

TABLE 4: Overview of ML, DL, feature selection, and feature extraction usage by existing literature review.

Reference	ML	DL	Feature selection	Feature extraction
[11]	No	Yes (GCN, LSTM, VAE)	Yes (preprocessing)	Yes (VAE)
[13]	Yes (SVM, NB, DT, RF)	No	Yes (RO+entropy)	Yes (PCA, ICA, SAE)
[15]	No	Yes (DNN)	Yes (MCC-based)	Yes (PCA)
[16]	Yes (RF, SVM, DT, GNB, KNN, XGB)	No	Yes (gene analysis)	Yes (pathway & network analysis)
[18]	No	No	Yes (NFS-based DIM)	Yes (hypergraph+PPI)
[19]	Yes (XGB, RF, SVM, KNN)	No	Yes (top-k XGB features)	No
[20]	No	Yes (RecNN)	Yes (LASSO)	Yes (NER)
[21]	Yes (SVM, LR, RF, Ensemble)	No	Yes (preprocessing)	No
[22]	Yes (NB, KNN, SVM, RF)	No	Yes (LASSO, mCGA)	No
[23]	Yes	Yes (BCC)	Yes (subtype refinement)	Yes (RNA-seq embedding)
[25]	Yes (DT, XGB, SVM, LR, etc.)	No	Yes (SMOTE+feature selection)	No
[26]	Yes (SVM)	No	Yes (KAO+AOA)	Yes (gene subset search)
[27]	Yes (KNN, SVM, RF)	No	Yes (LOCI+SHAP)	No
[28]	No	Yes (DL+SHAP)	Yes (SHAP genes)	Yes (ensemble learning)
[31]	No	Yes (DAE, DGBCox)	Yes (causal feature balancing)	Yes (latent representation via DAE)
[32]	Yes (meta-classification)	Yes (DL with imaging)	Yes (metadata analysis)	Yes (CNN for images)
[34]	Yes	No	Yes (key gene identification)	Yes (agent-based modeling)
[35]	Yes (E2E: XGB, RF, AB, etc.)	Yes (AlexNet, ResNet)	Yes (SMOTE)	Yes (image transformation)
[36]	Yes	No	Yes (sparsity-based)	Yes (SVD+graph regularization)
[38]	No	No	Yes (gene panel filtering)	No
[39]	Yes	Yes	Yes (reviewed LASSO, RF, etc.)	No
[40]	No	Yes (EMGP-net)	Yes (top 250 genes)	Yes (efficientformer+mambavision)
[43]	Yes	No	Yes (SHAP+hyperparameter tuning)	Yes (dimensionality reduction)
[44]	Yes	Yes (BiLSTM+CNN)	Yes (MRMR)	Yes (multi-omic integration)
[45]	No (review)	Yes	Yes (reviewed techniques)	Yes (imaging+genomic fusion)

DL: Deep learning; ML: Machine learning; SVM: Support vector machines; GCN: Graph-convolutional networks; LSTM: Long short-term memory; VAE: Variational autoencoders; NB: Naïve bayes; RF: Random forest; DT: Decision tree; GNB: Gaussian NB; KNN: K-nearest neighbors; XGB: eXtreme gradient-boosting; LR: Logistic-regression; E2E: Ensemble-of-ensemble; AB: AdaBoost; KAO: Kashmiri-apple optimization approach; AOA: Armadillo-optimization approach; LOCI: Leaving-one-covariate-in; SHAP: SHapley additive exPlanations; SMOTE: Synthetic minority oversampling technique; CNN: Convolutional neural network; SVD: Singular-value decomposition; MRMR: Minimum redundancy maximum relevance; BiLSTM: Bi-directional long short-term memory; RO: Remora-optimization; MCC: Mathew's correlation coefficient; NFS: Network-functional-score; DIM: Dynamic-incentive-model; PCA: Principal component analysis; SAE: Sparse auto-encoder; ICA: Independent component analysis; PPI: Protein-protein interaction; LASSO: Least-absolute-shrinkage and selection-operator.

The reviewed literature reveals notable progress in breast cancer prediction using ML and DL, but also highlights critical limitations in existing approaches. Many studies rely on either ML or DL alone, missing opportunities to leverage the strengths of both. ML models often offer high interpretability but may struggle with complex, non-linear patterns in omics data. On the other hand, DL models like CNNs, RNNs, and AEs provide superior feature representation and predictive ACC, but are frequently criticized for their black-box nature and high computational complexity. Feature selection techniques are often rudimentary, leading to suboptimal model performance, whereas feature extraction methods may reduce interpretability. Moreover, several approaches demonstrate promising results in limited datasets, but fail to generalize across diverse cohorts due to inadequate validation strategies. This underscores the growing need for DL-based frameworks that not only capture high-dimensional, nonlinear patterns in multi-omic and imaging data but also integrate explainability and domain knowledge. Combining DL with advanced feature selection and robust external validation could pave the way for more accurate, interpretable, and clinically applicable cancer prediction models, ultimately contributing to personalized and PRE oncology.

TABLE 5: Issues and challenges in existing approaches.	
Reference	**Issues and challenges**
11	DL-only method; no ML-to-DL comparison; potential loss of interpretable features during feature extraction using VAE.
13	Despite extensive feature extraction, ML-based classifiers may reach a performance plateau; BAC increased, but remained subpar for all classes.
15	PCA may ignore biologically significant features; however, the DL technique employed lacks diversity in classifiers.
16	Solely employs machine learning; fails to investigate DL models, which could more effectively capture non-linear dependencies; although gene-level network analysis is intricate, it might overlook more profound patterns.
18	Depends on network-based scoring (DIM), which might not generalize to noisy datasets; lacks DL/ML categorization.
19	The accuracy is comparatively low (72.7%); the feature-extraction approach is not robust; the feature selection is restricted to the top-k features via XGB.
20	RecNN is used, but no ML comparison is made. LASSO may fail to detect interactions among nonlinear features.
21	The study is ML-only; feature selection is straightforward, and DL is not used for deeper representation learning.
22	LASSO and mCGA were employed; however, no DL comparison was conducted. The biomarker finding was robust; however, there was no evidence of generalizability.
23	DL-based subtyping, but there isn't any obvious external validation; RNA-seq embeddings might vary depending on the dataset.
25	ML models were used; GB performed well, but test accuracy declined, suggesting overfitting.
26	DL is not integrated by ML with hybrid feature selection, which is restricted to classification without biological interpretability.
27	No DL model is employed; explainability is prioritized, yet predictive power may be weak; feature selection may overlook latent features.
28	Although the DL model is reliable, it does not integrate biological pathway information, and its generalizability has been validated only on a small number of datasets.
31	When DL is applied to causal inference, its complexity increases, and its interpretability and clinical applicability are constrained.
32	Multi-modal DL may require improved feature fusion, although its accuracy (88.78%) is lower than that of DL-only methods.
34	No DL model; ABM lacks real-time flexibility and is strong for simulation but not predictive.
35	High performance can be achieved using complex ensemble methods and DL; however, model interpretability and computational cost remain significant obstacles.
36	There is no DL; bi-clustering and graph regularization are heavily used; interpretability is good but not predictively validated.
38	Gene panel analysis may overlook new biomarkers in more recent datasets because it is not inherently predictive.
39	Review; draws attention to the lack of extensive validation across datasets and the inconsistency in ML/DL model comparison.
40	The validation dataset for the gene expression-focused DL model is modest (8 and 23 patients), raising concerns about its generalizability.
43	Strong interpretability ML model without DL benchmarking; robustness may be impacted by gene expression variability.
44	Although BiLSTM+CNN works effectively, it is complex and difficult to interpret, and MRMR selection may exclude synergistic genes.
45	Multimodal DL techniques are reviewed; however, the incorporation of dynamic patient data and explainability remain two main gaps.

DL: Deep learning; ML: Machine learning; VAE: Variational autoencoders; BAC: Balanced accuracy score; PCA: Principal component analysis; DIM: Dynamic-incentive-model; XGB: eXtreme gradient-boosting; LASSO: Least-absolute-shrinkage and selection-operator; RecNN: Recursive-neural-network; CNN: Convolutional neural network; BiLSTM: Bi-directional long short-term memory; ABM: Agent-based modelling; MRMR: Minimum redundancy maximum relevance; GB: Gradient-boosting.

CONCLUSION

Breast cancer remains one of the most critical health challenges affecting women worldwide, with early and accurate diagnosis being essential for effective treatment and improved survival rates. This work began with a comprehensive review of ML and DL approaches applied to breast cancer prediction and classification. Although numerous studies have attempted to use ML and DL models with various genomic, transcriptomic, and clinical datasets, significant limitations persist. Common issues include over-reliance on either ML or DL models, lack of generalization, inadequate feature selection or extraction techniques, and inconsistent performance metrics across datasets. The research identified key gaps such as limited integration of multi-modal data, poor interpretability, and the absence of robust, unified frameworks capable of handling

complex and high-dimensional gene expression data. In response, the problem statement was formulated to address the need for a more accurate and generalizable approach to breast cancer classification. The objectives included analyzing existing techniques, identifying their limitations, and proposing a way forward. A systematic methodology was adopted, including a literature review, dataset exploration, evaluation of performance metrics, and comparison of ML and DL models. Findings revealed that DL models generally offer superior performance but suffer from a lack of transparency and consistency when applied across different datasets. Future work will involve developing a novel DL-based framework that incorporates advanced feature extraction and selection methods. The proposed system will be trained and validated using diverse datasets, such as CuMIDA, METABRIC, and TCGA-BRCA. The goal is to accurately predict and classify various subtypes of breast cancer while ensuring high interpretability, robustness, and clinical relevance.

Footnotes

Authorship Contributions

Concept: A.S.P., Design: A.S.P., Data Collection or Processing: A.S.P., Analysis or Interpretation: P.J., Literature Search: P.J., A.S.P., Writing: P.J., A.S.P.

Conflict of Interest: No conflict of interest was declared by the authors.

Financial Disclosure: The authors declared that this study received no financial support.

REFERENCES

1. Sathishkumar K, Chaturvedi M, Das P, Stephen S, Mathur P. Cancer incidence estimates for 2022 & projection for 2025: result from National Cancer Registry Programme, India. Indian J Med Res. 2022;156(4&5):598-607. [Crossref] [PubMed] [PMC]
2. Tian F, Liu D, Wei N, et al. Prediction of tumor origin in cancers of unknown primary origin with cytology-based deep learning. Nat Med. 2024;30:1309-1319. [Crossref]
3. Zhang Y, Ji Y, Liu S, et al. Global burden of female breast cancer: new estimates in 2022, temporal trend and future projections up to 2050 based on the latest release from GLOBOCAN. J Natl Cancer Cent. 2025;5(3):287-296. [Crossref] [PubMed] [PMC]
4. Cai Y, Dai F, Ye Y, et al. The global burden of breast cancer among women of reproductive age: a comprehensive analysis. Sci Rep. 2025;15:9347. [Crossref]
5. García-Sancha N, Corchado-Cobos R, Pérez-Losada J. Understanding susceptibility to breast cancer: from risk factors to prevention strategies. Int J Mol Sci. 2025;26(7):2993. [Crossref] [PubMed] [PMC]
6. Arnold M, Morgan E, Rumgay H, et al. Current and future burden of breast cancer: global statistics for 2020 and 2040. Breast. 2022;66:15-23. [Crossref] [PubMed] [PMC]
7. Abu Abeelh E, AbuAbeileh Z. Comparative effectiveness of mammography, ultrasound, and MRI in the detection of breast carcinoma in dense breast tissue: a systematic review. Cureus. 2024;16(4):e59054. [Crossref]
8. Carriero A, Groenhoff L, Vologina E, Basile P, Albera M. Deep learning in breast cancer imaging: state of the art and recent advancements in early 2024. Diagnostics (Basel). 2024;14(8):848. [Crossref] [PubMed] [PMC]
9. Jiang B, Bao L, He S, Chen X, Jin Z, Ye Y. Deep learning applications in breast cancer histopathological imaging: diagnosis, treatment, and prognosis. Breast Cancer Res. 2024;26(1):137. [Crossref] [PubMed] [PMC]
10. Khan K, Awang S, Talab MA, Kahtan H. A comprehensive review of machine learning and deep learning techniques for intraclass variability breast cancer recognition. Franklin Open. 2025;11:100296-100296. [Crossref]
11. Mahmoud A, Alhussein M, Aurangzeb K, Takaoka E. Breast cancer survival prediction modeling based on genomic data: an improved prognosis-driven deep learning approach. IEEE Access. 2024;(12):119502-119519. [Crossref]
12. Breast Cancer Gene Expression Profiles (METABRIC). Available from: https://www.kaggle.com/datasets/raghadalharbi/breast-cancer-gene-expression-profiles-metabric (accessed 06 Aug. 2025) [Crossref]
13. Bharanidharan N, Sanassi Chakravarthy SR, Vankatesan VK, Abbas M, Mahesh TR, Mohan E. Local entropy based remora optimization and sparse autoencoders for cancer diagnosis through microarray gene expression analysis. IEEE Access. 2024;(12)39285-39299. [Crossref]
14. Feltes BC, Chandelier EB, Grisci BI, Dorn M. CuMiDa: an extensively curated microarray database for benchmarking and testing of machine learning approaches in cancer research. J Comput Biol. 2019;26(4):376-386. [Crossref] [PubMed]
15. Kishore Khan S, Kanamarlapudi A, Singh AR. Diagnosis and classification of breast cancer using data visualization and deep learning techniques. 2024 5th International Conference for Emerging Technology (INCET), Belgaum, India. 2024;1-6. [Crossref]
16. Das SC, Tasnim W, Rana HK, Acharjee UK, Islam MM, Khatun R. Comprehensive bioinformatics and machine learning analyses for breast cancer staging using TCGA dataset. Brief Bioinform. 2024;26(1):bbae628. [Crossref] [PubMed] [PMC]
17. Cancer.gov, 2024. Available link: https://portal.gdc.cancer.gov/projects/TCGA-BRCA
18. Hu Z, Li G, Luo X, et al. Identification of cancer driver genes based on dynamic incentive model. IEEE/ACM Trans Comput Biol Bioinform. 2024;21(6):2371-2381. [Crossref] [PubMed]
19. Kurniadi FI, Saputri HA. Feature selection using XGBoost on METABRIC dataset for survivability breast cancer detection. 2024 International Conference on Information Management and Technology (ICIMTech), Bali, Indonesia. 2024;259-262. [Crossref]
20. Brahmatej Rupavath RVSS, Shnain AH, Pushpalakshmi GRG, Hemalatha K. A deep learning based metastasis prediction system using multi omics data and recursive neural network. 2024 4th International Conference on Mobile Networks and Wireless Communications (ICMNWC), Tumkuru, India. 2024;1-5. [Crossref]
21. Puttegowda K, Kumar DA, Ravi V, et al. Advanced machine learning techniques for prognostic analysis in breast cancer. The Open Bioinformatics Journal. 2025;18(1). [Crossref]
22. Ghosh N, Kumar Mridha S, Paul R. LASSO-mCGA: machine learning and modified compact genetic algorithm-based biomarker selection for breast cancer subtype classification. IEEE Access. 2025;13:17673-17682. [Crossref]

23. Turova P, Kushnarev V, Baranov O, et al. The breast cancer classifier refines molecular breast cancer classification to delineate the HER2-low subtype. NPJ Breast Cancer. 2025;11(1):19. [Crossref] [PubMed] [PMC]
24. Saal LH, Vallon-Christersson J, Häkkinen J, et al. The Sweden Cancerome Analysis Network - Breast (SCAN-B) Initiative: a large-scale multicenter infrastructure towards implementation of breast cancer genomic analyses in the clinical routine. Genome Med. 2015;7(1):20. [Crossref] [PubMed] [PMC]
25. Asfaw BB, Tegaw, EM. Explainable machine learning to compare the overall survival status between patients receiving mastectomy and breast conserving surgeries. Scientific Reports. 2025;15(1):10700. [Crossref]
26. Yaqoob A, Verma NK. Feature selection in breast cancer gene expression data using KAO and AOA with SVM classification. J Med Syst. 2025;49(1):40. [Crossref] [PubMed]
27. Kallah-Dagadu G, Mohammed M, Nasejje JB, et al. Breast cancer prediction based on gene expression data using interpretable machine learning techniques. Sci Rep. 2025;15(1):7594. [Crossref] [PubMed] [PMC]
28. Aliouane SE, Chehili H, Boulahrouf K, Abdelaziz A, Khlifa N, Hamidechi MA. Integrating deep learning and SHAP for breast cancer classification and biomarker discovery using gene expression data. IEEE Access. 2025;13:49693-49709. [Crossref]
29. Signol F, Arnal L, Navarro-Cerdán JR, Llobet R, Arlandis J, Perez-Cortes JC. SEQENS: an ensemble method for relevant gene identification in microarray data. Comput Biol Med. 2023;152:106413. [Crossref] [PubMed]
30. "MalaCards - human disease database," Malacards.org, 2017. Available link: https://www.malacards.org/
31. Li X, Liu L, Li J, Le TD. Stable breast cancer prognosis. in IEEE Transactions on Computational Biology and Bioinformatics. 2025;22(2):721-731. [Crossref]
32. Rabah CB, Sattar A, Ibrahim A, Serag A. A multimodal deep learning model for the classification of breast cancer subtypes. Diagnostics. 2025;15(8):995-995. [Crossref]
33. NgX T. The Chinese Mammography Database (CMMD) 2022. [Crossref]
34. Sridharan P, Ghosh M. Gene expression and agent-based modeling improve precision prognosis in breast cancer. Scientific Reports. 2025;15(1):17059. [Crossref]
35. Kunta JPKC, Lepakshi VA. Deep residual transfer ensemble model for mRNA gene-expression-based breast cancer. IEEE Access. 2025;13:105608-105628. [Crossref]
36. Li D, Song P, Wang J. A novel biclustering algorithm based on differential sparsity constraints and dynamic graph regularization for cancer gene expression data. IEEE Access. 2025;13:94681-94695. [Crossref]
37. National Cancer Institute. The Cancer Genome Atlas Program (TCGA) – NCI. Available link: https://www.cancer.gov/ccg/research/genome-sequencing/tcga [Crossref]
38. Goidescu IG, Rotar IC, Nemeti G, et al. Moderate-low risk breast cancer gene expression in a romanian population. Int J Mol Sci. 2025;26(11):5313. [Crossref] [PubMed] [PMC]
39. Rezaei S, Hamedani Z, Ahmadi K, et al. Role of machine learning in molecular pathology for breast cancer: a review on gene expression profiling and RNA sequencing application. Crit Rev Oncol Hematol. 2025;213:104780. [Crossref] [PubMed]
40. Thâalbi O, Akhloufi MA. EMGP-net: a hybrid deep learning architecture for breast cancer gene expression prediction. Computers. 2025;14(7):253-253. [Crossref]
41. Andersson A, Larsson L, Stenbeck L, et al. Spatial deconvolution of HER2-positive breast cancer delineates tumor-associated cell type interactions. Nat Commun. 2021;12(1):6012. [Crossref] [PubMed] [PMC]
42. He B, Bergenstråhle L, Stenbeck L, et al. Integrating spatial gene expression and breast tumour morphology via deep learning. Nat Biomed Eng. 2020;4(8):827-834. [Crossref] [PubMed]
43. Chowdhury TM, Kamal AMR. An efficient and interpretable machine learning model for classifying breast cancer subtypes using gene expression profiles. Engineering Technology & Applied Science Research. 2025;15(4):24196-24203. [Crossref]
44. Nasarudin NA, Al-Jasmi F, Abdul Aziz NH, et al. An improved deep learning algorithm for breast cancer survival prediction based on multi-omics data. F1000Research. 2025;14:765-765. [Crossref]
45. Maigari A, XinYing C, Zainol Z. Multimodal deep learning breast cancer prognosis models: narrative review on multimodal architectures and concatenation approaches. Journal of Medical Artificial Intelligence. 2025;8:61-61. [Crossref]

CASE REPORT

DOI: 10.37047/jos.galenos.2025.2025-7-5
J Oncol Sci 2026;12(1):94-7

Abiraterone Acetate Plus Prednisone Induced Bilateral Avascular Necrosis of the Femoral Head

Serhat SEKMEK[1], Bülent ÖZKURT[2], Mirmehdi MEHTİYEV[1], Öznur BAL[1], Efnan ALGIN[1]

[1]Ankara Bilkent City Hospital, Clinic of Medical Oncology, Ankara, Türkiye
[2]Ankara Bilkent City Hospital, Clinic of Orthopaedics and Traumatology, Ankara, Türkiye

ABSTRACT

Abiraterone acetate (AA) is an inhibitor of cytochrome P450c17 that suppresses androgen synthesis from steroid precursors. Prednisone (P) is coadministered with AA to correct the glucocorticoid deficiency resulting from AA-induced alterations in steroid synthesis and to suppress excessive mineralocorticoid effects. We report bilateral avascular necrosis of the femoral head in a patient treated with AA+P; this condition is usually seen with long-term, high-dose glucocorticoid use. A 54-year-old male patient was diagnosed with castration-resistant metastatic prostatic adenocarcinoma (Gleason score 4+5). Following progression on androgen deprivation therapy+docetaxel, AA+P treatment was initiated. During this treatment period, the patient was in remission for thirty months; later, he developed bilateral avascular necrosis of the femoral heads and was referred to orthopaedics. Core decompression surgery was performed on both femoral necks due to avascular necrosis. Management and outcome: AA+P treatment was not discontinued because of the highly successful results in treating prostate cancer, and the patient remains in remission while continuing this treatment. AA+P is a treatment for prostate cancer that inhibits androgen synthesis. Although P is administered in low doses to prevent abiraterone-induced reductions in glucocorticoid levels, serious glucocorticoid side effects may, in rare cases, develop in these patients. To our knowledge, this is the first report of such a side effect in the literature.

Keywords: Abiraterone; avascular necrosis; prednisone; prostate cancer

INTRODUCTION

Prostate cancer is the second most common cancer and the fifth leading cause of cancer-related death among men worldwide.[1] The risk of prostate cancer increases with age; incidence exceeds 60% in men older than 65 years.[2]

Firstly, in the Cougar Oncology (COU)-abiraterone acetate (AA)-301 study, longer overall survival (OS) was observed with AA than with placebo in patients with castration-resistant prostate cancer who had previously received docetaxel treatment.[3] Later, in the COU-AA-302 study, AA was tested against placebo in chemotherapy-naive patients, and both progression-free survival and OS were superior to those with placebo.[4] In the LATITUDE and STAMPEDE studies, androgen deprivation therapy (ADT) with AA plus prednisone (P) (AA+P) resulted in longer OS than ADT with placebo in patients with high-risk metastatic hormone-sensitive prostate cancer.[5,6] Since the results of these studies were reported, the use of abiraterone in the treatment of castration-naive metastatic prostate cancer has become widespread.

AA is a selective and irreversible inhibitor of cytochrome P450c17 (17α-hydroxylase/C17,20-lyase), an enzyme required for androgen biosynthesis. This inhibits the synthesis of testosterone precursors such as dehydroepiandrosterone and androstenedione, as well as glucocorticoids, since this enzyme is also involved in their synthesis. As a result of relatively increased mineralocorticoid activity, side effects such as hypertension, hyperkalemia, and edema occur.[5] P is administered to correct the glucocorticoid deficiency resulting from abiraterone-induced changes in steroid synthesis and to suppress excessive mineralocorticoid effects.[7]

Correspondence: Serhat SEKMEK MD,
Ankara Bilkent City Hospital, Clinic of Medical Oncology, Ankara, Türkiye
E-mail: serhatsekmek@gmail.com
ORCID ID: orcid.org/0000-0003-4650-248X

Received: 14.07.2025 **Accepted:** 19.12.2025 **Epub:** 22.01.2026 **Publication Date:** 18.03.2026

Cite this article as: Sekmek S, Özkurt B, Mehtiyev M, Bal Ö, Algın E. Abiraterone acetate plus prednisone induced bilateral avascular necrosis of the femoral head. J Oncol Sci. 2026;12(1):94-7

Available at journalofoncology.org

Since P is used in physiological doses to replace deficiencies, glucocorticoid-related side effects are not expected. This case report describes bilateral avascular necrosis of the femoral head —a condition usually seen with long-term, high-dose glucocorticoid use— in a patient treated with AA+P. Informed consent was obtained from the patient and the patient's family for publication of the case report.

CASE REPORT

A 54-year-old man with no prior medical history was admitted to the department of urology, presenting with intermittent haematuria and dysuria for approximately one year. In August 2020, the prostate-specific antigen (PSA) level was 10.57 ng/mL; a 12-quadrant prostate biopsy was performed, and Gleason 4+5 prostatic adenocarcinoma was diagnosed in all 12 quadrants. No visceral organ metastases were detected on the computed tomography (CT) scan for staging. Whole-body bone scintigraphy showed increased osteoblastic activity in the posterior aspect of the right ninth rib, suspicious for metastasis. Subsequently, prostate-specific membrane antigen (PSMA) positron emission tomography (PET)-CT revealed no bone metastases; however, the patient was referred to the oncology department due to diffuse involvement of the prostate gland and regional lymph nodes. Radiotherapy was considered inappropriate for the patient with diffuse lymph node involvement because of the high risk of toxicity. Treatment with ADT (leuprolide 225 mg every three months) plus docetaxel (75 mg/m^2 every three weeks) was then planned. After four cycles of docetaxel treatment, the patient's PSA decreased to 2.5 and testosterone level to; however, PSMA PET-CT revealed new bone metastasis in the seventh thoracic vertebra (T7) and new paraaortic and parailiac lymph nodes, findings that were not considered oligoprogression. Due to radiological progression, he was assessed as having castration-resistant metastatic prostate cancer. In February 2021, docetaxel was discontinued, and AA (four tablets of 250 mg daily) plus P (5 mg twice daily) treatment was initiated. The PSA level decreased to 0.1 ng/mL during AA+P+ADT treatment. In the first month of treatment, the patient experienced grade 1 elevations in liver function tests and grade 1 fatigue. These side effects sometimes improved during treatment and sometimes relapsed, but did not progress. PSMA PET-CT showed a near-complete response in the T7 lesion and a partial response in the lymph nodes; the current treatment was continued. He began complaining of severe bilateral hip pain in August 2023. When the patient's pain was evaluated using the visual analogue scale, he rated it 8 out of 10 (very severe). The patient reported that he had difficulty even performing his daily activities due to pain and that his quality of life was impaired. The patient did not require orthopaedic aids for ambulation. The patient was not taking any medications other than prostate cancer treatments when he experienced this pain. No increase in PSA levels was detected. Laboratory values showed normal calcium levels, and bone mineral density measurement showed no osteoporosis. The patient had an orthopaedic consultation, and magnetic resonance imaging of the hip revealed no findings compatible with metastasis but showed degenerative bone changes, millimetric bone infarcts, effusion, and areas of bone marrow edema compatible with bilateral femoral head avascular necrosis (Figures 1, 2). The patient was evaluated by the tumour board, which decided to perform orthopaedic surgery for avascular necrosis. Core-decompression surgery was performed on the left femoral neck in September 2023 and on the right femoral neck in December 2023. Pathology results did not show any findings compatible with malignancy. AA+P treatment was not discontinued due to the highly successful results obtained in the treatment of prostate cancer and the patient is still in remission under this treatment. The adverse event developed after the patient started abiraterone (2 points); no other cause that could have

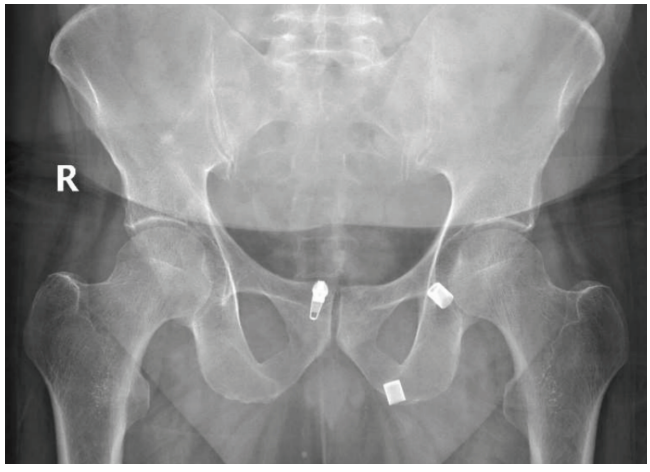

FIGURE 1: Pelvic X-ray of the patient.

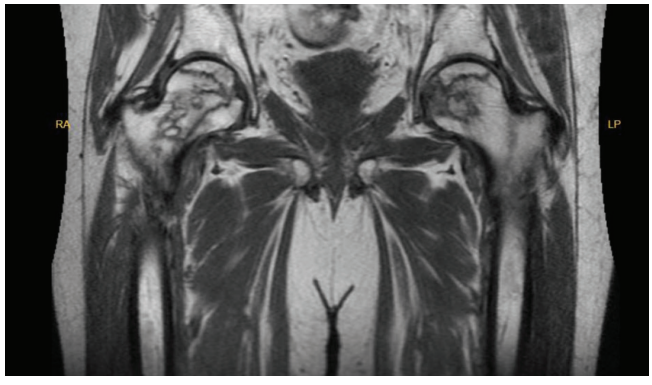

FIGURE 2: Pelvic magnetic resonance imaging of the patient.

led to this situation was identified (2 points); and the adverse event was objectively confirmed by imaging methods (1 point). The Naranjo Adverse Drug Reaction Probability scale score was calculated to be 5 in this case, indicating a probable association between this side effect and the drug (Figure 3). This side effect has not been reported to any local supervisory board or the pharmaceutical manufacturer.

DISCUSSION

AA is an androgen synthesis inhibitor used in the treatment of prostate cancer. In this case report, we describe the development of bilateral avascular necrosis of the femoral heads in a patient receiving abiraterone. To our knowledge, this is the first case in the literature of this association.

The most frequently observed side effects related to AA treatment are hypertension and hyperkalaemia. These side effects are due to abiraterone's inhibition of cytochrome P-450c17, which reduces both glucocorticoid and androgen synthesis, and to the consequent loss of negative feedback on adrenocorticotrophic hormone (ACTH), leading to increased ACTH secretion that stimulates mineralocorticoid synthesis in the adrenal glands. ACTH can be restored to its normal rhythm by physiological steroid replacement. This results in regularisation of mineralocorticoid synthesis and resolution of AA-related side effects.[8,9] To prevent these side effects related to the drug's mechanism of action, AA must be used in combination with physiological doses of cortisone.

Avascular necrosis of the femoral head may develop in patients receiving glucocorticoid therapy, depending on patients' comorbidities, the dose, and the duration of therapy. A meta-analysis showed that the risk of avascular necrosis increased by 3.6% per 10 mg/kg increase in glucocorticoid dose, particularly at doses higher than 20 mg/day.[10] In contrast, another study of 98,380 patients reported a 0.13% risk of avascular necrosis among patients receiving less than 15 mg of methylprednisolone daily.[11]

Patients using AA+P are not expected to experience side effects from physiological doses of glucocorticoids, which are

Adverse Drug Reaction Probability Scale

Question	Yes	No	Do Not Know	Score
1. Are there previous conclusive reports on this reaction?	+1	0	0	
2. Did the adverse event appear after the suspected drug was administered?	+2	-1	0	
3. Did the adverse event improve when the drug was discontinued or a specific antagonist was administered?	+1	0	0	
4. Did the adverse event reappear when the drug was readministered?	+2	-1	0	
5. Are there alternative causes that could on their own have caused the reaction?	-1	+2	0	
6. Did the reaction reappear when a placebo was given?	-1	+1	0	
7. Was the drug detected in blood or other fluids in concentrations known to be toxic?	+1	0	0	
8. Was the reaction more severe when the dose was increased or less severe when the dose was decreased?	+1	0	0	
9. Did the patient have a similar reaction to the same or similar drugs in any previous exposure?	+1	0	0	
10. Was the adverse event confirmed by any objective evidence?	+1	0	0	
	Total Score:			

Naranjo Algorithm - ADR Probability Scale

Score	Interpretation of Scores
Total Score ≥9	**Definite**. The reaction (1) followed a reasonable temporal sequence after a drug or in which a toxic drug level had been established in body fluids or tissues, (2) followed a recognized response to the suspected drug, and (3) was confirmed by improvement on withdrawing the drug and reappeared on reexposure.
Total Score 5 to 8	**Probable**. The reaction (1) followed a reasonable temporal sequence after a drug, (2) followed a recognized response to the suspected drug, (3) was confirmed by withdrawal but not by exposure to the drug, and (4) could not be reasonably explained by the known characteristics of the patient's clinical state.
Total Score 1 to 4	**Possible**. The reaction (1) followed a temporal sequence after a drug, (2) possibly followed a recognized pattern to the suspected drug, and (3) could be explained by characteristics of the patient's disease.
Total Score ≤0	**Doubtful**. The reaction was likely related to factors other than a drug.

FIGURE 3: Narenjo adverse drug reaction probability scale.

administered to replace the deficiency. However, in our case, bilateral avascular necrosis of the femoral head developed in a patient receiving AA+P treatment, who required surgical intervention. Other possible etiologies of avascular necrosis include alcohol addiction, rheumatological diseases such as systemic lupus erythematosus, genetic diseases such as sickle cell anaemia, and trauma.[12-14] Since our patient did not have any of these causes, and avascular necrosis occurred following administration of AA+P, we consider that this side effect is related to AA+P treatment. To our knowledge, our case is the first reported in the literature on this subject.

The conditions caused by hypercortisolemia are well known, and reports of hypercortisolemia and hypercortisolemia-related serious side effects in patients receiving AA+P treatment are very rare in the literature. Given the mechanism of action, studies and case reports have investigated the efficacy of AA in adrenocortical cell culture models and in the treatment of Cushing's syndrome.[15,16]

CONCLUSION

AA+P is a treatment used in prostate cancer and inhibits androgen synthesis. Although P treatment is in low doses and is used to prevent abiraterone-induced low glucocorticoid levels, serious glucocorticoid side effects may develop in these patients, in rare cases. Therefore, patients receiving AA+P treatment should be cautious about possible side effects.

Ethics

Informed Consent: Informed consent was obtained from the patient and the patient's family for publication of the case report.

Footnotes

Authorship Contributions

Surgical and Medical Practices: S.S., B.Ö., Concept: S.S., Ö.B., E.A., Design: S.S., E.A., Data Collection or Processing: S.S., B.Ö., M.M., Ö.B., E.A., Analysis or Interpretation: S.S., M.M., Literature Search: S.S., E.A., Writing: S.S.

Conflict of Interest: No conflict of interest was declared by the authors.

Financial Disclosure: The authors declared that this study received no financial support.

REFERENCES

1. Bray F, Laversanne M, Sung H, et al. Global cancer statistics 2022: GLOBOCAN estimates of incidence and mortality worldwide for 36 cancers in 185 countries. CA Cancer J Clin. 2024;74(3):229-263. [Crossref] [PubMed]
2. Sahoo CK, Sahoo NK, Sahu M, Gupta J. Liposomes for the treatment of prostate cancer therapy: a review. Cancer Treat Res Commun. 2024;39:100792. [Crossref] [PubMed]
3. de Bono JS, Logothetis CJ, Molina A, et al; COU-AA-301 Investigators. Abiraterone and increased survival in metastatic prostate cancer. N Engl J Med. 2011;364(21):1995-2005. [Crossref] [PubMed] [PMC]
4. Ryan CJ, Smith MR, de Bono JS, et al; COU-AA-302 Investigators. Abiraterone in metastatic prostate cancer without previous chemotherapy. N Engl J Med. 2013;368(2):138-148. Erratum in: N Engl J Med. 2013;368(6):584. [Crossref] [PubMed] [PMC]
5. Chi KN, Protheroe A, Rodríguez-Antolín A, et al. Patient-reported outcomes following abiraterone acetate plus prednisone added to androgen deprivation therapy in patients with newly diagnosed metastatic castration-naive prostate cancer (LATITUDE): an international, randomised phase 3 trial. Lancet Oncol. 2018;19(2):194-206. [Crossref] [PubMed]
6. James ND, de Bono JS, Spears MR, et al; STAMPEDE Investigators. Abiraterone for prostate cancer not previously treated with hormone therapy. N Engl J Med. 2017;377(4):338-351. [Crossref] [PubMed] [PMC]
7. Attard G, Merseburger AS, Arlt W, et al. Assessment of the safety of glucocorticoid regimens in combination with abiraterone acetate for metastatic castration-resistant prostate cancer: a randomized, open-label phase 2 study. JAMA Oncol. 2019;5(8):1159-1167. [Crossref]
8. Attard G, Reid AH, Yap TA, et al. Phase I clinical trial of a selective inhibitor of CYP17, abiraterone acetate, confirms that castration-resistant prostate cancer commonly remains hormone driven. J Clin Oncol. 2008;26(28):4563-4571. Erratum in: J Clin Oncol. 2012;30(15):1896. [Crossref] [PubMed]
9. Taplin ME, Montgomery B, Logothetis CJ, et al. Intense androgen-deprivation therapy with abiraterone acetate plus leuprolide acetate in patients with localized high-risk prostate cancer: results of a randomized phase II neoadjuvant study. J Clin Oncol. 2014;32(33):3705-3715. [Crossref] [PubMed] [PMC]
10. Mont MA, Pivec R, Banerjee S, Issa K, Elmallah RK, Jones LC. High-dose corticosteroid use and risk of hip osteonecrosis: meta-analysis and systematic literature review. J Arthroplasty. 2015;30(9):1506-1512.e5. [Crossref] [PubMed] [PMC]
11. Dilisio MF. Osteonecrosis following short-term, low-dose oral corticosteroids: a population-based study of 24 million patients. Orthopedics. 2014;37(7):e631-e636. [Crossref] [PubMed]
12. Fukushima W, Fujioka M, Kubo T, Tamakoshi A, Nagai M, Hirota Y. Nationwide epidemiologic survey of idiopathic osteonecrosis of the femoral head. Clin Orthop Relat Res. 2010;468(10):2715-2724. [Crossref] [PubMed] [PMC]
13. Slobogean GP, Sprague SA, Scott T, Bhandari M. Complications following young femoral neck fractures. Injury. 2015;46(3):484-491. [Crossref] [PubMed]
14. Adesina O, Brunson A, Keegan THM, Wun T. Osteonecrosis of the femoral head in sickle cell disease: prevalence, comorbidities, and surgical outcomes in California. Blood Adv. 2017;1(16):1287-1295. [Crossref] [PubMed] [PMC]
15. Sanders K, de Wit WL, Mol JA, et al. Abiraterone acetate for cushing syndrome: study in a canine primary adrenocortical cell culture model. Endocrinology. 2018;159(11):3689-3698. [Crossref] [PubMed]
16. Chacko R, Abdel-Razeq NH, Abu Rous F, Loutfi R. Abiraterone acetate for treatment of ectopic Cushing syndrome caused by ACTH-producing neuroendocrine tumor: a case report. J Gastrointest Oncol. 2022;13(5):2626-2632. [Crossref] [PubMed] [PMC]

CASE REPORT

DOI: 10.37047/jos.galenos.2025.2025-10-2

J Oncol Sci 2026;12(1):98-102

Diffuse Infiltration of both Breasts in Pregnant Women is the First Manifestation of Myeloid Sarcoma - A Case Report and Literature Review

Wei YANG[1], Chendong HE[2]

[1]Jiangsu Province Hospital of Chinese Medicine & Affiliated Hospital of Nanjing University of Chinese Medicine, Department of Radiology, Nanjing, China
[2]Nanjing Hospital of Chinese Medicine Affiliated to Nanjing University of Chinese Medicine, Department of Radiology, Nanjing, China

ABSTRACT

Myeloid sarcoma (MS) during pregnancy is rare, and cases initially presenting as bilateral breast infiltration are particularly misleading and difficult to diagnose. It is essential to differentiate MS from conditions such as mammary hyperplasia and breast cancer. We report a case of a 28-year-old woman who developed bilateral breast induration, distension, and serous discharge at seven months' gestation. The final diagnosis was MS secondary to acute myeloid leukemia. The patient is currently undergoing chemotherapy. Clinicians should increase their awareness of MS and, when necessary, recommend hematological and bone marrow cytomorphological examinations for pregnant women presenting with suspicious breast symptoms to ensure early diagnosis.

Keywords: Pregnancy; myeloid sarcoma; breast mass; acute myeloid leukemia; diagnosis

INTRODUCTION

Myeloid sarcoma (MS) is a malignant tumor composed of immature myeloid cells that forms a solid mass outside the bone marrow and disrupts the native tissue architecture. It is also known as extramedullary myeloid tumor, granulocytic sarcoma, or chloroma. MS can occur in any part of the body and typically manifests with symptoms of tissue infiltration and compression at the affected site. It most commonly involves the skin, lymph nodes, soft tissues, bones, and testes.[1] Breast involvement is rare and usually unilateral[2,3] with bilateral cases are even more uncommon.[4] We report a rare case of bilateral MS in a pregnant woman in whom diagnosis and treatment were delayed because of her pregnancy.

CASE REPORT

A 28-year-old pregnant woman presented to a local hospital at 7 months' gestation with bilateral breast swelling and clear discharge. The ultrasound finding was considered to represent a pregnancy-related breast secretion reaction and was not investigated further. After natural childbirth resulting in a healthy baby, she complained of persistent hardening and swelling of both breasts and clear nipple discharge. The patient was transferred to our hospital for further treatment.

Magnetic resonance imaging showed that both breasts appeared full, with diffuse hyperintensity on T2-weighted fat-suppressed imaging, high signal intensity on diffusion-weighted imaging, and low signal intensity on the apparent diffusion coefficient map. Contrast enhancement

Correspondence: Chendong HE MD,
Nanjing Hospital of Chinese Medicine Affiliated to Nanjing University of Chinese Medicine, Department of Radiology, Nanjing, China
E-mail: hcd1222@163.com
ORCID ID: orcid.org/0000-0002-2216-7245

Received: 06.10.2025 **Accepted:** 28.12.2025 **Epub:** 22.01.2026 **Publication Date:** 18.03.2026

Cite this article as: Yang W, He C. Diffuse infiltration of both breasts in pregnant women is the first manifestation of myeloid sarcoma - a case report and literature review. J Oncol Sci. 2026;12(1):98-102

Available at journalofoncology.org

was heterogeneous, with nodular thickening of the skin and areolae bilaterally (Figure 1). 18F- fluorodeoxyglucose positron emission tomography-computed tomography (CT) showed that both breasts were enlarged, with mass-like soft-tissue densities present. The radiotracer uptake is diffusely increased and heterogeneous, with an maximum standardized uptake value of 7.4. In addition, increased radiotracer uptake in bone and muscle was observed at multiple sites throughout the body. The imaging diagnosis was malignant breast cancer with multiple bone marrow metastases and multiple soft-tissue metastases (including muscle) throughout the body (Figure 2).

Hematological analysis showed a white blood cell count of 4.62×10^9/L, a red blood cell count of 5.13×10^{12}/L, hemoglobin concentration of 141 g/L, and a platelet count of 302×10^9/L. Differential counts revealed neutrophils at 32.1%, lymphocytes at 49.2%, and monocytes at 17.4%. The D-dimer level was 1.69 mg/L. Coagulation tests showed a prothrombin time of 12.9 seconds and an international normalized ratio of 0.99. Serum lactate dehydrogenase and uric acid were elevated, at 566 U/L and 496 μmol/L, respectively.

Bone marrow aspiration demonstrated that blasts comprised 58.1% of cells and were characterized by weak CD45 expression and low side scatter. Immunophenotyping showed expression of stem/progenitor and myeloid markers (HLA-DR, CD38, CD34, CD33, CD15, MPO) as well as B-cell markers (CD19, CD22, CD79a). CD10, CD20, CD13, and CD117 were not expressed. Bone marrow cellularity was markedly increased, with granulocytic, erythroid, and lymphocytic lineages accounting for 73.5%, 1.5%, and 25.0%, respectively, all showing normal morphology. Blasts constituted 65.0%, and the peroxidase positivity was 22.0%.

To confirm the diagnosis, a breast biopsy was performed under local anesthesia. Histopathological examination revealed diffuse infiltration by tumor cells. Immunohistochemical staining showed the following profile: CD3 (–), CD5 (–), CD20 (–), CD79a (–), CD21 (–), Ki-67 (75%+), BCL-6 (60%+), MUM1 (+), BCL-2 (+++), p53 (50%+), MPO (+++), CD43 (+++), CK (–), and EMA (+). Based on these findings, a diagnosis of MS was considered.

The patient received the IA chemotherapy regimen, comprising idarubicin (17 mg, intravenous infusion, days 1-3) and cytarabine (0.17 g, intravenous infusion, days 1-7), along with alkalization, hydration, antiemetic therapy, and gastric-protective measures. On June 26, 2023, a follow-up bone marrow examination showed a blast cell percentage of 2.0%. Blood cell analysis results were as follows: white blood cell count, 3.28×10^9/L; red blood cell count, 3.76×10^{12}/L; hemoglobin, 99 g/L; platelet count, 68×10^9/L; lymphocyte percentage, 40.9%; and absolute neutrophil count, 1.79×10^9/L.

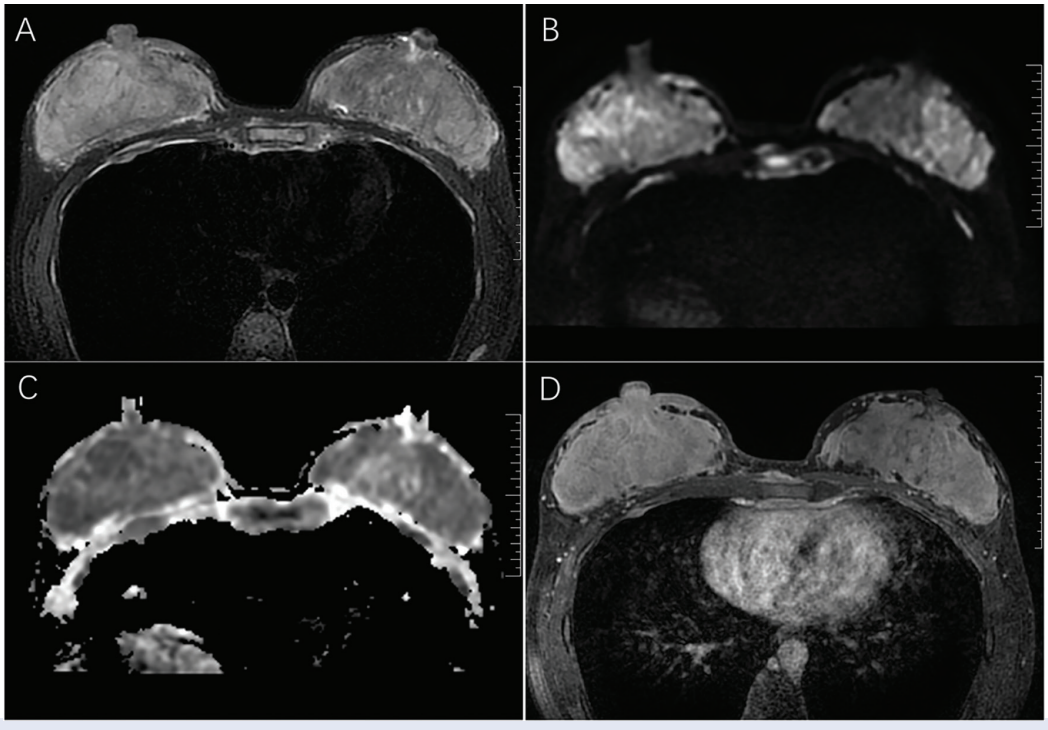

FIGURE 1: Breast magnetic resonance imaging examination, (A) T2-weighted fat-suppressed imaging shows diffuse high signal intensity in both breasts, (B) Diffusion-weighted imaging shows diffuse high signal intensity in both breasts, (C) The apparent diffusion coefficient map shows reduced signal intensity in both breasts, (D) Post-contrast imaging demonstrates heterogeneous enhancement, with skin thickening and enhancement in both breasts.

As the patient's blood parameters gradually recovered, they were discharged. Follow-up CT scans performed on July 7, 2023 (Figure 3A) and October 12, 2023 (Figure 3B) revealed a significant reduction in the breast mass.

DISCUSSION

MS commonly occurs secondary to hematologic malignancies, such as acute myeloid leukemia (AML), blast crisis of chronic myeloid leukemia, and myelodysplastic syndromes. MS can be categorized into two major types: leukemic MS - which includes extramedullary infiltration in AML or relapse following complete remission of AML. Isolated MS characterized by a solitary solid mass without accompanying bone marrow involvement.

The clinical manifestations of MS are non-specific, with initial symptoms primarily caused by mass effect and compression. MS can occur at any age and in various anatomical locations, but cases of AML with multisite

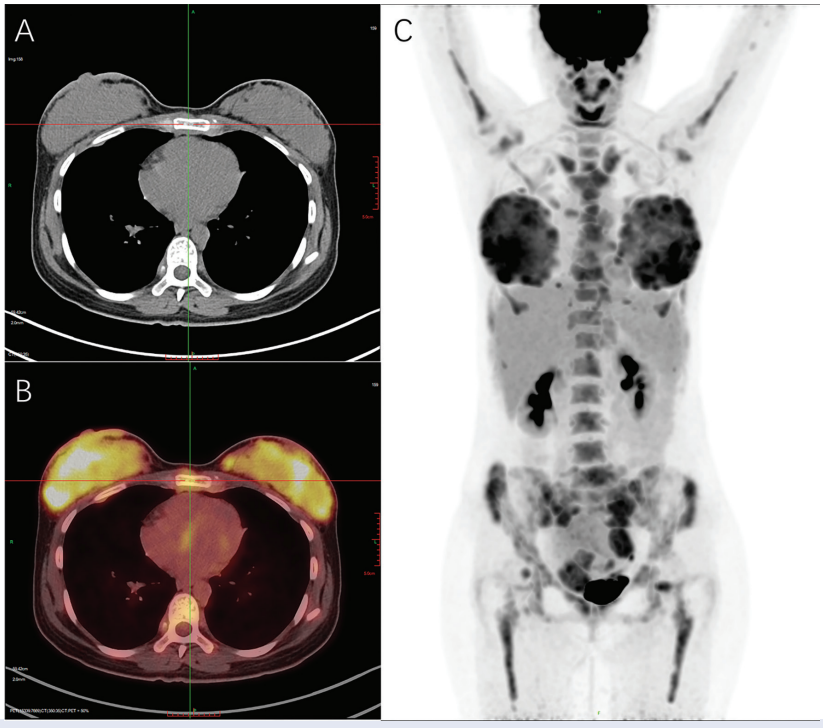

FIGURE 2: F-18 FDG PET-CT findings, (A) CT images show bilateral, dense, and full breast tissue with skin thickening, (B) PET images reveal diffusely increased but uneven radiotracer uptake in both breasts, with an SUV_{max} of 7.4, (C) Coronal maximum-intensity projection images demonstrate widespread systemic metastases.

PET: Positron emission tomography; CT: Computed tomography; FDG: Fluorodeoxyglucose; SUV: Standardized uptake value

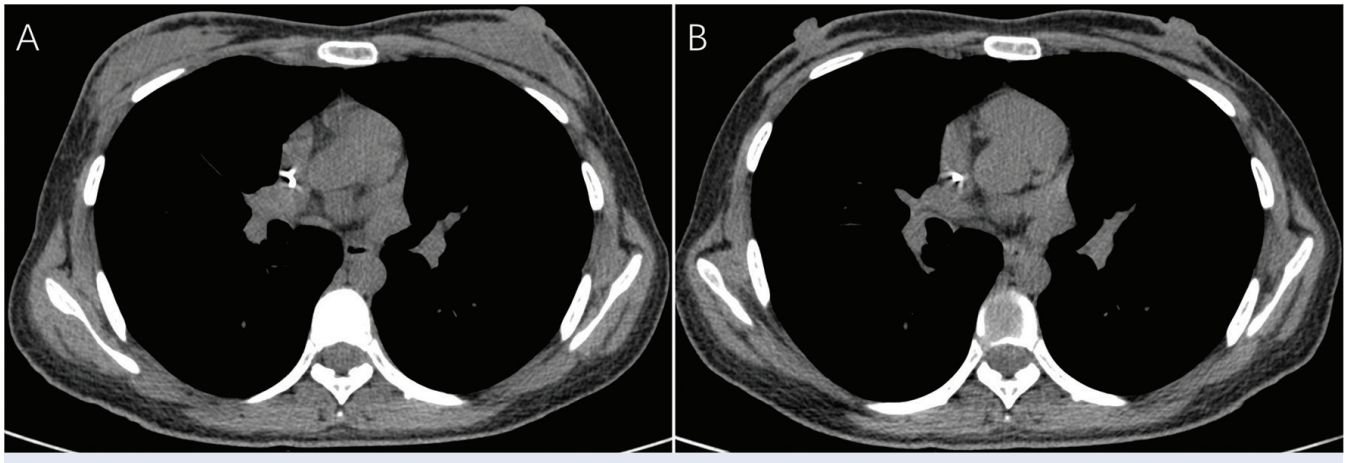

FIGURE 3: Post-treatment follow-up computed tomopraphy findings, (A) The computed tomography image reveals dense bilateral breast tissue and mild thickening of the skin, (B) The breast masses have mostly resolved.

systemic MS are extremely rare and are associated with a poor prognosis, as reported in the literature. Diagnosing MS in patients with a known history of AML is relatively straightforward. However, diagnosis of primary MS remains challenging, with an initial misdiagnosis rate of 75%, most commonly misdiagnosed as large-cell lymphoma. Advances in cytogenetic analysis, immunohistochemistry, flow cytometry, and fluorescence in situ hybridization have reduced the misdiagnosis rate to 25%-47%, although it remains high.[5] In this case, the patient presented with a breast mass and was initially misdiagnosed with breast cancer. Further investigation revealed the involvement of the pancreas, bone marrow, pleura, and multiple muscle and soft-tissue sites throughout the body. The definitive diagnosis was established through pathological and immunohistochemical analysis.

Histopathological examination of biopsy specimens is crucial for diagnosing MS. Morphologically, MS is characterized by myeloid cell infiltration and can be classified, based on cell origin, as granulocytic sarcoma, primitive monocytic sarcoma, or trilineage hematopoietic MS. Additionally, based on the degree of cell differentiation, MS can be categorized into blastic, immature, and differentiated subtypes. Immunohistochemical staining plays a vital role in assisting the diagnosis of MS. The most commonly expressed antigens in MS are MPO, CD34, CD43, CD45, CD56, CD68, CD117, and lysozyme; CD11, CD13, and CD33 are also frequently expressed. Among these, CD43 and lysozyme are the most sensitive markers, showing nearly 100% positivity.[5] MPO has a positive expression rate ranging from 66% to 96% and exhibits a characteristic green appearance when exposed to air.[5-7] However, some MS cases may abnormally express B-cell or T-cell markers, leading to misdiagnoses such as diffuse large B-cell lymphoma, peripheral T-cell lymphoma, or small lymphocytic lymphoma. A high Ki-67 index (typically >60%) is also common in MS. In this case, MPO, CD34, and Ki-67 were strongly positive, whereas CD3, CD5, CD20, CD79a, and CD21 were negative, ruling out B- and T-cell origins. Together with bone marrow aspiration and hematological analysis, these findings confirmed the diagnosis of MS.

Common chromosomal abnormalities in MS include MLL rearrangements, t(8;21), inv(16), and monosomies. Among genetic mutations in MS8, NPM1 is the most frequently mutated gene. Other reported cytogenetic abnormalities include the translocations t(9;11), t(8;17), t(8;16), and t(1;11), and the deletion 16q.[1,5] The clinical presentation of MS is closely linked to molecular abnormalities. Orbital MS in children is often associated with t(8;21), whereas inv(16) is related to extramedullary disease in AML, which is associated with a higher incidence of gastrointestinal and breast MS.[7-9]

MS during pregnancy poses a diagnostic challenge. During pregnancy, Cases involving the cervix, spinal cord, and stomach have been reported in which compression symptoms at the affected sites were the initial presentation.[10-12] Breast MS typically exhibits a diffuse or single-cell infiltrative growth pattern and can be classified, based on cellular differentiation5, into mature, immature, or blastic subtypes. Its single-cell infiltration pattern may mimic invasive lobular carcinoma, but MS usually does not disrupt the ductal and lobular structures of the breast. Immunohistochemistry is crucial for differentiating between these conditions.[13] Breast MS is primarily treated with chemotherapy and radiotherapy; in some cases, stem-cell transplantation may be considered. The prognosis is generally poor, making early and accurate diagnosis essential for timely and intensified treatment, which may improve long-term survival and the potential for cure.

CONCLUSION

MS presenting as bilateral breast masses is extremely rare. In pregnant women, physiological breast changes can obscure symptoms, making misdiagnosis highly likely, most commonly as mastitis, hyperplasia, breast cancer, or breast lymphoma. In patients presenting with breast masses, particularly those with suspected myeloid leukemia, MS should be considered in the differential diagnosis. Early histopathological examination and immunohistochemical analysis are recommended to establish a definitive diagnosis and to avoid treatment delays. We obtained the patient's consent.

Ethics

Informed Consent: Informed consent was obtained.

Footnotes

Authorship Contributions

Concept: W.Y., C.H., Data Collection or Processing: W.Y., Analysis or Interpretation: W.Y., C.H., Literature Search: F W.Y., C.H., Writing: W.Y.

Conflict of Interest: No conflict of interest was declared by the authors.

Financial Disclosure: The authors declared that this study received no financial support.

REFERENCES

1. Huang C, Fei S, Yao J, et al. Breast myeloid sarcoma presenting as a palpable breast lump after allogeneic stem cell transplantation for acute myelomonocytic leukemia: a rare case report. World J Surg Oncol. 2021;19(1):289. [Crossref] [PubMed] [PMC]
2. Ding Y, Xi D, Chen Y, Gu W. Myeloid sarcoma of the breast as a first manifestation of acute myeloid leukemia: a case report. Asian J Surg. 2022;45(8):1622-1623. [Crossref] [PubMed]

3. Nicosia L, Latronico A, Farina M, et al. Myeloid sarcoma of the breast: a pathology that should not be forgotten. Ecancermedicalscience. 2020;14:1160. [Crossref] [PubMed] [PMC]
4. Ozsoy A, Akdal Dolek B, Barca N, Aktas H, Araz L, Kulacoglu S. Ultrasound findings in a case of myeloid sarcoma of the breast. J Belg Soc Radiol. 2016;100(1):15. [Crossref] [PubMed] [PMC]
5. Magdy M, Abdel Karim N, Eldessouki I, Gaber O, Rahouma M, Ghareeb M. Myeloid sarcoma. Oncol Res Treat. 2019;42(4):224-229. [Crossref] [PubMed]
6. Chiu AM, Yoon JG, Tirumani SH, Ramaiya NH, Smith DA. Myeloid sarcoma: a primer for radiologists. J Comput Assist Tomogr. 2023;47(3):475-484. [Crossref] [PubMed]
7. Almond LM, Charalampakis M, Ford SJ, Gourevitch D, Desai A. Myeloid sarcoma: presentation, diagnosis, and treatment. Clin Lymphoma Myeloma Leuk. 2017;17(5):263-267. [Crossref] [PubMed]
8. Fu L, Zhang Z, Chen Z, Fu J, Hong P, Feng W. Gene mutations and targeted therapies of myeloid sarcoma. Curr Treat Options Oncol. 2023;24(4):338-352. [Crossref] [PubMed]
9. Ramia de Cap M, Chen W. Myeloid sarcoma: an overview. Semin Diagn Pathol. 2023;40(3):129-139. [Crossref] [PubMed]
10. Al-Sobhi EM, Jeha TM, Al-Taher MI. Granulocytic sarcoma causing cord compression in a pregnant woman with acute myeloid leukemia and t(8;21). Saudi Med J. 2008;29(11):1658-1661. [Crossref] [PubMed]
11. Gill H, Loong F, Mak V, Chan K, Au WY, Kwong YL. Myeloid sarcoma of the uterine cervix presenting as missed abortion. Arch Gynecol Obstet. 2012;286(5):1339-1341. [Crossref] [PubMed] [PMC]
12. Sekaran A, Darisetty S, Lakhtakia S, Ramchandani M, Reddy DN. Granulocytic sarcoma of the stomach presenting as dysphagia during pregnancy. Case Rep Gastrointest Med. 2011;2011:627549. [Crossref] [PubMed] [PMC]
13. Amiraian D, McDonough M, Geiger X. Bilateral myeloid sarcoma of the breast: a case report with radiological and pathological correlation. Cureus. 2022;14(5):e24731. [Crossref] [PubMed] [PMC]

CASE REPORT

DOI: 10.37047/jos.galenos.2026.2025-7-10

J Oncol Sci 2026;12(1):103-10

Unveiling the Uncommon: A Comprehensive Review and Case Report on Targeting Rare MET Fusions in NSCLC

Harun MUĞLU, Jamshid HAMDARD, Banu KARAALİOĞLU, Erdem SÜNGER, Mehmet Haluk YÜCEL, Ebru ENGİN DELİPOYRAZ, Ömer Fatih ÖLMEZ

İstanbul Medipol University Faculty of Medicine, Department of Medical Oncology, İstanbul, Türkiye

ABSTRACT

Advancements in molecular diagnostics and targeted therapies have significantly transformed the management of non-small cell lung cancer (NSCLC). Rare mesenchymal-epithelial transition (MET) rearrangements, including novel fusions such as human leukocyte antigen (HLA)-DRB1-MET and HLA-DQB2-MET, represent actionable genetic alterations with critical therapeutic implications. This review synthesizes findings from multiple case reports to highlight the efficacy of MET tyrosine kinase inhibitors (TKIs) in MET-driven oncogenesis. A literature review of published case reports and studies on MET rearrangements in NSCLC was conducted. Data were analyzed to assess the clinical outcomes of patients treated with MET TKIs, such as crizotinib and tepotinib. Additionally, our case report demonstrates the utility of comprehensive next-generation sequencing (NGS) in identifying rare MET fusions and guiding personalized treatment strategies. Our case illustrates the potential of NGS to detect rare MET fusions, thereby enabling durable disease control with crizotinib. Comparative analyses indicate the necessity of individualized treatment approaches, particularly in cases with central nervous system involvement and a prior treatment history. The review further emphasizes that MET alterations are more frequently identified in never-smoking female patients, in whom driver mutation detection rates exceed 60%. Precision oncology plays a pivotal role in addressing rare MET rearrangements in NSCLC. Despite advancements, challenges persist in early identification, therapeutic sequencing, and access to advanced diagnostics. Collaborative efforts among researchers, clinicians, and policymakers are crucial to refining treatment strategies and improving patient outcomes.

Keywords: Non-small cell lung cancer; MET rearrangements; tyrosine kinase inhibitors; HLA-DRB1-MET fusion; precision oncology

INTRODUCTION

Lung cancer is a leading cause of cancer-related mortality worldwide, responsible for approximately 1.8 million deaths annually. Non-small cell lung cancer (NSCLC) accounts for approximately 85% of all lung cancer cases, with adenocarcinoma being the most common histologic subtype.[1] Advances in molecular profiling, particularly next-generation sequencing (NGS), have significantly reshaped the diagnostic and therapeutic landscape of NSCLC. The mesenchymal-epithelial transition (MET) proto-oncogene encodes a transmembrane receptor tyrosine kinase that plays a critical role in regulating cell growth, survival, and motility.[2] Among the actionable mutations, those alterations affecting the MET proto-oncogene have garnered significant attention due to their oncogenic potential and therapeutic implications. Aberrations such as MET exon 14-skipping mutations, amplifications, and fusions result in constitutive activation of the MET signaling pathway, contributing to tumor progression.[3] MET fusions, although rare and accounting for approximately 0.5% of NSCLC cases, frequently involve novel partners such as human leukocyte antigen (HLA)-DRB1 and HLA-DQB2. These partners retain the MET kinase domain and drive oncogenesis through ligand-independent dimerization and activation.[4] Recent findings underscore the mounting importance of MET fusions in various malignancies, including NSCLC. These rare structural rearrangements have also been

Correspondence: Harun MUĞLU MD,
İstanbul Medipol University Faculty of Medicine, Department of Medical Oncology, İstanbul, Türkiye

E-mail: hm1635@hotmail.com

ORCID ID: orcid.org/0000-0001-9584-0827

Received: 30.07.2025 **Accepted:** 07.01.2026 **Epub:** 22.01.2026 **Publication Date:** 18.03.2026

Cite this article as: Muğlu H, Hamdard J, Karaalioğlu B, et al. Unveiling the uncommon: a comprehensive review and case report on targeting rare MET fusions in NSCLC. J Oncol Sci. 2026;12(1):103-10

Available at journalofoncology.org

identified in other tumor types. A notable example is that of a pediatric glioblastoma patient with a MET fusion who achieved a partial response to the MET inhibitor crizotinib, demonstrating the potential of targeted therapies in addressing such oncogenic drivers. This underscores the critical need for further research into the therapeutic landscape of MET fusions, especially given the promising, albeit preliminary, outcomes seen in early clinical cases.[5-7] Aberrant MET activation has also been associated with cancer cell proliferation and angiogenesis across different tumor types. Adenosine triphosphate (ATP)-competitive tyrosine kinase inhibitors (TKIs) have demonstrated antitumor activity in NSCLC patients with MET alterations, particularly in cases with MET exon 14 skipping mutations. However, the therapeutic impact of MET TKIs on more complex structural rearrangements, such as MET fusions, remains poorly understood and warrants further investigation.[8,9] Crizotinib has demonstrated favourable response rate in the treatment of lung adenocarcinomas harboring MET gene alterations. Additionally, other MET-targeting agents, including cabozantinib, savolitinib, capmatinib, and tepotinib, have shown therapeutic potential in this context.[10-12] In this review, we analyse a range of cases reported in the literature and emphasise a unique case at Medipol University involving an HLA-DRB1-MET fusion. This case exemplifies the role of molecular diagnostics in guiding targeted therapy decisions. Additionally, we aim to contextualize this case within the broader spectrum of MET rearrangements to provide a comprehensive understanding of their therapeutic implications.

Literature Search Strategy

A focused literature review was conducted to identify published case reports and case series describing MET gene rearrangements in NSCLC. The PubMed/MEDLINE and Scopus databases were searched for articles published from January 2010 to December 2024. The search strategy used combinations of the following keywords: "non-small cell lung cancer", "NSCLC", "MET fusion", "MET rearrangement", "HLA-DRB1-MET", "HLA-DQB2-MET", and "TKIs."

Articles were screened based on titles and abstracts, followed by full-text review when relevant. Studies were included if they reported clinical cases of NSCLC with confirmed *MET* gene rearrangements and provided molecular, therapeutic, and clinical outcome data. Reviews without original patient data, preclinical studies, and reports lacking sufficient clinical or molecular information were excluded. Reference lists of included articles were also manually reviewed to identify additional relevant publications.

Clinical Cases and Therapeutic Insights

Tepotinib in HLA-DRB1-MET Fusion-positive NSCLC (Blanc-Durand et al.[13])

A 41-year-old female patient diagnosed with stage IIIA NSCLC and subsequent brain metastases was found to harbor an *HLA-DRB1-MET* gene fusion. Initial treatment with cisplatin and vinblastine combined with radiotherapy resulted in a partial response, but the disease progressed within seven months, leading to brain, liver, and bone metastases. Molecular profiling identified the HLA-DRB1-MET fusion, and targeted therapy was initiated. Crizotinib was administered as first-line treatment, resulting in a complete response that lasted six months. However, disease progression occurred, manifesting as symptomatic cerebral metastases. Following disease progression, tepotinib was introduced as a second-line therapy. This resulted in a near-complete intracranial response and significant systemic disease control, which was maintained for nine months. Subsequently, cabozantinib was administered as the third-line therapy, further stabilizing the disease, preserving the patient's quality of life, and causing minimal adverse effects. This case underscores the significance of NGS in identifying actionable mutations and demonstrates the potential efficacy of tepotinib in managing NSCLC with central nervous system (CNS) involvement.[13]

Crizotinib in HLA-DRB1-MET Fusion-positive NSCLC (Davies et al.[4])

A 74-year-old female patient, who had never smoked, had a history of stage I lung adenocarcinoma, which was treated with a wedge resection of the right lower lobe. Nine years later, a new left upper lobe mass was detected; following lobectomy, the tumor was confirmed as stage II lung adenocarcinoma. Initial testing of the second tumor sample revealed no epidermal growth factor receptor (EGFR) mutations or anaplastic lymphoma kinase (ALK) rearrangements. Adjuvant chemotherapy was declined by the patient. Eighteen months later, surveillance imaging revealed multiple new lung lesions and nodal involvement, and a biopsy confirmed adenocarcinoma, morphologically similar to previous samples, without ALK or ROS1 rearrangements. After four cycles of carboplatin-pemetrexed followed by maintenance pemetrexed, the disease remained stable, but progressed slowly after treatment cessation, which was due to fatigue. Subsequent NGS of a resected tumor specimen identified a novel HLA-DRB1-MET fusion with MET exon 15. Crizotinib was initiated off-label, as the patient's tumor was negative for other actionable mutations [EGFR, kirsten rat sarcoma (KRAS), ALK, ROS1, rearranged during transfection]. Within

six weeks, the patient achieved a complete response, which was maintained for eight months with manageable side effects, including fatigue and mild hypokalemia. This case highlights the value of comprehensive NGS in uncovering rare actionable fusions, such as HLA-DRB1-MET, and demonstrates the efficacy of crizotinib as a targeted therapy for such patients.[4]

Crizotinib in HLA-DRB1-MET Fusion-positive NSCLC (Kunte and Stevenson[14])

A 59-year-old woman with a history of stage IA lung adenocarcinoma underwent radiation therapy for recurrent pleural-based nodules. Despite treatment, disease control was not achieved. Molecular profiling with NGS identified a rare *HLA-DRB1-MET* gene fusion. Pembrolizumab monotherapy was initiated, resulting in disease stabilization for eight months before progression occurred. Subsequently, crizotinib was introduced based on the molecular findings, leading to a rapid and significant reduction in pleural lesions. A complete radiographic response was achieved within four months. Crizotinib was well tolerated, with only mild, manageable side effects, including fatigue and nausea. This case illustrates the clinical value of NGS in identifying rare MET fusions and substantiates the efficacy of crizotinib as a targeted therapy for patients with these actionable alterations.[14]

Tepotinib in HLA-DQB2-MET Fusion-positive NSCLC (Dias E Silva et al.[15])

A 73-year-old female patient with advanced NSCLC (stage IVA) presented with a large left upper lobe mass, pleural effusion, and mediastinal lymph node involvement. Initial treatment with a combination of carboplatin, pemetrexed, and pembrolizumab resulted in temporary disease stabilization, but progression was noted following maintenance therapy. Molecular profiling via NGS identified a novel HLA-DQB2-MET fusion. Tepotinib, a selective MET inhibitor, was initiated at a dose of 450 mg daily. This treatment achieved significant tumor reduction and sustained disease control for over 12 months. Tepotinib was well tolerated, with no treatment-related adverse events reported.

These findings support the use of selective MET inhibitors, such as tepotinib, to manage rare MET fusion variants and emphasize the importance of comprehensive genomic testing in identifying actionable therapeutic targets.[15]

Sequential TKI Therapy in ALK-HLA-DRB1 Fusion-positive NSCLC (Gao et al.[16])

A 48-year-old female patient with advanced NSCLC presented with bilateral pulmonary nodules and mediastinal lymphadenopathy. Molecular profiling via NGS identified a rare ALK-HLA-DRB1 rearrangement that retains the kinase domain of ALK and drives oncogenesis. Crizotinib was administered as the patient's initial treatment, resulting in rapid clinical improvement and a substantial radiographic response. Disease control was maintained for six months. Due to economic constraints, the patient was transitioned to ceritinib, which further extended progression-free survival (PFS), resulting in 18 months of disease control. This case demonstrates the efficacy of sequential ALK TKI therapy in managing rare ALK rearrangements and highlights the critical role of precision oncology in improving outcomes for complex cases.[16]

Crizotinib in HLA-DRB1-MET Fusion-positive NSCLC: Our Experience

A 59-year-old female patient, a never-smoker, presented with complaints of persistent dry cough and mid-thoracic back pain lasting several weeks. She had no history of cancer and had only a diagnosis of hypertension, which was managed with amlodipine. No other chronic illness or ongoing medication use was reported. Her family history was negative for cancer or hereditary disorders, and she reported no significant psychosocial stressors. On physical examination, decreased breath sounds and dullness to percussion were noted in the left lower lung field. No cyanosis or digital clubbing was observed. Palpation of the thoracic spine revealed tenderness, particularly in the mid-thoracic region, suggesting skeletal involvement. No peripheral lymphadenopathy or hepatosplenomegaly were detected. The patient's performance status was Eastern Cooperative Oncology Group-1.

Initial imaging included a thoracoabdominal computed tomography (CT) scan, which revealed a large mass in the left lung. A tru-cut biopsy of the pulmonary lesion confirmed the diagnosis of primary lung adenocarcinoma.

Further staging with positron emission tomography-CT imaging demonstrated a hypermetabolic hilar mass in the left lung, mediastinal lymphadenopathy, and multiple bone metastases, consistent with stage IV NSCLC (Figure 1).

Molecular analysis showed that the tumor was negative for EGFR mutations and for *ALK* and *ROS1* gene rearrangements. However, programmed death-ligand 1 expression was positive, with a tumor proportion score of 40%, placing it in the 1-50% expression category.

Based on these findings, the patient was started on first-line chemoimmunotherapy comprising carboplatin, pemetrexed, and pembrolizumab. After four cycles, imaging revealed a partial response, and the regimen was modified

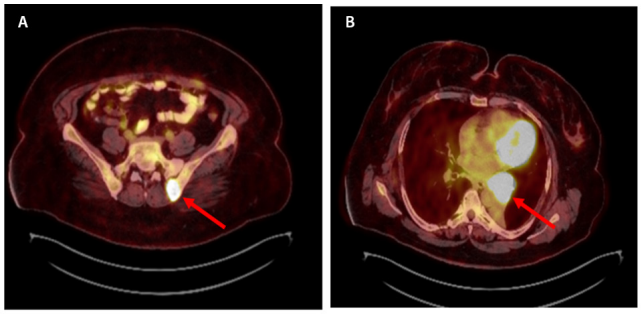

FIGURE 1: PET-CT at the time of diagnosis, A: Left iliac bone metastasis, B: Primary mass in the left lung.

PET-CT: Positron emission tomography-computed tomography

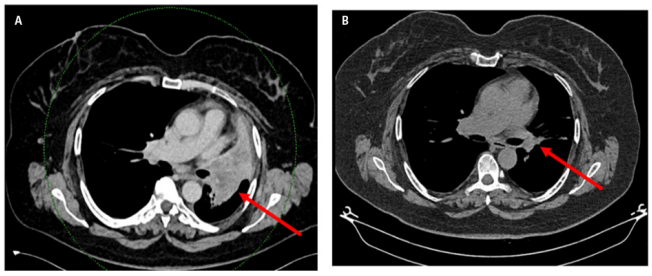

FIGURE 2: Thoracic computed tomography, (A) Before crizotinib: A right hilar mass (red arrow), likely representing a tumor or lymph node enlargement, causing partial compression of adjacent structures. (B) After crizotinib: Significant reduction in the size of the right hilar mass (red arrow), indicating a positive therapeutic response.

to maintenance pemetrexed and pembrolizumab, with carboplatin discontinued.

However, during the 11th cycle of pembrolizumab, radiological progression was noted in the primary lung lesion, suggesting acquired resistance (Figure 2A).

Given the patient's non-smoking status, female sex, and progression despite standard therapy, the presence of rare driver mutations was suspected. A comprehensive NGS panel was performed. The results identified CDKN2A underexpression and a HLA-DRB1-MET chromosomal rearrangement, which was considered actionable. No other driver mutations were detected. Microsatellite status was stable, and the tumor mutational burden was low (2.1 mutations/Mb).

In October 2024, the patient was started on crizotinib 250 mg twice daily based on the NGS results. Within two weeks of starting crizotinib, the patient reported marked symptomatic relief, including resolution of cough and back pain. No adverse effects or drug-related toxicities were noted. At the three-month follow-up, thoracic CT imaging demonstrated a substantial reduction in tumor size compared to baseline (Figure 2B). The patient was completely asymptomatic, and treatment was well-tolerated. This robust response suggests the potential utility of crizotinib in MET-rearranged NSCLC, even in rare fusion types such as HLA-DRB1-MET.

A subsequent series of imaging tests confirmed a significant decrease in the size of the tumor and a stabilization of the metastatic disease. At the most recent follow-up, the patient continues to receive crizotinib with excellent tolerability and a sustained clinical and radiological response. There is no evidence of new metastatic lesions, and the patient maintains a high quality of life. Overall, this experience demonstrates the successful integration of chemotherapy, immunotherapy, and molecularly targeted therapy in the management of advanced NSCLC, highlighting the transformative impact of personalized medicine. Written informed consent was obtained from the patient for the publication of this case report and the accompanying clinical information. A comparative analysis of all cases is presented in the following table (Table 1).

DISCUSSION

The present report highlights the potential of personalized therapy in advanced-stage NSCLC, particularly in cases harboring rare gene fusions such as HLA-DRB1-MET. As the fourth reported instance of an *HLA-DRB1-MET* gene rearrangement in the extant literature, this case underscores the importance of comprehensive molecular profiling, including NGS, in identifying actionable mutations and guiding tailored treatment strategies. HLA-DRB1-MET rearrangements, which are rare driver mutations in lung adenocarcinoma, are detected using comprehensive molecular profiling. In this instance, crizotinib was initiated following disease progression on chemo-immunotherapy, leading to significant disease control. The patient remains on crizotinib therapy with ongoing clinical and radiological stability, demonstrating the sustained efficacy of this targeted approach. Five months after treatment initiation, the patient remained progression-free with a sustained partial response and a PFS of 5 months (ongoing).

Although prospective data for MET fusions remain limited to small series and case reports, outcomes from larger MET-driven NSCLC cohorts provide clinically useful benchmarks for MET inhibition. In the long-term follow-up of the phase 2 VISION trial evaluating tepotinib in MET exon 14-skipping NSCLC, objective response rates (ORR) were approximately 51-56% across lines of therapy, and responses were durable (median duration of response approximately 18-21 months in the overall population), supporting sustained clinical benefit in appropriately selected patients with MET-altered disease.[3,17]

TABLE 1: Comparative analysis of cases.

Case	Age gender	Smoking status	Molecular findings	Treatment	Response	Current status	PFS/disease control duration
Crizotinib in HLA-DRB1-MET fusion-positive NSCLC Davies et al.[4]	74 Female	Never-smoker	HLA-DRB1-MET fusion	-Pemetrexed plus Carboplatin (1st line) -Crizotinib (2nd line)	Complete radiographic response within 6 weeks, maintained for 8 months	Stable with manageable side effects (fatigue, mild hypokalemia)	Crizotinib PFS: 8 mo.
Tepotinib in HLA-DRB1-MET fusion-positive NSCLC Blanc-Durand et al.[13]	41 Female	Never-smoker	HLA-DRB1-MET fusion	-Crizotinib (1st line) -Tepotinib (2nd line) -Cabozantinib (3rd line)	Complete intracranial response to tepotinib, sustained control for 9 months	Stable with good tolerance to treatment	Crizotinib PFS: 6 mo. Tepotinib PFS: 9 mo. Cabozantinib PFS: NR
Crizotinib in HLA-DRB1-MET fusion-positive NSCLC Kunte and Stevenson[14]	59 Female	Never-smoker	HLA-DRB1-MET fusion	-Curative RT (1st line) -Pembrolizumab (2nd line) -Crizotinib (3rd line)	Complete radiographic response within 4 months	Stable with mild side effects (fatigue, nausea)	Crizotinib PFS: at least 4 months (Ongoing at last follow-up)
Tepotinib in HLA-DQB2-MET fusion-positive NSCL Dias e Silva et al.[15]	73 Female	Never-smoker	HLA-DQB2::MET fusion	-Pemetrexed plus Carboplatin plus Pembrolizumab (1st line) -Tepotinib (2nd line)	Sustained disease control for over 12 months	Stable, no treatment-related adverse events	Tepotinib PFS: 12 mo.
Sequential TKI therapy in ALK-HLA-DRB1 fusion-positive NSCLC Gao et al.[16]	48 Female	Never-smoker	ALK-HLA-DRB1 fusion	-Crizotinib (1st line) -Ceritinib (2nd line)	24 months progression-free survival (crizotinib plus ceritinib)	Stable after sequential TKI therapy	Crizotinib PFS: 6 mo Ceritinib PFS: 18 mo.
Crizotinib in HLA-DRB1-MET fusion-positive NSCLC: Our experience	59 Female	Never-smoker	HLA-DRB1-MET fusion	-Pemetrexed plus Carboplatin plus Pembrolizumab (1st line) -Crizotinib (2nd line)	Significant tumor regression and symptomatic relief	Ongoing treatment with sustained good response	Crizotinib PFS: At least 8 months (ongoing at last follow-up)

TKI: Tyrosine kinase inhibitor; PFS: Progression-free survival; NR: Not reached; RT: Radiotherapy; NSCLC: Non small cell lung cancer; HLA: Human leukocyte antigen; MET: Mesenchymal-epithelial transition.

A comparison of the present case with that reported by Kunte and Stevenson[14] reveals notable distinctions. While both cases involved crizotinib administration following immunotherapy, Kunte and Stevenson[14] administered it after disease progression on pembrolizumab monotherapy. In contrast, crizotinib was employed in the present case after progression on a chemo-immunotherapy combination. In a similar vein, Davies et al.[4] reported a dramatic and rapid response to crizotinib in the absence of prior systemic treatments. Conversely, the progression-driven use of crizotinib for this patient exemplifies a more complex treatment trajectory and underscores the need to integrate targeted therapies into a comprehensive therapeutic framework. By comparison, Blanc-Durand et al.[13] demonstrated the efficacy of tepotinib in a case involving CNS metastases, in which the choice of therapy was influenced by the drug's ability to penetrate the blood-brain barrier. The absence of CNS involvement in this case enabled crizotinib to achieve effective disease control, emphasizing the need to tailor therapy to individual clinical profiles. Another comparison involves the report by Dias E Silva et al.[15], in which tepotinib was employed following progression on prior systemic treatments. Both cases underscore the critical role of comprehensive genomic analysis in identifying rare fusions. However, the absence of CNS metastases in this instance simplified management and enabled a straightforward treatment strategy. In contrast, the sequential use of crizotinib and ceritinib, as described by Gao et al.[16], involved crizotinib monotherapy, which was sufficient to achieve durable disease control.

From a biological perspective, MET fusions, such as HLA-DRB1-MET, act as oncogenic drivers by activating hepatocyte growth factor receptor (HGFR)-mediated signaling. Fusion events involving MET's exon 15 preserve the kinase domain, leading to constitutive activation and disruption of regulatory regions. Mechanistically, MET fusion proteins can promote ligand-independent receptor activation and downstream signaling through pathways such as MAPK/ERK and PI3K/AKT, reinforcing oncogenic dependence on MET. In addition to DNA-based detection, RNA-based assays can improve sensitivity for identifying expressed fusion transcripts and defining fusion breakpoints, which is particularly relevant when rare partners or complex rearrangements are present.[18,19] These advances have been instrumental in detecting such rearrangements. These assays facilitate the concurrent evaluation of multiple genes, thereby enabling precise therapeutic decisions, particularly in cases where conventional testing might miss rare alterations.[20] The efficacy and safety of targeted therapies, such as crizotinib and tepotinib, have been demonstrated in numerous cases, with improvements in patient outcomes and quality of life. Crizotinib's established activity against MET exon 14-skipping mutations and rare fusions has been attributed to its inhibition of HGFR-mediated signaling. Other MET inhibitors, such as capmatinib, have emerged as promising alternatives, particularly in cases involving CNS metastases or resistance to first-line MET inhibitors.[21,22]

Consistent with this, the Phase 2 GEOMETRY mono-1 study of capmatinib in MET exon 14-skipping NSCLC reported clinically meaningful activity in both treatment-naïve and previously treated populations: ORR of approximately 68% and 41%, respectively, and median PFS of approximately 12 months and 5 months, respectively. These data support the broader concept that dependence on the MET pathway can translate into substantial radiographic responses and meaningful disease control in patients treated with MET-selective TKIs.[23,24]

Beyond de novo MET-altered tumors, MET activation is also a key mechanism of acquired resistance. In the insight 2 phase 2 trial in patients with EGFR-mutant NSCLC and MET amplification after progression on first-line osimertinib, tepotinib plus osimertinib achieved an ORR of 50%, with a median duration of response of 8.5 months, median PFS of 5.6 months, and median OS of 17.8 months, illustrating how MET-directed therapy is increasingly incorporated into rational combination strategies when MET drives resistance.[25]

Despite meaningful initial responses, both on-target and off-target resistance mechanisms can limit the durability of MET TKI benefit. On-target resistance may arise through secondary MET kinase-domain mutations (commonly involving residues such as D1228 and Y1230) that reduce binding of type I MET inhibitors; other mutations (e.g., solvent-front alterations) can differentially affect sensitivity across MET inhibitors and may inform switching strategies. Off-target (bypass) resistance has been linked to activation of parallel signaling networks—such as ERBB-family signaling and reactivation of downstream PI3K/AKT or RAS/MAPK pathways—and to genomic events such as KRAS pathway alterations. These resistance patterns underscore the rationale for repeat molecular testing at progression and for tailoring subsequent therapy (switching MET inhibitor class, combination approaches, or clinical trial enrollment) based on the emergent mechanism.[18,26,27] The rarity of MET rearrangements, which occur in approximately 0.5% of lung adenocarcinomas, underscores the importance of advanced diagnostic tools. Techniques combining RNA and DNA analysis are expanding the scope of detectable alterations, enabling broader applications of precision oncology. This case aligns with global evidence supporting the integration of targeted therapies following standard treatments, showcasing the nuanced strategies required to manage NSCLC with rare MET rearrangements.

CONCLUSION

This review synthesizes evidence from a variety of case reports, emphasizing the transformative impact of molecularly targeted therapies in NSCLC with MET rearrangements. While significant progress has been made in understanding and treating these rare alterations, challenges persist in their early identification, standardized management, and access to advanced diagnostics and therapies. Addressing these challenges will require coordinated efforts in research, healthcare policy, and patient advocacy. The efficacy of MET TKIs, particularly in cases involving novel fusions such as HLA-DRB1-MET and HLA-DQB2-MET, underscores the potential of precision oncology to deliver highly personalized and effective treatments. The case study presented here further illustrates the importance of a multidisciplinary approach combining advanced diagnostics with innovative therapies. This case provides further evidence supporting the efficacy of crizotinib in achieving durable disease control in patients with HLA-DRB1-MET fusions and is consistent with global evidence supporting targeted therapy. Furthermore, comparative analyses of involving tepotinib and sequential TKI therapies underscore the necessity to customize treatment strategies based on individual clinical profiles, including CNS involvement and prior therapies. For instance, the efficacy of tepotinib in patients with CNS metastases and the sequential use of TKIs to overcome resistance highlight the complexities inherent in the management of MET-altered NSCLC. Notably, among never-smoking female patients with NSCLC,

the detection rate of driver mutations can be as high as 60%, underscoring the critical importance of comprehensive NGS profiling in this subgroup. Such advanced molecular diagnostics are pivotal in guiding precise therapeutic decisions and have a significant impact on survival outcomes. Consequently, the integration of comprehensive NGS into the diagnostic workup of these patients should be prioritized to ensure optimal clinical management and to improve overall survival. As our understanding of MET rearrangements progresses, so too will the strategies to optimize outcomes and improve the quality of life for affected patients. Continued innovation and collaboration among researchers, clinicians, and industry stakeholders are essential to ensure that emerging therapies reach the patients who need them most. In conclusion, these findings contribute to the growing body of evidence that MET TKIs are effective treatments for NSCLC with MET rearrangements. The adaptive integration of molecular profiling and personalized therapy offers new hope for improved patient outcomes. Future research should aim to optimize therapeutic sequencing, explore the efficacy of emerging MET inhibitors, and further elucidate the mechanisms underlying MET-driven oncogenesis, thereby enhancing the precision and efficacy of cancer care.

Ethics

Informed Consent: Written informed consent was obtained from the patient for the publication of this case report and the accompanying clinical information.

Footnotes

Authorship Contributions

Surgical and Medical Practices: H.M., J.H., B.K., Concept: H.M., B.K., M.H.Y., Ö.F.Ö., Design: H.M., E.S., M.H.Y., Ö.F.Ö., Data Collection or Processing: H.M., J.H., Analysis or Interpretation: H.M., M.H.Y., Literature Search: H.M., E.S., E.E.D., Writing: H.M., Ö.F.Ö.

Conflict of Interest: No conflict of interest was declared by the authors.

Financial Disclosure: The authors declared that this study received no financial support.

REFERENCES

1. Bade BC, Dela Cruz CS. Lung cancer 2020: epidemiology, etiology, and prevention. Clin Chest Med. 2020;41(1):1-24. [Crossref] [PubMed]
2. Salgia R. MET in lung cancer: biomarker selection based on scientific rationale. Mol Cancer Ther. 2017;16(4):555-565. [Crossref] [PubMed]
3. Paik PK, Felip E, Veillon R, et al. Tepotinib in non-small-cell lung cancer with MET exon 14 skipping mutations. N Engl J Med. 2020;383(10):931-943. [Crossref] [PubMed] [PMC]
4. Davies KD, Ng TL, Estrada-Bernal A, et al. Dramatic response to crizotinib in a patient with lung cancer positive for an HLA-DRB1-MET gene fusion. JCO Precis Oncol. 2017;2017(1):PO.17.00117. [Crossref] [PubMed] [PMC]
5. Stransky N, Cerami E, Schalm S, Kim JL, Lengauer C. The landscape of kinase fusions in cancer. Nat Commun. 2014;5:4846. [Crossref] [PubMed] [PMC]
6. International Cancer Genome Consortium PedBrain Tumor Project. Recurrent MET fusion genes represent a drug target in pediatric glioblastoma. Nat Med. 2016;22(11):1314-1320. [Crossref] [PubMed]
7. Zehir A, Benayed R, Shah RH, et al. Mutational landscape of metastatic cancer revealed from prospective clinical sequencing of 10,000 patients. Nat Med. 2017;23(6):703-713. Erratum in: Nat Med. 2017;23(8):1004. [Crossref] [PubMed] [PMC]
8. Santarpia M, Massafra M, Gebbia V, et al. A narrative review of MET inhibitors in non-small cell lung cancer with MET exon 14 skipping mutations. Transl Lung Cancer Res. 2021;10(3):1536-1556. [Crossref] [PubMed] [PMC]
9. Plenker D, Bertrand M, de Langen AJ, et al. Structural alterations of MET trigger response to MET kinase inhibition in lung adenocarcinoma patients. Clin Cancer Res. 2018;24(6):1337-1343. [Crossref] [PubMed]
10. Yu H, Ahn M-J, Kim S-W, et al. TATTON phase Ib expansion cohort: osimertinib plus savolitinib for patients (pts) with EGFR-mutant, MET-amplified NSCLC after progression on prior first/second-generation epidermal growth factor receptor (EGFR) tyrosine kinase inhibitor (TKI). Cancer Research. 2019;79(Suppl 13): CT032. [Crossref]
11. Wolf J, Seto T, Han J-Y, et al. Capmatinib (INC280) in METΔex14-mutated advanced non-small cell lung cancer (NSCLC): Efficacy data from the phase II GEOMETRY mono-1 study. American Society of Clinical Oncology. 2019;37(Suppl 15). [Crossref]
12. Reungwetwattana T, Liang Y, Zhu V, Ou SI. The race to target MET exon 14 skipping alterations in non-small cell lung cancer: the why, the how, the who, the unknown, and the inevitable. Lung Cancer. 2017;103:27-37. [Crossref] [PubMed]
13. Blanc-Durand F, Alameddine R, Iafrate AJ, et al. Tepotinib efficacy in a patient with non-small cell lung cancer with brain metastasis harboring an HLA-DRB1-MET gene fusion. Oncologist. 2020;25(11):916-920. [Crossref] [PubMed] [PMC]
14. Kunte S, Stevenson J. A case of HLA-DRB1-MET rearranged lung adenocarcinoma with rapid response to crizotinib. Clin Lung Cancer. 2021;22(3):e298-e300. [Crossref] [PubMed]
15. Dias E Silva D, Mambetsariev I, Fricke J, et al. A novel HLA-DQB2::MET gene fusion variant in lung adenocarcinoma with prolonged response to tepotinib: a case report. Transl Lung Cancer Res. 2024;13(5):1163-1168. [Crossref] [PubMed] [PMC]
16. Gao P, Tang K, Hao Y, et al. Case report: patient with lung adenocarcinoma with ALK-HLA-DRB1 rearrangement shows impressive progression-free survival after sequential crizotinib and ceritinib treatment. Front Oncol. 2022;12:762338. [Crossref] [PubMed] [PMC]
17. Mazieres J, Paik PK, Garassino MC, et al. Tepotinib treatment in patients with MET exon 14-skipping non-small cell lung cancer: long-term follow-up of the VISION phase 2 nonrandomized clinical trial. JAMA Oncol. 2023;9(9):1260-1266. Erratum in: JAMA Oncol. 2023;9(9):1300. [Crossref] [PubMed] [PMC]
18. Rivas S, Marín A, Samtani S, González-Feliú E, Armisén R. MET signaling pathways, resistance mechanisms, and opportunities

for target therapies. Int J Mol Sci. 2022;23(22):13898. [Crossref] [PubMed] [PMC]

19. Rolfo C, O'Brate A, Menzel C, et al. Liquid and tissue biopsies for identifying MET exon 14 skipping NSCLC: analyses from the phase II VISION study of tepotinib. Clin Cancer Res. 2025;31(13):2675-2684. [Crossref] [PubMed] [PMC]
20. Awad MM. Impaired c-Met receptor degradation mediated by MET exon 14 mutations in non-small-cell lung cancer. J Clin Oncol. 2016;34(8):879-881. [Crossref] [PubMed]
21. Ettinger D, Wood D. NCCN guidelines version 3.2020 non-small cell lung cancer. National Comprehensive Cancer Network. 2020:1-244. [Crossref]
22. Paik PK, Veillon R, Cortot AB, et al. Phase II study of tepotinib in NSCLC patients with MET ex14 mutations. American Society of Clinical Oncology. 2019;37(Suppl 15). [Crossref]
23. Heist R, Vansteenkiste J, Smit E, et al. MO01. 21 phase 2 GEOMETRY mono-1 study: capmatinib in patients with METex14-mutated advanced non-small cell lung cancer who received prior immunotherapy. Journal of Thoracic Oncology. 2021;16(1):S24-S25. [Crossref]
24. Ferreira M, Swalduz A, Greillier L, et al. Capmatinib efficacy for METex14 non-small cell lung cancer patients: Results of the IFCT-2104 CAPMATU study. Lung Cancer. 2024;196:107934. [Crossref] [PubMed]
25. Wu YL, Guarneri V, Voon PJ, et al.; INSIGHT 2 investigators. Tepotinib plus osimertinib in patients with EGFR-mutated non-small-cell lung cancer with MET amplification following progression on first-line osimertinib (INSIGHT 2): a multicentre, open-label, phase 2 trial. Lancet Oncol. 2024;25(8):989-1002. Erratum in: Lancet Oncol. 2024;25(10):e472. [Crossref] [PubMed]
26. Yao Y, Yang H, Zhu B, et al. Mutations in the MET tyrosine kinase domain and resistance to tyrosine kinase inhibitors in non-small-cell lung cancer. Respir Res. 2023;24(1):28. [Crossref] [PubMed] [PMC]
27. Kang J, Deng QM, Feng W, et al. Response and acquired resistance to MET inhibitors in de novo MET fusion-positive advanced non-small cell lung cancer. Lung Cancer. 2023;178:66-74. [Crossref] [PubMed] [PMC]

CASE REPORT

DOI: 10.37047/jos.galenos.2026.2025-10-7

J Oncol Sci 2026;12(1):111-4

Synchronous Adrenocortical Carcinoma, Renal Cell Carcinoma, and Mediastinal Mature Teratoma with Heterozygous Variants in SMARCA4, APC, and MYBP3: A Case Report

Ferit ASLAN[1], Burcu ERKILIÇ[2], Şeref Barbaros ARIK[3], Fisun ARDIÇ YÜKRÜK[4], Ersin ATABEY[5], Fatih YILDIZ[6], Hakan TABAN[1]

[1]Yüksek İhtisas Afiliated Medicalpark Ankara Hospital, Clinic of Medical Oncology, Ankara, Türkiye
[2]Yüksek İhtisas University Faculty of Medicine, Department of Internal Medicine, Ankara, Türkiye
[3]Yüksek İhtisas Afiliated Medicalpark Ankara Hospital, Clinic of Radiology, Ankara Türkiye
[4]University of Health Sciences Türkiye, Dr. Abdurrahman Yurtaslan Oncology Training and Research Hospital, Department of Pathology, Ankara, Türkiye
[5]Yüksek İhtisas Afiliated Medicalpark Ankara Hospital, Clinic of Urology, Ankara, Türkiye
[6]University of Health Sciences Türkiye, Dr. Abdurrahman Yurtaslan Oncology Training and Research Hospital, Department of Medical Oncology, Ankara, Türkiye

ABSTRACT

We describe an exceptionally rare case of a 46-year-old woman diagnosed with three synchronous primary tumors: adrenocortical carcinoma (ACC), renal cell carcinoma (RCC), and an anterior mediastinal mature teratoma. Cross-sectional imaging demonstrated distinct lesions of comparable size (each measuring 6-7 cm) in the right adrenal gland, right kidney, and the mediastinum. The patient underwent radical nephrectomy, adrenalectomy, and excision of the mediastinal mass. Histopathology confirmed clear cell RCC, ACC, and a mature teratoma without malignant transformation. Molecular testing revealed heterozygous variants in SMARCA4, APC, and MYBP3, suggesting a permissive background for multiple tumorigenic events. Importantly, all tumors were diagnosed at an early stage and completely resected, thereby enabling curative surgery without the need for adjuvant therapy. This unique presentation underlines the importance of integrated radiological, pathological, and molecular evaluation in patients with multiple synchronous tumors and highlights the role of vigilant follow-up in long-term management.

Keywords: Adrenocortical carcinoma; renal cell carcinoma; mediastinal mature teratoma; SMARCA4 variant; synchronous primary tumors

INTRODUCTION

The occurrence of multiple synchronous primary tumors is uncommon and often poses diagnostic as well as therapeutic challenges. While some cases are associated with well-defined hereditary cancer syndromes such as Li-Fraumeni, Lynch, or von Hippel-Lindau disease, the coexistence of independent tumors outside these classical syndromes is exceedingly rare.[1-3]

Adrenocortical carcinoma (ACC) and renal cell carcinoma (RCC) have occasionally been reported in combination, and mediastinal germ cell tumors are recognized entities, but the simultaneous presence of ACC, RCC, and a mediastinal mature teratoma of comparable size in the same patient has not previously been described.[4-6] Rare reports have described atypical RCC presentations with poor prognosis.[7] In contrast, our patient presented with three synchronous tumors that were completely resected at an early stage, allowing curative surgery without the need for adjuvant therapy.

Molecular profiling revealed heterozygous variants in SMARCA4, APC, and MYBP3, suggesting a permissive genetic

Correspondence: Prof. Ferit Aslan,
Yüksek İhtisas Afiliated Medicalpark Ankara Hospital, Clinic of Medical Oncology, Ankara, Türkiye
E-mail: feritferhat21@gmail.com
ORCID ID: orcid.org/0000-0002-9153-6921

Received: 14.10.2025 **Accepted:** 01.02.2026 **Epub:** 09.03.2026 **Publication Date:** 18.03.2026

Cite this article as: Aslan F, Erkılıç B, Arık ŞB, et al. Synchronous adrenocortical carcinoma, renal cell carcinoma, and mediastinal mature teratoma with heterozygous variants in SMARCA4, APC, and MYBP3: a case report. J Oncol Sci. 2026;12(1):111-4

Available at journalofoncology.org

background for multiple tumorigenic events. This emphasizes the importance of integrating radiological, pathological, and molecular evaluation in patients with rare tumor associations, where clinical outcomes may vary widely depending on stage and genetic profile.

CASE REPORT

A 46-year-old woman presented with a two-week history of retrosternal chest pain. The physical examination was unremarkable. Thoracic computed tomography (CT) revealed a 6.2 cm anterior mediastinal mass with cystic and necrotic components, while abdominal CT demonstrated two distinct lesions: a 6.5 cm heterogeneously enhancing mass in the upper pole of the right kidney and a 6.7×5.1 cm well-circumscribed adrenal mass (Figure 1).

Fluorodeoxyglucose positron emission tomography/CT confirmed metabolic activity in all three lesions (maximum standardized uptake value: mediastinal 2.19, renal 3.32, adrenal 11.58) without evidence of distant metastasis. A comprehensive endocrine evaluation, including measurements of cortisol, dehydroepiandrosterone sulfate, aldosterone, and catecholamines, as well as an overnight dexamethasone suppression test, revealed no hormonal excess, a finding consistent with a non-functioning ACC. Additionally, tumor markers commonly associated with germ cell tumors—alpha-fetoprotein, beta human chorionic gonadotropin, and lactate dehydrogenase—were within normal limits, supporting the diagnosis of a benign mediastinal teratoma.

The patient underwent right radical nephrectomy, right adrenalectomy, and excision of the mediastinal mass. Histopathological analysis confirmed three independent primary tumors (Figure 2).

- **Renal tumor:** Clear cell RCC, World Health Organization/International Society of Urological Pathology grade 2, confined to kidney, paired box gene 8 and epithelial membrane antigen positive.
- **Adrenal tumor:** ACC, Weiss score 3, inhibin and Melan-A positive, non-functioning.
- **Mediastinal mass:** Mature teratoma composed of gastrointestinal, pancreatic, thymic, and mesenchymal elements, without malignant transformation.

Molecular analysis identified heterozygous variants in SMARCA4, APC, and MYBP3, while no alterations were detected in classical hereditary cancer genes. Importantly, both RCC and ACC were diagnosed at an early stage and were completely resected; therefore, no adjuvant systemic therapy was indicated. The patient has been followed for 20 months after surgery without evidence of recurrence.

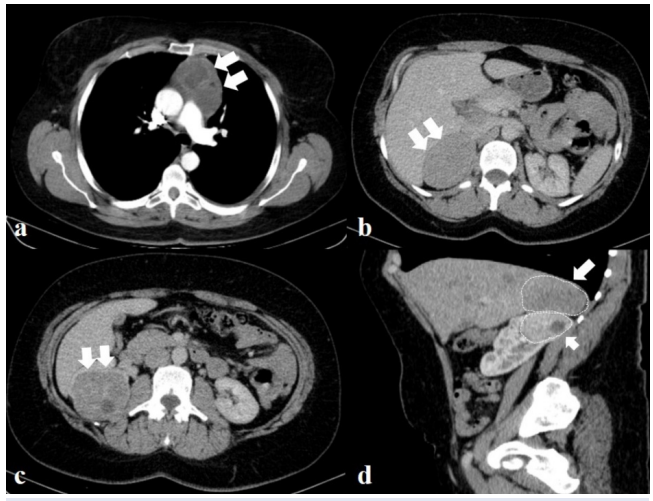

FIGURE 1: Contrast-enhanced computed tomography (CT) images of the same patient demonstrating three distinct masses, (a) An axial thoracic CT image shows a retrosternal mass with heterogeneous enhancement and cystic components (white arrows), (b) Axial abdominal CT image in the portal venous phase shows a homogeneously enhancing right adrenal mass; on dedicated dynamic adrenal CT, the absolute washout was indeterminate (white arrows), (c) Axial abdominal CT image in the portal venous phase demonstrates a heterogeneous right renal mass with residual contrast washout and cystic areas (white arrows), (d) Sagittal multiplanar reconstruction CT image in the arterial phase depicts both the right adrenal and right renal masses in the same plane (white arrows).

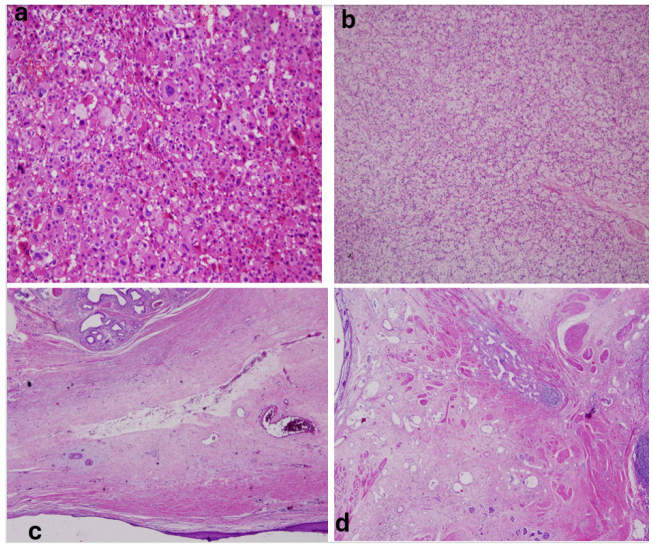

FIGURE 2: Histopathology. (a) Adrenocortical tumor showing marked cellular atypia and pleomorphism without necrosis, mitosis, or vascular invasion (H&E, ×200), (b) Clear cell renal cell carcinoma composed of nests of clear cells with delicate vasculature and minimal nuclear atypia (H&E, ×100), (c) Mature mediastinal teratoma with a cystic component lined by squamous epithelium and subepithelial skeletal muscle fibers (H&E, ×40), (d) Mature mediastinal teratoma containing gastric-type glands and pancreatic tissue elements (H&E, ×40).

H&E: Hematoxylin and eosin

DISCUSSION

The coexistence of three distinct primary tumors in a single patient is exceptionally rare and raises multiple clinical, prognostic, and molecular questions. In the setting of synchronous tumors, outcomes are often worse than for solitary primaries, largely due to diagnostic complexity, increased cumulative tumor burden, or limited therapeutic options. In one large series, the 1-year survival was 56.9%, but the 3-year survival dropped to 20.9%.[8] Other population-based data confirm that synchronous metastases are associated with a poorer prognosis than metachronous ones.[9,10] Case reports also emphasize the rarity and clinical challenges of managing synchronous malignancies.[11]

Demographically, most published reports of synchronous tumors involve middle-aged or older patients, often with a slight male predominance. Younger age has occasionally been associated with better outcomes, whereas unusual presentations in women have also been described in the literatüre.[7,8] These observations underline the importance of age and sex as potential prognostic modifiers in synchronous malignancies.

Clinically, both RCC and ACC were diagnosed at an early stage in our patient. Radical nephrectomy and adrenalectomy achieved complete resection; given the absence of adverse pathological features or hormonal activity, adjuvant systemic therapy was not required. The mediastinal teratoma was also completely excised and confirmed as benign. At 20 months' follow-up, the patient remains recurrence-free, demonstrating that early detection and curative surgery can mitigate the otherwise poor prognosis often reported for synchronous tumors.

From a molecular perspective, heterozygous variants in SMARCA4, APC, and MYBP3 were identified. SMARCA4 is a catalytic subunit of the switch/sucrose non-fermentable chromatin-remodeling complex, and its inactivation has been strongly linked to aggressive tumor biology. In small cell carcinoma of the ovary and thoracic sarcomas, SMARCA4-deficient tumors are associated with poor prognoses; median survival is often below one year.[1,2] In non-small cell lung cancer, SMARCA4 alterations similarly predict shorter overall and progression-free survival.[3,12] Interestingly, some studies suggest that SMARCA4-deficient tumors may respond more favorably to immune checkpoint inhibitors, raising the possibility of immunotherapy as a targeted therapeutic strategy.[12-14]

APC mutations, by contrast, are central to Wnt/β-catenin pathway activation and have been associated with colorectal and adrenal carcinogenesis, often contributing to aggressive tumor biology.[4,5] MYBP3 variants, although less well characterized, have been reported in pan-cancer sequencing efforts and may reflect underlying genomic instability rather than acting as true driver mutations.[6]

In our patient, the coexistence of three synchronous tumors harboring molecular alterations contrasts with the otherwise favorable clinical outcome achieved following complete resection. This underscores the importance of multidisciplinary evaluation: while genetic findings raise concerns for long-term risk, the absence of recurrence after nearly two years highlights that surgical management at an early stage remains the most decisive prognostic factor. Future studies may clarify whether patients with SMARCA4-altered tumors should benefit from closer surveillance or early inclusion in immunotherapy protocols.

CONCLUSION

This case represents an exceptionally rare coexistence of three synchronous primary tumors: RCC, ACC, and a mediastinal mature teratoma. Despite harboring molecular alterations including heterozygous SMARCA4, APC, and MYBP3 variants—changes usually associated with aggressive behavior—the patient achieved a favorable outcome with curative surgery alone. At 20 months' follow-up, she remains disease-free without adjuvant systemic therapy. This case highlights that early-stage diagnosis and complete resection can outweigh adverse molecular markers while emphasizing the importance of vigilant follow-up and the consideration of molecular risk in surveillance planning.

Ethics

Informed Consent: Informed consent was obtained from the patient and the patient's family for publication of the case report.

Footnotes

Authorship Contributions

Surgical and Medical Practices: F.A., Ş.B.A., F.A.Y., E.A., F.Y., H.T., Concept: F.A., B.E., H.T., Design: F.A., B.E., H.T., Data Collection or Processing: F.A., B.E., Ş.B.A., F.A.Y., E.A., H.T., Analysis or Interpretation: F.A., Ş.B.A., F.A.Y., E.A., F.Y., Literature Search: F.A., B.E., Writing: F.A., B.E.

Conflict of Interest: No conflict of interest was declared by the authors.

Financial Disclosure: The authors declared that this study received no financial support.

REFERENCES

1. Witkowski L, Carrot-Zhang J, Albrecht S, et al. Germline and somatic SMARCA4 mutations characterize small cell carcinoma of the ovary, hypercalcemic type. Nat Genet. 2014;46(5):438-443. [Crossref] [PubMed]
2. Yoshida A, Kobayashi E, Kubo T, et al. Clinicopathological and molecular characterization of SMARCA4-deficient thoracic sarcomas with comparison to potentially related entities. Mod Pathol. 2017;30(6):797-809. [Crossref] [PubMed]

3. Naito T, Umemura S, Nakamura H, et al. Clinical impact of SMARCA4 mutations in non-small cell lung cancer. J Thorac Oncol. 2020;15(6):947-955. [Crossref]
4. Assié G, Letouzé E, Fassnacht M, et al. Integrated genomic characterization of adrenocortical carcinoma. Nat Genet. 2014;46(6):607-612. [Crossref] [PubMed]
5. Cancer Genome Atlas Research Network; Kandoth C, Schultz N, Cherniack AD, et al. Integrated genomic characterization of endometrial carcinoma. Nature. 2013;497(7447):67-73. [Crossref] [PubMed] [PMC]
6. Liu J, Lichtenberg T, Hoadley KA, et al; Cancer Genome Atlas Research Network; Hu H. An integrated TCGA pan-cancer clinical data resource to drive high-quality survival outcome analytics. Cell. 2018;173(2):400-416.e11. [Crossref] [PubMed] [PMC]
7. Aslan F, Erkılıç B, Türkmen G, Günaydın E, Hasanov C. Renal cell carcinoma in pregnancy with breast metastasis: a case report and literature review. Cureus. 2025;17(9):e92550. [Crossref] [PubMed] [PMC]
8. Lv M, Zhang X, Shen Y, et al. Clinical analysis and prognosis of synchronous primary malignancies: a single-center study of 1,104 cases. J Surg Oncol. 2017;115(3):282-289. [Crossref]
9. Reboux N, Xu J, Faron M, et al. Incidence and survival in synchronous and metachronous metastases. JAMA Netw Open. 2022;5(9):e2233063. [Crossref]
10. Singnurkar AM, Ma C, Qiu Y, et al. Impact of synchronous cancers on survival in stage I lung cancer: a population-based study. Lung Cancer. 2020;145:12-18. [Crossref]
11. Al Laham O, Elhage J, Alorjani MS, et al. An exceedingly rare simultaneous incidental occurrence of synchronous malignancies. Int J Surg Case Rep. 2022;92:106823. [Crossref]
12. Cancer Genome Atlas Research Network. Comprehensive molecular profiling of lung adenocarcinoma. Nature. 2014;511(7511):543-550. Erratum in: Nature. 2014;514(7521):262. Rogers, K [corrected to Rodgers, K]. Erratum in: Nature. 2018;559(7715):E12. [Crossref] [PubMed] [PMC]
13. Schrock AB, Zhu VW, Hsieh WS, et al. Receptor tyrosine kinase fusions and SMARCA4 mutations as potential targets for immunotherapy in NSCLC. J Thorac Oncol. 2019;14(10):1887-1896. [Crossref]
14. Henon C, Blay JY, Massard C, et al. Efficacy of immune checkpoint inhibitors in SMARCA4-deficient thoracic tumors: a multicenter retrospective study. Ann Oncol. 2021;32(6):702-710. [Crossref]